



The influence of methyl donor status on cervical cancer cell behaviour *in vitro*

NATWADEE POOMIPARK

Human Nutrition Unit

Department of Oncology

The Faculty of Medicine, Dentistry, and Health

University of Sheffield

A thesis submitted for the degree of Doctor of Philosophy

OCTOBER, 2013

Acknowledgements

I am heartily thankful to my supervisor, Professor Hilary Powers, whose encouragement, guidance and persistent support has enabled me to develop an understanding of the subject of my PhD study.

I am indebted to many of my colleagues who have also supported me: Barbara, who helps, teaches, and supports me: Janet, who is always there to help me in a million things and Marilyn, who gives me a hand when I don't know how to deal with an experiment.

I would like to thank Dr Paul Heath for his kindness and help for microarray analysis and Dr Nigel Manning for methionine analysis.

I owe my deepest gratitude to Dr Carolyn Staton and Sapna Lunji for their time, guidance and discussion about a scratch assay.

I wish to thank Danny for his friendship and his brilliant ideas and I owe my deepest gratitude to Eun-Sook for helping me in everything and supporting me through my PhD.

I would like to show my gratitude to my teacher-Associate Professor Dr Kanoktip Packdibamrung and my friend-Dr Kuakarun Krusong who have supported me since my undergraduation at Chulalongkorn University. I would like to express the deepest appreciation to Associate Professor Dr Nusiri Lerdvutthisopon, Associate Professor Dr Treetip Ratanavarachai, Assistant Professor Dr Pintusorn Hansakul, Associate Professor Dr Jarunee Kualpiboon, Dr Ammara Chaikan, Dr Wanwarang Hiriote and all my colleagues at the Department of Pre-medical Science, Faculty of Medicine, Thammasat University who are always as my backups.

I would like to thank Dr Phakpoom Phraprasert, Dr Patompon Wongtrakoongate, Dr Supathra Narawatthana, Oratai Weeranantanapan, Nisa Patikarnmonthon, Sujunya Boonpradit and a number of Thai students who have shared their love and support throughout my study at Sheffield.

Lastly, this thesis is dedicated to all of my family, the Poomiparks and the Rittirongs, in Thailand. They have made available their support in a number of ways throughout my life and they are the wind beneath my wings.

Finally, my PhD scholarship was supported by Royal Thai Government.

Statement of Involvement

Certain measurements, which required the use of facilities to which there was limited researcher access, were made by others. These were: intracellular methionine concentration, which was measured by Dr Nigel Manning in the Department of Clinical Chemistry at the Children's Hospital in Sheffield, and the Gene microarray, which was carried out by Dr Paul Heath in the Department of Neuroscience at University of Sheffield.

Abstract

Epidemiological studies suggest that the availability of methyl-donor nutrients may influence the risk of cervical cancer and of cancer progression. This effect may be mediated by altered DNA instability and aberrant DNA methylation. The aim of this study was to develop and validate an appropriate *in vitro* model of methyl donor depleted cervical cancer cells and to use this model to investigate effects of methyl donor depletion on cell processes relevant to cancer risk and progression.

The human cervical cancer cell lines, C4-II and SiHa were selected for study. Cells were grown in complete medium and in medium depleted of folate alone and in medium depleted of methionine and folate. Growth rate, intracellular folate, intracellular methionine, and extracellular homocysteine were measured to validate the cervical cancer cell model of methyl donor depletion. The depleted cells showed >20-fold reduction of intracellular folate concentration in both cell models and a 60% reduction of methionine concentration in C4-II cells. Methyl donor depletion led to a greater reduction in the growth rate of C4-II than SiHa cells. Extracellular homocysteine was significantly raised by methyl donor depletion compared with controls.

Global DNA methylation was measured using a flow cytometric method. Combined depletion of folate and methionine led to an 18% reduction in global DNA methylation in C4-II cells but had no significant effect in SiHa cells; accordingly, only C4-II cells were used for further study. The expression of DNA methyl transferases (DNMTs) was measured using semi quantitative RT-PCR. Methyl donor depletion led to a significant down-regulation of DNMT3a and DNMT3b, which showed a 2.62 ($P= 0.024$) and 3.60-fold ($P= 0.001$) reduction in expression respectively. Total DNMT activity was increased by folate and methionine depletion cells ($P= 0.001$), although there are concerns about the quality of the assay used. Effects of folate and methionine depletion on cell growth, and DNMT3a and DNMT3b expression were reversed by transferring depleted cells to growth in complete medium.

Gene microarray analysis was carried out in order to identify genes and pathways affected by methyl donor depletion. A high proportion of genes associated with cell death, cell communication, and cell motion were up-regulated whilst a high proportion of genes associated with regulation of the cell cycle, cytoskeleton organisation, and chromosome organisation were down-regulated. Despite findings from the gene microarray were suggestive of effects on cell migration rate this was not found to be significantly influenced by methyl donor depletion, using the scratch assay.

Methyl donor status reversibly influences DNMT expression in cervical cancer cells *in vitro*, which may explain effects on global hypomethylation. Alterations in expression of other genes in response to methyl donor depletion are suggestive of cancer-promoting effects.

Contents

Acknowledgements	ii
Statement of Involvement	iii
Abstract	iv
List of Figures	ix
List of Tables	xii
Abbreviations	xiii
Chapter 1 Introduction	1
1.1 Cancer.....	1
1.2 Cervical Cancer	5
1.2.1 Epidemiology	5
1.2.2 Pathology	5
1.2.3 Causation.....	7
1.2.4 Diet as a modulator of cervical cancer risk	10
1.3 Folate	12
1.3.1 Folate metabolism.....	12
1.3.2 Importance of folate in DNA Synthesis and Repair	15
1.3.3 Importance of folate to DNA methylation	16
1.4 DNA methyltransferase (DNMT)	21
1.4.1 DNA methyltransferase (DNMT).....	21
1.4.2 Regulation of DNA methyltransferases.....	23
1.4.3 Dietary determinants of DNA methyltransferase expression /activity	24
1.4.4 DNA methyltransferase expression/activity as determinants of DNA methylation profile.....	25
1.4.5 DNA methyltransferases and cancer	26
1.4.6 DNA methylation, gene expression and cervical cancer	26
1.5 Folate as a modulator of cervical cancer risk	28
1.5.1 Folate and history of cervical cancer	28
1.5.2 MTHFR polymorphisms and cervical cancer	29
1.5.3 Folate and the natural history HPV.....	31
1.6 Methionine as a methyl donor	32
1.7 Hypothesis, aim, and objectives	35
Chapter 2 Materials and Methods	36
2.1 Materials.....	36
2.1.1 Cell lines	36

2.1.2 Media	36
2.1.3 Cell culture	37
2.1.4 Measurement of intracellular folate	37
2.1.5 Measurement of intracellular methionine	38
2.1.6 Measurement of homocysteine	38
2.1.7 Determination of DNA methylation	38
2.1.8 RNA extraction	41
2.1.9 cDNA synthesis.....	42
2.1.10 DNMTs gene expression by qRT-PCR.....	42
2.1.11 Gene expression analysis by microarray	43
2.1.12 Nuclear extraction	44
2.1.13 Protein quantification.....	44
2.1.14 DNMT activity.....	44
2.1.15 Cell migration	44
2.2 Methods	45
2.2.1 Cell culture	45
2.2.2 Determination of growth rate	46
2.2.3 Measurement of intracellular folate	48
2.2.4 Measurement of intracellular methionine	48
2.2.5 Measurement of homocysteine	48
2.2.6 DNA extraction.....	49
2.2.7 Determination of global DNA methylation	50
2.2.8 RNA extraction.....	52
2.2.9 cDNA synthesis.....	53
2.2.10 Determination of DNMT gene expression.....	53
2.2.11 Gene expression analysis by microarray	54
2.2.12 Nuclear protein extraction	55
2.2.13 Protein quantification.....	56
2.2.14 Determination of DNMT activity.....	56
2.2.15 Determination of cell migration	57
2.2.16 Statistic analysis.....	58
Chapter 3 Model development and validation.....	59
3.1 Introduction.....	59
3.2 Aims	61
3.3 Methods	61
3.3.1 Determination of cell growth and cell characteristics	61

3.3.2 Methyl-donor depletion.....	61
3.3.3 Measurement of intracellular folate	62
3.3.4 Measurement of intracellular methionine (C4-II only)	62
3.3.5 Measurement of homocysteine	62
3.3.6 Statistical analysis.....	62
3.4 Results	62
3.4.1 Cell characteristics	62
3.4.2 Effect of methyl-donor depletion on cell growth	63
3.4.3 Effect of methyl donor depletion on intracellular folate concentration	73
3.4.4 Effect of methyl donor depletion on Intracellular methionine concentration	75
3.4.5 Effect of methyl donor depletion on intracellular and extracellular homocysteine	77
3.5 Discussion.....	81
3.5.1 Cell culture.....	81
3.5.2 Effect on growth rate	81
3.5.3 Effect on intracellular folate concentration	83
3.5.4 Effect on intracellular methionine concentration	85
3.5.5 Effect of growth in a folate-depleted medium on methyl cycling: measurement of intracellular homocysteine and homocysteine export	85
3.6 Summary	86
Chapter 4 Effects of methyl donor depletion on DNMTs expression and DNA Hypomethylation.....	89
4.1 Introduction.....	89
4.2 Aims	89
4.3 Methods	90
4.3.1 Cell sample preparation	90
4.3.2 Development of the global DNA methylation assay	90
4.3.3 RNA extraction and cDNA synthesis (C4-II cells only).....	91
4.3.4 Determination of DNMTs expression (C4-II cells only)	91
4.3.5 Determination of DNMT activity (C4-II cells only)	92
4.3.6 Repletion study (C4-II cells only).....	92
4.3.7 Statistical analysis.....	92
4.4 Results	92
4.4.1 Development of the global DNA methylation assay	92
4.4.2 Determination of Global DNA methylation	102
4.4.3 DNMT expression (C4-II cells only).....	103
4.4.4 Total DNMT activity.....	104

4.4.5 Folate and methionine repletion (only C4-II cells).....	104
4.5 Discussion.....	109
4.5.1 Effect of methyl donor depletion on global DNA methylation	109
4.5.2 Effect on DNMTs expression.....	112
4.5.3 Effect of methyl donor repletion on cell growth and DNMT expression.....	114
4.5.4 Effect on DNMT activity.....	115
4.6 Summary.....	117
Chapter 5 Gene expression.....	118
5.1 Introduction.....	118
5.2 Aims	119
5.3 Methods	119
5.3.1 Microarray.....	119
5.3.2 Data analysis	119
5.4 Results and discussion.....	120
Chapter 6 Cell Migration.....	143
6.1 Introduction.....	143
6.2 Aims	144
6.3 Methods	144
6.3.1 Cell culture.....	144
6.3.2 Mitomycin C optimisation	145
6.3.3 Scratch assay	146
6.4 Results	147
6.4.1 Mitomycin C optimisation	147
6.4.2 Scratch assay	151
6.5 Discussion.....	154
6.6 Summary.....	157
Chapter 7 Discussion and Conclusion.....	158
7.1 Conclusion.....	158
7.2 Discussion.....	159
REFERENCES	164

List of Figures

Figure 1: <i>Integrated circuits derived from multiple hallmark capabilities.....</i>	4
Figure 2: <i>Incidence and mortality rate of cervical cancer update 2011</i>	6
Figure 3: <i>Diagram of CIN progression to invasive cancer.....</i>	7
Figure 4: <i>Structure of folate.....</i>	13
Figure 5: <i>Structure of important folate coenzymes</i>	13
Figure 6: <i>Methyl cycle showing two important mechanisms involved in one-carbon metabolism.</i>	14
Figure 7: <i>Purine synthesis: adding 8-carbon atom to purine ring.....</i>	17
Figure 8: <i>Purine synthesis: adding 2-carbon atom to purine ring.....</i>	17
Figure 9: <i>Folate is involved in pyrimidine synthesis.....</i>	18
Figure 10: <i>The position of methylation at a cytosine base</i>	18
Figure 11: <i>Hypermethylation on CpG rich-region at a promoter site</i>	22
Figure 12: <i>Global hypomethylation on CpG-rich regions</i>	22
Figure 13: <i>Effects of folate in cancer risk.....</i>	30
Figure 14: <i>The haemocytometer gridline</i>	47
Figure 15: <i>Growth of C4II cells cultured in complete medium for 20 days.....</i>	64
Figure 16: <i>Characteristics of C4-II cells after 4, 11 and 18 days of culture</i>	64
Figure 17: <i>Growth of SiHa cells cultured for 15 days in complete medium</i>	65
Figure 18: <i>Characteristics of SiHa cells after 4, 8 and 12 days of growth in complete medium</i>	65
Figure 19: <i>The growth curves of C4-II cells grown in folate and methionine-depleted medium compared with controls</i>	66
Figure 20: <i>The growth curves of SiHa cells growing in folate and methionine- depleted medium compared with controls.....</i>	66
Figure 21: <i>Effects of methyl donor depletion on growth of C4-II cells</i>	67
Figure 22: <i>Growth of C4-II cells (A), and SiHa cells (B) in complete medium, folate-deplete and combined folate and methionine-deplete medium</i>	70
Figure 23: <i>Characteristics of C4-II cells grown in (A) F+M+ (B) F-M+, and (C) F-M-after 4, 8 and 12 days of culture.....</i>	71
Figure 24: <i>Cell size of C4-II cells grown in F+M+, F-M+, and F-M- after 4, 8 and 12 days of culture.....</i>	71
Figure 25: <i>Characteristics of SiHa cells grown in (A) F+M+ (B) F-M+, and (C) F-M-after 4, 8 and 12 days of culture.....</i>	72
Figure 26: <i>Intracellular folate concentration of C4-II cells grown in folate and methionine-depleted medium and complete medium.....</i>	74

Figure 27: Intracellular folate concentration of SiHa cells grown in complete, folate-deplete, and, folate and methionine-depleted medium after 6 passages (42 days).....	74
Figure 28: Intracellular folate concentration of SiHa cells grown in folate-deplete, folate and methionine depleted medium and complete medium	76
Figure 29: Intracellular methionine concentration of C4-II cells grown in folate and methionine depleted medium, folate-depleted medium, and, complete medium.....	76
Figure 30: Extracellular homocysteine concentration of C4-II cells cultured in complete, folate-deplete, and, folate and methionine-deplete medium	79
Figure 31: Intracellular homocysteine of SiHa cells grown in complete, folate-deplete, and, folate and methionine-deplete medium for 6 passages (42 days).....	80
Figure 32: Extracellular homocysteine for SiHa cells cultured in complete, folate-deplete, and, folate and methionine-deplete medium.....	80
Figure 33: Methyl donor depletion protocol for C4-II.....	87
Figure 34: Methyl donor depletion protocol for SiHa.....	88
Figure 35: Global DNA methylation of C4-II cells grown in complete and folate and methionine-depleted medium, using the methyl acceptor assay.....	94
Figure 36: Global DNA methylation of SiHa cell DNA determined using the DNA methyl acceptor assay.....	95
Figure 37: Detection of 5-methylcytosine of C4-II DNA by immunocytochemistry.....	96
Figure 38: Pattern of 5-methylcytosine detection of C4-II cells by flow cytometry	99
Figure 39: Detection of 5-methylcytosine of C4-II DNA by flow cytometry	100
Figure 40: Detection of 5-methylcytosine of SiHa DNA by flow cytometry	101
Figure 41: DNMT expression of C4-II cells grown in folat depleted medium, folate and methionine-depleted medium and complete medium	105
Figure 42: Total DNMT activity of methyl-donor depleted cells in comparison with control	106
Figure 43: Growth of cells depleted of methyl donors for 8 days and then grown in complete medium for a further 4 days	106
Figure 44: Effects of methyl donor repletion on DNMTs expression in C4-II cells.....	108
Figure 45: Example of functional annotation clustering using DAVID Bioinformatics. This screen shot shows a few clusters from the up-regulated gene list.....	121
Figure 46: Example of functional annotation clustering using DAVID Bioinformatics. This screen shot shows a few clusters from the down-regulated gene list	122
Figure 47: Example of genes from the cell death cluster which were up-regulated in methyl-donor depleted cells.....	132
Figure 48: Example of genes from the cell cycle cluster which were down-regulated in methyl-donor depleted cells	133
Figure 49: The Wnt signalling pathway from KEGG database.....	134

Figure 50: <i>The focal adhesion pathway from KEGG database</i>	136
Figure 51: <i>Example of functional annotation clustering using DAVID Bioinformatics. This screen shot shows some clusters from the up-regulated gene list (re-analysis)</i>	140
Figure 52: <i>Example of functional annotation clustering using DAVID Bioinformatics. This screen shot shows some clusters from the down-regulated gene list (re-analysis)</i>	141
Figure 53: <i>The flow chart of mitomycin C optimisation protocol</i>	145
Figure 54: <i>The flow chart of the scratch assay protocol</i>	146
Figure 55: <i>The effect of mitomycin C on cell proliferation</i>	148
Figure 56: <i>Mitomycin C optimisation considering the effect on cell proliferation</i>	149
Figure 57: <i>The effect of mitomycin C on F-M- cell proliferation (repeat)</i>	150
Figure 58: <i>Scratch wound model</i>	150
Figure 59: <i>The percentage of gap closure of the C4-II cells grown under four different conditions</i>	152
Figure 60: <i>The effect of mitomycin C treatment on cell proliferation</i>	152
Figure 61: <i>Scratch wound model from time-lapse microscopy</i>	153

List of Tables

Table 1: <i>Reagent volumes used for different packed cell volumes.....</i>	56
Table 2: <i>Intracellular homocysteine concentration ($\mu\text{mol/L}$) of C4-II cells grown in complete, folate-deplete, and folate and methionine-deplete medium</i>	77
Table 3: <i>Intracellular homocysteine concentration ($\text{pmol}/10^6$ cell) of C4-II cells in complete, folate-deplete, and, folate and methionine-deplete medium</i>	78
Table 4: <i>The percentage reduction in global DNA methylation in C4-II cells depleted of methyl donors, compared with control cells.....</i>	102
Table 5: <i>The percentage reduction of global DNA methylation in SiHa cells depleted of methyl-donors, compared with control.....</i>	103
Table 6: <i>Summary of selected gene clusters from both up- and down-regulated genes of methyl-donor depleted cells</i>	123
Table 7: <i>Example of genes which were up-regulated in methyl-donor depleted cells and their relevance to biological function</i>	127
Table 8: <i>Example of genes which were down-regulated in methyl-donor depleted cells and their relevance to biological function</i>	130
Table 9: <i>The list of up-regulated genes of focal adhesion pathway in F-M- cells compared with in F+M+ cells</i>	137
Table 10: <i>The list of down-regulated genes of focal adhesion pathway in F-M- cells compared with in F+M+ cells.....</i>	138
Table 11: <i>Summary of selected gene clusters from both up- and down-regulated genes of methyl-donor depleted cells (re-analysis with multiple corrections)</i>	139

Abbreviations

CIN	Cervical intraepithelial neoplasia
DNA	Deoxyribonucleic acid
RNA	Ribonucleic acid
OC	Oral contraceptive
OR	Odds ratio
CI	Confidence interval
HPV	Human papillomavirus
ROS	Reactive oxygen species
RBC	Red blood cell
THF	Tetrahydrofolate
DHF	Dihydrofolate
SAM	S-adenosyl methionine
SAH	S-adenosyl homocysteine
MTHFR	Methylene tetrahydrofolate reductase
IMP	Inosine monophosphate
AMP	Adenosine monophosphate
GMP	Guanosine monophosphate
HR-HPV	High-risk human papillomavirus
LR-HPV	Low-risk human papillomavirus
Rb, RB	Retinoblastoma
E2F	E2 transcription factor
IL	Interleukin
HIF	Hypoxia inducible factor
5-mc	5-methylcytosine
5-Azadc	5-aza-2'-deoxycytidine
F+M+	Folate and methionine-replete medium
F+M-	Methionine-depleted medium
F-M+	Folate-depleted medium
F-M-	Folate and methionine-depleted medium
FCS	Fetal calf serum
PBS	Phosphate buffer saline
DTT	Dithiothreitol
DAB	Diaminobenzidine
DPM	Disintegrations per minute
HPLC	High performance liquid chromatography

qRT-PCR	Quantitative real-time reverse transcription polymerase chain reaction
dNTP	Deoxynucleotide triphosphate mix
BSA	Bovine serum albumin
FCS	Fetal calf serum
DNMT	DNA methyltransferase
RIN	RNA integrity number
ECM	Extracellular matrix
MTS	[3-(4,5-dimethylthiazol-2-yl)-5-(3-carboxymethoxyphenyl)-2-(4-sulfophenyl)-2H-tetrazolium]

Chapter 1 Introduction

Micronutrient deficiency is known to play an important role in the development of many conditions including night blindness, anaemia, and peripheral neuropathy. Additionally, there is evidence that some micronutrients have an important influence on the risk of cancer at various sites (Jacobs *et al.*, 2003; Powers, 2005; Park *et al.*, 2007). There are various factors which seem to be important for cancer risk and cancer progression such as smoking, infection, and diet. A few nutrients have been clearly shown to have a role in determining cancer risk (García-Closas *et al.*, 2005); there is particular interest in the role of methyl donors because of their importance to DNA synthesis/repair and DNA methylation, which are known to influence carcinogenesis (Duthie *et al.*, 2004; Kim, 2005).

1.1 Cancer

This thesis described and investigation of methyl-donor deficiency on aspect of DNA methylation, gene expression and the cervical cancer phenotype. The interpretation of our findings necessitated an understanding of those processes thought to be especially pertinent to the cancer process. This understanding is informed by the work of Hanahan and Weinberg (2000 and 2011) who proposed hallmarks of cancer to characterise the cancer process (Hanahan & Weinberg, 2000; Hanahan & Weinberg, 2011). The hallmarks of cancer are summarized below.

I. Sustaining proliferative signalling

Normal tissues work to ensure a balance between cell death and proliferation through cell cycle signals. In contrast, cancer cells have their own signals and deregulate the cell cycle (Collins *et al.*, 1997). Our understanding of the mechanisms of cell signalling in normal cells is fairly limited, research into cell signalling in cancer cells is better understood. Cancer cells may organize their own growth factor ligands to produce autocrine proliferative stimulation or send the stimulated signal to normal cells to send back the various supporting growth factors (Bhowmick *et al.*, 2004; Cheng *et al.*, 2008). Cancer cells may also increase their receptor proteins in order to access more signals and operate an independent downstream signalling pathway within the cells. This hallmark is likely to involve the activation of downstream pathways such as the mitogen activated protein (MAP)-kinase pathway and phosphoinositide 3-kinase (PI3-kinase) (Castellano & Downward, 2011). Cancer cells also have mechanisms which disrupt the intrinsic negative-feedback, therefore, they can sustain proliferative signals. Moreover, the elevation of oncogenic signals from

RAS, MYC, and RAF in cancer cells leads to cell adaptation by disabling senescence- or apoptosis-inducing circuitry (Lowe *et al.*, 2004; Evan & d'Adda di Fagagna, 2009; Collado & Serrano, 2010).

II. Evading growth suppressors

To sustain growth stimulating signals, the cancer cells do not operate to negatively regulate cell proliferation. Two well-known key tumour suppressors, RB (retinoblastoma-associated) and TP53, play an important role in this. Generally, the RB and/or TP53 pathway is defective in cancer cells (Kastan & Bartek, 2004). In addition, the loss of contact inhibition can disrupt growth suppressors; this has occupied researchers for about the last four decades of research, but the mechanism is only just being understood. Moreover, interference in the TGF- β pathway (antiproliferative effect) is reported to promote malignancy (Derynck *et al.*, 2001).

III. Resisting cell death

Cancer cells evolve their ability to limit apoptosis, commonly by the functional loss of the TP53 tumour suppressor gene (Fridman & Lowe, 2003). For the same purpose, cancer cells may increase their expression of antiapoptotic regulators such as Bcl-2 and Bcl-x_L, and also up-regulate survival signals (IGF1/2) (Shortt & Johnstone, 2012). A defect in autophagy is also a mechanism to drive cancer cells to resist cell death. Autophagy is a self-degradation process which is up-regulated by stress signals such as growth factor deprivation, starvation, and pathogen infection (He & Klionsky, 2009). In addition, necrotic cancer cells can release proinflammatory signals to the surrounding microenvironment, which promote angiogenesis, proliferation, and invasion, such as IL-1 α to facilitate cancer progression (Apte *et al.*, 2006).

IV. Enabling replicative immortality

Immortalization is the ability to proliferate without evidence of senescence or crisis. There is evidence that unlimited proliferation results from telomeres protecting the end of the chromosomes (Shay & Wright, 2000; Blasco, 2005) and the presence of telomerase (DNA polymerase which adds telomere segments) is associated with a resistance to entering senescence and crisis/apoptosis (Reddel, 2000).

V. Inducing angiogenesis

To support their metabolism, in terms of receiving nutrients and oxygen or removing waste products, cancer cells generate neovasculature. Important angiogenesis factors are vascular endothelial growth factor-A (VEGF-A) and thrombospondin-1 (THBS-1). VEGF-A is an angiogenic inducer which is up-regulated by hypoxia and oncogenic signals (Carmeliet,

2005; Gabhann & Popel, 2008; Ferrara, 2009). The VEGF ligands can be activated by extracellular matrix-degrading proteases such as MMP-9 (Kessenbrock *et al.*, 2010). TSP-1 is an angiogenic inhibitor which binds to transmembrane receptor and counterbalances proangiogenic stimuli (Kazerounian *et al.*, 2008). The chronic up-regulation of fibroblast growth factor (FGF) is also one of the proangiogenic signals (Baeriswyl & Christofori, 2009).

VI. Activating invasion and metastasis

The key factor in this hallmark is the cell-to-cell adhesion molecule, E-cadherin. This molecule supports the assembly of epithelial cell sheets. The down-regulation of E-cadherin indicates the promotion of invasion and metastasis (Cavallaro & Christofori, 2004; Berx & van Roy, 2009). The genes expressing cell-to-cell and cell-to-ECM adhesion molecules, which support cytotaxis, are typically down-regulated in this hallmark. In contrast, genes which encode adhesion molecules involved in cell migration, are up-regulated such as N-cadherin in the migrating neuron (Hazan *et al.*, 2000).

VII. Reprogramming energy metabolism

In order to supply sufficient energy for unlimited proliferative potential and rapid division, cancer cells need to adapt themselves to deal with an estimated 18-fold higher requirement of ATP by an up-regulation of glucose transporters (GLUT1) (DeBerardinis *et al.*, 2008; Hsu & Sabatini, 2008; Jones & Thompson, 2009). An increased Ras oncoprotein and hypoxia in cancer cells also leads to an increase in HIF1 α and HIF2 α transcription factors in order to up-regulate glycolysis (Kroemer & Pouyssegur, 2008; Semenza, 2010b; Semenza, 2010a).

VIII. Evading immune destruction

Basically, the immune system has a responsibility to destroy pathogens or foreign bodies in the body. In a similar way to pathogens, cancer cells should be recognised and eliminated by the immune system. However, the existence of cancer cells at all somehow indicates that cancer cells can avoid elimination (Dunn *et al.*, 2002; Schreiber *et al.*, 2011). Cancer susceptibility is not only limited to the immunocompromised patients with virus-induced cancer, but occurs in non-virus-induced cancers. According to tumour-host immunological interactions, the immune system of the host can be destroyed by highly immunogenic cancer cells.

All 8 hallmarks are coordinated to maintain cancer cell characteristics such as the alteration of genes in the Wnt signalling pathway, which leads to changes in cell motility and also is linked to changes in the expression of other genes important to carcinogenesis. **Figure 1** illustrates the integrated circuits from individual signals. The 4 sub-circuits show an

interconnection between signalling pathways in cancer cells. Individual sub-circuits are comprised of multiple hallmark capabilities and lead to the main characteristics of cancer cells. Characteristics of cancer cells at specific sites do not necessarily include all of the hallmarks summarised above. Furthermore, cervical cancer has the added complexity of requiring the presence of the human papillomavirus (HPV).

The details concealed within the circuits in figure 1 are examined in some depth when discussing the findings of our microarray study.

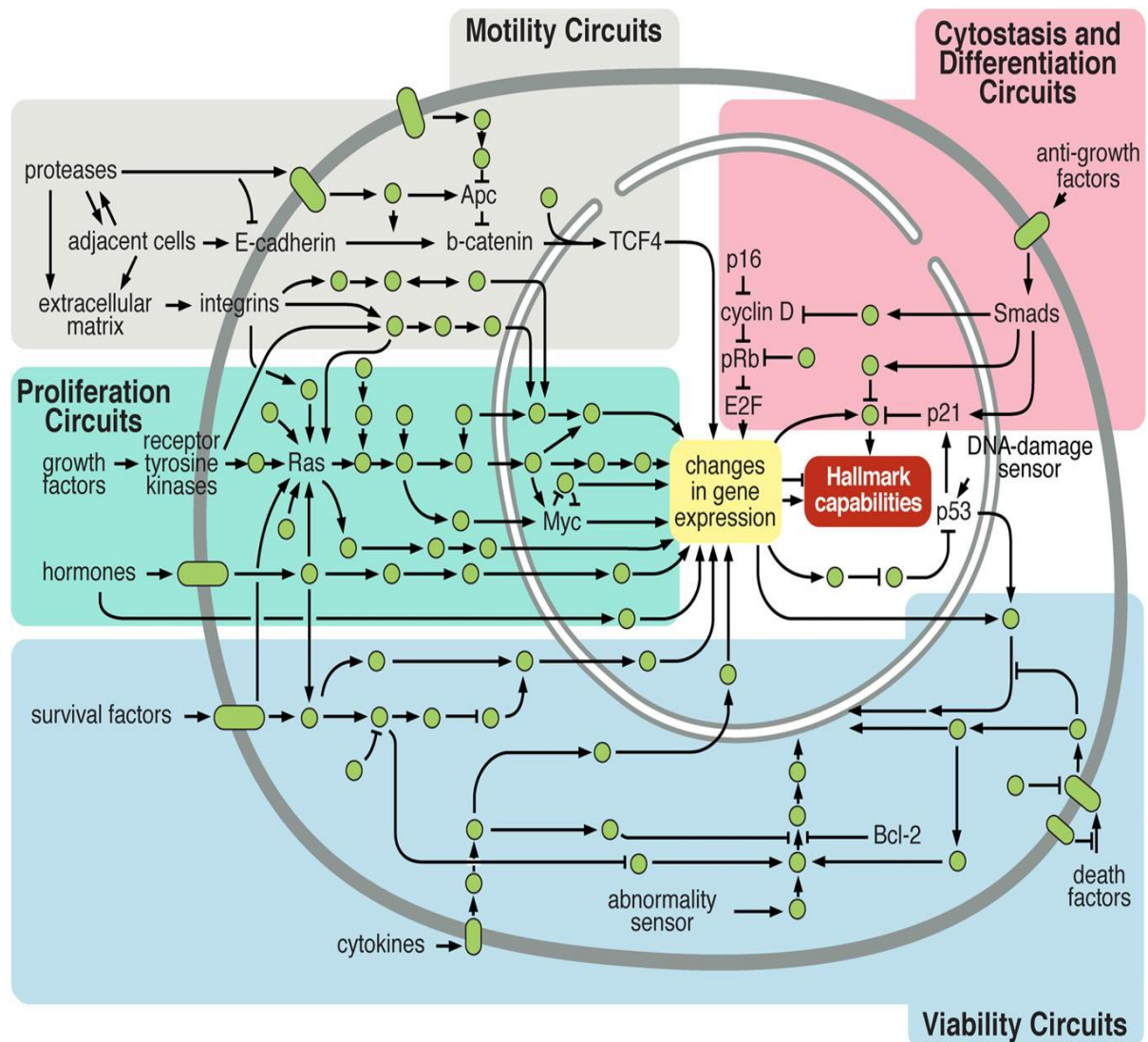


Figure 1: Integrated circuits derived from multiple hallmark capabilities

(Hanahan & Weinberg, 2011)

This figure identifies particular cellular functions and expresses these as signalling pathways, which Hanahan & Weinberg visualise as circuits. This figure focuses on some of the circuits which proved important in the gene microarray study of methyl donor depleted cells.

1.2 Cervical Cancer

1.2.1 Epidemiology

In the 1930s cervical cancer was the most common cancer in American women (Schoell *et al.*, 1999). Recent cancer statistics indicate that **(figure 2)**, cervical cancer is the third most diagnosed cancer and the fourth major cause of cancer death in women worldwide, accounting for 9% (529,800) of new cancer cases and 8% (275,100) of total cancer deaths among females (Jemal *et al.*, 2011). Chronologically, the world burden of cervical cancer has improved; specifically, since the introduction of the Papanicolaou (Pap) smear for screening pre-invasive cervical cancer, the incidence has decreased in developed countries (Garner, 2003).

Cervical cancer used to have a relatively high incidence in middle-aged women, but now the peak incidence has shifted toward younger women. In European countries, twenty years ago the highest rate of incidence was in women aged between 44 and 49 years, whereas in Latin America, Asia and Africa the peak occurred between the ages of 50 and 55 (1987). In 2006, data from Cancer Research UK reported that the highest incidence of cervical cancer in UK occurred between the ages of 30-40years (CancerresearchUK, 2009). Trends in cervical cancer incidence in most Latin American countries, in African countries, and in several Asian countries, have not decreased in the way they have in developed countries because of a lack of effective screening programs. About 80% of new cases each year are in developing countries (Powers, 2005).

1.2.2 Pathology

Cervical cancer can be divided into two types: squamous cell carcinomas (SCC) which are the transformation of squamous epithelial cells of ectocervix, and adenocarcinomas (AC) which are transformation of glandular epithelial cells of endocervix. According to the International Federation of Gynecology of Obstetrics (FIGO), cervical cancer can be classified by four stages from the less severe level I to the most severe level IV. In the context of Bethesda criteria, abnormality of cervical cells can be classified into various grades of cervical intraepithelial neoplasia (CIN). CIN 1 (grade I) is a mild dysplasia or a low grade squamous intraepithelial lesion (LSIL), which deeply expands into 1/3 of the layer of epithelial cells. CIN 2 (grade II) is a moderate dysplasia, which expands for 2/3 of epithelial cells. And CIN 3 (grade III) is a severe dysplasia or a high grade squamous intraepithelial lesion (HSIL), which expands into more than 2/3 of the epithelial cell layer. Women who have dysplasia grade far beyond the CIN 3 are diagnosed as having cervical cancer **(figure 3)**.

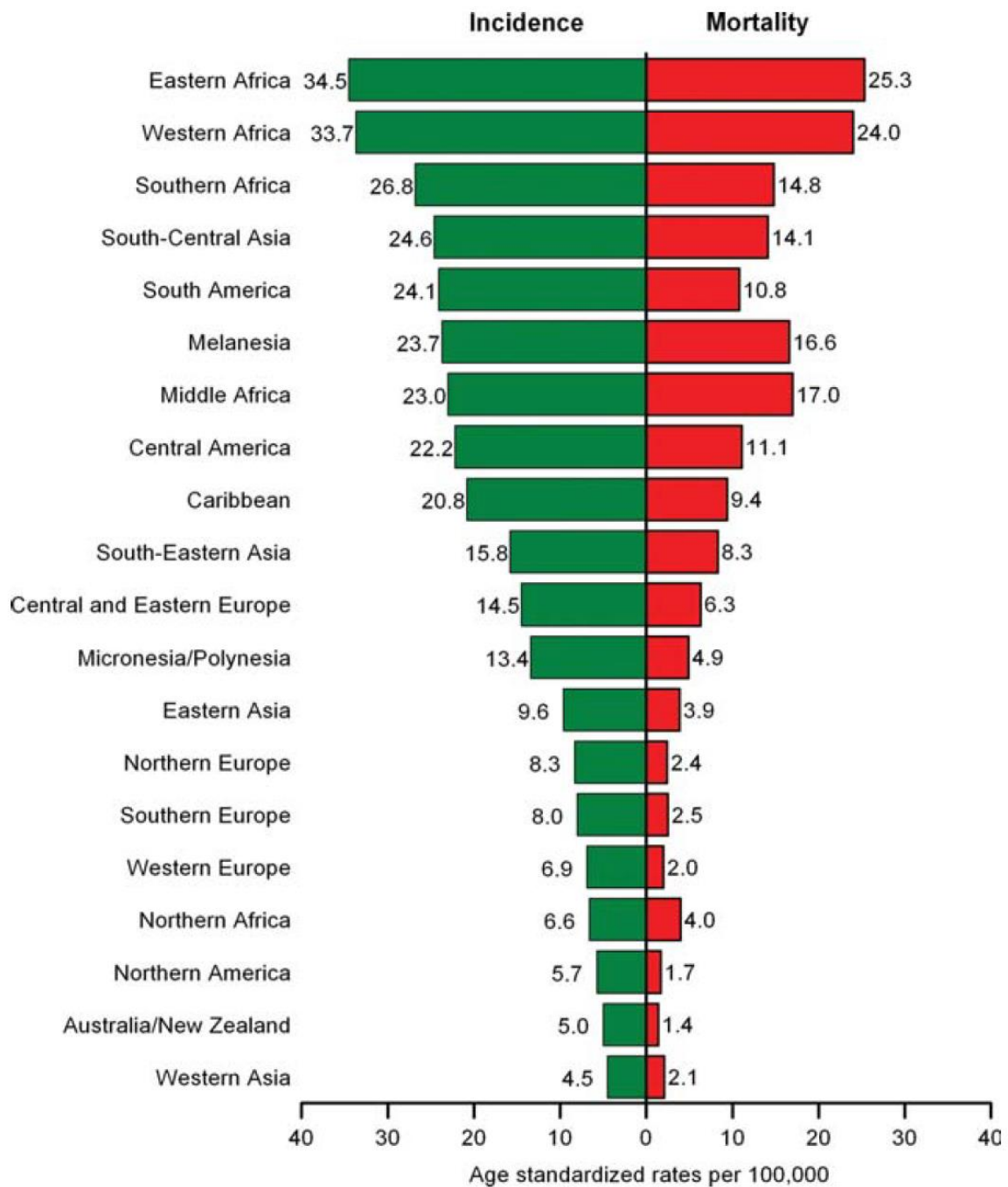


Figure 2: Incidence and mortality rate of cervical cancer update 2011

(Jemal et al., 2011)

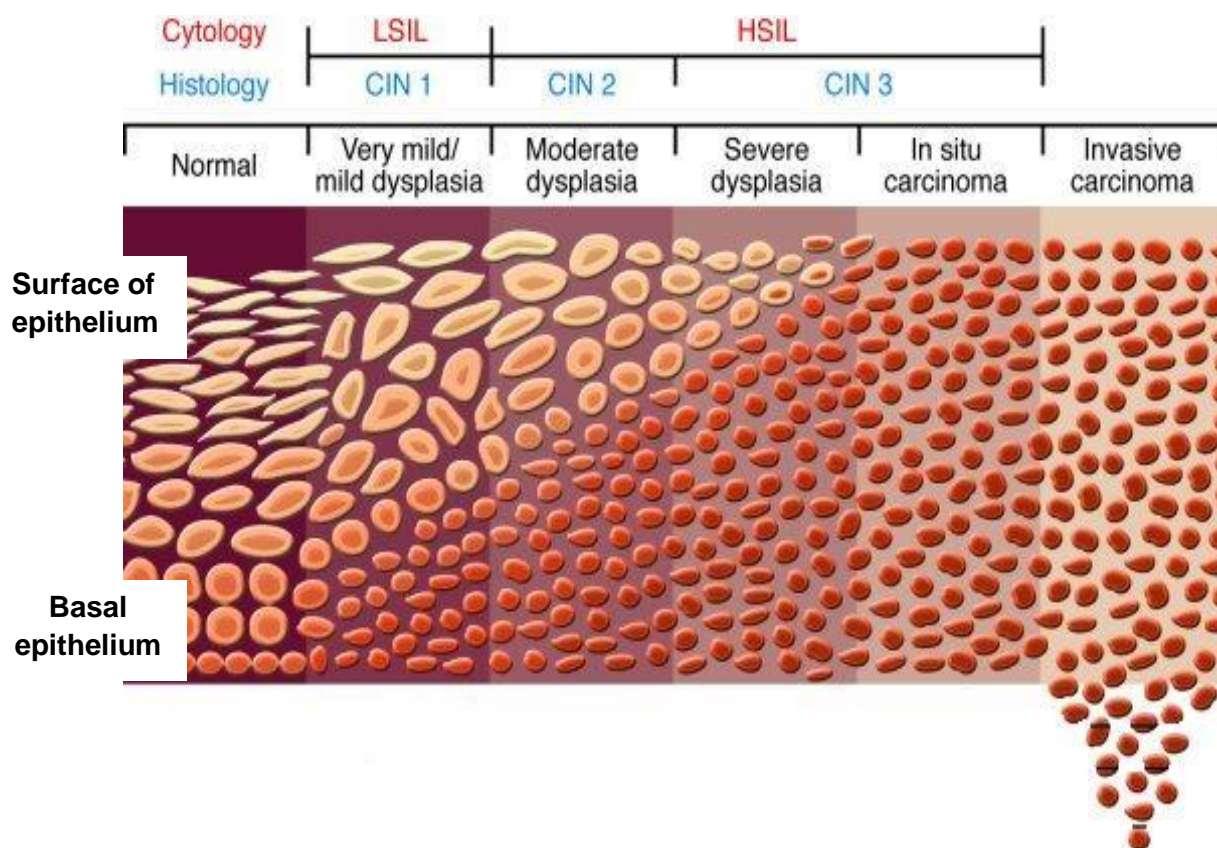


Figure 3: Diagram of CIN progression to invasive cancer

Adapted from (Lowy & Schiller, 2006)

Although CIN 1 is the first stage for development of cervical cancer, not all women who are diagnosed with CIN 1 develop cervical cancer. The follow-up study in USA of Ostor in 1993, found that more than fifty percent of cases of CIN 1 could regress to normal. This study also reported that 32% of stage CIN 1 persisted while the progression of CIN 1 to CIN 3 was 11% and 1% of cases progressed to invasive cancer (Ostor, 1993). The progression from CIN 1 to CIN 3 may take a long time or not depending on the individual. Furthermore even though the grade of CIN is classified on the basis of a cytological classification system, it can be difficult to be certain about the diagnosis of the earliest stage of abnormality, CIN1.

1.2.3 Causation

There are several established risk factors for cervical cancer. Owing to many chemical carcinogens in tobacco, smoking is associated with an increased risk of several kinds of cancer including cervical cancer. Carcinogens cause DNA damage and mutations

which lead to cancer. A short communication suggested that both smokers and even non-smokers who are passive smokers are at risk of cancer (Whidden, 1994). In 2006 The International Collaboration of Epidemiological Studies of Cervical Cancer reported their analysis of 23 studies, and stated that current smokers were inclined to have a greater risk of squamous cell carcinoma of the cervix than women who had never smoked (Relative Risk (RR) = 1.60 (95% CI: 1.48–1.73), $p < 0.001$). Women who smoke a greater number of cigarettes per day (≥ 15) tend to be at higher risk for cervical cancer than never smokers (RR= 1.98 (95% CI: 1.78–2.21), (Appleby *et al.*, 2006). However, early studies of risk factors for cervical cancer did not take HPV infection into account, which would alter relative risks from other factors.

Parity appears also to influence the risk of cervical cancer. A case-control study in four Latin American countries during 1986-1987 found that women with 12 or more live births have a four-fold increased risk over women with one or never live births and the relative risk for those with 14 or more pregnancies was 5.1(95% CI: 2.7–9.7) (Brinton *et al.*, 1989). This study also suggested that the high risk of parity for cervical cancer may be because of the greater risk of a trauma lesion of the cervix during delivery. The increase in risk does not seem to be restricted to only women with very high parity. In 2002, Muñoz *et al* reported results of a cross-cultural study. They gathered parity data from ten case-control studies carried out in populations at different risk of cervical carcinoma in eight countries: high risk-Morocco, Brazil, Peru, Paraguay, and Colombia; intermediate risk-Thailand and Philippines; and low risk-Spain. The Odd Ratios for seven or more pregnancies compared with nulliparous women was 3.8 (95% CI: 2.7-5.5) and was 2.3 (95% CI: 1.6-3.2) when compared with one or two pregnancies (Muñoz *et al.*, 2002).

Oral contraceptive (OC) use is also a risk factor for cervical cancer. Brinton and colleagues conducted a case-control study in Panama, Costa Rica, Columbia and Mexico. They demonstrated that long-term users have a higher risk of cervical cancer especially of adenocarcinomas (Brinton *et al.*, 1990). There was also a report from the Oxford Family Planning Association contraceptive study, which conducted a cohort study of 17000 women incorporated within a nested case-control study, which demonstrated that users of various OCs had a slightly increased risk for all types of cervical neoplasia compared with non-users; the Odd Ratio (OR) was 1.40 (95% CI 1.00-1.96). They also pointed out that Odds Ratios were highest for invasive carcinoma (OR=4.44, 95% CI 1.04-31.6) and lowest for dysplasia (OR=1.07, 95% CI 0.69-1.66). The increasing risk associated with OC use appeared to be specific to the group of long-term users of OCs (Zondervan *et al.*, 1996). Moreover, a report from 24 epidemiological studies (26 countries worldwide) from the

International Collaboration of Epidemiological Studies of Cervical Cancer in 2007, concluded that the greater duration of use of combined oral contraceptives, the greater the risk of cancer (relative risk = 1.90, 95% CI 1.69–2.13) for five or more years use versus never use (Appleby *et al.*, 2007).

The major risk factor for cervical cancer is infection with human papillomavirus (HPV). Many groups have established the importance of HPV which was summarized in the publication of Stanley (Stanley, 2006). There are:

(1) 90-100% of cervical cancer cases have HPV detected. The frequent detection were HPV16 (40-60%) and HPV (10-20%) (Lowy *et al.*, 1994).

(2) HPV DNA can be found in 90% of high grade CIN. HPV-induced lesion was the major cause of cytological abnormalities (Kiviat & Koutsky, 1993).

(3) Prospective studies show that HPV infections bring about CIN and its progression

(4) Primary human keratinocytes can be immortalized by High risk types HPV (HR-HPVs)

HPV is a DNA virus, which usually infects the epithelium of the host cell. There are at least 200 types of HPV and these are usually classified by the potential to induce malignant transformation. High risk types HPV (HR-HPV) include HPV16, 18, 31, 33, 35, 39, 45, 51, 52, 56, 58, 59, 68, 73 and 82. The probable high-risk types are HPV26, 53, and 66. The low-risk types are HPV6, 11, 40, 42, 43, 44, 54, 61, 70, 72, and 81 (Muñoz *et al.*, 2003).

The expression of E6 and E7 oncogenes of HPV has a major role in cervical cancer causation through inactivating cell cycle regulators. E6 inhibits tumor suppressor protein function by binding to p53 and induces the degradation of the protein, whereas E7 promotes cell growth by binding to retinoblastoma (Rb) gene product (Howley, 1991). Normally, Rb forms complexes with the transcription factor, E2F-1, and functions as transcriptional repressor. E7-Rb binding leads to the dissociation of Rb-E2F-1 complex, which makes transcription factor E2F-1 free for action as a transcriptional activator. A high level of E2F-1 causes the up-regulation of S-phase genes (Boulet *et al.*, 2007).

However, despite the evident importance of HPV infection as a cause of cervical cancer, not every woman who acquires an HPV infection develops cervical cancer. Clearly, other factors must be important in not only determining whether a woman acquires an HPV infection but whether an HPV infection persists. Dietary factors may be important. There have been several studies of the role of nutrients in cancer not only in the case of cancer formation, but also in the case of cancer progression and recurrence. In 1996, The American Cancer Society estimated that diet was responsible for one third of cancer deaths in United States (The American Cancer Society Advisory Committee on Diet & Cancer, 1996).

Potischman and Brinton (1996) also suggested the role of diet on cervical carcinogenesis (Potischman & Brinton, 1996).

1.2.4 Diet as a modulator of cervical cancer risk

The evidence linking dietary behaviour with cervical cancer risk is quite limited. Early studies failed to take account of the importance of HPV infection as a causal factor, and therefore, results from these studies may be confounded and need to be considered cautiously.

To evaluate the association of dietary factors with the risk of invasive cervical cancer, a case-control study of nutrients in the diet and plasma biomarkers of status and risk of *in situ* cervical cancer was conducted among Australian women. They found that high intakes of β -carotene, folate and vitamin C are associated with a lower risk of cervical cancer (Brock *et al.*, 1988). In 1991, a case-control study in four Latin American countries was carried out by interviewing 748 cases and 1,411 controls, about diet consumption and other important details such as sexual behavior and medical history. This study found that women who have a high consumption of fruit and fruit juice tend to have a low risk of invasive cervical cancer. They also found that a high intake of vitamin C, β -carotene, and other carotenoids was associated with a decrease risk of the cancer (Herrero *et al.*, 1991). In the US, a case-control study focusing on vitamin C and folate demonstrated an inverse association between dietary and serum folate and vitamin C and cervical intraepithelial neoplasia. Moreover, investigation of vitamin C in CIN women also gave the same result as folate (VanEenwyk *et al.*, 1992).

It has been suggested that the inverse association between intakes or plasma concentrations of some nutrients and cervical cancer risk may be explained by their antioxidant function in diminishing the damage caused by reactive oxygen species (ROS). ROS are products of normal cell metabolism and are generated daily in both normal and abnormal cells. The oxidation of DNA bases can lead to altered cellular function and increased risk of mutations. Nutrients which act as anti-oxidants include vitamin A, vitamin C and vitamin E but studies of their protective role in carcinogenesis have not generated consistent results (Goodman *et al.*, 2004). Furthermore, effects of confounding factors have not always been taken into account. For example, in the case of vitamin C, although vitamin C status has been reported to be associated with risk of all grades of cervical neoplasia, vitamin C status is also known to be lower in smokers than nonsmokers. Given that smoking is also a risk factor for cervical cancer, the relationship between low vitamin C status and cervical cancer may be confounded by smoking status. Moreover, the epidemiological studies of vitamin C may be limited by its instability in blood (Potischman, 1993).

In their review, Potischman and Brinton summarized studies of the role of nutrition in cervical cancer risk at that time, concluded that a low intake of vitamin C, carotenoids, vitamin E and folate may be associated with an increased risk of cervical neoplasia. A low concentration of vitamin C and carotenoids may be associated with both pre-invasive and invasive cervical cancer, whereas folate may have an effect only on preneoplastic cervical lesions. However, in this review, the author pointed out that most studies did not take other factor risks into account and especially lacked information about HPV infection. Overall, it can be cautiously proposed that nutritional factors play an important etiologic role in cervical carcinogenesis (Potischman & Brinton, 1996).

More recently García-Closas *et al.* (2005) tried to summarise findings regarding the role of diet in cervical cancer risk by conducting a systematic review and classification of all studies published between 1995 and 2003 with a consideration of HPV infection. The authors concluded that a sufficiency of nutrients such as vitamins C, E, beta-and alpha-carotene, and lycopene, may have a possible protective effect on HPV persistence. Nutrients including folate, retinol, vitamins C and B12 and vitamin E may have a possible protective effect on cervical neoplasia (García-Closas *et al.*, 2005).

There has been particular interest in the possible role of folate as a determinant of cervical cancer risk (Piyathilake, 2007). Some studies have focused on folate and HPV infection/persistence (Sedjo *et al.*, 2002; Piyathilake *et al.*, 2004) and some studies have considered the role of folate in DNA methylation and gene expression (Narayan *et al.*, 2003; Flatley *et al.*, 2009; Liu *et al.*, 2011). The relevance of folate to cervical cancer will be discussed below.

1.3 Folate

1.3.1 Folate metabolism

Folate is a water soluble B vitamin. Although humans cannot synthesise folate, we are able to find folate in many foods such as nuts, beans, green leafy vegetables, fruits and liver (mainly in the form of polyglutamates). Low dietary folate intake has been associated with conditions such as neural tube defects (Czeizel & Dudas, 1992; Pitkin, 2007), Down's syndrome (James *et al.*, 1999; Patterson, 2008), and cancer (Eichholzer *et al.*, 2001; Kim, 2007). Folate fortification of flour has been introduced into several countries including USA, Canada, and Australia, with the specific purpose of reducing the incidence of neural tube defects. Current dietary reference values (DRVs) for the UK state that the amount of folate required to meet the requirements of 97.5% of the UK population is 200µg/day for adults and that women should take 400µg/day. The Recommended Dietary Allowance (RDAs) for the USA and the Joint Food and Agriculture Organization of the United Nation/World Health Organization (FAO/WHO) is set at 400µg/day for adults and 600µg/day for pregnant women (Geissler & Powers, 2011).

Folate is a term used to describe a group of naturally-occurring compounds, whereas folic acid is the synthetic form. If we look into the structure of folate, we will find that folate is composed of a pteridine ring, para-aminobenzoic acid, and glutamic acid residues (**figure 4**). Within the complex of its structure, folate can be related to more than 150 compounds by modifying the pteridine ring and forming a polyglutamate tail (Shane, 2010). Food folates can be absorbed in the proximal jejunum and the efficiency of absorption seems to be dependent on the hydrolysis of the polyglutamate chain. Once taken up into the enterocyte folate can be converted to dihydrofolate (DHF) and tetrahydrofolate (THF) by dihydrofolate reductase (DHFR). There are many forms of pteroylmonoglutamates including 5-formylTHF, 5,10-methenylTHF, 5,10-methyleneTHF, 5-methylTHF, 10-formylTHF, and tetrahydrofolate (THF) (**figure 5**).

Pteroylmonoglutamates, mostly in the form of 5-methylTHF, are transported to the liver from which they are distributed to other tissues (Halsted, 1980). 5-methylTHF is taken up into tissues via folate receptors or reduced folate carriers. After being taken up into cells, pteroylmonoglutamates are converted by folypolyglutamate synthetases (FPGS) to form folypolyglutamate derivatives. The major function of folate is as a one-carbon carrier, which plays an important role in several biochemical reactions (**figure 6**).

There are two main features of this one-carbon cycle, which underpin the biochemical basis for a role of methyl donors in cancer prevention. These are DNA synthesis/repair and DNA methylation.

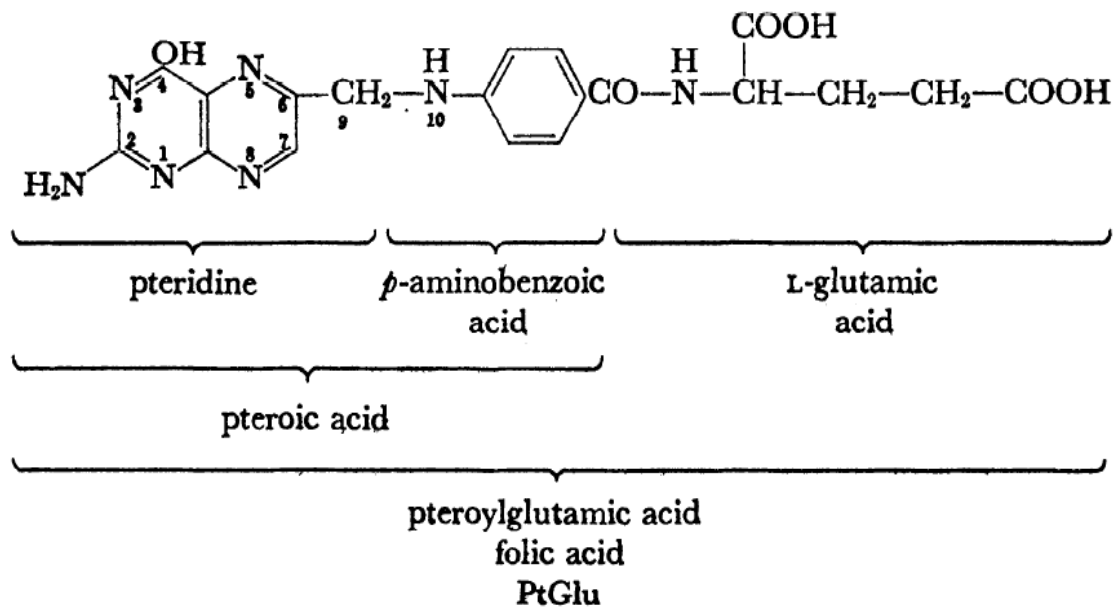
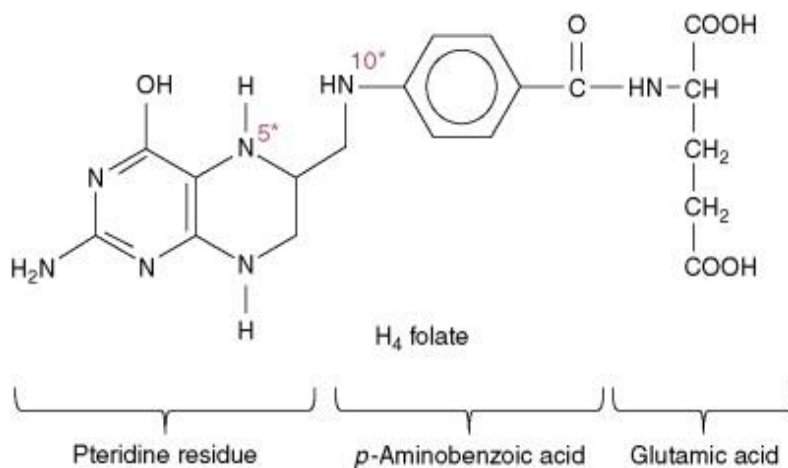


Figure 4: Structure of folate
 (Stokstad & Koch, 1967)



Coenzyme	Substituent at:	
	N-5	N-10
5-FormylTHF	-HCO	-H
5,10-MethenylTHF	=CH ⁺ -	
5,10-MethyleneTHF	-CH ₂ -	
5-MethylTHF	-CH ₃	
10-FormylTHF	-H	-HCO
THF	-H	-H
Folic acid	-H	Nil

Figure 5: Structure of important folate coenzymes
 (Liu *et al.*, 2010)

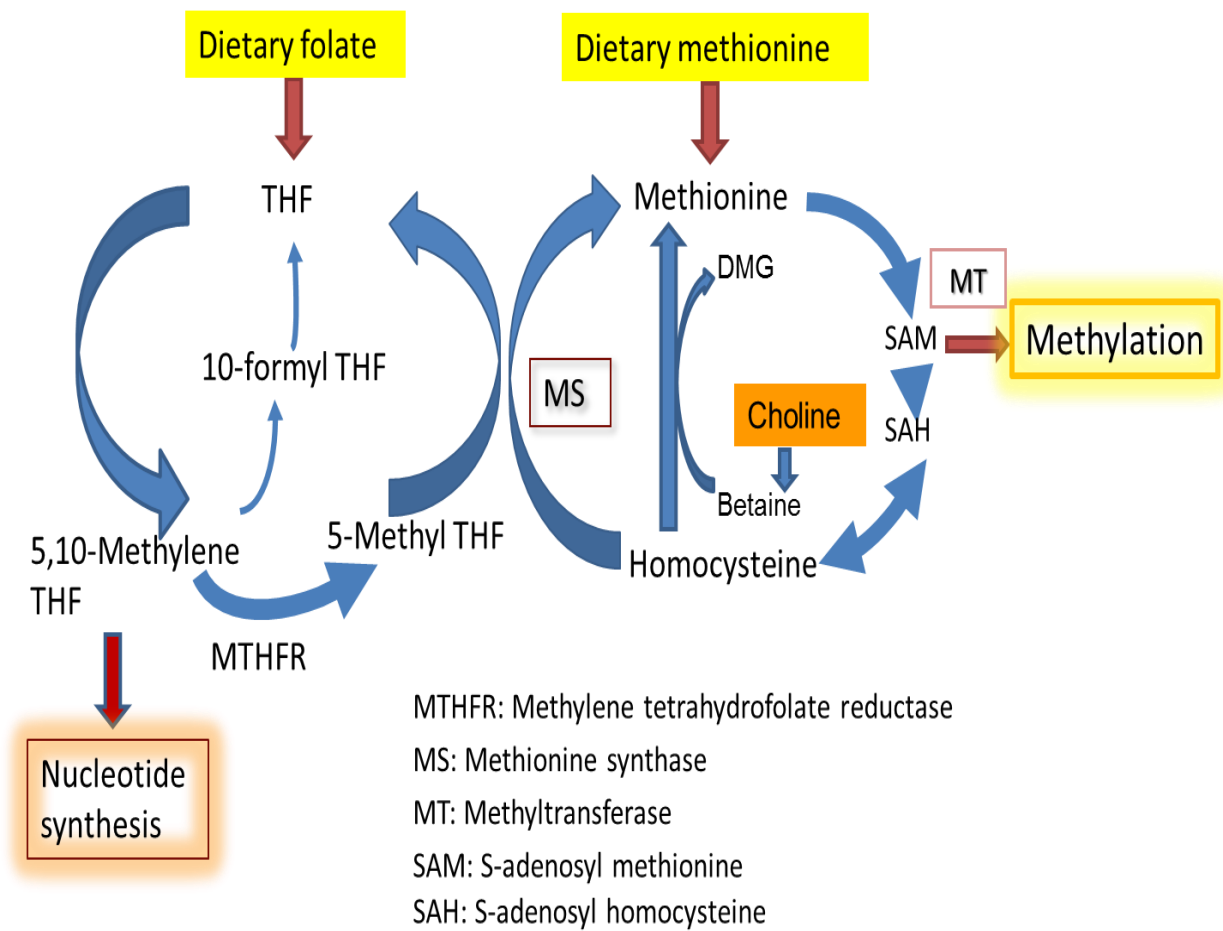


Figure 6: Methyl cycle showing two important mechanisms involved in one-carbon metabolism.

1.3.2 Importance of folate in DNA Synthesis and Repair

Folate is essential for DNA synthesis and repair. In this case, tetrahydrofolate acts as methyl carrier for both purine and pyrimidine synthesis. In *de novo* process of purine synthesis, there are two steps in which folate is involved: the addition of carbon in the positions 2 and 8 of the purine ring. The first step is the process to add 8-carbon atom to glycinamide ribonucleotide by N^{10} -formyl-THF to form formylglycinamide ribonucleotide (**figure 7**) and then, the ring of purine forms. The second step is the addition of 2-carbon atom to aminoimidazolecarboxamide ribonucleotide by N^{10} -formyl-THF to form formylaminoimidazolecarboxamide ribonucleotide (**figure 8**), and after that, inosine monophosphate (IMP) is formed. IMP is the precursor of adenosine monophosphate (AMP) and guanosine monophosphate (GMP); therefore, purine nucleotides are produced.

In pyrimidine synthesis (**figure 9**), N^5, N^{10} -methylene-THF is one-carbon donor, which helps transfer a methyl group from deoxyuridine monophosphate (dUMP) to deoxythymidine monophosphate (dTMP) in a reaction catalysed by thymidylate synthase. After N^5, N^{10} -methylene-THF has donated a methyl group, it will be converted into DHF in order to start a cycle of one-carbon donor again.

If folate is limiting, there will be an accumulation of dUMP. Moreover, there will be limited formation of both purine nucleotides and dTMP, so an imbalance of nucleotides will result. Consequently, the cell attempts to remove misincorporated uracil nucleotide by developing DNA strand breaks, but this can cause genetic instability and increase cancer risk. Folate-deficient chinese hamster ovary (CHO) cells were shown to have a 10-fold greater frequency of chromosomal aberrations in mitotic cells (Libbus *et al.*, 1990). In a study of lymphocytes in culture, DNA strand breaks and uracil misincorporation increased as a result of folate depletion (Duthie & Hawdon, 1998). Duthie *et al.* (2002) reviewed the impact of folate deficiency on DNA stability. She cultured CHO cells in folate-deficient media and found that cellular uracil increased; the misincorporation of uracil also increased threefold. Moreover, when folate-deficient human colonocytes were exposed to an alkylating agent (which integrates into DNA and disrupts the cross-linking of DNA strands), these cells were unable to repair DNA strand breakage (Duthie *et al.*, 2002). In his review, Ames (2001) reported that folate deficiency led to an increased uracil misincorporation into DNA (4 million/cell) and subsequent chromosome break in 10% of US population. He associated this observation with an increase in colon cancer risk (Ames, 2001).

1.3.3 Importance of folate to DNA methylation

1.3.3.1 DNA methylation

In general, methyl transfer can take place onto several types of biomolecules such as proteins, lipids, hormones, RNA, and DNA. Methylation is important for several cell activities, for example, noradrenaline accepts a methyl group to form adrenaline, lipids accept a methyl group to turn into phospholipids, guanidoacetic acid accepts a methyl group to produce creatine, and DNA can be found in the form of methylated DNA. DNA methylation is considered to be part of an ancient component of a protection mechanism which recognized parasitic viral DNA sequence integration into the genome. This methyl mark serves to be a suppressed or deleted location in order to establish normal genome function. DNA methylation now has been reported to have additional functions such as X-chromosome inactivation, imprinting, and transcriptional regulation.

Cytosine is a target for methylation (**figure 10**) when it forms part of a dinucleotide with guanine (CpG). CpG dinucleotides are distributed unevenly throughout DNA (0.75-1% of human genome). However, there are regions, often in the promoter regions of genes, which are rich in CpG, called CpG islands. Normally, 70-90% of CpG dinucleotides are methylated (Ehrlich *et al.*, 1982), but CpG islands are unmethylated. Recently, it was reported that CpG island “shores” are another important region for DNA methylation. CpG island shores are CpG-containing regions which are up to 2kb away from CpG islands and located at tissue-specific differential methylated sites in normal tissue (Irizarry *et al.*, 2009).

1.3.3.2 Folate and DNA methylation

(Please refer to figure 5). Folate is relevant to methylation via its role in the SAM-SAH cycle. DNA methylation is the addition of a methyl group onto the cytosine ring in DNA. Methionine, in the form of S-adenosyl methionine (S-AdoMet or SAM), is a methyl donor. By using methyltransferases, a methyl group transfers from SAM to a methyl acceptor, after which SAM itself is converted into S-adenosyl-homocysteine (SAH). SAH will cleave into homocysteine and adenosine. If homocysteine accepts a methyl group, for example, from methyl-tetrahydrofolate (methyl-THF), it will be remethylated to methionine and complete a cycle (**figure 5**). Considering the role of folate as a methyl donor, the SAM-SAH cycle is expected to be impaired in the absence of folate.

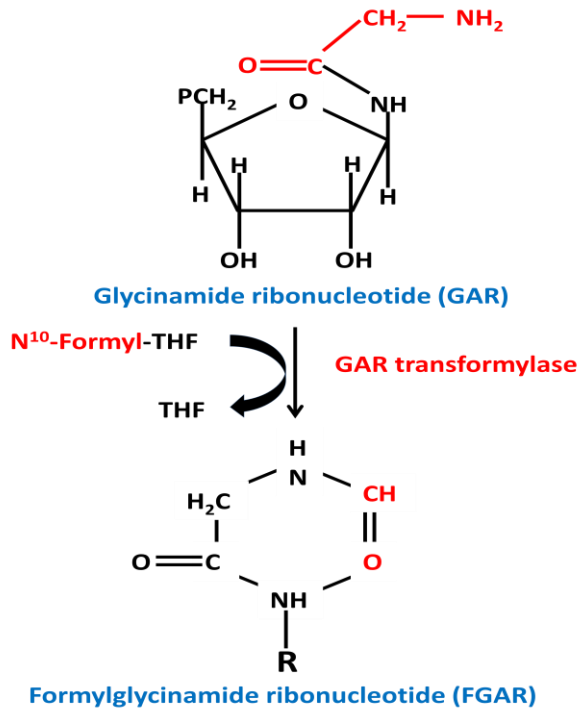


Figure 7: Purine synthesis: adding 8-carbon atom to purine ring

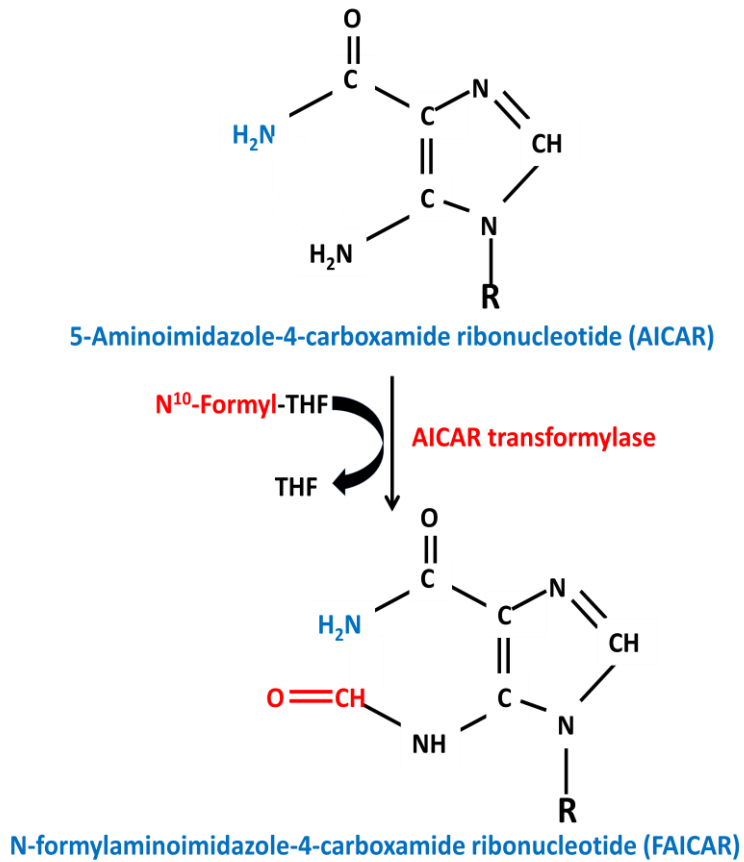


Figure 8: Purine synthesis: adding 2-carbon atom to purine ring

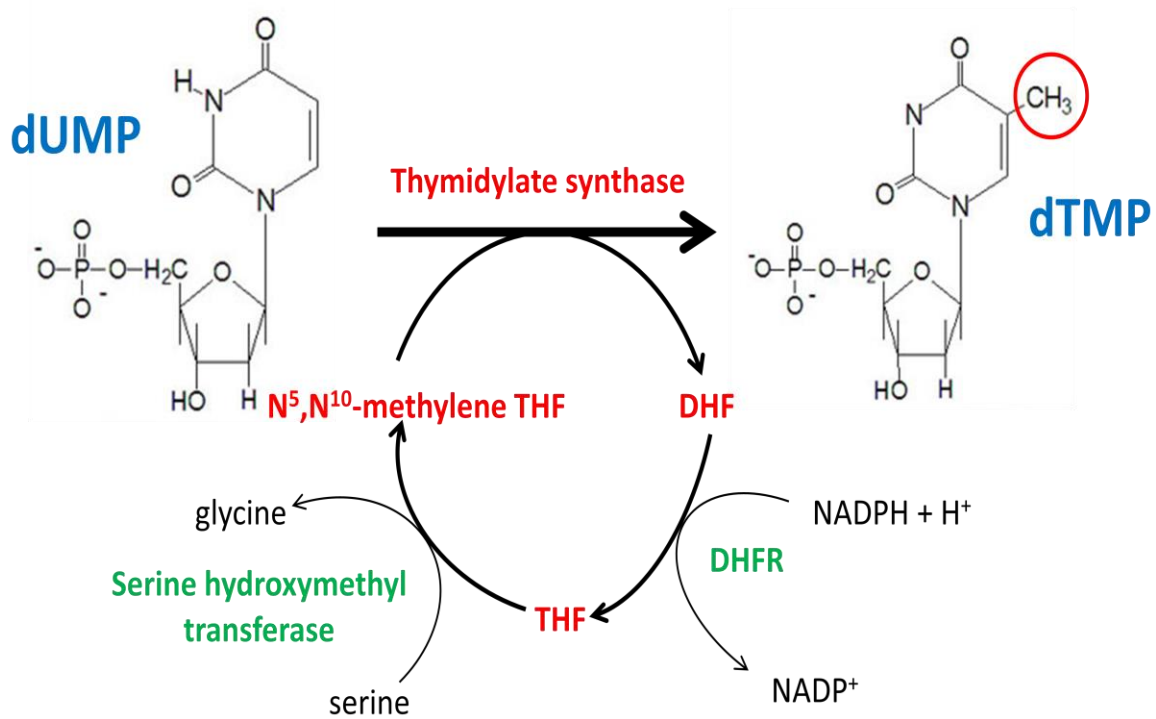


Figure 9: Folate is involved in pyrimidine synthesis

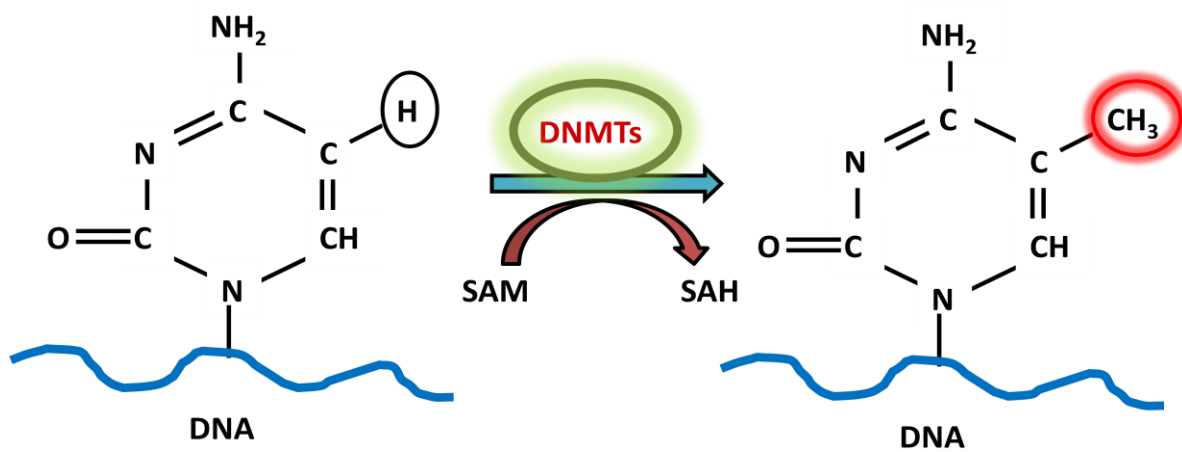


Figure 10: The position of methylation at a cytosine base

Studies of folate and methylation have been conducted in various systems. In their *in vitro* study, Stempak *et al.* (2005) reported that global DNA methylation was decreased in folate-deficient untransformed cells (NIH/3T3 and CHO-K1 cell lines), but not significantly changed in folate-deficient transformed cells (HCT116 and Caco-2 colon cancer cell lines). In their study of Min mice to investigate the effect of DNMT1 deficiency on DNA methylation in folate-depletion, Trasler *et al.* found no change in global DNA methylation (Trasler *et al.*, 2003). Sohn *et al.* (2003) conducted a study to determine the effect of folate deficiency in rats and found that although plasma homocysteine was increased, and colonic SAM concentration was decreased, there was no change in colonic DNA methylation (Sohn *et al.*, 2003). Kotsopoulos *et al.* (2008) also conducted a study in folate-deficient rats. Rats were fed a folate-deficient diet (0 mg folic acid/kg rat) from weanling to young adulthood for 8 weeks and then supplemented with 2mg/kg (control diet) at puberty for 22 weeks. There was a significant increase in global DNA methylation in the liver of 34-48% at adulthood. On the other hand, rats fed with a folate-deficient diet throughout their life until adulthood, and rats fed with the control diet until puberty and then changed to folate-deficient diet until 30 weeks of age, showed no change in their hepatic genomic DNA methylation. This suggested that the timing in exposure of folate deficiency influences epigenomic programming (Kotsopoulos *et al.*, 2008).

Some studies have been conducted in humans either depleted of folate or given folic acid supplements. For example, in order to link plasma folate status with the DNA methylation profile in gastric cancer samples, Fang *et al.* (Fang *et al.*, 1997) found a decrease in global DNA methylation in association with low plasma folate status and related this to gastric carcinogenesis. In 1998, Cravo *et al.* set up a controlled, cross-over study to evaluate the effect of folate supplementation on global DNA methylation in 20 patients with colonic adenomas. They found that supplementation with folic acid (5 mg/day) increased global DNA methylation in 7 of 20 patients who had one polyp (Cravo *et al.*, 1998). This however was a very small study and the folic acid dose was high, and so the generalisability of their findings is not certain. Jacob *et al.* (1998) conducted a study to determine the effect of folate status on DNA methylation in healthy postmenopausal women. Women aged between 49-63 years were fed for 5 weeks with a low folate diet (56 µg/day) followed by repletion with 111 µg/day of folic acid for 4 weeks and then 286-516 µg/day for 3 weeks. They found a decrease in plasma folate concentration, a lowering of lymphocyte DNA methylation, and an increase of plasma homocysteine in the first two time periods. After repletion with 286-516 µg/day of folic acid the lymphocyte DNA methylation level was normalised and plasma homocysteine decreased with 516 µg/day, but not with 286 µg/day of folic acid (Jacob *et al.*, 1998). Moreover, in 2000, Rampersaud and colleagues studied

the effect of folate depletion on DNA methylation of leukocytes in elderly women (60-85 years) by investigation of the incorporation level of ³H-methyl group into DNA. They demonstrated that elderly women who consumed a folate-depleted diet (118 µg folate/day) for 7 weeks had a low level of DNA methylation compared with those consuming a folate adequate diet (P=0.0025) (Rampersaud *et al.*, 2000). However, in this study, the 7-week repletion with 200 or 415µg folate/day after depletion did not change the DNA methylation level. Research so far suggests that folate status has variable effects on DNA methylation dependent on pathological stage, cell type, and age.

1.3.3.3 DNA methylation and gene expression

DNA methylation occurs in order to regulate gene expression to “switch on” or “switch off” genes, which is important for cell function. For example, (1) methylation of cytosine inhibits access of transcription factors to DNA via methylation-binding proteins, therefore inhibiting transcription (**figure 11**), and also, (2) methylation can change the DNA structure in the context of chromatin remodeling, which is important for regulating transcription (**figure 12**). By influencing the epigenetic modification of histones in chromatin, it is known that histone modification can determine whether chromatin is in the “opened” or “closed” configuration, which determines whether transcription is allowed or not.

Aberrant DNA methylation, both hypo- and hypermethylation, is considered a cause of abnormal expression of genes. This may be undermethylation of the entire genome (hypomethylation) or hypermethylation in CpG-rich regions (islands), often locating upstream of promoter regions. Approximately sixty percent of human genes have CpG-rich regions (Antequera & Bird, 1993), not only housekeeping genes but also genes with tissue-specific pattern of expression.

Specifically in relation to hypomethylation, there is interest in decreased global DNA methylation, which results in decreased ability to maintain a normal level of DNA replication and DNA repair. Uncontrolled replication and repair of DNA brings about mutations. Gene mutation can affect a protein’s efficiency. Sometimes, mutation may influence the transformation of a proto-oncogene to an oncogene, such evidence is critical in terms of tumorigenesis and oncogenesis (**please refer to figure 12**). DNA hypomethylation is mostly found in highly repeated DNA sequences (Hoffmann & Schulz, 2005; Weisenberger *et al.*, 2005), which include tandem centromeric satellites, juxtacentromeric (centromere-adjacent) satellite 2, interspersed Alu and long interspersed element (LINE)-1 (Ehrlich, 2009). Hypomethylation of satellite DNA (Sat2) of chromosome 1 was found in about 45% of 25 breast adenocarcinomas (Narayan *et al.*, 1998). LINE-1 DNA hypomethylation was also found in cancers such as cervical cancer (Shuangshoti *et al.*, 2007) and colorectal cancer

(Estéicio *et al.*, 2007). Gene specific hypomethylation can also be found in cancer. For example, urokinase (uPA) which is a serine protease, was found to be hypomethylated and overexpressed in breast cancers (Pakneshan *et al.*, 2004).

On the other hand, in the case of hypermethylation, we are interested in an increase of DNA methylation, which has been shown to lead to gene silencing. With regard to transcription, hypermethylation will obstruct transcription factor binding, so that transcription cannot occur and in turn a gene is silenced (**please refer to figure 11**). When tumour suppressor genes are silenced this invariably leads to unlimited division of cells. In cancer, hypermethylation usually occurs on specific genes which play an important role in cancer pathways. For example, hypermethylation at the 5'-end of the Rb gene, which is important to regulation of the cell cycle, was found in blood and tumour cells of 21 retinoblastoma patients (Greger *et al.*, 1989). Regarding genes involved in DNA mismatch repair, hypermethylation at the 5' CpG island of *hMLH1* was found in colorectal mucosa and primary sporadic colorectal tumour specimens (Herman *et al.*, 1998). Promoter methylation of the DNA repair gene, *O*⁶-methylguanine DNA methyltransferase (MGMT), was found in about 40% of colorectal carcinoma patients (Esteller *et al.*, 1999). In the Wnt signalling pathway, colorectal cancer is often associated with promoter DNA hypermethylation in one or more genes, including *APC*, *β-catenin*, *AXIN2*, *TCF4* and *WISP3* (Thorstensen *et al.*, 2005).

The process of DNA methylation is dependent on the activity of a group of enzymes called DNA methyltransferases, which are responsible for transferring a methyl group onto DNA.

1.4 DNA methyltransferase (DNMT)

1.4.1 DNA methyltransferase (DNMT)

The DNA methylation process is catalysed by DNA methyltransferases (DNMTs). DNMTs catalyse the donation of methyl groups from S-adenosylmethionine (SAM) to the C5 of cytosine nucleotide. Together with the availability of methyl donors, factors influencing their expression and activity might be expected to influence DNA methylation.

There are 3 distinct enzymatically active forms of DNMTs: DNMT1, DNMT3a, and DNMT3b. Also there is one related protein called DNMT3L which is lacking catalytic activity. DNMT1 is classified as a DNA maintenance enzyme, preferring hemi-methylated CpG sites as substrate over unmethylated DNA. This enzyme is located at the replication fork to maintain parental methylation during the synthesis of daughter strand DNA in S phase.

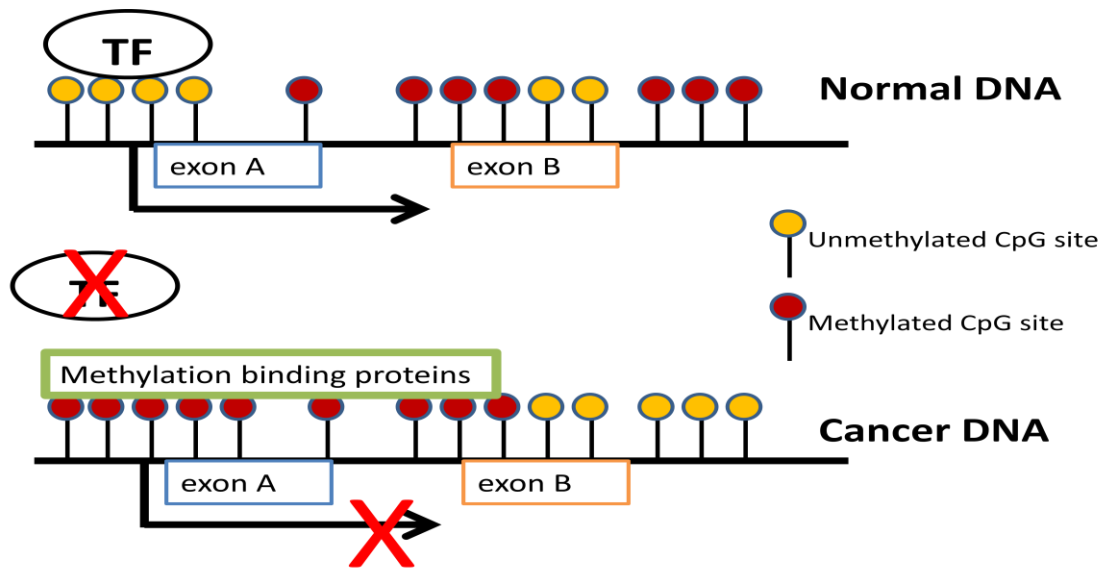


Figure 11: *Hypermethylation on CpG rich-region at a promoter site*

This inhibits the binding of transcription factor (TF), switches off some genes to further transcription such as tumor suppressor genes.

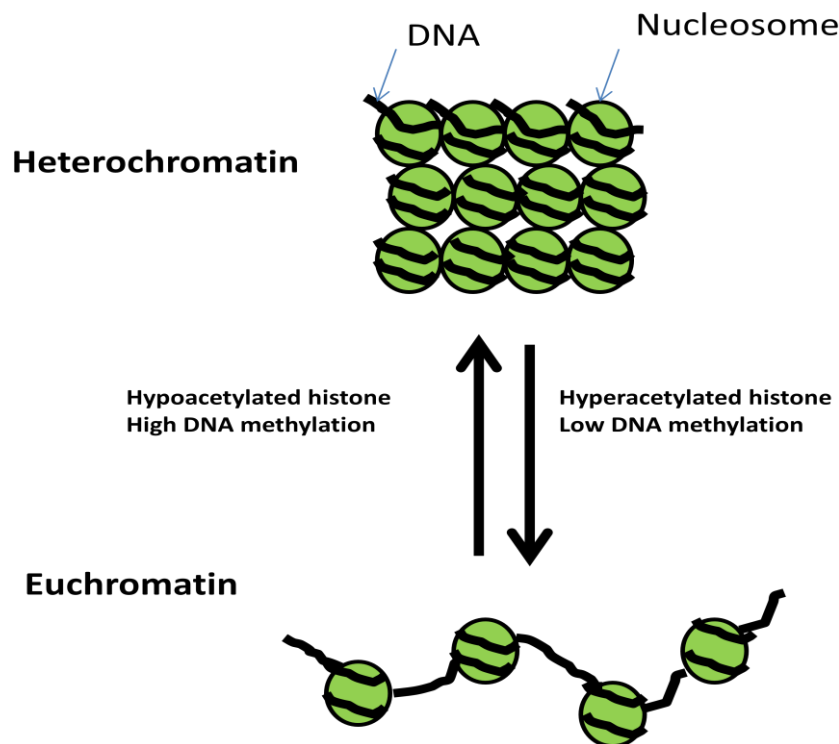


Figure 12: *Global hypomethylation on CpG-rich regions*

This can change the morphology of chromatin, which turns from a condensed structure to an open structure and allowed some genes such as oncogenes to switch on.

Knocked down DNMT1 of human colorectal carcinoma cells led to loss of cell proliferation and progressive cell death (Chen *et al.*, 2007). The mRNA expression level of DNMT1 is dynamically changed during the cell cycle, being the highest in S phase of proliferating cells (Lee *et al.*, 1996). Besides playing a maintenance role, other functions are unclear. However, Clements *et al.* examined the function of DNMT1 in the form of inactive catalytic methyltransferase and found that there were target genes for which DNMT1 functions as a transcriptional repressor (Clements *et al.*, 2012). This repressive function may relate to a role for scaffolding target genes which induce a deficiency of the active histone mark.

On the other hand, DNMT3a and 3b, which are reserved as *de novo* DNA methyltransferases, mostly catalyse the addition of methyl-groups to unmethylated CpG sites on both strands of the DNA (Fatemi *et al.*, 2002). However, there is evidence showing that DNMT1 also has a *de novo* function and works together with DNMT3a (Fatemi *et al.*, 2002). DNMT3a and 3b are stably located at chromatin containing methylated DNA (Jeong *et al.*, 2009). Yanagisawa *et al.* (Yanagisawa *et al.*, 2002) proposed that, like DNMT1, DNMT3a and 3b have multiple transcriptional start points (TSPs) which are controlled by multiple promoters. These promoters are in the form of CpG-rich and CpG-poor regions, which may comprise distinct transcription regulation.

Regarding gene expression, Robertson *et al.* (2000), from his work in MCF7 breast cancer cells, suggested that DNMT1 and DNMT3b are down-regulated during G₀/G₁ of the cell cycle while DNMT3a sustains its expression level throughout the whole cell cycle. The change in DNMT expression during different phases of the cancer cell cycle suggested that there are determinants of DNMT expression which in turn influence DNA methylation, leading to development of cancer (Ahluwalia *et al.*, 2001).

1.4.2 Regulation of DNA methyltransferases

The regulation of DNMT activity is not well understood but various post-transcriptional and post-translational modifications as well as the interaction with non-coding RNA (ncRNA) and non-coding microRNA (miRNA), are thought to modify stability including methylation (Denis *et al.*, 2011).

Regarding DNMT1, three miRNAs, which are miR-148, miR-152 and miR-126, showed their ability to down-regulate DNMT1. Moreover, it has been reported in human colorectal HT-29 cells that mutation of APC (adenomatous poliposis coli) led to an upregulation of DNMT1 promoter activity and mRNA (Campbell & Szyf, 2003). The activity of DNMT1 was regulated via post-translational mechanisms through phosphorylation, methylation, acetylation and sumoylation-small ubiquitin-like modifiers (Denis *et al.*, 2011). It has been shown that sumoylation of DNMT1 led to an increase of its activity in HCT116

cancer cell lines (Lee & Muller, 2009). In addition, a histone methyltransferase, SET7, has been suggested to regulate protein stability of DNMT1. SET7 methylated Lys-142 of DNMT1 resulted in the promotion of proteosomal degradation and also enhanced the absence of lysine-specific demethylase 1 (LSD1). Thus the overexpression of SET7 resulted in a reduction of DNMT1 expression (Estève *et al.*, 2009).

Post-transcriptional modification of DNMT3a and 3b via an interaction with miR-29s, led to a down-regulation of their mRNA level (Fabbri *et al.*, 2007). Additionally, it has been reported that DNMT3b was also down-regulated by miR-148 (Duursma *et al.*, 2008). On the other hand, Hu-antigen R (HuR) seemed to enhance the stability of DNMT3b mRNA (López de Silanes *et al.*, 2009). DNMT3a is also regulated by post-translational mechanisms through sumoylation of a Pro-Trp-Trp-Pro motif which is located in the N-terminal region. This sumoylation modifies DNMT3a ability to interact with other components such as HDACs and results in the disruption of its ability to repress the transcription of reporter genes (Ling *et al.*, 2004).

DNMTs interact with several components at the regulatory domain such as other DNMTs, histone deacetylase 1 and 2, the Rb and E2F1 transcription factors, and proliferating cell nuclear antigen (PCNA). All of those components can act as activators/suppressors of methylation. Abnormal interactions resulting from any alteration of those components influence DNMTs functions (Robertson, 2001).

1.4.3 Dietary determinants of DNA methyltransferase expression /activity

Several nutrients have been found to affect DNMTs expression/activity such as choline, selenium, and folate. Regarding choline, rats fed a choline-deficient diet showed an up-regulation of DNMT1 gene expression in fetal liver, and choline supplemented diets led to a decrease in DNMT3a gene expression (Vacheva *et al.*, 2007). This group also found a significant correlation between DNMT1 mRNA level and 5-methylcytosine content in fetal liver DNA ($r=0.66$, $P<0.02$). Fiala *et al.* (1998) determined the effect of selenium compounds benzyl selenocyanate (BSC), 1,4-phenylenebis(methylene)selenocyanate (*p*-XSC), and sodium selenite) on DNMTs activity and found that the DNMTs activity of cell lysate from both human colonic carcinoma cells and human colon carcinoma cell lines (HCT116) was inhibited by selenium compounds. The concentrations of selenite, BSC, and *p*-XSC which could decrease DNMTs activity by 50% were 3.8, 8.1, and 5.2 mM, respectively (Fiala *et al.*, 1998). However, this study was an *in vitro* model and the relevance to the *in vivo* situation is not clear. In contrast, a study in Fischer-344 rats fed a selenium-deficient diet up to 70 days from weaning found no change in hepatic DNMTs activity although the activity tended to decrease in colon ($P<0.06$)(Ross & Davis, 2006). A study in the liver of F344 rats fed a folate

deficient diet (Ghoshal *et al.*, 2006) demonstrated that folate and methyl donor deficiency led to a decrease in mRNA and protein of DNMT1, an increase in DNMT3a mRNA, and an increase in MBD1-3 mRNA. They also found an elevation of protein of MBD 1, 2, and 4 in folate and methyl deficient rats. In their mouse model of folate deficiency, Ding *et al.* (2012) demonstrated an elevation in DNMT1, 3a, and 3b expression in endometrial cells during pregnancy (Ding *et al.*, 2012).

1.4.4 DNA methyltransferase expression/activity as determinants of DNA methylation profile

Since aberrant DNMTs expression/function may lead to an abnormal methylation level, some studies have suggested that aberrant DNMT expression influences DNA methylation profile, but results are not consistent (Fatemi *et al.*, 2002; Sawada *et al.*, 2007). There is still no clarity about the relationship between DNMT expression and DNA methylation profile.

Some research has reported a link between DNMT expression and DNA methylation profile. For example, disruption of DNMT1 expression led to hypomethylation of mouse embryonic stem (ES) cells (Li *et al.*, 1992). A study in colorectal and stomach cancer samples found an association between overexpression of DNMT1 and DNMT3b and cancer. Overexpression of DNMT1 mRNA was associated with a CpG island methylator phenotype (CIMP), but overexpression of DNMT3b was not related to CIMP or DNA hypomethylation of pericentromeric satellite regions (Kanai *et al.*, 2001). This is important because the cancer phenotype is associated with a concentration of methylation at CpG islands and pericentromeric satellite regions seem to be the mutation target site (Hansen *et al.*, 1999; Saito *et al.*, 2002). In their investigation of 67 hepatocellular carcinomas (HCCs), Saito *et al.* (2001) found that the mRNA level of DNMT1 and DNMT3a of noncancerous liver tissues was higher than HCCs. DNA hypomethylation of pericentromeric satellite regions was detected in both noncancerous liver tissues and HCCs. The CpG island hypermethylation of p16, methylated in tumour1, 2, 12, 25, and 31 genes was greater in HCCs than noncancerous liver tissues. DNA hypomethylation of pericentromeric satellite regions led to a centromeric decondensation and increased chromosome recombination resulted in chromosome instability (Saito *et al.*, 2001).

In addition, the examination of DNA methylation and DNMT expression in a mouse prostate cancer model suggested that even though the overexpression of all DNMTs was seen in all stages of transgenic adenocarcinoma of mouse prostate (TRAMP), hypermethylation of specific genes was only seen in early and late stage of tumorigenesis and only related to the overexpression of DNMT1. Also, the overexpression of DNMTs

protein was not associated with genomic hypomethylation or specific gene hypermethylation (Morey Kinney *et al.*, 2008). A study in human prostate cancer, which reported both an increase and decrease of DNA methylation level at CpG sites compared to normal prostate, demonstrated that those alterations were associated with the overexpression of DNMT3a and 3b (Kobayashi *et al.*, 2011).

In their review Wild and Flanagan (Wild & Flanagan, 2010) suggested that the DNA methylation profile was associated with both an alteration in DNMT expression and a change in their activity and function. However, Choi *et al.* (Choi *et al.*, 2003) demonstrated that DNMT1 activity was not correlated with its expression.

1.4.5 DNA methyltransferases and cancer

There are numerous observational studies reporting overexpression of DNMTs in tumour tissues. An immunohistochemical examination of DNMT1 in cervical cancer samples demonstrated that DNMT1 was increased in low-grade CIN and was even higher in high-grade CIN, but the level was decreased in invasive stage. This suggested that the increased DNMT1 was associated with the early stage of cervical carcinogenesis (Sawada *et al.*, 2007). In their hepatocellular carcinoma study, Oh *et al.* found that all DNMTs were up-regulated (RT-PCR) and the expression level was progressively increased from normal livers through chronic hepatitis, cirrhosis to HCCs (Oh *et al.*, 2007). The overexpression of DNMT1 was also found in gastric cancer samples using immunohistochemistry and correlated with hypermethylation at CpG islands of the human MutL homologue 1 (hMLH1), E-cadherin, and thrombospondin-1 (THBS-1) (Etoh *et al.*, 2004). There is also some evidence that overexpression of DNMTs may influence liver cancer progression (Choi *et al.*, 2003).

Robertson *et al.* (Robertson *et al.*, 1999) demonstrated that the expression of all DNMTs in normal tissue was coordinated. Unlike normal tissues, most tumour cells presented with a significantly increased DNMT3b expression, but only very modest increases in DNMT1 and DNMT3a. This suggested that the alteration of DNMT3b expression had a specific influence on tumor development. Ahluwalia *et al.* found an increased level of DNMT1 and DNMT3b transcripts in ovarian cancer cell lines and they suggested that DNMT activity was increased in association with the progression of cancer (Ahluwalia *et al.*, 2001). Beaulieu *et al.* indicated that DNMT3b has a site selectivity, which plays an important role in regulation of gene expression, associated to cancer survival, and the down regulation of DNMT3b led to cancer cell apoptosis (Beaulieu *et al.*, 2002).

1.4.6 DNA methylation, gene expression and cervical cancer

Although cervical cancer has not been a major focus of interest in terms of associations between epigenetic determinants of gene expression, there is a modest

literature which can be discussed. In 1994, Kim *et al.* studied the relationship between various grades of cervical neoplasia and DNA hypomethylation status in 41 patients with abnormal cervical epithelial cells. They found that DNA hypomethylation level increased with the grade of cervical neoplasia. DNA hypomethylation increased from normal cervical tissue to cervical neoplasia and cancer by threefold and sevenfold, respectively. In other words, the more severe the progress of the disease, the greater the level of DNA hypomethylation (Kim *et al.*, 1994b). Also, in 1998, Fowler *et al.* further described the above relationship by conducting a study in 83 patients with various grades of cervical neoplasia. They found that the largest increase in hypomethylation appeared in the early stage of cervical neoplasia and then was stable through CIN3, and then increased again when the disease progressed to cancer (Fowler *et al.*, 1998). A more recent study (Flatley *et al.*, 2009) also showed significantly more hypomethylation in cervical cell DNA from women with cervical cancer than in those women with neoplasia or normal cytology.

Regarding hypermethylation, in 2001, Virmani *et al.* studied aberrant promoter hypermethylation in cervical cancer in 73 patients and 10 cervical cancer cell lines. They found that the rate of DNA methylation in cervical cell DNA from cancer patients was greater than controls, moreover, the pattern of methylation of 6 genes important in DNA replication and cell division, *p16*, *RARB*, *FHIT*, *GSTP1*, *MGMT*, and *hMLH1*, was altered. They showed that the frequency of methylation in those 6 genes was greater than 20%, except *hMLH1*. Methylation is a tumour-associated event as *RARB* and *GSTP1* methylation were found in early stage cellular abnormality, *p16* and *MGMT* methylation were found in the intermediate stage, and *FHIT* methylation was found in the late stage (Virmani *et al.*, 2001). Narayan *et al.* (2003) also studied hypermethylation of 16 gene promoters in 82 tumour biopsies derived from primary invasive cervical cancers and 8 cervical cancer cell lines. They found that *CDH1*, *DAPK*, *RARB* and *HIC1* gene promoters have a high level of methylation in cancer compared to normal cervical cells. The percentage of promoter methylation of *CDH1*, *DAPK*, *RARB* and *HIC1* gene in cervical cancer cases was 51.1%, 43.3%, 33.3%, and 22.2%, respectively (Narayan *et al.*, 2003). In this study, they included cervical cancer cell lines to investigate the reversible effect of methylation by treatment with the hypo-methylating agent, 5-aza-2'-deoxycytidine, and found that expression of those genes with a previously hypermethylated promoter, was up-regulated. In addition, Flatley *et al.* (2009) conducted a cross-sectional study in various grades of CIN in 308 women. They demonstrated that six of seven selected tumor suppressor genes showed a trend towards an increased promoter methylation from normal cervical cells towards cancer. Among those genes, three genes (*CDH1*, *DAPK*, and *HIC1*) showed a significant increase in promoter methylation from cells with normal cytology through neoplasia to cervical cancer ($P < 0.05$). Although it is generally

accepted that promoter methylation leads to gene silencing this need not always be the case. Recently, Guenin *et al* (2012) conducted a study of promoter methylation profile and expression pattern of stem cell (SC) genes during cervical carcinogenesis and they demonstrated that an increase in hypermethylation of undifferentiated cell transcription factor 1 (UTF1) promoter was associated with lesion severity. In this study, the hypermethylation of this promoter resulted in the increase of mRNA and protein expression. They also reported that the disruption of methylation using 5-aza-2'-deoxycytidine was related to a decrease in UTF1 gene methylation and expression in epithelial cancer cell lines (Guenin *et al.*, 2012). This study suggests that the hypermethylated promoter does not necessarily result in gene silencing.

All of the above suggests that folate might play an important role in maintaining normal cellular metabolism and thereby influence cancer risk. A fall in folate intake will reduce folate status in tissues. This may lead to an altered methylation status of DNA, which may be DNMT-mediated. There also will be dNTP pool imbalance in folate deficiency, which will disrupt DNA repair. Finally, this may bring about the alteration of gene expression such as DNA methyltransferase, the disruption of DNA integrity, and an increase in DNA damage. These changes can increase cancer risk. These considerations are illustrated in **figure 13**.

1.5 Folate as a modulator of cervical cancer risk

1.5.1 Folate and history of cervical cancer

A number of studies have examined the association between folate status and cervical cancer risk. In 1973, Whitehead *et al.* found that abnormal cervical cells were similar in appearance to those of megaloblastic anemia seen in folate and vitamin B12 deficiency. They also reported observations correlating folate status with cervical neoplasia in 22 women using oral contraceptives. After they gave folic acid to eight women with cervical abnormality, who also took oral contraceptives, for three weeks, all of the women showed an improvement in abnormal cytology (Whitehead *et al.*, 1973). However, this study was not robust because of the small number of subjects and the lack of a control group. In 1982, Butterworth *et al.* set up an experiment by giving oral folic acid supplement or placebo (ascorbic acid) for three months to 47 women who had mild or moderate cervical intraepithelial neoplasia and who also used oral contraceptive. They found that the cytology of women who received a folic supplement appeared to be better than the women in the placebo group ($P < 0.05$). Therefore, they concluded that folate could decrease the severity of CIN. They also demonstrated that red blood cell folate concentrations of oral contraceptive users are lower than non-users (Butterworth *et al.*, 1982). However, ten years later, in 1991, Potischman *et al.* conducted a case-control study in order to further examine the role of

folate. By collecting serum sample from 330 cases (varying stages of neoplasia and cervical cancer) and 555 controls (normal cervical cytology), they found that the concentration of folate was no different between the groups. Therefore, they concluded that folate is not correlated with the stage of cervical neoplasia (Potischman *et al.*, 1991). In a nested-case control conducted by Alberg *et al.* (2000), there was no association between serum folate status and cervical cancer (Alberg *et al.*, 2000).

However, the determination of folate status using serum or plasma folate may be confounded by recent dietary intake. Moreover, these early studies of the role of folate on cervical neoplasia produced mixed results. In 2001, Weinstein *et al.* conducted a case-control study in the United States in order to examine the relationship between serum and red blood cell (RBC) folate and incidence of invasive cervical cancer. In this study, they tried to control for all potential confounders such as age, smoking, oral contraceptive use, Pap smear history, and detection of HPV. Folate status was measured using four assays. The mean result for serum folate showed a lower concentration in cervical cancer cases than controls. For RBC folate, microbiological and radiobinding assays showed an Odds Ratio for cervical cancer for low versus high folate status of 1.2 (95% confidence interval (CI) 0.6-2.2) and 1.5 (95% confidence interval (CI) 0.8-2.7), respectively, which was not statistically significant (Weinstein *et al.*, 2001).

1.5.2 MTHFR polymorphisms and cervical cancer

There are several studies investigating the metabolism of folate in the context of polymorphism in the methylene tetrahydrofolate reductase (MTHFR). MTHFR is an enzyme used to convert 5,10-methylenetetrahydrofolate to 5-methyltetrahydrofolate, which is the key methyl donor for producing methionine. Thus, this enzyme influences folate metabolism and methylation in cells. Decreased activity of MTHFR can occur via two single nucleotide polymorphisms (SNPs) in the MTHFR gene: (1) changing from C to T at the position of 677 (C677T), and, (2) changing from A to C at the position of 1298 (A1298C). Both SNPs bring about an amino acid change in the enzyme, and may modify enzyme configuration, which has an influence on substrate binding. The prevalence of these genotype variants of MTHFR is different between populations; C677T polymorphism has a low frequency in sub-Saharan Africa and Northern Canada, whereas a high frequency is found in Southern Europe and South America.

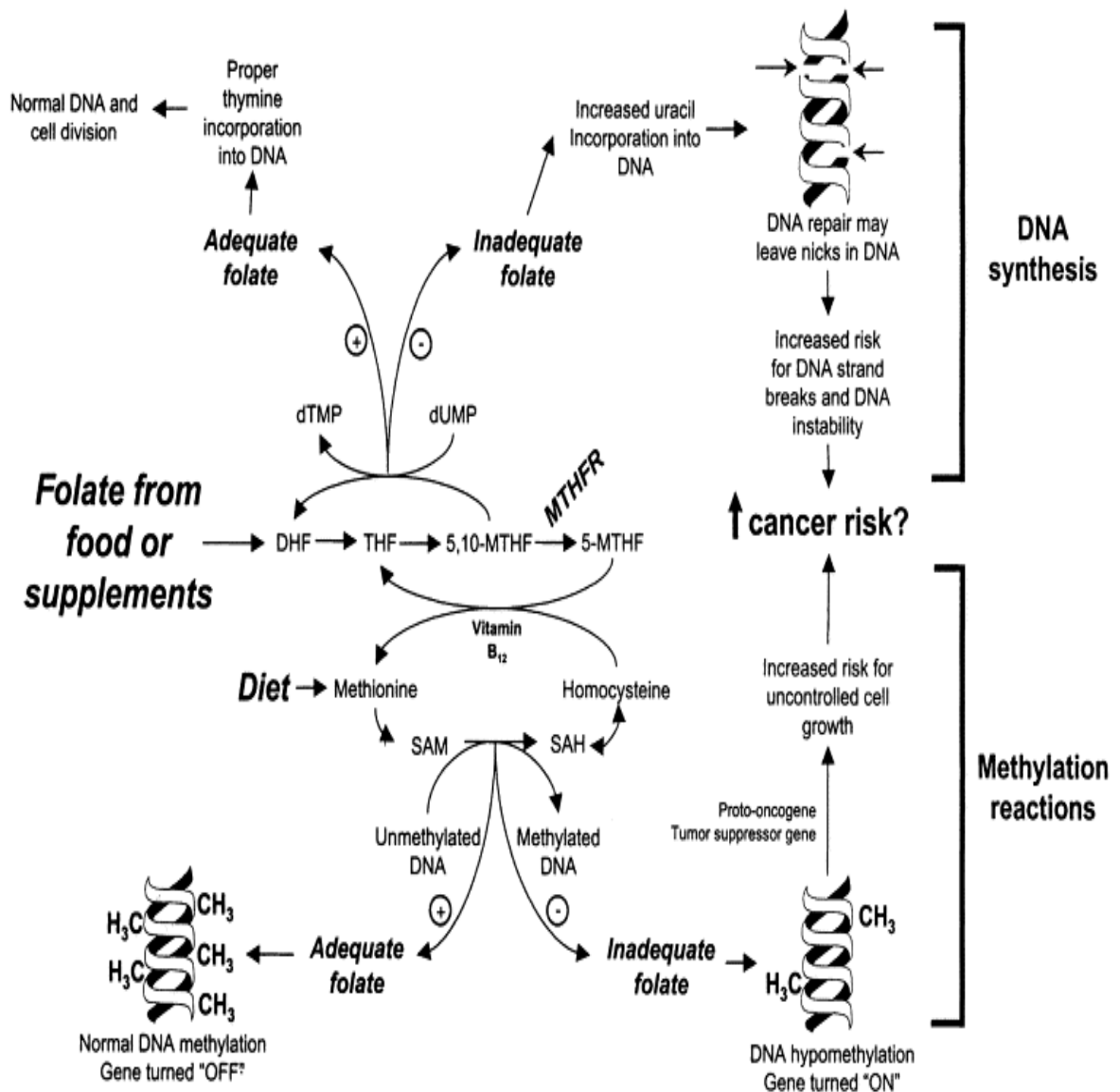


Figure 13: Effects of folate in cancer risk

(Rampersaud et al., 2002)

Folate deficiency led to an alteration of DNA synthesis and methylation process.

In 2001, Goodman *et al.* conducted a multiethnic case-control study of 150 cases and 179 controls in Hawaii to find variations in allele frequencies. They found that the CT-genotype and TT-genotype MTHFR had twofold [OR, 2.0; 95% confidence interval (CI), 1.1-3.7] and threefold risk (OR, 2.9; 95% CI, 1.0-8.8) of CIN, respectively, compare to CC-genotype. They also demonstrated that women who had the variant T allele (CT or TT) with low folate intake had more risk of cervical dysplasia than those women with the CC alleles and high folate intake (OR, 5.0; 95% CI, 2.0-12.2). Moreover, the risk from HPV infection in CIN also had strong impact among women carrying the TT-genotype or CT-genotype (OR, 46.6; 95% CI, 15.9-136.2) (Goodman *et al.*, 2001). On the other hand, in 2002, Gerhard *et al.* conducted a study in USA into the association between the MTHFR polymorphic variation (C677T and A1298C) and invasive cervical cancer by using family-based transmission/disequilibrium test (TDT) in 102 families of women who had invasive cervical cancer. They found that there was no influence of the prevalence of these two MTHFR variants (Gerhard *et al.*, 2003). This study did not use a traditional case-control study design, which can generate false-positives due to the difficulty in properly matching cases and controls. In addition, the study in Korea of Kang *et al.* (2005) also failed to find an increase in cervical cancer risk in association with the MTHFR C677T polymorphism in 82 cervical cancer specimens (Kang *et al.*, 2005).

1.5.3 Folate and the natural history HPV

Because of the well-accepted importance of HPV infection as a risk factor for cervical cancer, factors which influence susceptibility to infection, and HPV clearance, are relevant to cervical cancer risk. In the context of folate and HPV risk of cervical cancer, there is evidence to suggest that the role of folate status and DNA methylation may be important for HPV gene expression in host cells. The chromosome fragile site which is sensitive to folate deficiency coincides with an HPV-16 integrating site in primary cervical carcinomas (Wilke *et al.*, 1996). In 2004, Piyathilake *et al.* conducted a study of the association between folate status and high risk-HPV infection in a cohort of 345 women who were at risk of the progression of CIN. After 24 months with at least three consecutive visits HPV test and the measurement of folate status, they found that women having high folate status tended to show a negative result for the HR-HPV test (OR: 2.50; 95% CI, 1.18-5.30; P = 0.02) (Piyathilake *et al.*, 2004). In 2007, this group conducted research in the same population to find out whether circulating folate concentration influenced the risk of CIN in high stage cytological abnormality (CIN \geq 2) in women with HR-HPV. They found that HPV-16 infected women who also had low red blood cell folate, were more likely to show high CIN stage than non HPV-16 infected women who had high red blood cell folate (odds ratio 9, 95% confidence interval 3.3-24.8) (Piyathilake *et al.*, 2007). In their recent study, Flatley and

colleagues demonstrated that folate status was significantly lower in women with HR-HPV infection than those with no infection ($P=0.031$)(Flatley *et al.*, 2009). A further study in 100 human cervical biopsy samples including normal, SIL, and cervical cancer (Pathak *et al.*, 2012) also found that low folate status modulated the risk of HPV infection and cervical cancer.

Overall, these findings suggest that folate status may modulate cervical cancer risk and/or progression, through effects on one-carbon metabolism. However, in the one-carbon cycle, folate is not the sole methyl donor. Other intermediates in the cycle, including dietary methionine and betaine, may be important determinants of DNA methylation and therefore gene expression.

1.6 Methionine as a methyl donor

Methionine is an essential amino acid which can be found in any protein products such as egg white, chicken breast, and fish. Methionine plays an important role in protein synthesis. Methionine itself is also required for cell growth and serves as one of the methyl donors which is essential for methylation processes. **Figure 5** indicates the co-operation between folate, choline, and methionine in methyl donor function. Methionine biosynthesis occurs through 2 pathways. The first pathway involves the remethylation of homocysteine with 5-methyltetrahydrofolate, which requires the vitamin B12-dependent enzyme 5-methyltetrahydrofolate-homocysteine methyltransferase. The second pathway is the remethylation of homocysteine with betaine, which is a product of choline metabolism; this reaction is catalysed by betaine-homocysteine methyltransferase. All of these methyl donors work in harmony to supply methyl groups for cellular metabolism and the availability of one methyl donor can affect the requirement for other methyl donors (Niculescu & Zeisel, 2002). Several studies have demonstrated that folate and choline deficiency lead to a lowering in hepatic methionine and SAM (Finkelstein *et al.*, 1982; Zeisel *et al.*, 1989; Pomfret *et al.*, 1990). In addition, it has been shown that a defect in the transmethylation of folate or choline leads to a perturbation in the other. Either choline depletion or choline and methionine depletion resulted in a decrease in hepatic folate concentration (Horne *et al.*, 1989; Selhub *et al.*, 1991). Severe folate deficiency also led to a significant depletion of hepatic choline and phosphocholine concentration (Kim *et al.*, 1994a).

There has been no study linking methionine status with cervical cancer. However, there have been a few *in vitro* studies conducted in various cell types. Kokkinakis *et al.* (2004) developed a methionine deficient model in central nervous system tumor cell lines in order to investigate the expression level of several genes. After Western blot confirmation, they found that methionine stress led to changes in genes in cell cycle checkpoints and proapoptotic pathways. This research group also used a methionine-depleted model in

pancreatic tumour cell lines. Their results suggested that methionine deficiency led to a disruption of mitosis and enhanced cell cycle arrest and increased the number of micronuclei cells (Kokkinakis *et al.*, 2005). In 2009, Najim *et al.* also used a methionine-depleted model of central nervous system tumor cell lines and reported that glutathione was increased and O⁶-methylguanine-DNA-methyltransferase (MGMT) activity, which plays an important role in DNA repair, was decreased in Daoy cells (Najim *et al.*, 2009).

Studies of combined methyl donor deficiency have been conducted mostly in animal models. For example, Duthie *et al.* (2000) studied the effect of deficiency in a combination of methyl donors (methionine and choline, and folate, methionine and choline) in Male Hooded-Lister rats. After 10 weeks of feeding methyl-deficient diets, they found DNA strand breakage in colonocytes, but no significant change in global DNA methylation of colonic scrapings (Duthie *et al.*, 2000b). Pogribny *et al.* (2004) also investigated the effects of methionine-choline-folate-deficiency in male weanling F344 rats. They reported DNA hypomethylation and an increase in DNA methyltransferase of rat liver after 36 weeks of depletion, but found no effect on pancreas, spleen, kidney, and thymus. This suggested that the alteration of DNA methylation was specific to hepatocarcinogenesis (Pogribny *et al.*, 2004). In addition, Ghoshal *et al.* (2006) demonstrated an alteration of DNA methylation machinery in the liver of F344 rats which were fed with a folate-methionine-choline deficient diet (Ghoshal *et al.*, 2006). These studies suggested that effects of combined folate-methionine-choline deficiency targeted the liver. However, an effect of a combined folate-methionine-choline deficient diet was also found in the brains of F344 rats, but in the opposite direction to effects seen in the liver. In brain, global DNA methylation was increased, as detected by an increase in the genomic 5-methylcytosine content. This global DNA hypermethylation was also associated with an increase in protein expression of DNMT3a and methyl-CpG-binding protein 2 (Pogribny *et al.*, 2008). Although combined folate-methionine-choline deficiency has been studied in a number of groups, there has been no study of the combination of only folate and methionine deficiency before.

According to the evidence cited above there are plausible reasons why folate and methionine status may influence cervical cancer risk and progression. Low folate status affects one-carbon transferring processes, which are required for nucleotide synthesis/repair and methylation. Low methionine status also affects the distribution of folate derivatives and disturbs methylation processes. A combined methyl donor deficiency may maximize the effects of methyl donor depletion on cells. Therefore, low folate and methionine status may lead to reduced DNA stability and disturbed DNA or histone methylation. Consequently, fragile sites may occur in DNA which cause difficulty in repair, and which might allow greater ease of entry of pathogenic DNA such as high-risk HPV. Moreover, normal cell division is

affected not only by an HPV-gene expression mechanism itself, but also by incorporation of unusual DNA methylation profile in the host cell, which occurs in folate deficiency. Since abnormal DNA methylation can cause “switch on” or “switch off” of regulatory genes, HPV persistence or HPV latency stage in the host cell may occur differently depending on DNA methylation level and therefore HPV DNA expression.

As folate and methionine both serve as methyl donors, this study was conducted to determine the effects of folate deficiency alone or in combination with methionine depletion, on the global DNA methylation level of cervical cancer cells. Since the DNA methylation process is catalysed by DNA methyltransferase, DNMTs expression was also examined to investigate the association between DNA methylation level and gene expression. As aberrant DNA methylation is an epigenetic process which may lead to an alteration of gene expression profile and might lead to several changes in phenotype, cell characteristics resulting from the effects of folate and methionine deficiency were also examined.

1.7 Hypothesis, aim, and objectives

1.7.1 Hypothesis

Methyl-donor depletion alters DNA methylation status and DNA methyltransferase expression. Furthermore, it is hypothesised that methyl-donor depletion will lead to an alteration of global gene expression, which affects the phenotype of cervical cancer cells.

1.7.2 Aim

The overall aim of this study is to examine how methyl donor status influences DNA methylation, DNA methyltransferase gene expression, global gene expression, and cervical cancer phenotype.

1.7.3 Objectives

1. To develop the methyl donor depleted model using cervical cancer cell lines.
2. To validate the methyl donor depleted model by examining intracellular folate concentration, intracellular methionine concentration, and extracellular homocysteine.
3. To investigate the effects of methyl donor on;
 - DNA methylation status
 - DNA methyltransferases expression
 - DNA methyltransferase activity
 - global gene expression
 - phenotype of cervical cancer cells

Chapter 2 Materials and Methods

2.1 Materials

2.1.1 Cell lines

Cervical cancer C4-II cells were obtained from HPA Culture Collections, United Kingdom. The cells are derived from a cervical carcinoma of a 41 year old Caucasian female. C4-II cells have been reported to contain human papilloma virus 18 (HPV-18) DNA sequences and to express HPV-18 RNA. C4-II is the most similar to cervical cancer biopsies in gene expression when comparing with other kinds of cervical cancer cell lines (Carlson *et al.*, 2007).

SiHa is a cervical cancer cell line which was established from fragments of a primary tissue sample obtained after surgery from a CIN II -grade Japanese patient. SiHa is reported to harbor an integrated human papillomavirus type 16 genome (HPV-16, 1 to 2 copies per cell).

NIH 3T3 fibroblast cells were used as a positive control in the immunocytochemistry method for methylcytosine.

2.1.2 Media

- A. Waymouth MB 752/1: GIBCO, UK** (Cat. No. 31220072) was used for the normal culture of C4-II. This medium contains sufficient nutrients for cell growth. It is described in the text as complete medium or F+M+ medium (900nM of folic acid and 300µM of methionine).The medium was prepared by supplementation with 10% fetal calf serum gold (FCS Gold: PAA, Cat. No. A15-151), 200 nM L-glutamine, and 1% penicillin/streptomycin antibiotics (GIBCO, Cat. No. 15140-122)
- B. Waymouth MB folate and methionine-free medium: GIBCO, UK** (Cat. No. 04196306) was used for folate and methionine depletion of cells. It is described in the text as depleted medium or folate and methionine-depleted medium or F-M- medium. The medium was supplemented with 10%FCS Gold, 200 nM L-glutamine, and 1% penicillin/streptomycin antibiotics. This medium contained a low concentration of folate and methionine from FCS (12-30 nM of folate and ~20 µM of methionine).
- C. Dulbecco's Minimum Essential Medium (DMEM): GIBCO, UK** (Cat. No. 22320022) was used for normal culture of NIH 3T3 cells (control cell for immunocytochemistry) and initial culture of SiHa
- D. Waymouth MB folate and methionine-free medium + 900 nM folinic acid** (folinic acid calcium salt hydrate: SIGMA CAS No. 1492-18-8, MW= 511.50) was used for the folate

repletion experiment. It is described in the text as methionine-depleted medium or F+M-medium.

E. Waymouth MB folate and methionine-free medium + 300 μ M L-methionine (L-methionine: SIGMA CAS 63-68-3, MW=149.21) was used for the methionine repletion experiment. It is described in the text as folate-depleted medium or F-M+ medium.

2.1.3 Cell culture

Centrifuge (Sorvall RT6000B refrigerated centrifuge, USA)

Culture flasks and plates (Nunc)

FCS Gold (foetal calf serum gold: PAA, Cat. No. A15-151)

Folinic acid (folinic acid calcium salt hydrate, SIGMA: CAS 1492-18-8)

Haemocytometer

Hand tally counter

L-Glutamine (200 nM L-Glutamine: GIBCO)

L-Methionine (SIGMA: CAS 63-63-3)

Microscope (Diaphot: Nikon, Japan)

PBS pH 7.3 \pm 0.2 (phosphate buffered saline tablets: OXOID, England)

Penicillin/ Streptomycin (1% Penicillin/Streptomycin: GIBCO, Cat. No. 15140-122)

Trypan blue stain 0.4% (GIBCO)

Trypsin-EDTA (0.25% trypsin-EDTA: GIBCO)

2.1.4 Measurement of intracellular folate

Beckman coulter folate access Kit (Beckman coulter, UK)

Centrifuge (MIKRO 22R: Hettich Zentrifugen, Germany)

Precellyse[®]24 lysis and homogenization machine (Bertin technologies, France)

Sonicator (UCD-200TM: Bioruptor diagenode, Belgium)

2.1.5 Measurement of intracellular methionine

Biochrom Amino Acid Analyser30 (Biochrom, UK)

Centrifuge (MIKRO 22R: Hettich Zentrifugen, Germany)

Precellyse[®]24 lysis and homogenization machine (Bertin technologies, France)

Sonicator (UCD-200TM: Bioruptor diagenode, Belgium)

2.1.6 Measurement of homocysteine

Centrifuge (MIKRO 22R: Hettich Zentrifugen, Germany)

Heat box (FALC supplied by Scientific Ltd. UK)

HPLC Analysis of homocysteine kit (order no. 45000: CHROMSYSTEMS, Germany)

HPLC module (Gilson model no. 811C, USA)

Precellyse[®]24 lysis and homogenization machine (Bertin technologies, France)

Sonicator (UCD-200TM: Bioruptor diagenode, Belgium)

2.1.7 Determination of DNA methylation

2.1.7.1 DNA methyl acceptor assay

2.1.7.1.1 DNA extraction

Centrifuge (MIKRO 22R: Hettich Zentrifugen, Germany)

Heat box (FALC supplied by Scientific Ltd. UK)

Nanodrop spectrophotometer (Labtech international, UK)

QIAamp[®] DNA Mini kit (QIAGEN: cat no. 51304)

2.1.7.1.2 [³H]-SAM donor assay

Absolute ethanol (BDH, EC 200-578-6)

Beckman counter LS 6500 multi-purpose scintillation counter

CpG methyltransferase (*M.SssI* 20000 unit/ml: Bio Labs , M00226M)

DTT (dithiotreitol: SIGMA D9779-5G CAS no. 3483-12-3MW 154.2)

EDTA (Ethylene diamine tetraacetic acid disodium salt solution: SIGMA E7889)

³H-SAM (250 µCi-9.25 MBq [10.0 Ci/mmol in 0.455 ml of 10mM H₂SO₄: EtOH 9:1] S-[methyl]-3H: Perkin Elmer, USA)

Incubator, centrifuge, micropipette, microfuge tube

Methylated control (100 µg/ml CpG methylated Jurkat genomic DNA: N4002S BioLabs)

NaCl (sodium chloride: BDH AnalaR product no. 102415K MW 58.44)

Plastic box and scintillation vial

SAM (S-adenosylmethionine: BioLabs, 32 mM 10%ethanol in H₂SO₄, #B90035)

Scintillation fluid (ULTIMA GOLD High flash-point LSC-cocktail for aq. and non-aq. Samples: Perkin Elmer)

Sodium phosphate monobasic (SIGMA CAS no. 7558-80-7 MW 119.98 g/mol)

TE buffer (Tris-EDTA buffer solution pH 8.0: Fluka)

Tris (Tris (hydroxymethyl) methylamine: BDH GPR EC no. 201-064-4 MW 121.14)

Unmethylated control (100 µg/ml 5-Azadc treated Jurkat genomic DNA: N4003S, BioLabs)

Whatman ion-exchange filter paper (wipe out: 90mmØ circle cat no. 1001090, spot: 2.3 cm Ø grade DE81 cat no. 3658-023)

2.1.7.2 Immunocytochemistry of 5-methylcytosine

Blocking solution (0.2% fish gelatin + 0.3M glycine in PBS)

Broad-tipped Forceps, point-tipped forceps, fine-tipped forceps

Cell of interest (C4-II cell lines, Positive control is NIH 3T3 cells)

Citric acid (SIGMA, CAS no. 5949-29-1, FW=210.1)

Culture slide (Lab-Tek® Chamber slide Cat. No. 177399)

DAB chromogen solution (mixture of substrate buffer, diaminobenzidine tetrahydrochloric acid, and hydrogen peroxide: reagent D1, D2, and D3 of Histostatin®-Plus Kits, respectively)

DAB Staining kit (Histostatin®-Plus Kits Invitrogen®2nd Generation Cat no. 85-9643)

Enzyme conjugate (streptavidin-peroxidase conjugate: reagent C of Histostatin®-Plus Kits Invitrogen)

Fish gelatin (gelatin from cod water fish skin: SIGMA, G7765-250ML)

Formaldehyde (formaldehyde solution for molecular biology 36.5%: SIGMA CAS no. 50-00-0)

Glycine (Fisher Biotech, USA CAS no. 56-40-6 FW=75.07)

Haematoxylin counterstain (Haematoxylin Gill II: Surgipath, product code 01521E)

Hydrochloric acid (36%: Fisher Scientific, CAS. No. 7647-01-0, FW=36.46)

Hydrogen peroxide (SIGMA, CAS no. 7722-84-1)

Microscope (Nikon ECLIPSE e400)

Mounting medium (Clearmount™ Mounting Solution: ZYMED®Laboratories invitrogen Immunodetection)

PBS pH 7.3±0.2 (phosphate buffered saline tablets: OXOID, England)

Permeabilizing solution (0.2% (v/v) Triton X-100 in PBS)

Primary antibody (anti 5-methylcytosine mouse mAb: MERCK 162 33 D3)

Primary antibody diluents (0.1% tween 20 in PBS)

Secondary antibody (biotinylated secondary antibody: reagent B of Histostatin®-Plus Kits Invitrogen)

Tissue culture medium appropriate for the cells

2.1.7.3 Flow cytometric analysis of 5-methylcytosine

5-azadeoxycytidine (SIGMA)

BSA (Albumin from bovine serum: SIGMA EC 232-936-2)

Cell of interest (C4-II and SiHa cell lines)

Centrifuge (Sorvall RT6000B refrigerated centrifuge, USA)

Donkey serum (SIGMA D9663 PA-TEC-0005)

FACS tube (5 ml Polystyrene Round Bottom tube 12x75 mm : Becton Dickinson 352058)

FACS CALIBUR flow cytometer (Becton Dickinson)

FCS (FCS Gold: PAA, Cat. No. A15-151)

Formaldehyde (formaldehyde solution for molecular biology 36.5%: SIGMA CAS no. 50-00-0)

Haemocytometer

Hydrochloric acid (36%: Fisher Scientific, CAS. No. 7647-01-0, FW=36.46)

Isotype control Ab negative control (mouse IgG1: AbD SEROTEC MCA928)

Methanol (Fisher Scientific: CAS. No. 67-56-1, FW=32.04)

PBS (phosphate buffered saline tablets: OXOID, England)

Primary antibody (anti 5-methylcytosine mouse mAb: MERCK 162 33 D3)

Secondary antibody (anti-mouse IgG: Alexa fluor 488 donkey anti-mouse IgG (H+L), Invitrogen A21202)

Sodium borate pH8.5 (SIGMA CAS 1303-96-4)

Tissue culture medium appropriate for the cells

Tween20 (Polyoxyethylene sorbitan monolaurate: SIGMA P7949 CAS 9005-64-5)

Water bath

2.1.8 RNA extraction

Absolute ethanol (BDH, EC 200-578-6)

Bevelled Filter Tips (sterile): RNase, DNase, DNA and pyrogen free

Herarus PICO17 centrifuge (Thermo scientific, UK)

Micropipette (Gilson, USA)

Nanodrop spectrophotometer (Labtech international, UK)

Precellyse[®] 24 lysis and homogenization machine (Bertin technologies, France)

Precellyse tube

RNase-free DNase I (New England Biolabs: cat no. M0303S)

RNase-free DNase set (QIAGEN: cat no. 79254)

RNeasy[®] Mini kit (QIAGEN: cat. no. 74104)

Sodium Hydroxide solution (20mM: for experimental space cleaning)

2.1.9 cDNA synthesis

0.2ml single thin wall PCR tubes (Starlab, Germany: Cat. No. 1 1402 4300)

5X First-Strand Buffer (Invitrogen: Cat. No. 18080-044)

Centrifuge: GmCLAB[®] for PCR tube (Gilson, USA)

dNTP mix (Invitrogen: Cat no. 18427-013)

DTT (Dithiothreitol:Invitrogen)

Nuclease-Free water (Ambion: Cat. No. AM9937)

PCR machine: G-strom (Catcombe, UK)

Random primers (Promega, USA: Cat. no. C1181)

RNase OUT[™] Ribonuclease Inhibitor Recombinant (Invitrogen: Cat no. 10777-019)

SuperScript[™] III Reverse transcriptase (RT) (Invitrogen: Cat no.18080-044)

2.1.10 DNMTs gene expression by qRT-PCR

Bevelled Filter Tips (sterile): RNase, DNase, DNA and pyrogen free

Fast optical 96 well reaction plate: Micro AMP[®] with Barcode 0.1 ml (Applied Biosystems, Singapore)

Mini Plate Spinner (Labnet MPS1000)

Optical adhesive film: Micro Amp™ (Applied Biosystems, USA)

Primers (SIGMA, USA)

Probes (Applied Biosystems, USA)

StepOne Plus™ Real-Time PCR (Applied Biosystems, USA)

TaqMan®: Fast Universal PCR Master Mix (2X) No AmpErase®UNG (Invitrogen, USA:
cat no. 4367846)

2.1.11 Gene expression analysis by microarray

Agilent 2100 Bioanalyzer (Agilent Technologies, Germany)

Agilent RNA 6000 Nano Kit (Agilent Technologies, Germany)

David Bioinformatics Resource 6.7

GeneChip® 3'IVT Express Kit (Affymetrix, UK)

GeneChip® Command Console® Software (Affymetrix,UK)

GeneChip® Fluidics Station 450 (Affymetrix,UK)

GeneChip® Human Genome U133 Plus 2.0 Array (Affymetrix, UK)

GeneChip® Hybridisation Oven 640 (Affymetrix, UK)

GeneChip® Hybridisation, wash, and Stain kit (Affymetrix, UK)

GeneChip® Scanner 3000 enabled for high-Resolution Scanning (Affymetrix,UK)

GeneSpring Software version11 (Agilent Technologies, Germany)

Herarus PICO17 centrifuge (Thermo scientific, UK)

Micropipette Thermal Cycler with heated Lid

Nanodrop spectrophotometer (Labtech international, UK)

RNase-free microfuge tube

Vortex Mixer multiple

2.1.12 Nuclear extraction

Centrifuge (MIKRO 22R: Hettich Zentrifugen, Germany)

NE-PER[®] Extraction Reagents (Thermo Scientific, USA: Cat no. 78833)

Protease Inhibitor Cocktail Tablet (Complete Mini in Easy Pack, Roche Applied Science, USA: Cat no. 04 693 124 001)

2.1.13 Protein quantification

96-well plate

Bio-Rad Bradford Reagent (Bio-Rad, UK: cat no. 500-0205)

Microplate reader (BioTek FLX800, USA)

Protein standard BSA liquid 2mg/ml (Sigma, UK: CAS number 9048-46-8, Cat no. P0834)

2.1.14 DNMT activity

EpiQuik[™] DNA Methyltransferase Activity/Inhibition Assay Kit (Epigentek, USA)

Incubator

Microplate reader (BioTek FLX800, USA)

Multichannel micropipette

2.1.15 Cell migration

96-well culture plate (Nunc[™] Cell Culture MicroWell Plates: Thermo scientific, UK)

CellTiter 96[®]Aqueous One Solution Cell Proliferation Assay (Promega: Cat no. G3580)

ImageJ Software

LAS software

Leica DMI AF600LX time-lapse microscope (USA)

Leica DMIL microscope (USA)

Microplate reader (BioTek FLX800, USA)

Mitomycin C (SIGMA)

Motic Image plus 2.0ML Software

2.2 Methods

2.2.1 Cell culture

2.2.1.1 Cell Thawing

Growth of the cell lines was initiated by propagation of the cells received from HPA. Cells were moved from vial to a new 50-ml tube and 11 ml normal (complete) medium were added to the cells and the suspension centrifuged at room temperature for 5 min. at 150xg. The supernatant was discarded and the cell pellet was suspended in 4 ml of normal medium. Cells were counted and checked under a microscope for viability (see section 2.2.1.3). Then, 11 ml of fresh and warm normal medium were added into new T75 flask and the cell suspension was transferred into the flask. Cells were cultured in a humidified incubator at 37°C with 5% carbon dioxide. Cell growth and cell characteristics were observed each day. The cells were subcultured when they reached 70-80% confluence.

2.2.1.2 Subculture

Cells were split when they reached 70-80% confluence. The culture medium was discarded and cells were washed with 10 ml. PBS. Then, 2 ml. of trypsin-EDTA were added into the culture flask and incubated in CO₂ incubator for about 8 min. Detached cells were checked under a microscope. Fresh warm normal medium was added into the culture flask and the cell suspension transferred to a new tube. Cells were centrifuged at room temperature for 5 min. at 150xg. The supernatant was discarded and cell pellet was suspended with 4 ml of fresh and warm normal medium. Then, 14 ml of fresh and warm normal medium were added into a new flask and 1 ml of the cell suspension was transferred into the flask (split 1:4 or 1.5x10⁶ cells of C4-II for 4-day culture in T75-flask : total cells may be 10000-30000 cell/cm² and split 1:3-1:10 for SiHa cell). Cells were cultured in a humidified incubator at 37°C with 5% carbon dioxide. Cell growth was observed daily according to confluence and cell morphology.

2.2.1.3 Counting

Viable cells were counted by mixing 20µl of cell suspension with 20µl Trypan Blue in a microfuge tube and 20µl were taken for counting using a haemocytometer (dead cells appear blue). Cells were counted in 4 big corner squares (**please see figure 14: area 1, 2,**

4, and 5) under 10x objective of microscope. The haemocytometer was designed so that the number of cells in one set of big corner squares was equivalent to the number of cells $\times 10^4$ per ml.

Cell number = (the sum of cells/4) $\times 2 \times 10^4$ cell/ml

(The number of cells was divided by 4 to produce an average and multiplied by 2 to adjust for the 1: 2 dilution in trypan blue)

Percentage viability = (no. viable cells/total cells) $\times 100$

2.2.1.4 Cryopreservation

Cell line stocks were frozen in liquid nitrogen. Cells were harvested when they reached 70-80% confluence. The culture medium was discarded and cells were washed with 10 ml. PBS. Then, 2 ml. of trypsin-EDTA were added to the culture flask and incubated in CO_2 incubator for about 8 min. Detached cells were checked under a microscope. Fresh and warm medium was added into the culture flask. The cell suspension was transferred to a new tube and cells were centrifuged at room temperature for 5 min. at 150xg. Supernatant was discarded and cell pellet was suspended with fresh and warm medium. Viable cells were counted (see 2.2.1.3). Then, DMSO was added to the cell suspension at 1:9 ratio of DMSO: cell suspension. The cell suspension was pipetted into a cryotube and frozen in a cryobox at -20°C overnight to slow the decrease in temperature before storage in liquid nitrogen.

2.2.2 Determination of growth rate

Cells were split when they reached 70-80% confluence. The culture medium was discarded and cells were washed with 10 ml PBS. Then, 2 ml of trypsin-EDTA were added to the culture flask and incubated in CO_2 incubator for about 8 min. Detached cells were checked under a microscope. Fresh and warm medium was added into culture flask. The cell suspension was transferred to a new tube and centrifuged at room temperature for 5 min. at 150xg. The supernatant was discarded and the cell pellet was suspended in 4 ml of fresh warm medium. Viable cells were counted (see 2.2.1.3). Then, 2.5 ml of fresh and warm medium were added into each well of a 6-well plate or 15 ml of fresh and warm medium were added into each T75-flask and the cell suspension transferred into each culture container (starting cell density 0.192×10^6 cell/ well in 6-well plate or 1.5×10^6 cell/flask: total cell may be 10000-30000 cell/ cm^2). Cells were cultured in a humidified incubator at 37°C with 5% carbon dioxide. Cell growth was observed daily and 1-3 wells of culture plates or one flask was selected for counting every 3-5 days for 12- 20 days.

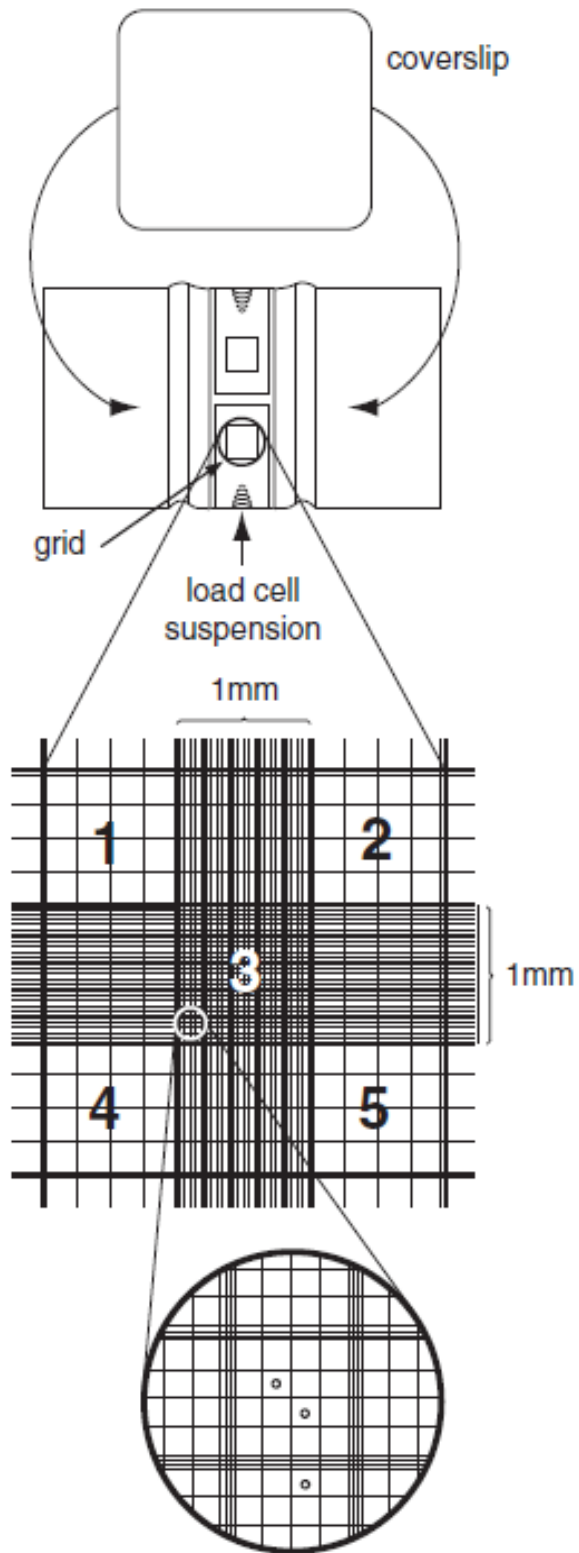


Figure 14: *The haemocytometer gridline*
 (Phelan, 1998)

2.2.3 Measurement of intracellular folate

More than 5 million cells were harvested at day 4, 8 and 12 of culture for C4-II cells, and at 2nd, 4th, and 6th passage (week 2, 4, and 6) for SiHa. Cells were trypsinised and washed with PBS. The cells were suspended with 500 µl of 0.5% (w/v) ascorbic acid in water. Cell lysates of the cell suspension were prepared by cell disruption using a sonicator (high pulse: 10 min.) followed by 2 cycles of precellys (1 cycle: 6000 rpm/pulse: 2 x 30 sec / pause: 20 sec). The supernatants were separated by centrifugation at 16000xg for 10 min at 4°C. The cell suspensions were diluted into 1:10 ratio in separate tubes and all diluted suspensions and non-diluted suspensions were kept at -80°C until analysis. Intracellular folate was measured in units of ng/ml by using an automated competitive folate protein binding assay (Beckman Access Kit) in the Department of Human Metabolism at the University of Sheffield. Intracellular folate concentration was expressed as pmol/10⁶ cells for C4-II and pmol/10⁶ cells for SiHa cells.

2.2.4 Measurement of intracellular methionine

More than 20 million cells were harvested at day 4, 8 and 12 of culture for C4-II cells. Cells were trypsinised and washed with PBS. The cells were suspended with 300 µl of PBS. Cell lysates of the cell suspension were prepared by cell disruption using a sonicator (high pulse: 10 min.) followed by 2 cycles of precellys (6000 rpm/pulse: 2 x 30 sec / pause: 20 sec). The supernatants were separated by centrifugation at 16000xg for 10 min at 4°C and kept at -80°C until analysis. Methionine was measured using Biochrom 30 amino acid analyzer at the Department of Clinical Chemistry, Sheffield Children Hospital, using a Biosys software v2.05 and analysed using EZChrom Elite software v3.4. The intracellular methionine was presented in nmol/L and expressed as pmol/10⁶ cells.

2.2.5 Measurement of homocysteine

Intracellular and extracellular homocysteine concentrations were determined by reverse-phase high-performance liquid chromatography using CHROMSYSTEMS HPLC Kit. Briefly, cell lysates (cell lysate preparation is the same as for the intracellular methionine measurement) and cultured medium were pipetted into a light protected reaction vial and incubated with internal standard and reducing reagent at room temperature for 10 min. Precipitation reagent was added and centrifuged at 9000xg for 5-7 min. The supernatant was transferred to a new light protected reaction vial. Derivatisation mix was added to the supernatant and incubated at 50-55°C for 10 min. Prepared samples were injected onto the HPLC system. Absorbance of eluted compounds was monitored using $\lambda_{\text{ex}} = 385 \text{ nm}$ and $\lambda_{\text{em}} = 515 \text{ nm}$. The retention time of the internal standard and homocysteine at a flow rate of 1.5 ml/min were taken as 3.3-3.5 min and 3.9-4.5 min, respectively. Chromatograms were

recorded with UniPoint™ LC System Software Version 5.1 with quantification accomplished by automatic peak area integration. Calibrator, control I, and control II with internal standard were used to identify the elution peaks and for calculation of homocysteine concentration.

$$C_{analyst, sample} \left[\frac{\mu mol}{L} \right] = \frac{(A_{sample} * IS_{calibrator})}{(A_{calibrator} * IS_{sample})} * C_{calibrator}$$

A sample = Peak area/height of substance A in the chromatogram of the sample

A calibrator = Peak area/height of substance A in the chromatogram of the calibrator

IS sample = Peak area/height of substance Internal standard in the chromatogram of the sample

IS calibrator = Peak area/height of substance Internal standard in the chromatogram of the calibrator

C calibrator = The concentration C of substance A in the calibrator (14.8 μmol/l)

2.2.6 DNA extraction

DNA was extracted by QIAamp®DNA Mini kit from QIAGEN (cat no. 51304) by following the manufacturer's protocol. Briefly, the cell pellet was removed from -20°C freezer and thawed. Then, 180 μl of buffer ATL was added in to the cell pellet followed by 20 μl of proteinase K. The cell suspension was mixed by vortexing and incubated at 56°C for 1-2 hours. Then, 200 μl of buffer AL were added followed by further incubation at 70°C for 10 min. After that, 200 μl of ethanol (96-100%) were added and the DNA mixture was applied to the QIAamp spin column. The column was centrifuged at 6000xg for 1 min. The filtrate was discarded and buffer AW1 was added and the column was centrifuged again at 6000xg for 1 min. The filtrate was discarded and Buffer AW2 was added and the column was centrifuged at 16000xg for 3 min. The filtrate was discarded and TE buffer was added and the sample incubated at room temperature for 5 min, followed by a centrifugation at 16000xg for 1 min. The filtrate consisted of a DNA suspension; DNA was quantified and the purity determined using the Nanodrop spectrophotometer. The DNA had an absorbance ratio of $A_{260}:A_{280}$

between 1.8 and 2.2. The DNA concentration was determined as the mean of three independent spectrophotometric readings.

2.2.7 Determination of global DNA methylation

2.2.7.1 DNA methyl acceptor assay

The modified method of Balaghi and Wagner (Balaghi & Wagner, 1993) was used. DNA suspension containing 0.5 µg of genomic DNA was prepared in triplicate from cells at day 4, 12, 20, and 24 of culture for C4-II and at day 8 of SiHa cells after 6 passages. The DNA was incubated with 0.455 µCi of [³H]-methyl-S-adenosylmethionine, 3 units of CpG methyltransferase and 6 µl of methylation buffer (pH 8.0: 50 mM tris, 600 mM NaCl, 50 mM EDTA, 5 mM DTT) in a total volume of 30 µl for 1 hour at 30°C. The incubation mixtures were spotted onto Whatman DE-81 ion exchange filter paper. After the papers were dried, the papers were washed 3 times with 0.5 M sodium phosphate buffer pH 7.0 for 10 min each followed by 10-minute washing with water. Then, the papers were washed with 70% ethanol 2 times and washed with absolute ethanol 2 times. The papers were dried for 30 min placed into scintillation vials and 5 ml of scintillation fluid was added. The radioactivity retained on the papers was measured by scintillation counting for 10 min. each. For a positive control, 0.5 µg of 5-azadeoxycytidine-treated Jurkat genomic DNA (5-azadeoxycytidine treatment demethylates DNA) was used instead of the cell DNA. For a negative control, 0.5 µg of CpG methylated Jurkat genomic DNA was used. The disintegration per minute (DPM) result reflected the [³H]-methyl incorporation into DNA. To calculate sample DNA hypomethylation, blank DPM (the mixture lacking CpG methyltransferase) was subtracted from sample DPM and reported as DPM/1 µg of DNA.

2.2.7.2 Immunocytochemistry of 5-methylcytosine

Cells were grown in T25 or T75 flasks, trypsinised and then were seeded onto 4-well slide chambers and incubated at 37°C/ 5%CO₂ for 24 hours, 8 days and 15 days. On the indicated day, cells were washed twice with cold PBS and fixed with p-formaldehyde for 20min and washed twice with PBS. Then, cells were permeabilized with 0.2%triton X-100 in PBS for 10 min and washed 3 times with PBS. For antigen retrieval, the cultured slide was placed into 0.01M citric acid pH 6.0 and heated at full power in a microwave oven for 12 min and rinsed with deionized water. The slide was then placed into 3.5N HCl for 15 min followed by rinsing with deionized water. Endogenous peroxidases were quenched with a solution of 3% hydrogen peroxide in methanol for 10 min and washed 3 times with PBS. The slide was then incubated with blocking solution (0.2% fish gelatin and 0.3 M glycine in PBS) for 30 min at room temperature to block nonspecific staining. After draining off the solution, the slide

was incubated with 5 µg/ml of primary antibody (anti 5-methylcytosine mouse monoclonal antibody) for 1 hour at room temperature. This antibody is known to recognize 5-methylcytosine in methylated DNA or RNA in NIH 3T3 cells, which were used as a positive control. After washing 3 times with PBS, the secondary antibody (biotinylated secondary antibody: reagent B of Histostatin®-Plus Kits Invitrogen) was added for 10 min. The slide was then washed 3 times with PBS and incubated with enzyme conjugate solution (streptavidin-peroxidase conjugate: reagent C of Histostatin®-Plus Kits Invitrogen) for 10 min, and then washed 3 times with PBS. For staining, DAB chromogen solution was added for 3-10 min and rinsed with deionized water. For counterstaining, Gill's Haematoxylin was used for 15 seconds and rinsed with Scott's Tap water. Finally, the mounting medium was placed on the cell surface until completely dried. Cells were visualized using Nikon ECLIPSE e400 microscope. NIH 3T3 cells with and without primary antibody were used as a positive and negative control, respectively. Cells positive for 5-methylcytosine had DAB brown stained nuclei, negative cells were haematoxylin blue counterstained.

2.2.7.3 Flow cytometric analysis of DNA methylation

More than 5×10^6 trypsinised cells were collected into 6 ml of appropriate medium in a 50ml centrifuge tube and pelleted by centrifugation (150xg). The supernatant was decanted and cells were washed twice by resuspending in 10ml of washing solution (PBST/BSA: 0.1% tween20, 1%BSA in PBS) and pelleted by centrifugation. The cell pellet was resuspended in 5ml of 4%formaldehyde for 30 min at 37°C and cooled at 4°C for 10 min for fixation. Cells were incubated with 9 volumes of 88%methanol/12%PBS at -20°C for 30 min. Cell pellets were centrifuged and the supernatants were discarded. The cells were washed twice by centrifugation in 10ml PBST/BSA. Antigen retrieval was performed by incubating each cell pellet in 5ml of 2N HCl for 30 min at 37°C and pelleting by centrifugation, and resuspending in 5ml of 0.1M sodium borate pH8.5 for 5 min at room temperature. Cells were washed twice by centrifugation in washing solution. The cells were blocked in blocking solution (10%FCS or donkey serum in PBST/BSA) overnight at 4°C. Cells were counted and aliquots of 0.5×10^6 cells placed into FACS tubes. Cell aliquots were immunostained with primary antibody anti-5 methylcytosine (100µl of a 1:250 dilution of anti 5-mc in PBST/BSA) **OR** 10µl IgG1 isotype control + 90µl PBST/BSA per tube and incubated at 37°C for 45 min. Cells were washed 3 times by centrifugation in washing solution. Secondary antibody was added (100µl of 1:1000 of 2°antibody in PBS+5% BSA solution) and incubated at 37°C for 45min in the dark. Cells were washed 3 times by resuspending pellet in washing solution and pellet by centrifugation. Cells were kept at 4°C before analysis by BD FACSCalibur™. Appropriate controls were utilized and included unstained cells, secondary antibody alone and 5-Aza, 2-deoxycytidine

treated cells for a negative control. Nonspecific antibody binding was monitored with a mouse IgG1 isotype. Data analysis was run by BD CELLQuest software.

2.2.8 RNA extraction

RNA was extracted by RNeasy[®] Mini kit from QIAGEN. The 500 μ l of PBS was added in to the cell pellet followed by homogenizing by precellys (6000 rpm, 2x30 sec-pulse, 20 sec-puase). Then, 350 μ l of RLT buffer was added to the cell lysate and mixed by vortexing. Then, 1 volume of 70% ethanol was added to the homogenized lysate and mixed by pipetting. After that, the sample was applied to the RNeasy spin column. The column was centrifuged at 10000xg for 15 seconds. The filtrate was discarded and buffer RW1 was added and the column was centrifuged again at 10000xg for 15 seconds. The filtrate was discarded and DNase mix (The RNase-Free DNase Set, QIAGEN cat. no. 79254) was added. The column was incubated at room temperature for 15 min. The buffer RW1 was added and the column was centrifuged again at 10000xg for 15 seconds. The filtrate was discarded and 500 μ l of RPE buffer was added and the column was centrifuged again at 10000xg for 15 seconds. The filtrate was discarded and 500 μ l of RPE buffer was added and the column was centrifuged again at 10000xg for 2 min. The filtrated was discarded and 30-50 μ l of RNase-free water was added. The column was incubated at room temperature for 10 min. followed by a centrifugation at 10000xg for 1 min. The filtrate consisted of a RNA suspension; ice-cold RNA suspension was quantified and the purity determined using the Nanodrop spectrophotometer. The RNA had an absorbance ratio of A260:A280 between 1.8 and 2.2. The RNA concentration was determined as the mean of three independent spectrophotometric readings. However, the absorbance ratio of A260:A280 does not indicate whether the RNA suspension was contaminated by DNA.

To remove the remaining genomic DNA from RNA, DNase digestion (DNase 1: RNase-free, New England Biolabs, M0303S) was done again. Briefly, the 2-10 μ g of RNA suspensions were added by 2 unit of DNase I in the total reaction volume of 100 μ l and incubate at 37^oC for 10 minutes. The one μ l of 0.5M EDTA (5mM in final concentration) was added to prevent the RNA from degradation and incubated at 75^oC for 10 minutes in order to inactivate the DNase I activity. The treatment was stopped by placing the tube on ice. The RNA suspension was cleaned to remove the protein and excess salt by following the RNA cleanup protocol of QIAGEN. Following this, the 350 μ l of RLT buffer was added to the cell lysate and mixed by vortexing. Then, 250 μ l of absolute ethanol was added to the RNA suspension and mixed by pipetting. After that, the sample was applied to the RNeasy spin column. The column was centrifuged at 10000xg for 15 seconds. The filtrate was discarded and 500 μ l of RPE buffer was added and the column was centrifuged at 10000xg for 15

seconds. The filtrate was discarded and 500 µl of RPE buffer was added and the column was centrifuged again at 10000xg for 2 min. The filtrate was discarded and 30-50 µl of RNase-free water was added. The column was incubated at room temperature for 10 min. followed by a centrifugation at 10000xg for 1 min. The filtrate can be re-loaded into the column and centrifuged at the same speed again in order to increase the RNA yield. RNA was quantified again and the purity determined using the Nanodrop spectrophotometer. RNA with an absorbance ratio of A260:A280 between 1.8 was used for further work.

2.2.9 cDNA synthesis

Each first-strand cDNA synthesis was carried out using the SuperScript™ III Reverse Transcriptase (Invitrogen, USA) according to the manufacturer's recommendations for random primer. The cDNA synthesis was performed on 1.5-2 µg of total RNA in a volume of 20µl. In brief, 50 ng of random hexamer (Promega, USA) and 0.5mM of dNTP mix (Invitrogen, USA) were added to RNA sample. The mixture was heated at 65°C for 5 min and incubated on ice for at least 1 min. Then, the master mix, which is comprised of 5X first-strand buffer (Invitrogen : 250 mM Tris-HCl pH 8.3 at room temperature, 375 mM KCl, 15 mM MgCl₂), 5mM of DTT, 40U of RNaseOUT™ Recombinant RNase Inhibitor (Invitrogen, USA), and 200U of SuperScript™ III RT (Invitrogen, USA), was added to the mixture. The mixture was incubated at 25°C for 10 min followed by 50°C for 50 min. The reaction was terminated by heating at 85°C for 5 min and chilled at 4°C. The cDNA products were diluted into a concentration of 25-50 ng/µl and used them immediately or kept in aliquots at -80°C.

2.2.10 Determination of DNMT gene expression

DNMT gene expression was determined using semi-quantitative RT-PCR. Two µl of cDNA product (50 ng) were taken for PCR amplification. The reaction was in a total volume of 25 µl, which included TaqMan® Fast Universal PCR Master Mix 2X, No AmpErase UNG (Applied Biosystems, USA), 125 nM of probe, 300 nM of each forward primer, and 300 nM of each reverse primer. All Primers were purchased from Sigma (Balada *et al.*, 2008). Taqman probes were used in all cases (Balada *et al.*, 2008). All reactions were run in triplicate in Fast optical 96-well Reaction plates with Barcode sealed with optical adhesive covers (Applied Biosystems, USA) on a StepOnePlus™ Real-time PCR System (Applied Biosystems, USA). Taqman dual probes were labelled with a reporter dye [6-carboxy-fluorescein (6-FAM) or VIC® (Applied Biosystems, USA)] and a fluorescent quencher [6-carboxy-tetramethylrhodamine (TAMRA)]. Forward primers, reverse primers and probe sequences were as follows.

β-actin: 5'-TCACCCACACTGTGCCCATCTACGA-3',
5'-CAGCGGAACCGCTCATTGCCAATGG-3', and

5'-VIC-ATGCCCTCCCCCATGCCATCCTGCGT-TAMRA-3'

DNMT1: 5'-CGGTTCTTCCTCCTGGAGAATGTCA-3',

5'-CACTGATAGCCCATGCGGACCA-3', and

5'-6-FAM-AACTTTGTCTCCTTCAAGCGCTCCATGGTC-TAMRA-3'

DNMT3a: 5'-CAATGACCTCTCCATCGTCAAC-3', 5'-CATGCAGGAGGCGGTAGAA-3', and

5'-6-FAM-AGCCGGCCAGTGCCCTCGTAG-TAMRA-3';

DNMT3b: 5'-CCATGAAGGTTGGCGACAA-3', 5'-TGGCATCAATCATCACTGGATT-3', and

5'-6-FAM-CACTCCAGGAACCGTGAGATGTCCCT-TAMRA-3'.

Thermocycling parameters were: 20 sec at 95°C and 40 cycles consisting of 1 sec at 95°C for denaturation and 20 sec at 60°C for annealing.

2.2.11 Gene expression analysis by microarray

A whole Microarray analysis was processed by Dr Paul R Heath, Department of Neuroscience, SiTRans, University of Sheffield.

2.2.11.1 Sample preparation

RNA was extracted (see section 2.2.8) from F+M+ and F-M- C4-II cells grown for 8 days of three-independent experiments and determined the RNA purity and integrity by Agilent RNA 6000 Nano kit using Agilent 2100 bioanalyzer. The ratio of A260/A280 should be more than 1.8. The ratio of 28S/18S RNA should be more than 1.0 and RNA integrity number (RIN) should be more than 5.0. The higher RIN the more intact the RNA (Schroeder *et al.*, 2006). The RNA of each sample was used for gene microarray target preparation.

2.2.11.2 Microarray target preparation

The target RNA was prepared by using the GeneChip® 3' IVT Express Kit protocol in order to get linear RNA amplification and process T7 *in vitro* transcription. Briefly, the RNA was synthesised to first-strand cDNA containing T7 promoter and then converted into double-strand DNA by the Eberwine or reverse transcription-IVT (RT-IVT) reagents provided by the kit. The double-strand DNA was then transcribed and tagged with biotin-conjugated nucleotide to get cRNA or aRNA (amplified RNA). The aRNA was further purified by magnetic-bead aRNA purification to clean from salts, enzyme, unincorporated NTP, and inorganic phosphate. The biotin-modified aRNA was fragmented into ~800 nucleotides and to be ready for hybridisation.

2.2.11.3 Hybridisation and probe array scan

The biotin-modified aRNA fragment was mixed with hybridisation cocktail followed the GeneChip® Hybridisation, Wash, and Stain Kit protocol and loaded into GeneChip Human Genome U133 Plus 2.0 Array. Each array was comprised of more than 54,000 probe sets which can be used to analyze the human expression level of over 47,000 transcripts. The array was incubated in GeneChip® Hybridisation Oven 640 for 16 hours. After hybridisation, the array chip was washed and stained. The whole steps of washing and staining were all automatically processed by GeneChip® Fluidics Station 450. The array was scanned to define the probe signals and stored as a CEL image file by using GeneChip® Scanner 3000.

2.2.12 Nuclear protein extraction

Nuclear extracts were prepared by using NE-PER® Extraction Reagents. The cytoplasmic and nuclear protein extraction was processed using the reagent volumes indicated in the manufacturer's protocol (**Table 1**) with the volume ratio of CER I: CER II: NER reagents at 200:11:100µl, respectively. The protease inhibitor cocktail solution was added to CER I and NER prior to use and all of the extraction processes were run at 4°C. After trypsinization, the cells were washed twice with PBS and the cell pellets were collected by centrifugation and carefully remove supernatant. The ice-cold CER I reagent was added to the cell pellet and vortexed vigorously for 15 seconds. The cell suspension tube was incubated on ice for 10 minutes. The ice-cold CER II was added to the cell suspension and vortexed on the highest setting for 5 seconds followed by incubation on ice for 1 minute. The cell suspension was vortexed for 5 second s and centrifuged at 16,000xg for 5 minutes. The supernatant (cytoplasmic extract) was transferred to a new pre-chilled tube and placed on ice or stored at -80°C until use. The pellet fraction was suspended with ice-cold NER reagent and vortexed vigorously for 15 seconds every 10 minutes 4 times. The cell suspension was vortexed for 5 seconds and centrifuged at 16,000xg for 10 minutes. The supernatant (nuclear extract) was transferred immediately to a new pre-chilled tube and placed on ice or stored at -80°C until use.

Table 1: Reagent volumes used for different packed cell volumes

Packed Cell volume (µl)	CER I* (µl)	CER II* (µl)	NER I* (µl)
10	100	5.5	50
20	200	11	100
50	500	27.5	250
100	1000	55	500

*CER I = cytoplasmic extraction reagent I, CER II= cytoplasmic extraction reagent II, NER = nuclear extraction reagent

2.2.13 Protein quantification

The BSA protein standard was made to 1.0, 0.75, 0.5, 0.25, 0.125, and 0.0625 mg/ml. The BSA standard series can be kept at 4°C and used for several measurements. Protein quantification was determined by Bio-Rad Bradford assay. The Bio-Rad reagent was diluted in to the ratio of 1:5, and, the samples were diluted in to the ratio of 1:2, 1:4, and 1:8 in distilled water. 4 µl of water (blank), diluted standard, and, samples were pipetted in to a 96-well plate in duplication for standard s and triplication for blank and samples. 200 µl of diluted Bio-Rad reagent were added into each well containing the standards, samples, and blank, mixed by pipetting. Absorbance at 595nm was measured by a microplate reader within 30 minutes. A standard curve of protein concentration was plotted and the protein in the samples quantified using the standard curve.

2.2.14 Determination of DNMT activity

Nuclear extracts were prepared by using NE-PER® Extraction Reagents following the manufacturer's protocol (Thermo Scientific). Protein concentrations of the nuclear extracts were determined by using Bio-Rad protein assay before running the global DNA methyltransferase activity (EpiQuik™ DNA Methyltransferase Activity/Inhibition Assay Kit, Epigentek, USA). The activity assay followed the manufacturer's protocol. Briefly, 3 µl nuclear extracts were incubated with methylation substrate at 37°C for 1.5 hours. The capture antibody was added and incubated at room temperature for 60 min on an orbital shaker. Then, the detection antibody was added and incubated for 30 min. The colour developing solution was added followed by the stop solution. The absorbance was determined by using a microplate reader at 450 nm. The global DNMT activity (O.D./h/mg) was calculated referring to the formula: (Sample OD – blank OD)/(sample protein amount

: $\mu\text{g} \times 1000$), according to manufacturer's instructions. The results are given in activity units detected in treatments (F-M+ and F-M-) relative to the activity level detected in control (F+M+) at day 8.

2.2.15 Determination of cell migration

2.2.15.1 Cell proliferation assay (MTS assay)

Proliferation of C4-II cells cultured in a 96-well plate was determined for 6-technical replicates for each sample. The proliferation rate was investigated by measuring the number of living cells at given time points. The CellTiter 96® AQueous One Solution Reagent (Promega, USA) was used and the measurement was made followed the manufacturer's protocol. The reagent stock was thawed and aliquoted into several 1-ml microcentrifuge tubes and stored at -20°C in the dark. At three hours prior to each given time point, $20\mu\text{l}$ of reagent were added into each well of the 96-well plate containing the cells in $100\mu\text{l}$ of culture medium. The plate was incubated in the dark at 37°C for 3 hours in a humidified, 5% CO_2 incubator. The absorbance at 490 nm was measured using a colorimetric microplate reader. A higher absorbance indicates a higher cell proliferation. The change in cell proliferation was compared with the control at 24-hours.

2.2.15.2 Mitomycin C optimisation

After treatment for 8 days cells were trypsinised and re-plated into 96-well culture plates at a cell density anticipated to give 50-70% confluency after 24hours, Following 3 hours of re-plating, cells were treated with mitomycin C in the range of 0.1-1.0 $\mu\text{g}/\text{ml}$ for 2 hours. The cells were washed with PBS and then the $100\mu\text{l}$ of particular fresh medium was added. Cells were cultured in a humidified incubator at 37°C with 5% carbon dioxide. Prior to 24, 48, and 72-hour culture period (at 21, 45, and 69 hour, respectively), the proliferation was determined (see section 2.2.15.1).

2.2.15.3 Scratch assay

After 8-days treatment C4II cells were trypsinised and re-plated into 96-well culture plates at a cell density anticipated to give 100% confluency by the next day (100,000 cells /well). After the cells reached 100% confluency, the cells were treated with 0.7 $\mu\text{g}/\text{ml}$ of mitomycin C for 2 hours. The cells were washed by PBS and the particular fresh medium was added. The cells were incubated at 37°C for 1 hour and then a straight-line scratch was made for every cultured well by using p200-micropipette tips. The cells were washed twice by PBS to remove cell debris and the particular fresh medium was added. A scratch at 0, 24, and 48 hours was imaged under 4x objective microscope. The width of the scratch was

measured and analysed by using ImageJ program for 20 measurements in at least 6 areas (wells). The cell migration rate was expressed as a percentage of mean gap closure in comparison between control cells, mitomycin C-treated control cells, methyl-donor depleted cells, and mitomycin C-treated methyl-donor depleted cells.

2.2.16 Statistic analysis

Statistical analyses were carried out using SPSS statistics version 20 for Windows. Two-way ANOVA was used to compare treatments for experiments involving more than one time point. The results were considered significant if *P-values* were ≤ 0.05 . Where a significant difference effect of time or treatment was indicated, one-way ANOVA and a Bonferroni or Dunnett T3 post-hoc test was carried out depending on the raw data homogeneity.

Chapter 3 Model development and validation

3.1 Introduction

Methyl donor metabolism plays an important role in both DNA synthesis and methylation. Deficiency in one carbon donors can induce DNA instability (Duthie *et al.*, 2002) and alter methylation (Kim, 2004; Crider *et al.*, 2012) which may in turn affect carcinogenesis (Kim, 2005). In order to study the effect of one carbon donor depletion on cervical cancer development and progression, a cervical cancer cell model of folate and methionine depletion was constructed.

Many models of methyl-donor depletion have been generated both in different animal species and different cell types. These studies differ not only in terms of the model system itself but also the nature and severity of the depletion and the outcomes of interest. Several studies in *in vitro* models have been developed. Duthie *et al.* (2000a) investigated the effect of folate deficiency on uracil misincorporation and DNA methylation level in immortalized normal human colon epithelial cells. They reported a decrease in DNA stability was in cells at folate concentrations associated with folate concentrations found in human plasma (1-10ng/ml), but DNA hypomethylation was not folate concentration dependent. In 2001, Chern *et al.* (2001) conducted a folate-depletion study in HepG2 cells and suggested that the accumulation of homocysteine in cells depleted of folate led to oxidative stress and apoptosis (Chern *et al.*, 2001). Similarly, Novakovic *et al.* (2006) demonstrated that the expression of 5 and 12 genes involved in apoptosis were altered in folate-deficient human colon adenocarcinoma cell lines, HCT116 and Caco-2 cells, respectively. However, there was only one gene, baculoviral IAP repeat-containing 3 (*BIRC3*; apoptosis inhibitor), which was altered in the same direction (up-regulation) in this study (Novakovic *et al.*, 2006).

The investigation of the one-carbon homeostasis resulting from folate deficiency is another focus of interest. A study in breast cancer cells, MCF-7/MR, of Ifergan *et al.* in both long-term (Ifergan *et al.*, 2004) and short-term folate deficiency (Ifergan *et al.*, 2005) demonstrated almost total loss of breast cancer resistance protein (BCRP/ABCG2) and only 14% remaining in plasma membrane, respectively. BCRP is the transporter proteins, which exports folate mono-, di-, and triglutamate. Down-regulation of this protein was reported to increase [³H] folic acid accumulation in an experimental model and was associated with an increase in polyglutamate synthetase activity (FPGS: catalyses the conversion of folate to polyglutamate). This study suggested cell adaptation to manage the folate pool. An alteration of the transcript levels of genes related to folate metabolism was observed in folate deficient human colonic epithelial cell model was also determined by Hayashi *et al.* (2007).

They demonstrated the up-regulation of folate receptor (FR- α), FPGS, methylenetetrahydrofolate reductase (MTHFR) and DNMT1, and the down-regulation of reduced-folate carrier (RFC), thymidylate synthase (TS), methionine synthase reductase (MTRR), DHFR, serine hydroxymethyltransferase (SHMT), methionine synthase (MTR), and methyl DNA-binding domain protein 2 (MBD2) in HCT116, but these results different in some respects in Caco-2 cells. In Caco-2 cells, gene changes suggested that folate deficiency increased folate uptake and reduced folate hydrolysis. The authors also suggested that HCT116 adaptation indicated a preference of the shuttle of the flux of one-carbon units to the methionine cycle rather than nucleotide synthesis pathway (Hayashi *et al.*, 2007).

There have been a few studies of methionine-deficiency in *in vitro* models of the central nervous system tumour cell lines which found an alteration of gene in cell cycle checkpoints, proapoptotic pathways, and DNA repair (Kokkinakis *et al.*, 2004; Najim *et al.*, 2009) and pancreatic tumour cell lines which found a disruption of mitosis and enhanced cell cycle arrest (Kokkinakis *et al.*, 2005). Studies of combined methyl-donor depletion have been mostly conducted in animals and found an impact on liver such as an alteration of global DNA methylation and abnormal liver metabolism (Pogribny *et al.*, 2004; Ghoshal *et al.*, 2006; Romestaing *et al.*, 2008).

It is clear that there is a diversity of interest in terms of effects of moderate or severe methyl donor depletion on various functional outcomes and therefore the findings from these various model systems have only limited comparability. Our interest lies primarily in the importance of methyl donor status to cervical cancer risk and cancer progression. To our knowledge there have been no studies of methyl donor depletion in cervical cancer cells.

In this study, folate and methionine were the focus of interest, partly because they have a very close relationship in their metabolism, also because we have previous experience of the effects on the methyl cycle of depletion of one or both these methyl donors (Nakano *et al.*, 2005). Two cervical cancer cell lines were chosen, C4-II and SiHa cells. These two cervical cancer cell lines are derived from different sources and harbour different types of high risk HPV. The intention was to develop a model of moderate methyl donor depletion.

The proposal was to deplete cells of folate or folate and methionine, by culturing in media deficient in these substrates, to confirm a methyl donor-depleted state and to determine functional impact on the methyl cycle.

3.2 Aims

To develop a cervical cancer cell model of folate and combined folate and methionine depletion, to determine effects on growth characteristics and to validate the model by examination of intracellular folate concentration, intracellular methionine concentration, and homocysteine export.

3.3 Methods

3.3.1 Determination of cell growth and cell characteristics

C4-II and SiHa cells were thawed (see section 2.2.1.1) and a culture maintained through subculturing, as described (see section 2.2.1.2). Cells were transferred to appropriate culture containers and medium for the determination of cell growth and cell characteristics (see section 2.2.2). Cell size was examined by measurement of cell diameter (in pixel scale) from cell images using ImageJ software. Twenty cells were randomly chosen and measured from one area and the mean cell diameter of ten areas was reported.

3.3.2 Methyl-donor depletion

3.3.2.1 Combined folate and methionine depletion

In the first instance, a model of one-carbon donor depletion was established to maximize the likelihood of an effect on global DNA hypomethylation at a later date. C4-II and SiHa cells were cultured as 20,000 cell /cm² for 12-20 days in two types of media in parallel: complete medium (F+M+) and folate and methionine-depleted medium (F-M-). Cell growth was observed every day and one flask of cultured flasks was chosen for cell counting every 3-5th day for 12-20 days (see section 2.2.2).

3.3.2.2 Differentiation of the effects of folate depletion alone from methionine depletion alone

To differentiate the effects of folate depletion alone from methionine depletion alone, C4-II cells were cultured for 12-20 days in four types of media in parallel: complete medium (F+M+), folate and methionine-depleted medium (F-M-), folate and methionine-depleted medium to which folinic acid was added to a concentration of 900 nM (F+M-), and, folate and methionine-depleted medium to which L-methionine was added to a final concentration of 300 μM (F-M+). The growth rates were compared by cell counting (see section 2.2.2).

3.3.2.3 Folate depletion, and, folate and methionine depletion

C4-II and SiHa cells were cultured for 12-20 days in three types of media in parallel: complete medium (F+M+), folate and methionine-depleted medium (F-M-), and, folate and

methionine-free medium + 300 μ M L-methionine (F-M+). The growth rates were compared by cell counting (see section 2.2.2).

3.3.3 Measurement of intracellular folate

More than 5 million cells were harvested on days 4, 8 and 12 of culture for C4-II cells, and at week 2, 4 and 6 for SiHa cells. Cells were prepared for the measurement of intracellular folate as described (see section 2.2.3), using an automated competitive folate protein binding assay (Beckman Access Kit). Intracellular folate concentration was expressed as pmol/ 10^6 cells.

3.3.4 Measurement of intracellular methionine (C4-II only)

More than 20 million cells were harvested on days 4, 8 and 12 of culture for C4-II cells only. Cells were prepared for the measurement of intracellular methionine and sent to the Department of Clinical Chemistry, Sheffield Children's Hospital (see section 2.2.4). Intracellular methionine was measured using a Biochrom amino acid analyzer and expressed as pmol/ 10^6 cells.

3.3.5 Measurement of homocysteine

To determine intracellular homocysteine and extracellular homocysteine, cells were harvested and the culture medium was collected on days 0, 4, 8, and 12 of culture for C4-II cells or at 70-80% confluence of SiHa cells after 2, 4, and 6 passages (week 2, 4, and 6) in each treatment. Intracellular homocysteine and extracellular homocysteine were measured by HPLC (see section 2.2.5).

3.3.6 Statistical analysis

See section 2.2.16 and the Mann-Whitney U test was used for comparison between two samples.

3.4 Results

3.4.1 Cell characteristics

Figure15 shows the mean C4II cell number over 20 days from three independent experiments. Results from three-independent experiments showed that the number of C4-II cells doubled every 3 or 4 days of culture. Growth was exponential from the fourth day of culture.

C4-II cells reached 100% confluence by day 10 of culture. Cells were observed to form diffuse monolayer colonies with domes and pile up in post-confluence from day 10 (**figure 16**)

SiHa cells were initially grown in DMEM to determine growth rate. The results are from one experiment using the same seeding density as for C4-II cells. **Figure 17** shows SiHa cell growth and shows that SiHa cells double at approximately the same rate as C4-II. However, unlike C4-II cells, SiHa cells entered a plateau phase after day 10. Moreover, SiHa cells maintain a monolayer throughout the culture period, with few floating cells. **Figure 18** shows images of SiHa cells at three time points. SiHa cells reached 100% confluence by day 8.

3.4.2 Effect of methyl-donor depletion on cell growth

3.4.2.1 Folate and methionine depletion

Figure 19 shows the growth of C4-II cells over 20 days, when grown in complete medium and folate and methionine-deplete medium. C4-II cells grown in complete medium reached 100% confluence by day 8-10, after which the cells started to pile up in multilayers. C4-II cells cultured in folate and methionine-depleted medium also reached 100% confluence by day 8-10, but after which the cells still appeared as a monolayer. There was a difference of 40 and 50 million cells between treatments by the end of day 15 and 20, respectively, and by day 20 the number of cells in the depleted medium was only 30% of that of cells grown in the complete medium. By day 12, folate and methionine-deplete cells were growing more slowly and this persisted to day 20 ($P < 0.05$).

Figure 20 shows the results from three growth experiments using SiHa cells. Cells grown in folate and methionine-deplete medium appeared to grow at the same rate as cells grown in complete medium, until day 12. From day 18, there was a fall in cell number in the depleted cells. By day 20, the cell number in folate and methionine-depleted medium was about 30% lower than for cells grown in complete medium ($P < 0.05$).

3.4.2.2 Differentiation of the effects of folate depletion alone from methionine depletion alone (C4-II only)

In the first instance, C4-II cells were cultured in four different media; complete medium (F+M+), folate-depleted medium (F-M+), methionine-depleted medium (F+M-), and folate and methionine-depleted medium (F-M-). **Figure 21** shows growth rate during 20 days of culture.

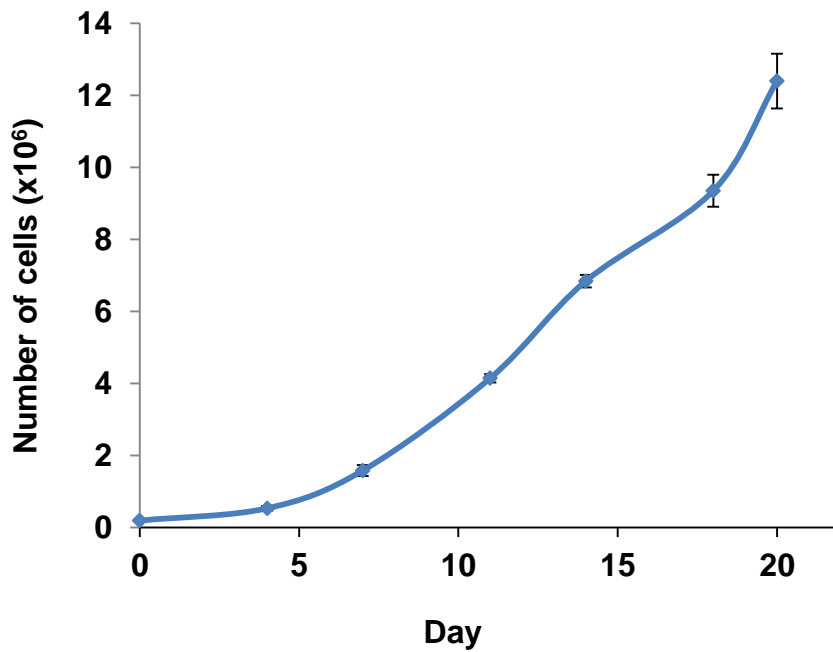


Figure 15: Growth of C4II cells cultured in complete medium for 20 days

Each value shows mean of three-independent experiments and error bars show SEM.

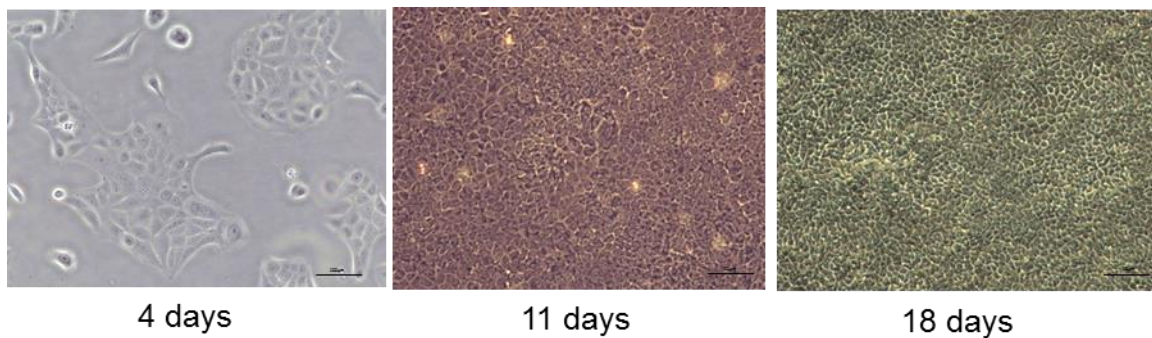


Figure 16: Characteristics of C4-II cells after 4, 11 and 18 days of culture

All of the images were taken under 10x objective lens.

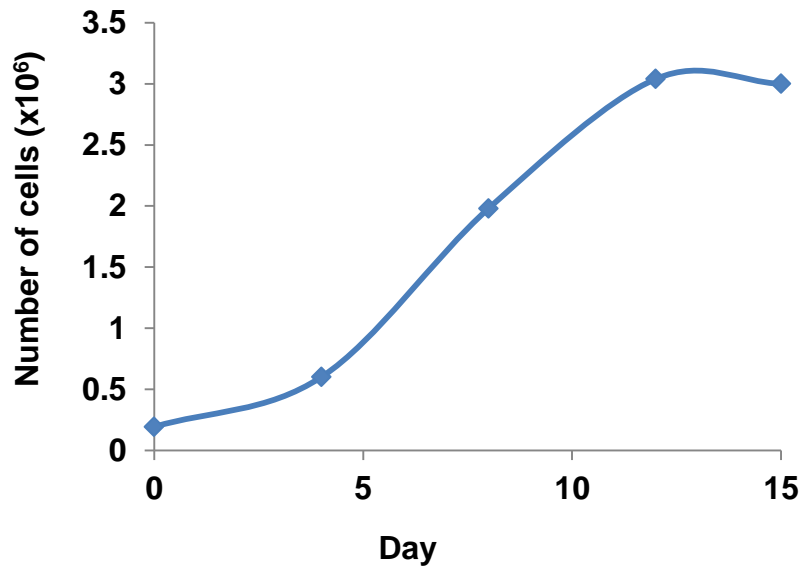


Figure 17: *Growth of SiHa cells cultured for 15 days in complete medium*

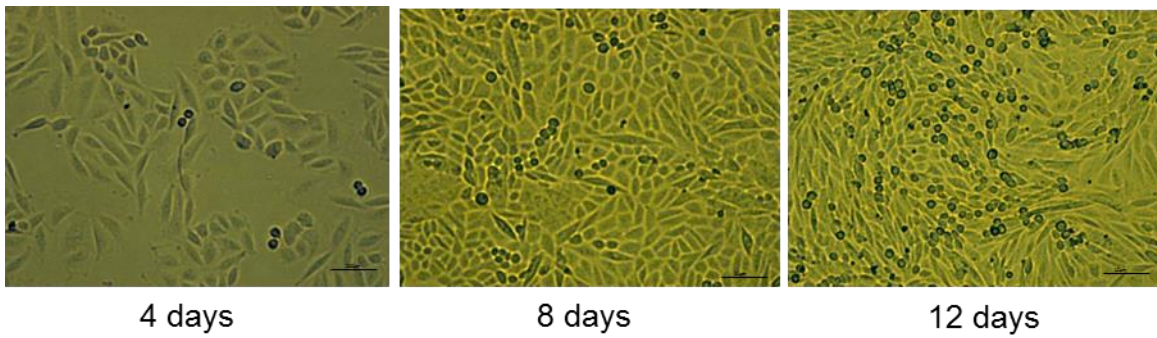


Figure 18: *Characteristics of SiHa cells after 4, 8 and 12 days of growth in complete medium*

All of the images were taken under 10x objective lens.

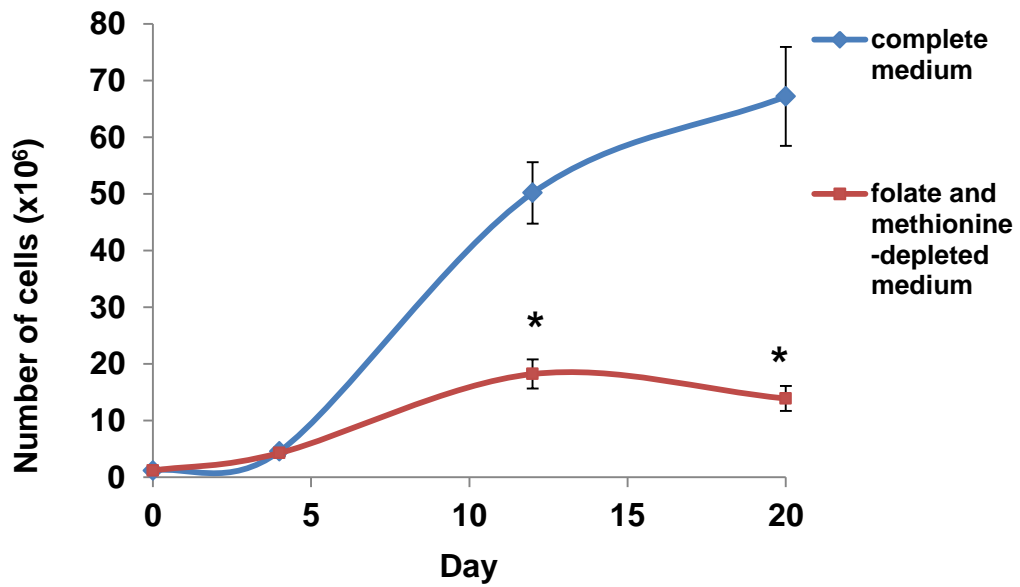


Figure 19: The growth curves of C4-II cells grown in folate and methionine-depleted medium compared with controls

Each value shows mean of three-independent experiments and error bars show SEM.
 *Cell number significantly different between treatments, $P < 0.05$ (Mann-Whitney U test).

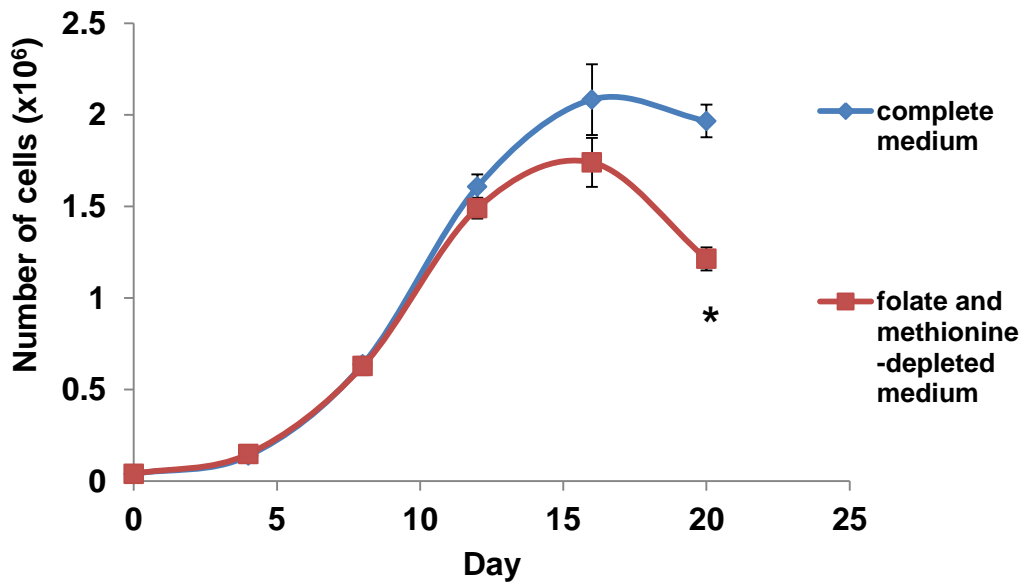


Figure 20: The growth curves of SiHa cells growing in folate and methionine-depleted medium compared with controls

Each value shows mean of three-independent experiments and error bars show SEM.
 *Cell number significantly different between treatments, $P < 0.05$ (Mann-Whitney U test).

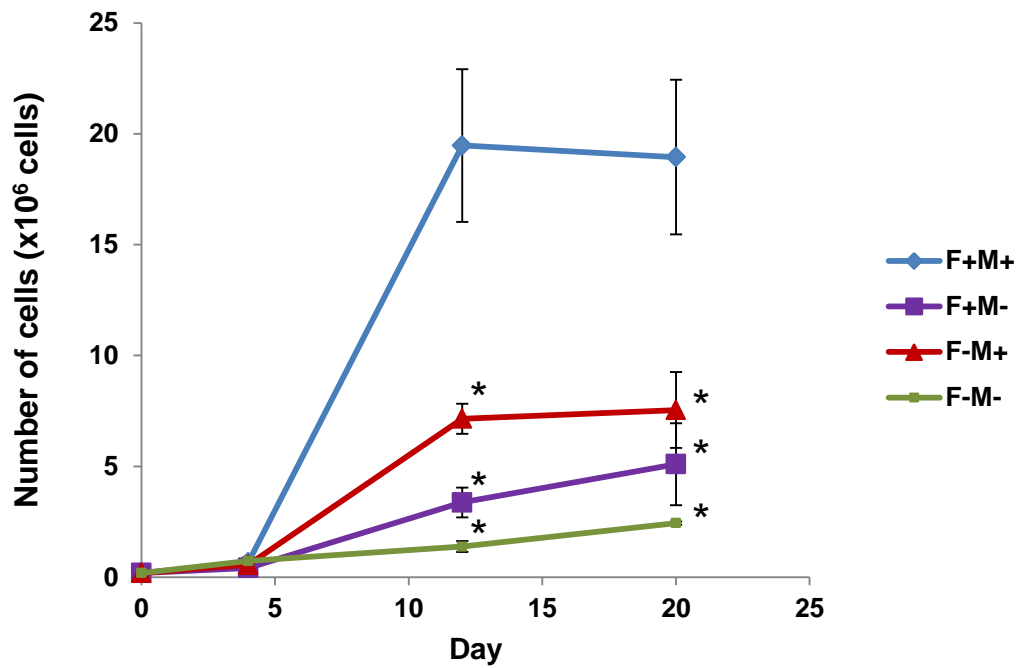


Figure 21: Effects of methyl donor depletion on growth of C4-II cells

Each value shows mean of three-independent experiments and error bars show SEM.

* Cell number significantly different from control, $P < 0.05$ (one-way ANOVA, post hoc test).

Growth was significantly influenced by time ($P < 0.001$) and treatment ($P < 0.001$), and a significant interaction occurred between these factors ($P < 0.001$). Cells appeared to grow at a similar rate under each of the four conditions, up to day 4, from which time cells grown in the complete medium appeared to grow faster than cells grown in either of the deplete media (**figure 21**). At day 12, there was a greater number of cells when grown in complete medium than under any other condition ($P < 0.01$) but the number of cells grown in the three depleted conditions did not differ from each other. This effect of treatment was also seen at day 20; there was a greater number of cells when grown in complete medium than all other conditions ($P < 0.05$) but the number of cells grown in those three depleted conditions did not differ from each other.

From three independent experiments, it was observed that a combined folate and methionine depletion was associated with a lower mean growth rate than for folate or methionine alone, even though this did not reach statistical significance. It was decided that further experiments would focus on folate depletion alone, and combined folate and methionine depletion.

3.4.2.3 Determination of effects on growth of folate depletion alone, and combined folate and methionine depletion

The effect of folate depletion alone on growth rate was determined in three independent experiments for C4-II and SiHa cells. Because of the tendency of C4-II cells to grow in a multilayer after 12 days all further experiments using these cells were carried out up to day 12 only. C4-II cells were grown in T75 flasks while SiHa cells were grown in 24-well plates, but in the same seeding ratio-20,000 cell/cm². **Figure 22A**) and **22B**) show the results for C4-II and SiHa cells, respectively. C4-II cells grown in complete medium gave the highest growth rate. By day 12, cell mean number was lowest for cells grown in folate and methionine-depleted medium, intermediate for cells grown in folate-deplete medium and highest for cells grown in complete medium.

In C4-II cells cell growth was significantly influenced by time ($P < 0.001$) and treatment ($P < 0.001$), and a significant interaction occurred between these factors ($P < 0.001$). C4-II cells appeared to grow at a similar rate under each of the three conditions, up to day 4, from which time cells grown in the complete medium appeared to grow faster than cells grown in either of the deplete media (**figure 22A**). One-way ANOVA and post hoc analysis with treatment as factor on day 8 showed a significantly greater number of cells grown in complete medium than that in folate and methionine-deplete medium ($P < 0.001$), and the cell number for cells grown in folate deplete medium was greater than that in folate and methionine deplete medium ($P = 0.017$). At day 12, the growth rate was significantly different

for all three treatments ($P < 0.001$). The doubling time (DB) of cells grown in combined folate and methionine depleted medium was 5.08 days compared with 2.77 days for control cells and 3.62 day for folate-depleted medium.

Growth of SiHa cells was influenced by time ($P < 0.001$), treatment ($P < 0.001$), and a significant interaction occurred between these factors ($P < 0.001$). SiHa cells appeared to grow at a similar rate under each of the three conditions, up to day 12, from which time cells grown in the folate and methionine-depleted medium grew more slowly, and by day 20, there was a lower cell number than for other treatments ($P < 0.001$) (**figure 22B**). The doubling time (DB) of SiHa cells grown in complete, folate-depleted, and, folate and methionine-depleted medium were 2.46 days, 2.52 days, and 2.57 days, respectively.

The cell size of C4-II cells grown in folate and methionine deplete medium was greater than the complete medium and folate deplete medium after 8 days of culture (**figure 23**). Two-way ANOVA showed effects of time and treatment ($P < 0.001$) and a significant interaction between the two factors ($P < 0.001$). From day 4 until day 12 there was a significant decrease in cell size for cells grown in either the complete medium or the folate deplete medium. In contrast, cells grown in the folate and methionine deplete medium increased in size from day 4 until day 8. As a result, by day 8, cells grown in the folate and methionine depleted medium were larger than those grown in complete medium or folate deplete medium, and this was also evident at day 12 (**figure 24**). The cell size and morphology of SiHa cells grown in all three media were similar throughout culture period (**figure 25**).

Growth of SiHa cells seemed resistant to growth in folate and methionine-depleted medium and therefore, in order to determine long-term effects, SiHa cells were exposed to long-term depletion for 6 weeks with subculture at 70-80% cell confluence every week.

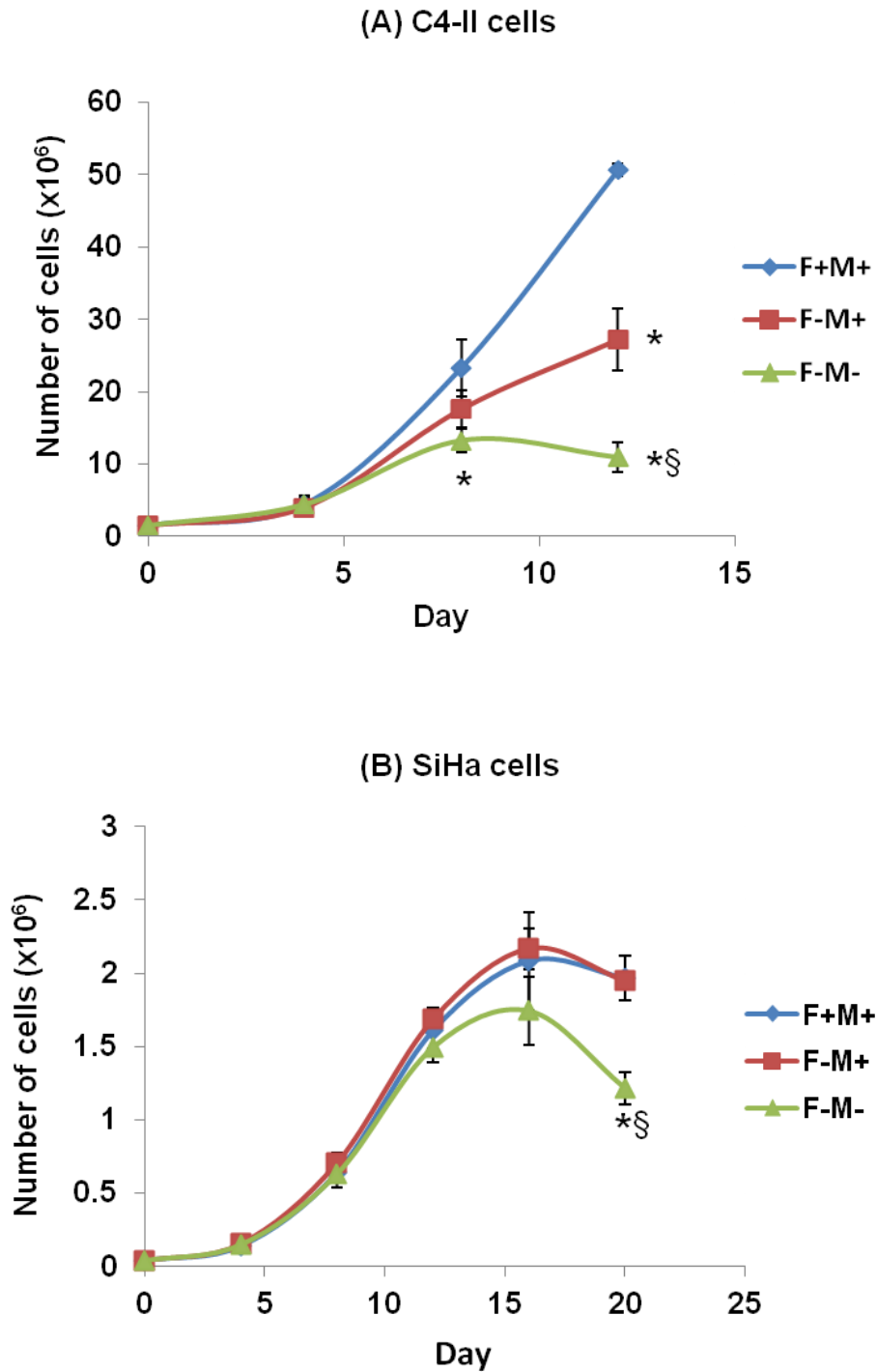


Figure 22: Growth of C4-II cells (A), and SiHa cells (B) in complete medium, folate-deplete and combined folate and methionine-deplete medium

Each value shows mean of three-independent experiments and error bars show SEM.
 *Significantly different from control, $P < 0.05$, § significantly different from F-M+, $P < 0.05$ (one-way ANOVA, post hoc test)

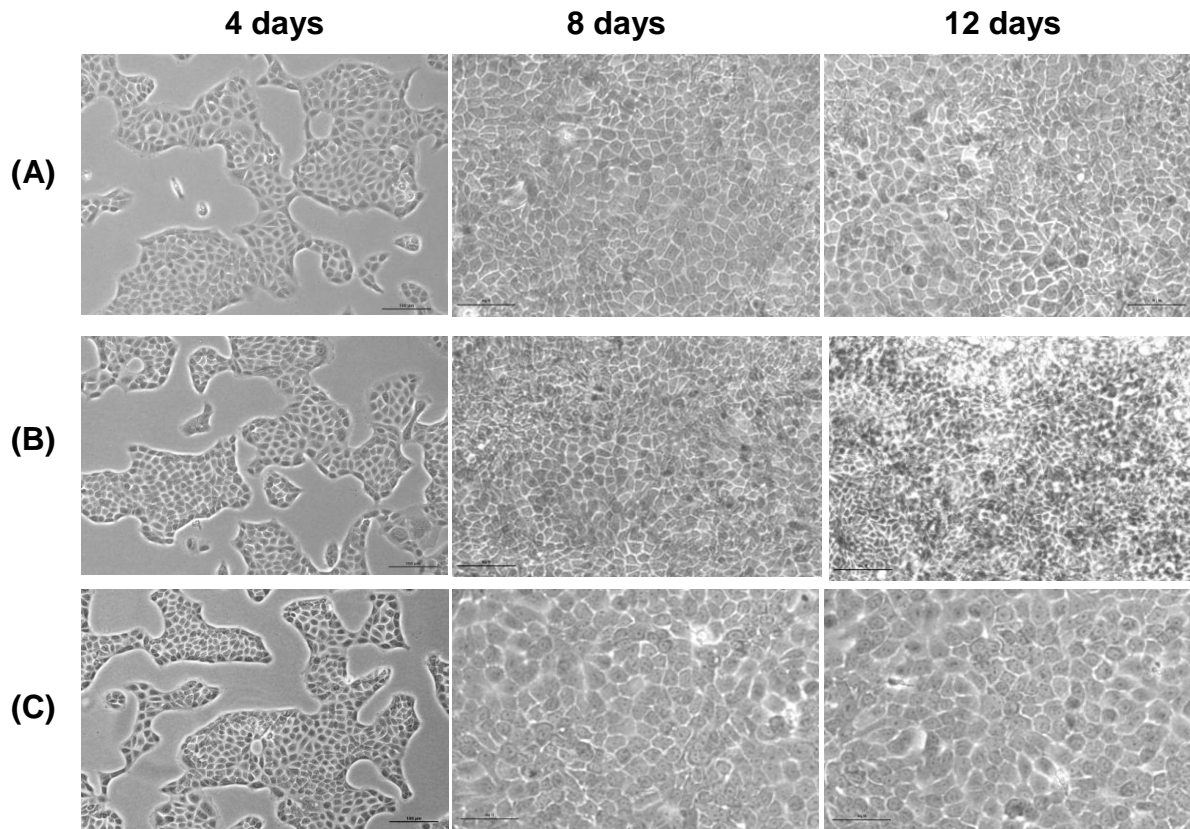


Figure 23: Characteristics of C4-II cells grown in (A) F+M+ (B) F-M+, and (C) F-M- after 4, 8 and 12 days of culture

All of the images were taken under 10x objective lens.

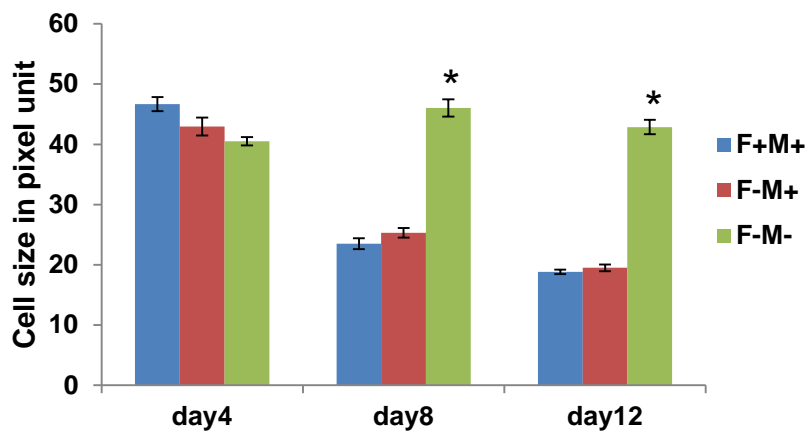


Figure 24: Cell size of C4-II cells grown in F+M+, F-M+, and F-M- after 4, 8 and 12 days of culture

Each value shows mean cell diameter from ten measurements and error bars show SEM. *significantly different from control and F-M+, $P < 0.05$ (one-way ANOVA, post hoc test)

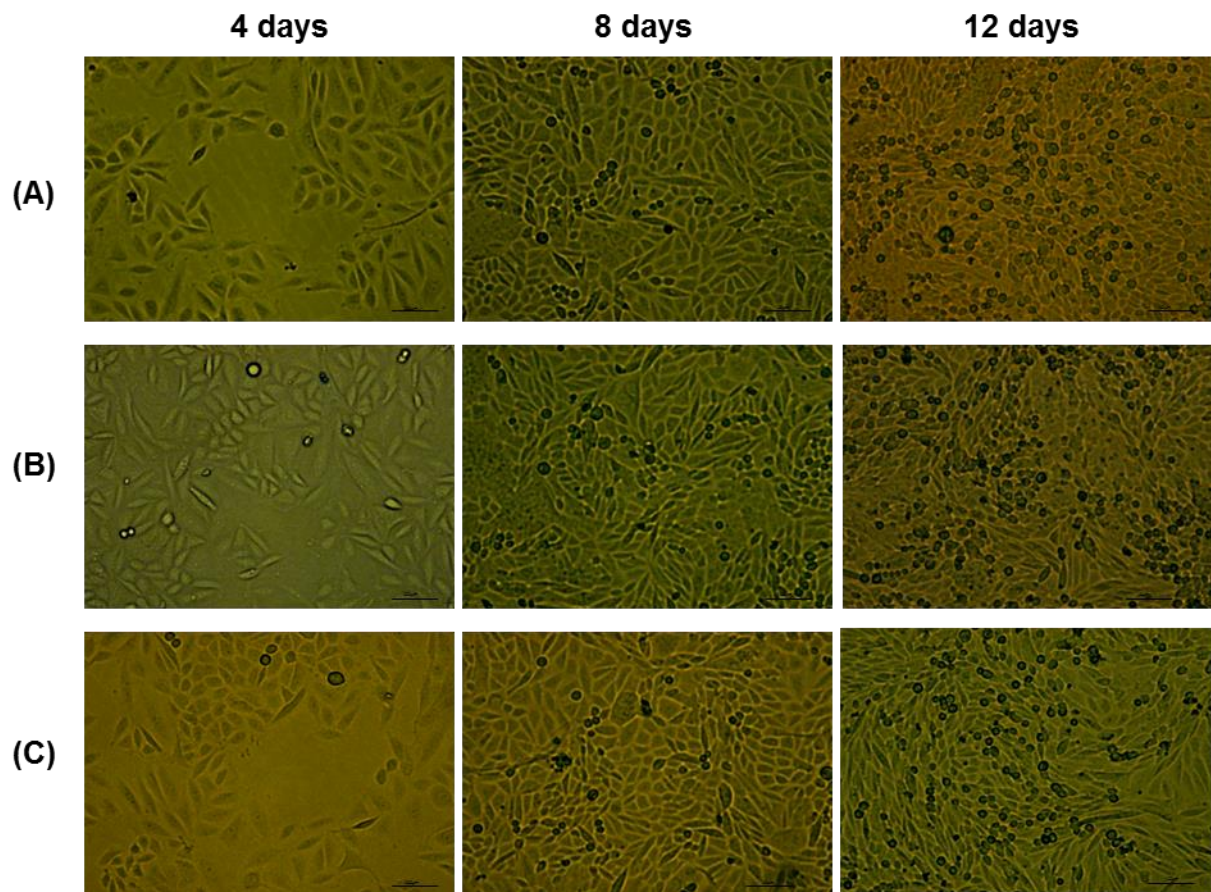


Figure 25: Characteristics of SiHa cells grown in (A) F+M+ (B) F-M+, and (C) F-M- after 4, 8 and 12 days of culture

All of the images were taken under 10x objective lens.

3.4.3 Effect of methyl donor depletion on intracellular folate concentration

For the cell lysate preparation, it was anticipated from experience with other cultured cells that a large number of cells would have to be available for the measurement of intracellular folate (more than 5×10^6 cells). To make the data comparable, intracellular folate concentration was corrected for cell number and calculated as nmol/ 10^6 cell or pmol/ 10^6 cell.

Intracellular folate fell by 90% within 4 days of culture of C4-II cells in folate –deplete or folate and methionine-deplete medium. C4-II cells grown in either folate-deplete or folate and methionine-deplete medium for only 4 days had an intracellular folate concentration of 0.1-0.3 pmol/ 10^6 cells compared with 2 pmol/ 10^6 cells in cells grown in complete medium (**figure 26**). Two-way ANOVA showed a significant effect of time and treatment on intracellular folate concentration ($P < 0.001$) and a significant interaction between these factors ($P < 0.001$). On day 4, 8, and 12 cells grown in folate deplete or folate and methionine deplete medium had significantly lower intracellular folate concentration than control cells ($P < 0.001$), but were not different from one another.

Intracellular folate concentration was lower at day 12 than day 4 for cells grown in folate and methionine deplete medium ($P = 0.036$), and lower at day 12 from that at day 8 for cells grown in folate deplete medium ($P = 0.05$). There was an unexpectedly higher folate concentration at day 8 compared with day 4 and day 12 in cells grown in complete medium ($P = 0.001$).

Since the preliminary experiments had indicated that growth of SiHa cells was relatively resistant to methyl donor depletion, effects of long term growth in folate-depleted medium were determined. The folate concentration in SiHa cells grown in complete, folate-deplete, and folate and methionine deplete medium was measured for one experiment after 6 passages (42 days), in cells at 70-80% confluence. **Figure 27** shows that intracellular folate in cells grown in both folate-deplete, and folate and methionine-deplete medium decreased to only about 2% of that in control cells. Further work was then carried out to determine how quickly SiHa cells become folate-deplete in order to establish the model.

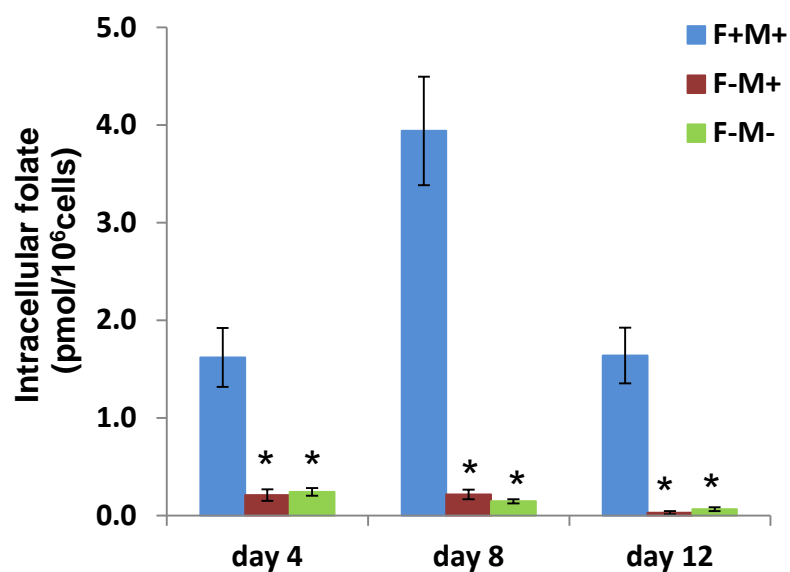


Figure 26: Intracellular folate concentration of C4-II cells grown in folate and methionine-depleted medium and complete medium

Each value shows mean values from three-independent experiments and error bars show SEM.

* Intracellular folate concentration was significantly different from control, $P < 0.05$ (one-way ANOVA, post hoc test)

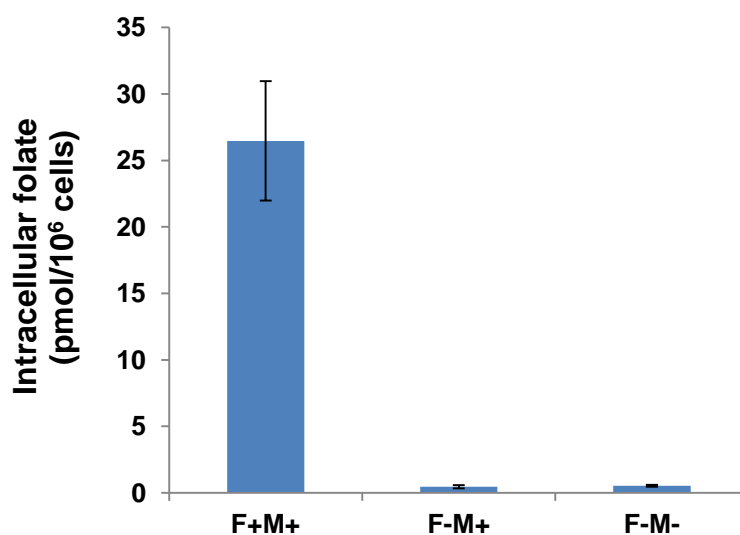


Figure 27: Intracellular folate concentration of SiHa cells grown in complete, folate-deplete, and, folate and methionine-depleted medium after 6 passages (42 days)

Each value shows mean values for two technical replicates from one experiment and error bars show SD.

A lower intracellular folate concentration was observed in SiHa cells after 6 passages of growth in folate and methionine-deplete medium, an experiment was set up to determine how quickly SiHa cells became folate-depleted. Cells were grown for 6-weeks and harvested every 2 weeks for the measurement of intracellular folate. **Figure 28** compares intracellular folate concentration of SiHa cells grown in three different conditions for a long term depletion. There was a significant effect of treatment on intracellular folate concentration ($P < 0.001$). At weeks 2, 4 and 6, cells grown in folate deplete and folate and methionine deplete medium had significantly lower intracellular folate concentration than control cells ($P < 0.001$), but were not different from one another. Folate concentrations were not different between weeks 2, 4 and 6.

3.4.4 Effect of methyl donor depletion on Intracellular methionine concentration

The intracellular methionine concentration was measured in only the C4-II cells because, at the time SiHa cells were still under study the measurement was not available. By the time the measurement was available, the SiHa cells were no longer under study. Time ($P = 0.05$) and treatment ($P = 0.001$) influenced the intracellular concentration of methionine. In C4-II cells grown in folate and methionine depleted medium showed a reduction in intracellular methionine from about 300 pmol/ 10^6 cells in control cells to 100 pmol/ 10^6 cells at day 4 (**figure 29**) and a further decrease to about 30 pmol/ 10^6 cells at day 8. Intracellular methionine was lower in folate and methionine-depleted cells than that in control ($P < 0.002$) and in folate-depleted cells ($P < 0.001$) on day 4 and day 8 ($P = 0.026$).

However, unexpectedly, at day 12 there was no significant difference in intracellular methionine concentration between treatment. One-way ANOVA with time as factor and post hoc analysis showed that intracellular methionine concentration was higher at day 12 than day 8 for cells grown in folate and methionine deplete medium ($P = 0.05$). However, unexpectedly, there was an increase in methionine between day 8 and 12 in cells grown in methionine-depleted.

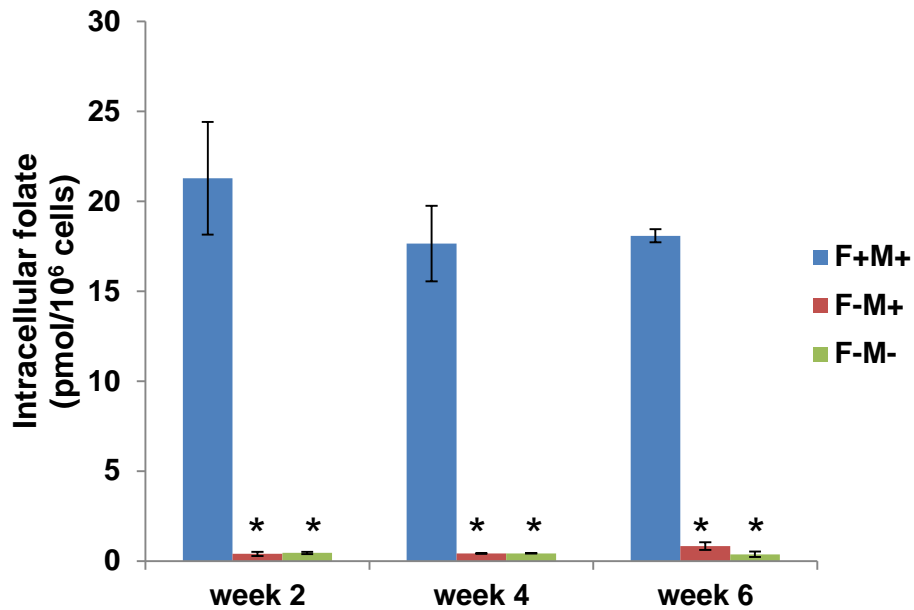


Figure 28: Intracellular folate concentration of SiHa cells grown in folate-deplete, folate and methionine depleted medium and complete medium

Each value shows the mean value from three-independent experiments and error bars show SEM.

* Intracellular folate concentration was significantly different from control, $P < 0.05$ (one-way ANOVA, post hoc test)

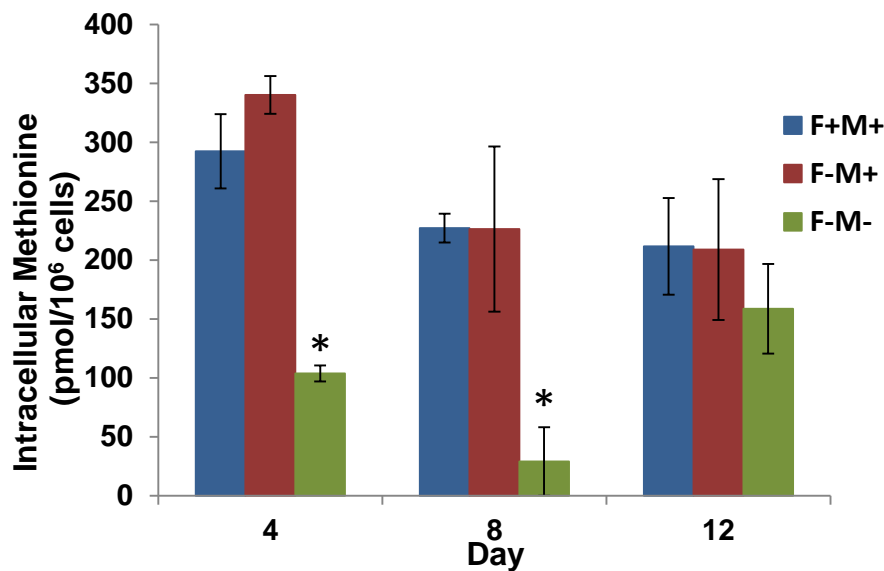


Figure 29: Intracellular methionine concentration of C4-II cells grown in folate and methionine depleted medium, folate-depleted medium, and, complete medium

Each value shows mean of three-independent experiments and error bars show SEM.

*Intracellular methionine concentration was significantly different from control, $P < 0.05$ (one-way ANOVA, post hoc test).

3.4.5 Effect of methyl donor depletion on intracellular and extracellular homocysteine

Intracellular homocysteine in C4-II cells

Elevated homocysteine concentration in the medium of cultured cells is an indicator of functional folate deficiency (Ueland *et al.*, 1993; Zittoun & Zittoun, 1999). This reflects accumulation of homocysteine intracellularly, due to a failure to remethylate homocysteine to methionine.

Table 2 shows the intracellular homocysteine concentration of C4-II cells expressed as $\mu\text{mol/L}$. There was an effect of time ($P < 0.001$) on homocysteine concentration, but no discernible trend. Unexpectedly, mean homocysteine concentration was lower at day 8 than at other time points ($P < 0.01$). The intracellular homocysteine of C4-II cells was not significantly different across the three treatments at any time point.

Table 3 shows intracellular homocysteine concentration of C4-II cells expressed as $\text{pmol}/10^6$ cells. Expressed in this way the mean homocysteine concentration was lower at day 8 than at other time points (as shown when expressed as $\mu\text{mol/L}$) but there was no significant difference across the three treatments at any time point. However, the concentration of intracellular homocysteine was extremely low, close to the lowest limitation of this method ($1.0\text{-}200 \mu\text{mol/L}$). Therefore, results need to be interpreted cautiously.

Table 2: *Intracellular homocysteine concentration ($\mu\text{mol/L}$) of C4-II cells grown in complete, folate-deplete, and folate and methionine-deplete medium*

Day of culture	Intracellular homocysteine ($\mu\text{mol/L}$)		
	F+M+ medium (mean \pm SEM)	F-M+ medium (mean \pm SEM)	F-M- medium (mean \pm SEM)
0	4.78 \pm 0.076	4.78 \pm 0.076	4.78 \pm 0.076
4	5.76 \pm 0.57	5.53 \pm 0.62	6.08 \pm 0.53
8	1.48 \pm 0.68*	3.18 \pm 0.48*	1.56 \pm 0.33*
12	7.74 \pm 0.54	8.49 \pm 0.64	6.70 \pm 0.64

*Values are mean values from three experiments. *significantly lower than other time points, $P < 0.01$ (one-way ANOVA, post hoc test).*

Table 3: Intracellular homocysteine concentration (pmol/10⁶ cell) of C4-II cells in complete, folate-deplete, and, folate and methionine-deplete medium

Day of culture	Intracellular homocysteine (pmol/10 ⁶ cells)		
	F+M+ medium (mean ± SEM)	F-M+ medium (mean ± SEM)	F-M- medium (mean ± SEM)
0	35.9 ± 0.58	35.9 ± 0.58	35.9 ± 0.58
4	47.6 ± 3.29	43.3 ± 3.75	42.4 ± 3.92
8	5.6 ± 0.42*	35.8 ± 1.34	1.6 ± 0.29*
12	31.4 ± 6.35	39.6 ± 1.62	51.9 ± 2.94

Values are mean values from three experiments. *significantly lower than other time points, $P < 0.01$ (one-way ANOVA, post hoc test).

Extracellular homocysteine C4-II cells

Figure 30 shows the homocysteine concentration in the medium when C4-II cells were grown under different conditions. Two-way ANOVA showed a significant effect of time and treatment on extracellular homocysteine concentration ($P < 0.001$) and a significant interaction between these factors ($P < 0.001$). At day 8 the concentration of homocysteine in the medium was greater for cells grown in folate-deplete medium than for cells grown in complete medium ($P = 0.001$), and greater than for cells grown in folate and methionine depleted medium ($P = 0.004$). At day 12, the concentration of homocysteine in culture medium of folate and methionine depletion was greater than of that in control ($P = 0.011$). The mean homocysteine concentration in the medium increased from day 4 to day 12 for cells grown in folate depleted medium ($P < 0.001$). The homocysteine concentration in the medium of cells grown in complete ($P = 0.001$) and folate and methionine depleted medium ($P = 0.002$) increased from day 4 to day 8, but showed no further increase thereafter.

Intracellular homocysteine SiHa cells

When considering the experiment for SiHa cells it was anticipated from experience with C4-II cells that a very large number of cells would have to be available for the measurement of intracellular homocysteine (more than 20×10^6 cells). For this reason, one single experiment was carried out in which intracellular homocysteine concentration was measured in cells at 70-80% cell confluence after 6 passages (42 days) when grown in complete, folate-deplete and folate and methionine-deplete medium. Homocysteine

concentration was measured in technical triplicates and shown in **figure 31**. Concentrations were similar to those observed for C4-II cells.

Mean concentrations of intracellular homocysteine, for both C4II cells and SiHa cells, were extremely low, close to the lower limit of this assay (range 1.0-200 $\mu\text{mol/L}$), and therefore the results need to be interpreted cautiously.

Extracellular homocysteine SiHa cells

Figure 32 shows extracellular homocysteine following growth of SiHa cells in different media over long-term culture. Two-way ANOVA showed a significant effect of treatment on extracellular homocysteine concentration ($P < 0.001$). The concentration of homocysteine in the medium was greater for cells grown in folate-depleted medium and folate and methionine depleted medium than for cells grown in complete medium ($P < 0.05$) at weeks 2 to week 6, but were not different from one another.

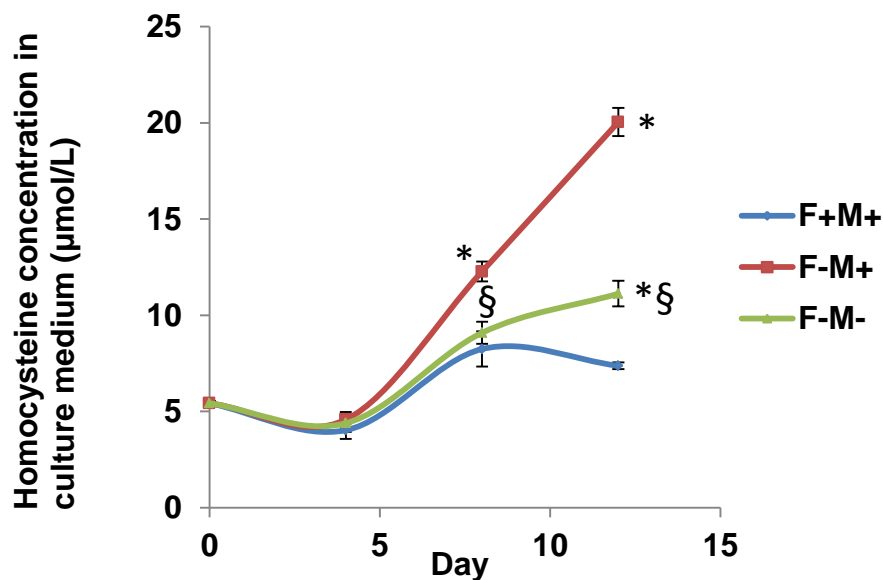


Figure 30: Extracellular homocysteine concentration of C4-II cells cultured in complete, folate-deplete, and, folate and methionine-deplete medium

Each value shows mean of three-independent experiments and error bars show SEM.
 * Significantly different from control, $P < 0.05$. § significantly different from F-M+, $P < 0.05$ (one-way ANOVA, post hoc test)

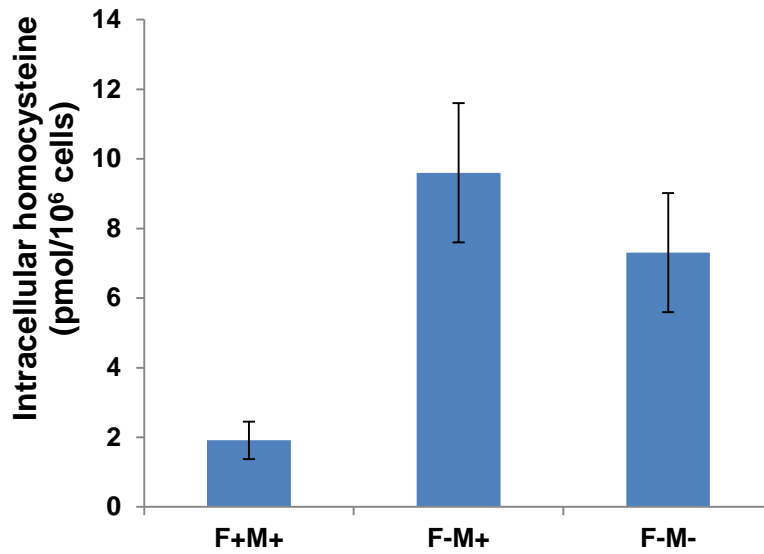


Figure 31: Intracellular homocysteine of SiHa cells grown in complete, folate-deplete, and, folate and methionine-deplete medium for 6 passages (42 days)

The values are expressed as pmol/10⁶ cells.

Each value shows mean values for technical replicates from one experiment and error bars show SD.

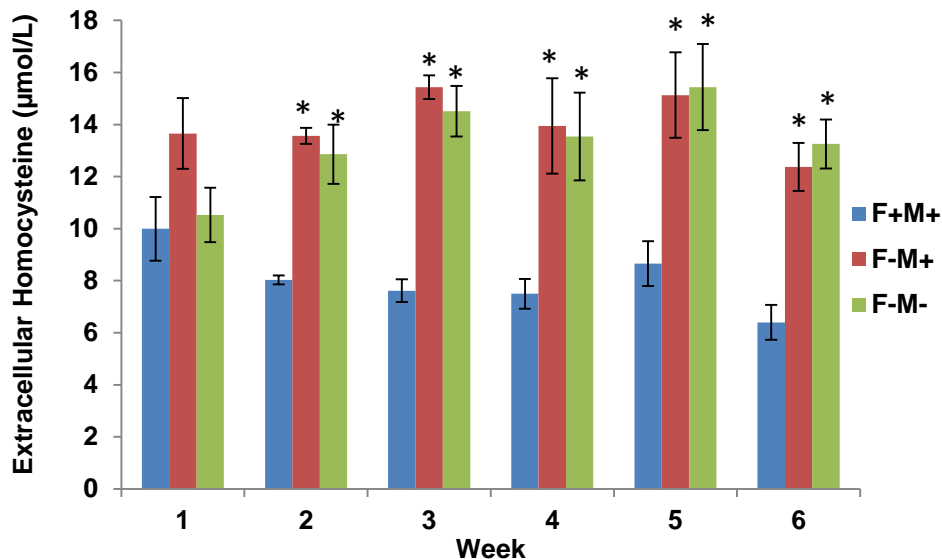


Figure 32: Extracellular homocysteine for SiHa cells cultured in complete, folate-deplete, and, folate and methionine-deplete medium

Each value shows mean of three-independent experiments and error bars show SEM.

* Significantly different from control, $P < 0.05$ (one-way ANOVA, post hoc test).

3.5 Discussion

In order to develop a model of one-carbon donor depletion, customized media was obtained representing two states of depletion; F-M+ (folate-depletion alone) and F-M- (folate and methionine-depletion). The folate and methionine concentrations in the F-M- medium were estimated to be 12-30 nM and 20 μ M, respectively, compared with 900 nM and 300 μ M, respectively in the complete medium. In comparison to the human physiological system, the normal folate concentration in human plasma is about 7-28 nM (Ruston *et al.*, 2004) and the methionine concentration is about 10-40 μ M (Garlick, 2006) so the model represents a moderate deficiency state, rather than an acute deficiency state.

3.5.1 Cell culture

C4-II is the most similar cell to cervical cancer cells in gene expression profile when compared with other cervical cancer cell lines (Carlson *et al.*, 2007). Therefore, C4-II was chosen for this research. C4-II is an epithelial cervical cancer cell line with hemicysts (domes) which are characteristic of transporting epithelia and respond to crowding by separation and shedding. A study showed that C4-II cell growth patterns in host tissue had characteristics of ectocervical basal cells and/or endocervical epithelium (Auersperg *et al.*, 1989). Our studies show that C4-II cells complete the first cell cycle within 2-3 days of culture (lag phase), after which C4-II cells were observed to divide faster and grow in a log phase for more than 20 days without entering a plateau phase. With 20,000 cell /cm² in the initial seeding, C4-II cells reach 100% confluence by 8-10 days. After C4-II cells reached 100% confluence they started to make domes and pile up in multilayers. To examine cell characteristics during culture, these early experiments involved examining cells in three phases of cell growth: pre-confluence, confluence, and post-confluence.

SiHa is another cervical cancer cell which shows genetic characteristics similar to human primary cervical cancer cells, although SiHa and C4-II cells have different cell characteristics. SiHa cells complete the first cell cycle within 2-3 days of culture (lag phase), after which SiHa cells were observed to divide faster and entered a plateau phase around day 16 of culture period. With 20,000 cell /cm² in the initial seeding, SiHa cells reach 100% confluence by 8-10 days. While C4-II cells showed a tendency to form multilayers, SiHa cells did not. Clearly a protocol which works well with one cell line may not be appropriate for another cell line.

3.5.2 Effect on growth rate

Growing C4-II cells in folate and methionine depletion retarded cell growth to a greater extent than folate or methionine depletion alone. Folate plays an important role in DNA synthesis by supplying tetrahydrofolate derivatives for construction of thymine. A

reduction in the availability of thymine leads to a decrease in the rate of cell proliferation and cells are arrested at S-phase of cell cycle (Jackson *et al.*, 1997). The methionine depletion together with folate deficiency resulted in enhanced growth retardation because methionine is an essential amino acid which is required not only for protein synthesis but also the methylation process. In our study, the effect on growth rate was profound and was evident from about 8 days of culture in depleted medium. The tendency of C4-II cells to multilayer after about day 12 of culture was unexpected. We reduced the seeding density in order to prevent C4-II cells reaching confluence before 8-10 days of culture, but this impaired early growth. Nevertheless, a comparison of effects of one-carbon donor depletion up to the point from which multilayering was evident, providing some useful information.

Interestingly, on days 8 and 12, the C4-II cells grown in folate and methionine-deplete medium were bigger than those grown in the complete and folate depleted state. Despite the hyperconfluence of cells grown in the complete and folate depleted medium at day 12, the confluence at day 4 and day 8 was the same. Therefore, a difference in available space did not obviously explain the difference in cell size. The loss of contact inhibition is one of the characteristics of cancer cells (Lipkin & Knecht, 1974; Abercrombie, 1979). The higher proliferation rate and the greater loss of cell contact inhibition for cells grown in complete and folate depleted medium may explain the difference in cell size. This suggests that sensitivity to contact inhibition is influenced by folate and methionine depletion.

Unlike C4-II cells, folate and/or folate and methionine depletion did not influence the growth rate of SiHa cells until cells were post-confluence. Growth curves of both complete and depleted cells started to diverge from about day 16 compared with day 8 for C4-II cells, and even dropped further at day 20. This may be because the SiHa cells started their apoptosis process.

For both cell models of methyl donor depletion, there is a small contribution to the folate and methionine pool from fetal calf serum, which is replenished at each point of medium replacement, thereby maintaining some growth in the depleted cells.

There have been numerous reports of folate-depletion studies in various kinds of cell lines and tissue types. The effect of folate deficiency seems to depend very strongly on the individual cell and the extent of folate depletion (Kim, 2005). Severe folate deficiency in untransformed NIH/3T3 and CHO-K1 cells, and human HCT116 and Caco-2 colon cancer cells led to a significant and progressive retarded growth by day 12 in untransformed cell lines and by day 20 in human colon cancer cell lines (Stempak *et al.*, 2005). Crott *et al.* (2008) studied the effect of folate depletion in three normal human colonic cell lines (HCEC, NCM460, and NCM356). Those cells were cultured for 30-32 days in various concentrations

of folic acid (25, 50, 75, and 150 nM). Cell growth of HCEC and NCM356 showed incremental growth retardation with decreasing folate concentration, whereas NCM460 growth was retarded only at the lowest concentration of folate, which was comparable to the concentration of folate in our depleted media. On the other hand, the growth of three clonal cell lines generated from prostate cell lines derived from the transgenic adenoma of the mouse prostate (TRAMP) was not affected by culture in what the authors described as folate-restricted (100 nM) medium even after 20 population doublings (Bistulfi *et al.*, 2010). It should be noted that folate concentration used by this group was about five-fold higher than the concentration used in our study.

There has been no previous study of methionine depletion of cervical cancer cells, although other cells have been studied. Hu & Cheung investigated effects of methionine depletion by methioninase in neuroblastoma and found that cell proliferation was inhibited and the cells were arrested at G2 phase (Hu & Cheung, 2009). Graziosi *et al* generated a methionine depletion of peritoneal carcinomatosis and xenograft model in gastric cancer cells. They showed evidence for increased apoptosis and decreased cellular adhesion and migration associated with reduction of the promoter methylation of E-cadherin gene (Graziosi *et al.*, 2013). Although the authors did not report methionine concentration, the gastric cancer cells in this study were grown in methionine-free RPMI supplemented with dialyzed serum, therefore, the final concentration might have been lower in methionine concentration than our methionine-depleted model.

3.5.3 Effect on intracellular folate concentration

Growth of C4-II cells in folate and methionine-depleted medium led to a decrease in the intracellular folate concentration compared with control cells, evident by day 4 of culture. C4-II cells grown in complete medium showed a fall in intracellular folate over 20 days of culture, presumably because of a competition for folate and methionine in the face of very rapid growth, eventually leading to multilayering. The decrease in intracellular folate concentration occurred before the decline in growth rate in the depleted cells, supporting a cause-effect relationship.

Effects of methyl donor depletion on intracellular folate at day 8 and 12 corrected for cell number may actually underestimate the effect, given that cell size increased in response to depletion. However, intracellular folate expressed in this way fell significantly by day 4 at which point cell diameter was unchanged. Also, the effect on cell diameter was only observed in the double depleted state, whilst intracellular folate was significantly lower in the folate-depleted state as well as the double-depleted state. It is therefore reasonable to

conclude that cells were profoundly folate depleted from day 4 of growth in folate depleted and folate and methionine depleted medium.

SiHa cells also showed a substantial decrease in intracellular folate concentration after 6 passages in folate and methionine-depleted medium. The intracellular folate in complete cells of SiHa was higher than that of C4-II more than 5 times, but the intracellular folate concentration of depleted cells in both cell lines was the same. Folate depletion in SiHa cells seemed to affect intracellular folate more than in C4-II. However, folate depletion in SiHa cells did not produce as great an effect on growth rate as for C4-II cells.

The response to folate depletion evidently depends on cell type. Effects on intracellular folate concentration of growth under folate-depleted conditions is reported from many studies and in various models. Growth of untransformed CHO-K1 Chinese hamster ovary cells and NIH/3T3 mouse fibroblasts and human colon adenocarcinoma cells-HCT116 and Caco-2 showed a significant decrease (~90%) in intracellular folate after 12-20 days of culture in folate-depleted medium (Stempak *et al.*, 2005). Depletion had a similar effect as in our study, in which the intracellular folate concentration dropped to 10% within 4 days and was sustained until day 12. Bistulfi *et al.* (2010) conducted a study of prostate cancer cell lines, which were generated from a primary prostate tumour in a TRAMP mouse, and demonstrated that folate-depleted medium also led to a significant depletion of intracellular folate. After culture in restricted folate medium (100nM) for 20 population doublings, intracellular folate concentration of prostate cancer cells in depleted medium was decreased to 10ng/5 million cells compared with 20-70 ng/5 million cells in control cells (Bistulfi *et al.*, 2010). The intracellular folate concentration in the depleted cells from our study was about 20-fold lower than this study. This may be because our study used a medium with a lower folate concentration. Therefore, our model seemed to be more folate depleted than this research group.

Although a reduction in extracellular folate can lead to cellular folate depletion cells do adapt to this folate restriction. A folate receptor gene may be up regulated by folate depletion (Kelemen, 2006). In cell culture studies, human KB (nasopharyngeal carcinoma) cells increased the uptake of folate by increasing the expression of the membrane folate receptor to maintain folate concentration of cells (Kane *et al.*, 1988; Chung-Tsen & Dolnick, 1993; Kelemen, 2006). Cells may extract enough nutrients from folate-depleted medium to survive, but at a slower proliferation rate (Antony, 1996). In our study, C4-II cells showed greater sensitivity to folate depletion than SiHa cells. This may suggest that SiHa cells might adapt themselves to folate depletion by upregulation of their folate receptor.

3.5.4 Effect on intracellular methionine concentration

Intracellular methionine of C4-II cells grown in folate and methionine-deplete medium dropped significantly by 4 days and fell further over the subsequent 4 days, confirming the combined depletion. Unlike the intracellular folate concentration which fell progressively over 12 days of culture in the double-depleted state, the intracellular methionine concentration increased from day 8 to day 12, suggesting that the cells can adapt to growth in methionine-deplete medium. A study in a rat model of sulphur amino acid deficiency demonstrated an up-regulation of activating transcription factor (ATF) and also an up-regulation of other genes involved in the solute carrier (SLC) family amino acid transporter (Sikalidis & Stipanuk, 2010). Therefore, cells grown for a prolonged period in methionine deplete medium may express more methionine transporter, and consequently, increase uptake of methionine and increase intracellular methionine concentration to support cell function.

3.5.5 Effect of growth in a folate-depleted medium on methyl cycling: measurement of intracellular homocysteine and homocysteine export

Intracellular homocysteine concentration depends on the activity of the methyl cycle, which is in turn dependent on the availability of enzyme co-factors and enzyme regulation. Accumulation of intracellular homocysteine leads to export from the cell (Svardal *et al.*, 1986; Nakano *et al.*, 2005). To determine whether folate depletion affects the methyl cycle, in cervical cancer cells both intracellular and extracellular homocysteine concentrations were examined in this study. From three-independent experiments in C4-II cells, it was concluded that the results of intracellular homocysteine concentration could not be relied on because of the very low concentrations observed. Homocysteine is rapidly exported from cells once they are no longer adherent, during cell harvesting (Antony *et al.*, 2004). We generated a very large number of cells for the measurement of intracellular homocysteine but we could not generate an intracellular homocysteine in the range that could be reliably detected. On the other hand, the results from the studies of extracellular homocysteine were consistent, and compatible with a functional folate depletion. Results indicated a higher homocysteine export from folate-depleted cells than folate-replete cells and this was greatest for cells depleted only of folate. Methionine will act as a methyl donor in the methyl cycle and drive the synthesis of homocysteine, therefore enhancing effects of folate depletion. The methionine cycle was evidently disturbed by folate depletion, so that homocysteine could not be efficiently remethylated to methionine, resulting in accumulation of homocysteine. Results are compatible with previous findings from this laboratory, in which the presence of methionine enhanced homocysteine export from folate-deficient human umbilical vein endothelial cells (HUVECs) (Nakano *et al.*, 2005).

In SiHa cells, also we found that homocysteine concentration (both intracellular and extracellular concentration) of methyl donor depleted cells was consistently higher than of the complete cells, reflecting the fact that impairment of the methionine cycle leads to intracellular homocysteine accumulation and enhanced export.

Few studies of methyl-donor depleted cells in culture have examined effects on homocysteine remethylation or on the effects of methionine in particular. Nakano and colleagues established a model using human umbilical vein endothelial cells (HUVECs) to determine the role of homocysteine in atherosclerosis. They showed that folate depletion of these cells led to enhanced homocysteine export, and that addition of folinic acid back into the medium mitigated this effect. Furthermore, they showed that the availability of methionine enhanced the effects of folate depletion on homocysteine export. Buemi *et al* (2001) showed that adding folic acid to human vascular monocytes in culture decreased homocysteine concentration in the medium (Buemi *et al.*, 2001). However, Brown *et al* (2006) investigated the effect of folate status on EA.hy926 endothelial cell line grown in two types of medium containing 23nM (LO) or 9µM folic acid (HI) with 10% FCS supplement for 13 weeks. They found no difference in either intracellular homocysteine concentration, SAM, SAH, SAM/SAH ratio or global DNA methylation of cells grown in these media. They also reported that the secreted homocysteine showed no consistent difference (Brown *et al.*, 2006). This study suggested that mild folate deficiency did not disturb methylation potential of the cells. However, they did report difference in cell size, morphology, and folate metabolites. They reported that cells grown in the lower folate concentration were larger, more elongated, more permeable, and formed a disordered monolayer. Also the intracellular THF, 5-methyl THF, and formylated THF of the LO cells were significant lower than the HI cells. It should be noted that the high folate concentration used in this study was much higher than in human plasma, and also, 10 fold higher than our study. And even though the low folate concentration used in this study was classified as a mild deficiency, the final concentration, including 10% FCS supplement in the medium, may be pronounced as normal.

Our results show clearly that growing cervical cancer cells in folate-deplete medium, and, folate and methionine-deplete medium has an adverse effect on the methyl cycle.

3.6 Summary

Growth of C4-II cells in both folate depleted medium, and folate and methionine-depleted medium led to growth retardation. A further reduction of growth rate was achieved by depleting the medium of methionine too. There was a profound decrease in the concentrations of intracellular folate and methionine, and as these effects occurred before

the decline in growth rate this supports a cause-effect relationship. Moreover, results from our study of extracellular homocysteine were consistent and compatible with a functional methyl-donor depletion. The increase in homocysteine export occurred after the decrease in intracellular folate and methionine, and occurred at the same time as the decline in growth rate in the depleted cells, again supporting a cause-effect relationship. Thus, a protocol was established to generate a model of methyl-donor deficiency using C4-II cells (**figure 33**).

On the other hand, SiHa cells were relatively resistant to methyl-donor depletion and these cells required long-term growth in depleted medium in order to a lower intracellular folate concentration and increase homocysteine export. Therefore, the depletion model of SiHa will be conducted using a long-term depletion protocol (**figure 34**).

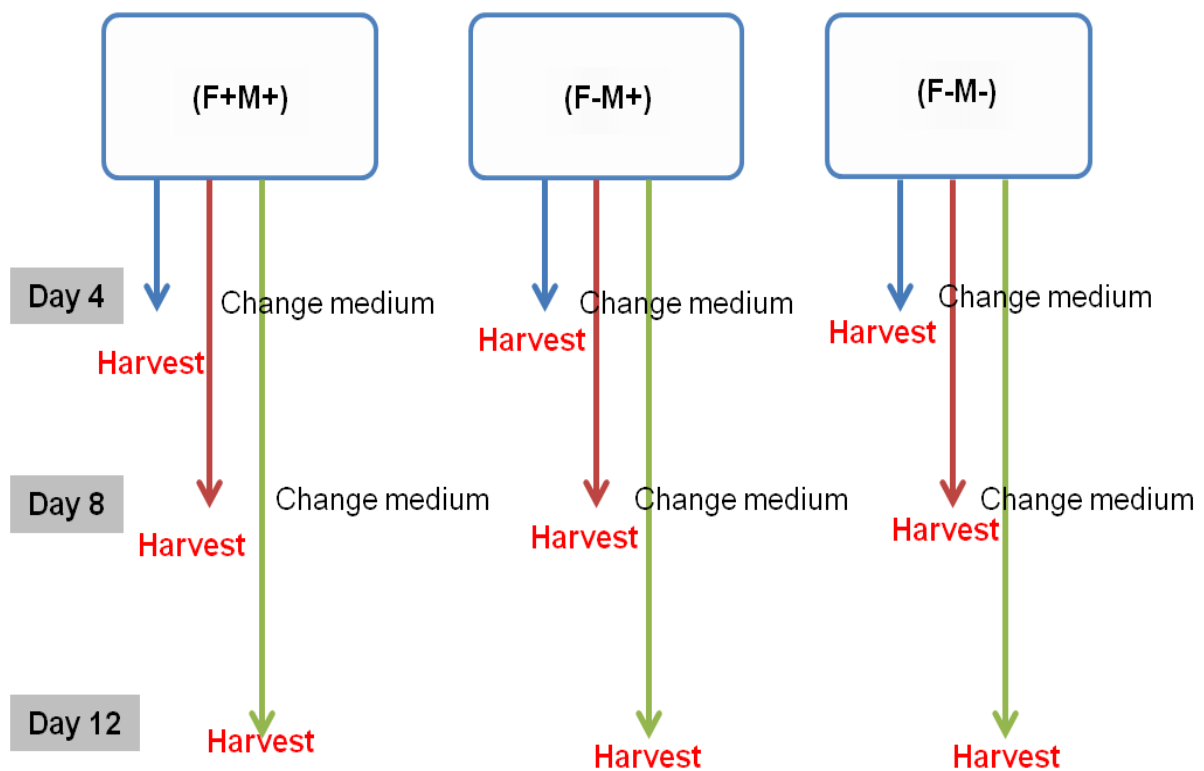


Figure 33: Methyl donor depletion protocol for C4-II

C4-II cells were cultured in particular medium up to 12 days and changed medium every 4 days to maintain cell growth. At day 4, 8, and 12, cells were harvested for further analysis.

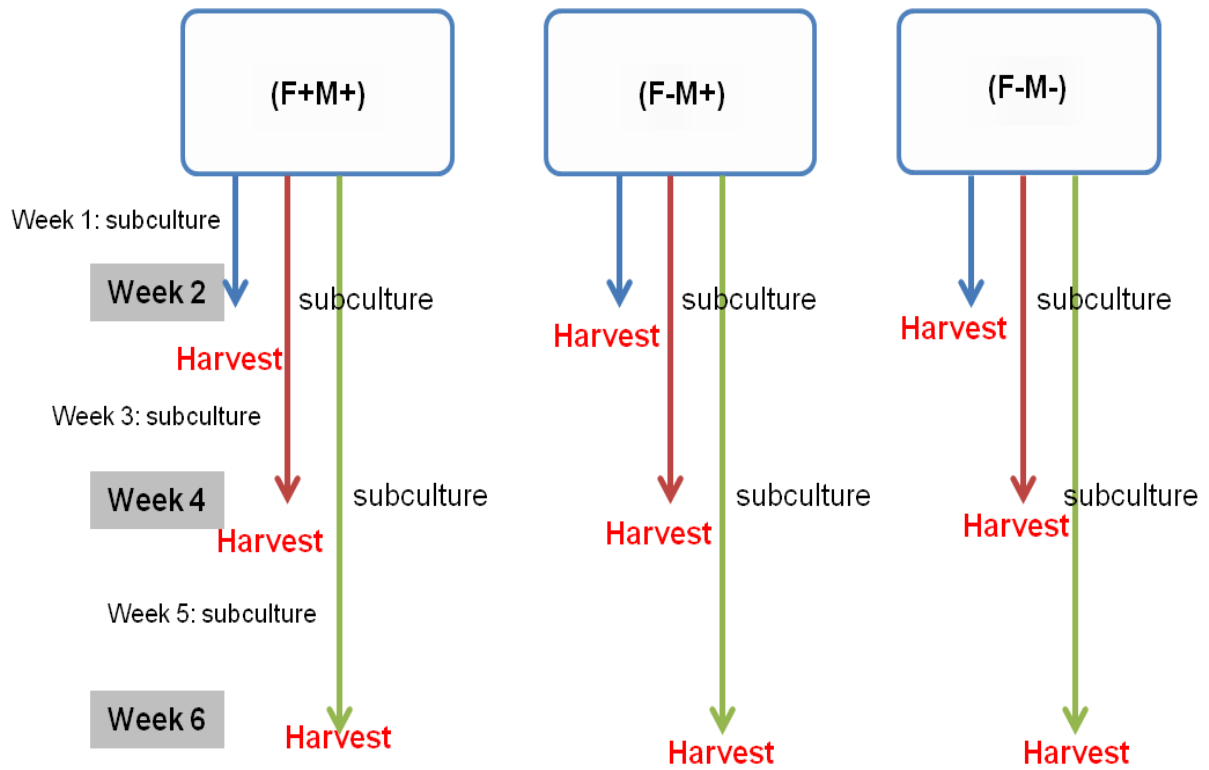


Figure 34: Methyl donor depletion protocol for SiHa

SiHa cells were cultured in particular medium and subcultured once a week up to 6 weeks. At week 2, 4, and 6, cells were harvested for further analysis.

Chapter 4 Effects of methyl donor depletion on DNMTs expression and DNA Hypomethylation

4.1 Introduction

DNA methylation is known to be a crucial process in the regulation of parental imprinting (Li *et al.*, 1993), X chromosome inactivation (Panning & Jaenisch, 1998), and the protection of genomic integrity by recruitment of retroviruses and transposons (Walsh *et al.*, 1998). In addition, the DNA methylation profile can affect gene expression (Lande-Diner *et al.*, 2007; Miranda & Jones, 2007), and thereby influence cancer risk and cancer progression (Jones & Baylin, 2007).

DNA methylation is catalysed by DNA methyltransferases (DNMT). DNMTs catalyse the donation of a methyl group from S-adenosylmethionine (SAM) to the C5 of the cytosine nucleotide. Some publications suggest strongly that aberrant DNMT expression influences the DNA methylation profile (Mizuno *et al.*, 2001; Biniszkiwicz *et al.*, 2002; Yin *et al.*, 2012), but there is a great deal of uncertainty in this area (Eads *et al.*, 1999; Oue *et al.*, 2001; Saito *et al.*, 2001; Oh *et al.*, 2007).

Several studies report the over expression of one or more DNMTs in cancer tissue such as gastric cancer (Etoh *et al.*, 2004), liver cancer (Choi *et al.*, 2003), ovarian cancer (Ahluwalia *et al.*, 2001), uterine cervix squamous cell carcinoma (Sawada *et al.*, 2007) cervical cancer (Piyathilake *et al.*, 2008) and breast cancer (Roll *et al.*, 2008). On the other hand, down-regulation of DNMTs has been linked with cancer progression (Yaqinuddin *et al.*, 2008; Gao *et al.*, 2011; Su *et al.*, 2013). The implications of altered DNMT expression or activity to carcinogenesis and progression are far from clear.

Despite the evident relevance of DNA global methylation and DNMT expression to cancer risk and expression the role of methyl donor status to these processes is still poorly understood. We have carried out a study to specifically investigate the effects of folate and methionine depletion in cervical cancer cells on DNMT expression and DNA global methylation.

4.2 Aims

To examine how methyl-donor status influences DNA methylation profile and DNA methyltransferase (DNMT) gene expression in cervical cancer cells, and to determine whether any such effects are reversible.

4.3 Methods

4.3.1 Cell sample preparation

A detailed description of cell culture is given for individual experiments. Generally, the C4-II cells were seeded at a density of 1.5 million cells / T75 flask and grown for 12 days, with a change of medium every 4 days. The cells were harvested at day 4, 8, and 12 for further analysis. The SiHa cells were seeded at a density of 0.8 million cells / T75 flask and grown for 6 weeks, with a passage every week. The cells were harvested at weeks 2, 4, and 6 for further analyses.

4.3.2 Development of the global DNA methylation assay

4.3.2.1 DNA Methyl Acceptor Assay

Cells were harvested on days 4, 12, and 20 of culture for C4-II cells, or at 70-80% confluence for SiHa cells after six passages in each treatment. Genomic DNA was extracted (see section 2.2.6) and DNA yield quantified by nanodrop spectrophotometric analysis. 0.5 µg DNA samples were taken for the determination of global DNA methylation status using the [³H]-SAM donor assay (see section 2.2.7.1). For a positive control, 0.5 µg of 5-azadeoxycytidine-treated Jurkat genomic DNA (5-azadeoxycytidine treatment demethylates DNA) was used instead of the cell DNA. For a negative control, 0.5 µg of CpG methylated Jurkat genomic DNA was used. The DPM result reflected the [³H]-methyl incorporation into DNA. To calculate sample DNA hypomethylation, blank DPM (the mixture lacking CpG methyltransferase) was subtracted from sample DPM and reported as DPM/1 µg of DNA.

4.3.2.2 Immunocytochemistry of 5-methylcytosine (C4-II cells only)

Cells were grown in T25 or T75 flasks, were trypsinised and then were seeded onto 4-well slide chambers and incubated at 37⁰C/ 5%CO₂ for 24 hours, 8 days and 15 days. On the indicated day, 5-methylcytosine was measured using immunocytochemistry (see section 2.2.7.2). Cells were visualized using a Nikon ECLIPSE e400 microscope and images were taken with an objective lens setting of X20. NIH 3T3 cells with and without primary antibody were used as a positive and negative control, respectively. Cells positive for 5-methylcytosine had DAB brown stained nuclei, negative cells were haematoxylin blue counterstained.

4.3.2.3 Flow cytometric analysis of DNA hypomethylation

The immunocytochemistry method modified from Habib et al (1999) and Mcmanus et al (2006) together with flow cytometry detection was used as the basis for the development and optimisation of this approach for 5-methylcytosine assessment in our system.

Initially, a protocol similar to the one used for immunohistochemistry was followed for staining of cells for flow cytometry, the difference being the cells were in suspension in tubes rather than being fixed to slides. In addition, the secondary antibody used was conjugated to a fluorochrome. However, initial experiments failed to show any positive staining for 5-methylcytosine and also many cells were lost during the microwaving stage of the procedure.

As the lack of positive staining may have been due to insufficient permeabilization of the cells, an incubation step with Triton X-100 was added to the staining procedure, and the fixation method was expanded to include an incubation with methanol at -20°C ; however results still proved unsatisfactory.

Further modification of the protocol included antigen retrieval, where cells were incubated with 2N HCl at 37°C followed by neutralisation with sodium borate pH8.5 Tween-20 and BSA were added into the washing solution to prevent cell clumping. The concentrations of primary and secondary antibody and also number of cells required were optimized. Problems of non-specific background staining were solved by including donkey serum in the blocking buffer. The combined modifications gave a consistent and reproducible result.

Cells were harvested on days 4, 8, and 12 of culture for C4-II cell, or at 70-80% confluence for SiHa cells after 2, 4, and 6 passages in each treatment, and 5-methylcytosine was quantified using flow cytometric detection method (see section 2.2.7.3). Cells were analysed by BD FACSCalibur™. Appropriate controls were utilized and included unstained cells, secondary antibody alone and 5-azadeoxycytidine treated cells for a negative control. Non-specific antibody binding was monitored with a mouse IgG1 isotype. Data analysis was run by BD CELLQuest software.

4.3.3 RNA extraction and cDNA synthesis (C4-II cells only)

Total RNA was extracted by RNeasy® Mini kit (see section 2.2.8) and quantified by nanodrop spectrophotometry. Each first-strand cDNA synthesis was carried out using the SuperScript™ III Reverse Transcriptase (see section 2.2.9). The cDNA was diluted to a concentration of 25-50 ng/ μl and kept in aliquots.

4.3.4 Determination of DNMTs expression (C4-II cells only)

DNMT gene expression was determined using semi-quantitative RT-PCR (see section 2.2.10). Negative controls (in which water instead of cDNA was added) were also run in each plate. Contamination of genomic DNA in the RNA samples was excluded by an

analysis with the cDNA synthesis products in the system without reverse transcriptase. Reactions for determining the expression of the gene of interest and the reference gene (β -actin) were carried out as separate PCR reactions. Normalization of RNA amounts was performed using β -actin expression analysed with the same procedure. Finally, expression ratios between the DNMTs from F+M+ (control), F-M+, and F-M- were calculated. The gene expression was analyzed and expressed as a relative gene expression by using the $2^{-\Delta\Delta C_T}$ Method (Livak & Schmittgen, 2001).

4.3.5 Determination of DNMT activity (C4-II cells only)

Nuclear extracts were prepared by using NE-PER[®] Extraction Reagents (see section 2.2.12). Protein concentrations of the nuclear extracts were determined by using the Bio-Rad protein assay (see section 2.2.13). The global DNA methyltransferase activity was measured by EpiQuik[™] DNA Methyltransferase Activity/Inhibition Assay Kit (see section 2.2.14). The global DNMT activity (OD/h/mg protein) was calculated referring to the formula: (sample OD – blank OD)/(sample protein amount : $\mu\text{g} \times 1000$), according to manufacturer's instructions. The results are given in activity units in treatments (F-M+ and F-M-) relative to the activity level in control (F+M+) on day 8.

4.3.6 Repletion study (C4-II cells only)

Cells were seeded at a density of 1.5 million cells / T75 flask and grown for 12 days, with a change of medium every 4 days. For methyl-donor repletion experiments, cells were grown for 8 days in folate-depleted medium (F-M+), and, combined folate and methionine-depleted medium (F-M-). Both depleted medium containing less than 30 nmol/L of folate. At day 8, the complete medium (F+M+) were transferred to the cultured cells for a further 4 days. Cells were processed for growth rate determination by cell counting (see section 2.2.2) and DNMT gene expression (see section 2.2.10) at days 4, 8, and 12.

4.3.7 Statistical analysis

See section 2.2.16

4.4 Results

4.4.1 Development of the global DNA methylation assay

4.4.1.1 DNA methyl acceptor assay

The DPM value represents the extent of incorporation of [³H]-methyl groups into DNA, therefore, the higher the DPM value, the lower the global DNA methylation. **Figure 35** shows the average DPM value for three independent experiments over 25 days. Two-way

ANOVA was run to determine the effect of culture time and/or treatment on hypomethylation level. Hypomethylation level increased significantly with time ($P=0.006$), but there was no significant effect of folate-depletion ($P=0.982$).

Post-hoc test (one-way ANOVA), revealed that global DNA hypomethylation for C4-II cells grown in folate depleted medium was significantly higher at day 24 than at days 4, 12, and 20 ($P=0.003$). In complete medium, the hypomethylation level was significantly greater at day 24 than day 4 ($P < 0.05$).

Figure 36 shows the average DPM value, from one experiment at day 8 (80% confluence) after 6th subculture in each treatment, for SiHa cells. At this time point, the incorporation of [³H]-methyl group into the DNA of SiHa cells was not significantly different between cells grown in F+M+, F-M+, and F-M- media. However, when the DPM value of the unmethylated DNA control and the DNA of all three treatments were compared, SiHa cervical cells grown in complete medium were found to have a high level of DNA hypomethylation.

4.4.1.2 Immunocytochemistry of 5-methylcytosine (C4-II only)

An immunocytochemical method was used to determine the 5-methylcytosine load of cells grown under different conditions. Anti 5-methylcytosine was used to detect 5-methylcytosine and results examined microscopically. Cells grown in folate and methionine-replete and folate and methionine-depleted media were compared at three time points. Cells grown for 24 hours, 8 days, and 15 days were chosen to represent sub-confluence, confluence, and post-confluence, respectively. Cells staining positively for methyl cytosine stained brown, cells staining negatively for methylcytosine stained blue. **Figure 37(A)** shows positive staining and negative staining. At 24 hours (**figure 37(B)**) there was no difference in the ratio of brown: blue staining between treatments. The second time point was 8-days, by which time cells under both treatments had increased in cell density, but the ratio of brown: blue staining was similar in the two treatments. By day 15 cells cultured in folate and methionine-replete condition (**figure 37(C), left**) had reached post-confluence, were multilayered and appeared to show more blue-stained cells than brown-stained cells. On the other hand, cells cultured in folate and methionine-depleted medium, which were still growing in a monolayer and had a lower cell density (**figure 37(D), right**), seemed to have more brown-stained cells than blue-stained cells.

It was difficult to obtain an accurate value for cell staining for cells growing at high density and for this reason this particular approach was considered unsuitable for our needs and no further experiments were performed using this technique.

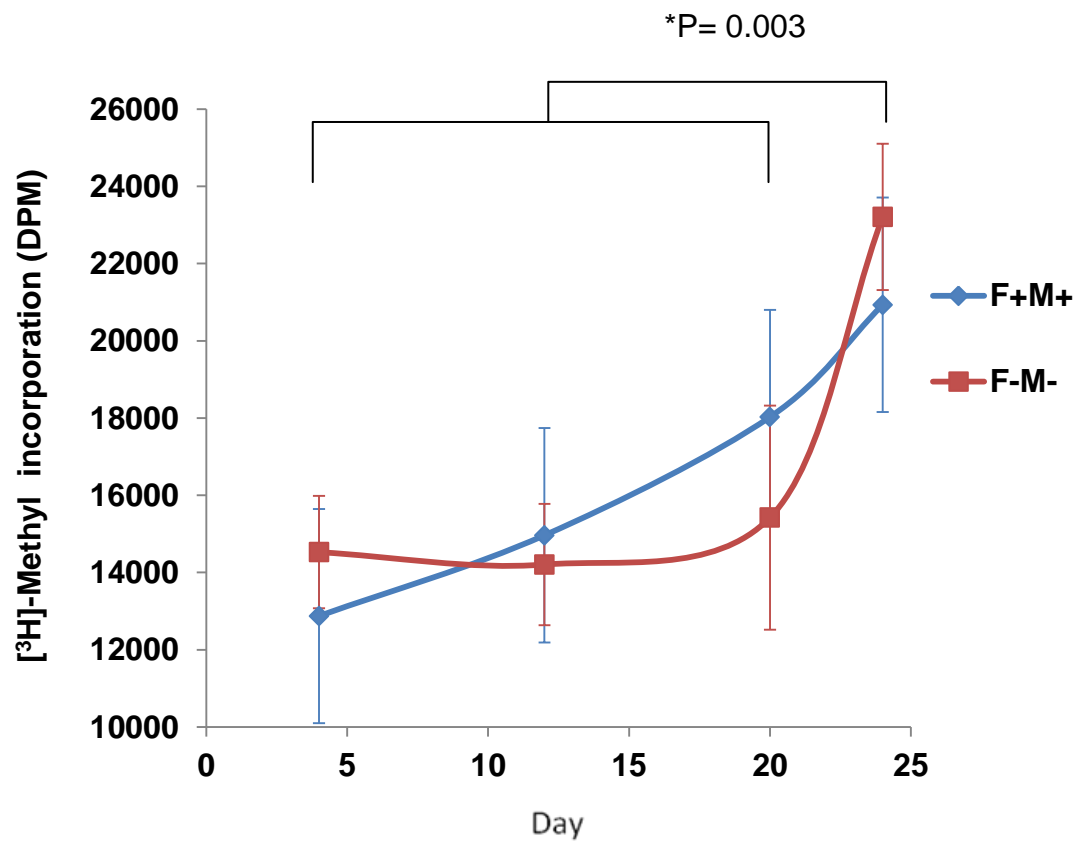


Figure 35: Global DNA methylation of C4-II cells grown in complete and folate and methionine-depleted medium, using the methyl acceptor assay

Each value shows mean of three-independent experiments and error bars show SEM.
 * Hypomethylation increased significantly with time, $P=0.003$ (one-way ANOVA)

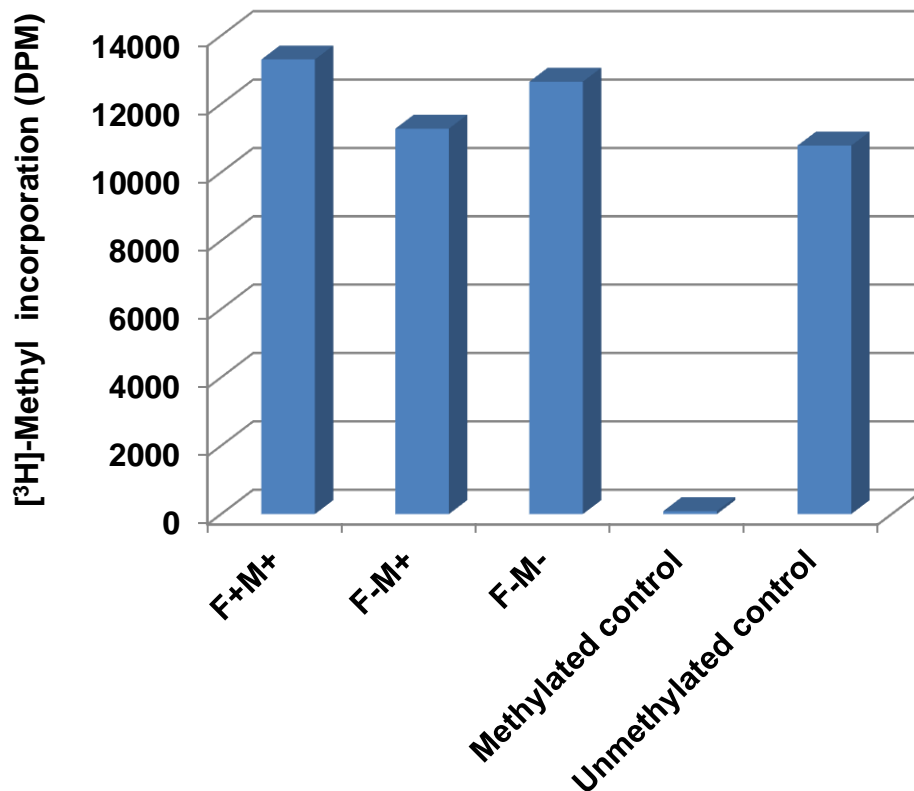


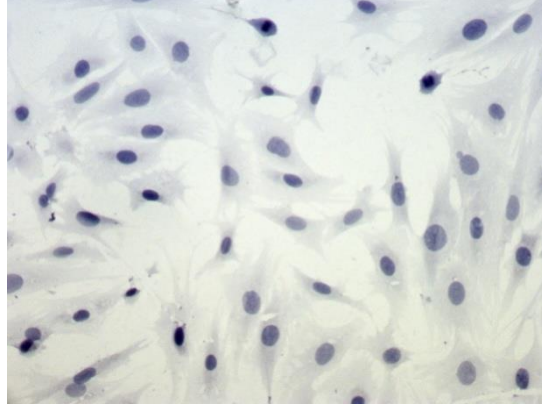
Figure 36: Global DNA methylation of SiHa cell DNA determined using the DNA methyl acceptor assay

The global DNA methylation was compared between the cells grown in complete, folate-depleted, and folate and methionine depleted medium using CpG methylated Jurkat genomic DNA as a negative control and using 5-azadeoxycytidine-treated Jurkat genomic DNA as a positive control. The more incorporation of [³H]-methyl group, the more hypomethylation of the DNA.

(A)

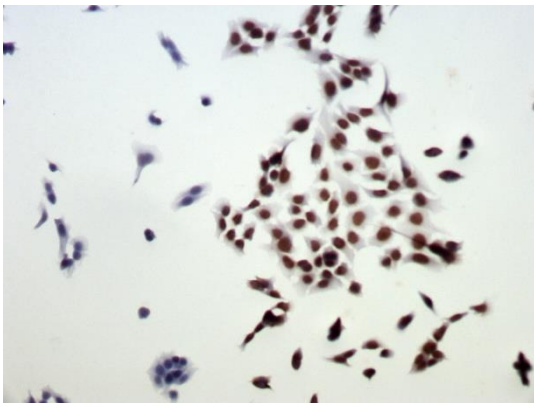


NIH 3T3 cells: positive control

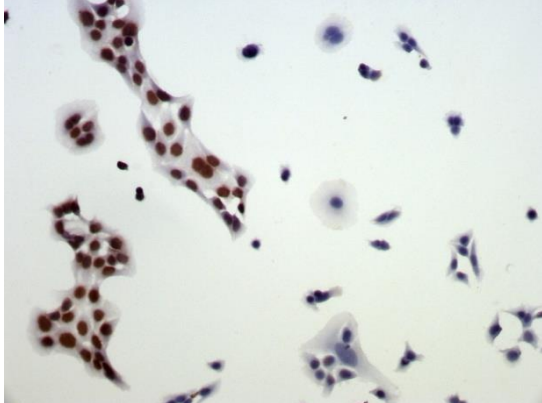


NIH 3T3 cells: negative control

(B)



C4-II 24hrs: complete cells

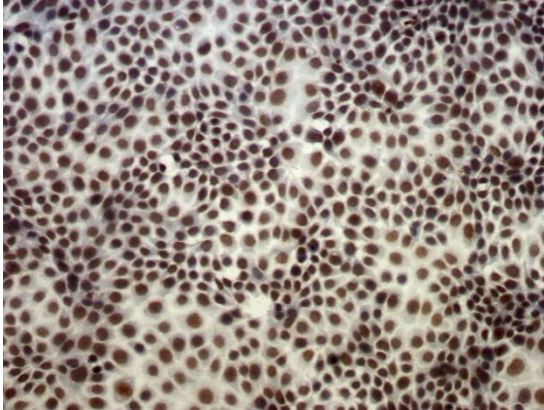


C4-II 24hrs: folate and
methionine-depleted cells

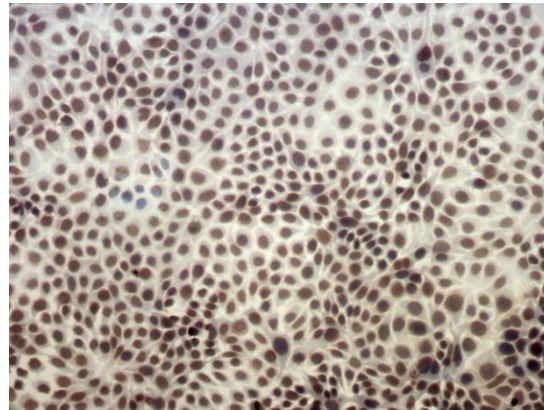
Figure 37: *Detection of 5-methylcytosine of C4-II DNA by immunocytochemistry*

NIH 3T3 fibroblast cells as control (A). C4-II cells grown in folate and methionine-depleted medium were compared with cells grown in complete medium at three different time points of culture: (B) 24 hrs

(C)

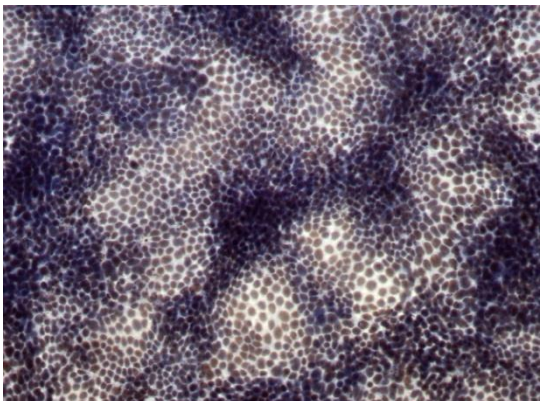


C4-II 8days: complete cells

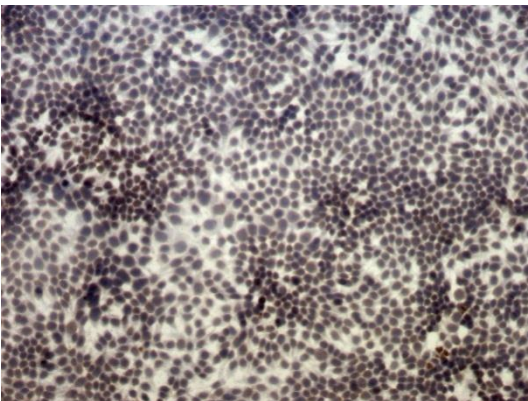


C4-II 8days: folate and
methionine-depleted cells

(D)



C4-II 15days: complete cells



C4-II 15days: folate and
methionine-depleted cells

Figure 37: *Detection of 5-methylcytosine of C4-II DNA by immunocytochemistry (continued)*

C4-II cells grown in folate and methionine-depleted medium were compared with cells grown in complete medium at three different time points of culture: (C) 8 days, and (D) 15 days.

4.4.1.3 Flow cytometric analysis of DNA methylation

Cells were stained for flow cytometry using a mouse monoclonal anti-5-methylcytosine antibody and a fluorescent donkey anti-mouse secondary antibody. Cell-staining controls included unstained, IgG1 isotype and secondary antibody only and also on one occasion, the primary antibodies alone were assessed. Graphs show cell count (Y-axis) versus fluorescence intensity, on a logarithmic scale (X-axis) (**figure 38**).

Figure 38 shows a negative result for controls (A-E) and a positive result in (F-H) from anti-5-methylcytosine antibody staining of C4-II cells. The right-shift in F indicates a greater concentration of 5-methylcytosine. Staining in graph B indicated a degree of positivity when compared with the unstained cells which suggested possible non-specific binding, which needed further consideration.

In order to compare the intensity of staining between growth conditions we looked at mean fluorescence. The higher the mean value the higher the average fluorescence and therefore cellular 5-methylcytosine content. The 5-azadeoxycytidine-treated cells were used as negative control and gave a lower mean fluorescence value, suggesting a demethylation effect and confirming the specificity of our primary antibody (**figure 38(F) and (G)**).

To assess the effect of folate depletion on 5-methylcytosine, C4-II cells were cultured in three conditions. At 3 time points (days 4, 8, and 12) cells were stained with anti-5-methylcytosine for flow cytometric analysis and this was done on three separate occasions. **Figure 39** shows the raw data from one experiment. A left shift in the mean channel of fluorescence in F-M- at day 8 and an even greater left shift at day 12 when compared with F+M+ and F-M+, indicating relative DNA hypomethylation. This was evident as a progressive decrease in the mean fluorescence of the cells depleted of both folate and methionine.

Figure 40 shows raw data for the flow cytometry for SiHa cells. Results are shown for unstained cells, three treatments (F+M+, F-M+, and F-M-), and from a negative control. On the basis of reproducibility of findings for both the C4-II cells and SiHa cells, the flow cytometry method was used to determine global DNA methylation status in our study.

However, frequency plots in figures 40 and for figure 41D, show a split peak, suggestive of two populations of cells. It was not possible to re-analyse the data. The software for the flow cytometry estimates the mean fluorescence for each treatment. The effects on mean fluorescence of what appears to be two populations of cells for some of the conditions is not known, but there may be implications for the calculated effects of methyl donor depletion. Further work would have to be carried out to explore this possibility further.

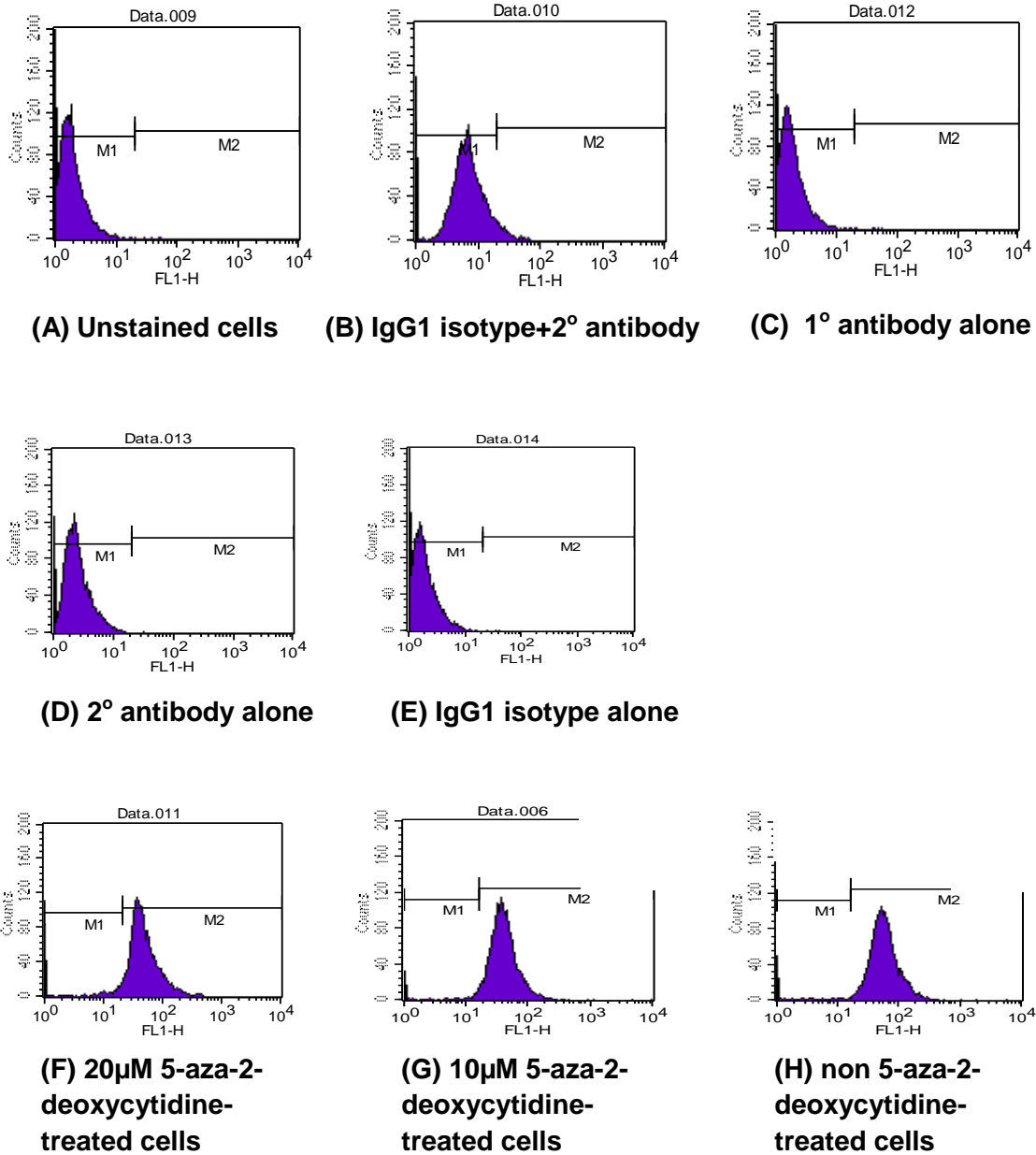
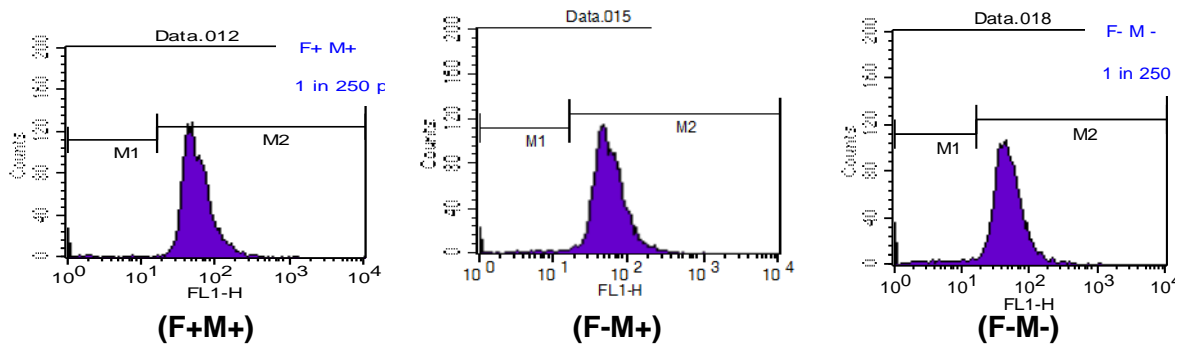


Figure 38: Pattern of 5-methylcytosine detection of C4-II cells by flow cytometry

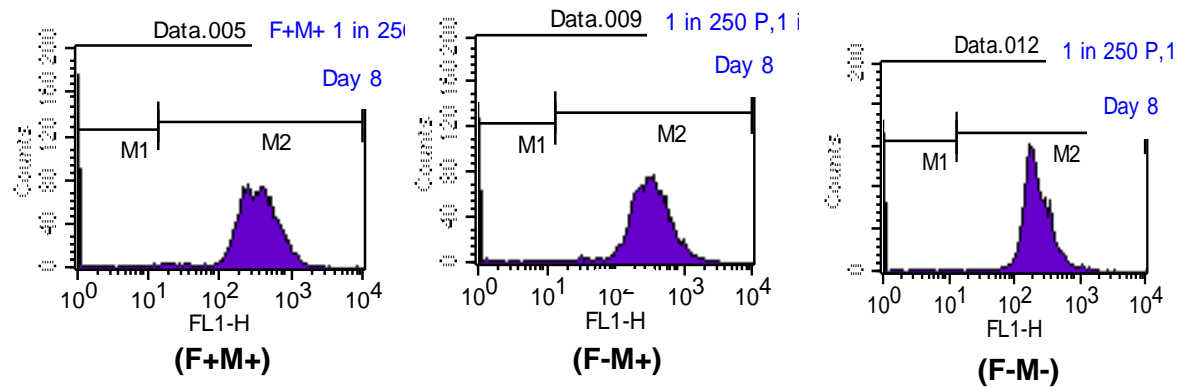
Unstained (A), IgG1 isotype+2° antibody (B), anti 5-methylcytosine (1°) antibody alone (C), 2° antibody alone (D), IgG1 isotype alone (E), 20µM 5-aza-2-deoxycytidine-treated cells (F), 10µM 5-aza-2-deoxycytidine-treated cells (G), and non 5-aza-2-deoxycytidine-treated cell (H), respectively.

The graphs show cell count (Y-axis) versus fluorescence intensity, on a logarithmic scale (X-axis). Graph in A to E shows an example of negative result for controls and F to H shows an example of positive result from anti-5-methylcytosine antibody staining. The right-shift in H indicates a greater concentration of 5-methylcytosine

Day 4



Day 8



Day 12

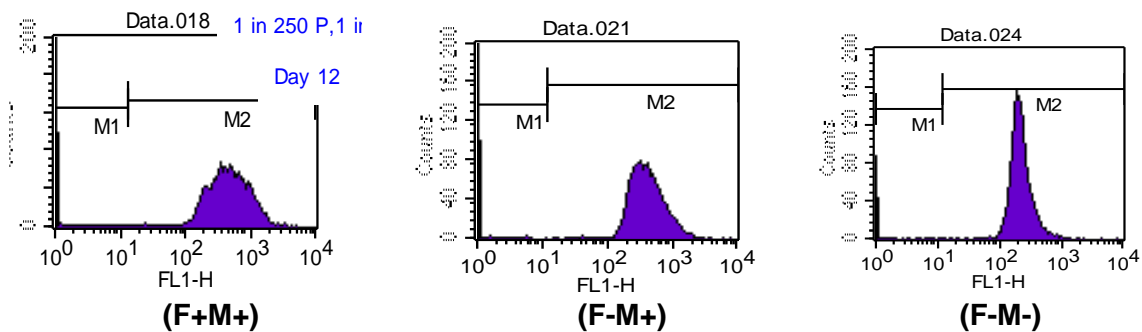
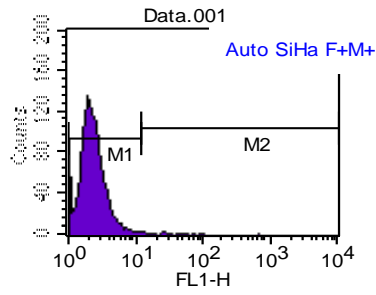
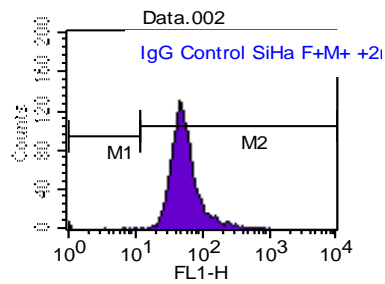


Figure 39: Detection of 5-methylcytosine of C4-II DNA by flow cytometry

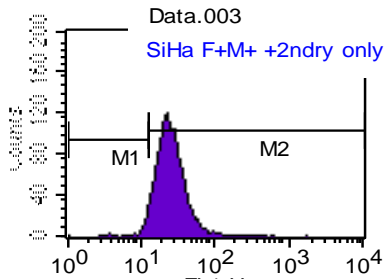
The graphs show 5-methylcytosine stained cells from three time points (day 4, 8, and 12) and three different conditions (from left F+M+, F-M+, and F-M-, respectively)



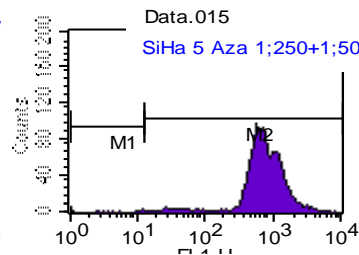
(A) Unstained



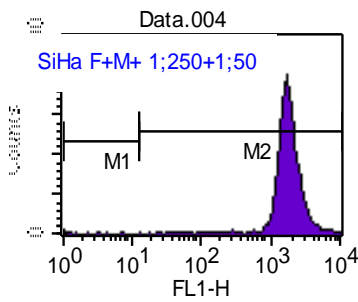
(B) IgG1 isotype+2° antibody



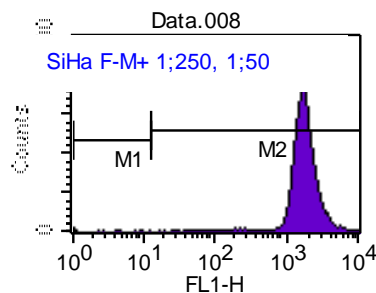
(C) 2° antibody alone



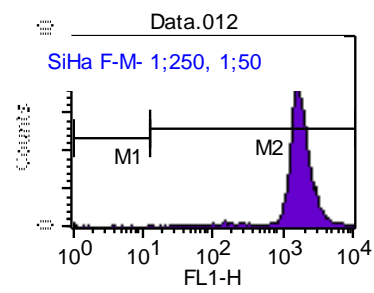
(D) 5-aza-2-deoxycytidine-treated cell



(E) F+M+ cells



(F) F-M+ cells



(G) F-M- cells

Figure 40: Detection of 5-methylcytosine of SiHa DNA by flow cytometry

Unstained (A), IgG1 isotype+2° antibody (B), 2° antibody alone (C), 5-aza-2-deoxycytidine-treated cell (D), anti 5-methylcytosine+2° antibody of F+M+ cells (E), anti 5-methylcytosine+2° antibody of F-M+ cells (F), and anti 5-methylcytosine+2° antibody of F-M- cells (G), respectively.

4.4.2 Determination of Global DNA methylation

In C4-II cells, there was evidence of a decrease in 5-methylcytosine in folate and methionine depleted cells in comparison with cells grown in complete medium, as seen in the data shown in **table 4**.

Results were expressed as a percentage reduction of global DNA methylation in treated cells compared with controls. There was a significant effect of time on global DNA methylation status from day 4 to day 8 ($P=0.016$). There was a progressive reduction in global DNA methylation in folate and methionine depleted cells compared with control cells. At day 4 there was a 2.03% reduction, at day 8 there was a 13.6% reduction, and by day 12 this had reached a 17.5% reduction, but the effect of time was not statistically significant ($P=0.08$). The mean percentage reduction in DNA methylation level was higher at all time points for cells grown in folate and methionine depleted medium compared with cells grown in complete medium and this reached statistical significance on day 8 ($P=0.024$). Effects of folate depletion alone on 5-methyl cytosine were more modest, resulting in a mean fall of 4-9% over 12 days of depletion, not significantly different from control cells.

Table 4: *The percentage reduction in global DNA methylation in C4-II cells depleted of methyl donors, compared with control cells*

Day of culture	Percentage reduction in global DNA methylation	
	F-M+ medium (mean \pm SEM)	F-M- medium (mean \pm SEM)
4	4.39 \pm 4.93	2.03 \pm 11.85
8	8.99 \pm 4.35	13.61 \pm 1.46*
12	6.94 \pm 9.66	17.46 \pm 2.78

Values are mean values from three-independent experiments

**significantly different from control, $P<0.05$ (one-way ANOVA, post hoc test)*

In SiHa cells, the mean percentage reduction in global DNA methylation was greater in cells depleted of both folate and methionine than control cells at weeks 4 and 6 but the effect just failed to reach statistical significance ($P=0.052$) (**table 5**).

Table 5: The percentage reduction of global DNA methylation in SiHa cells depleted of methyl-donors, compared with control

Week of culture	Percentage reduction in global DNA methylation	
	F-M+ medium (mean ± SEM)	F-M- medium (mean ± SEM)
2	2.51±1.04	2.39±0.65
4	1.17±1.63	10.17±3.75
6	1.28±8.23	8.40±4.12

Values are mean values from three-independent experiments

4.4.3 DNMT expression (C4-II cells only)

As an effect of methyl donor depletion on global DNA methylation was only observed to be significant in C4-II cells, the relative quantification (RQ) real-time PCR of DNMT expression was examined in C4-II cells only

There was a downregulation in expression of DNMT3a and 3b, in response to methyl donor depletion, in contrast with DNMT1 which was not significantly influenced by methyl donor depletion (**Figure 41**). Although the mean expression of DNMT1 was lower in folate and methionine-depleted cells than control cells or folate-depleted cells at day 8, the difference was not statistically significant (**figure 41A**). DNMT3a expression was significantly influenced by treatment ($P=0.001$) (**figure 41B**). At day 4 the expression was significantly lower in folate depleted ($P=0.02$) and folate and methionine depleted cells ($P=0.001$) than in the control. At day 8, the difference was only significant between the folate and methionine depleted cells and the controls ($P=0.024$). There was 2.62-fold lower expression of DNMT3a on this day compared with control cells. The folate depleted and folate and methionine depleted cells were not different from one another on either day. DNMT3a gene expression decreased from day 4 to day 8, in cells depleted of both folate and methionine ($P=0.03$).

DNMT3b expression was also significantly influenced by time ($P=0.004$) and by treatment ($P<0.001$), and a significant interaction was observed between these factors ($P=0.038$) (**figure 41C**). On day 4, there was a significantly lower expression of DNMT3b in folate deplete ($P=0.032$) and folate and methionine depleted cells ($P=0.006$) than control, and this difference was also evident on day 8 ($P<0.05$). On this day, DNMT3b expression was 3.60-fold lower in folate and methionine depleted cells compared with control. Folate

depleted cells were not different from folate and methionine depleted cells on either day. There was a significant fall in DNMT3b gene expression in folate and methionine depleted cells from day 4 to day 8 ($P=0.008$).

4.4.4 Total DNMT activity

As global DNA methylation was lower in folate and methionine depleted cells than cells grown in complete medium and expression of both DNMT3a and 3b was downregulated in response to methyl donor depletion, it was anticipated that methyl donor depletion would lead to a fall in the activity of DNMTs. Thus total nuclear DNMT activity was measured in cells grown under different methyl donor conditions.

Unexpectedly, cells depleted of folate and methionine showed a 2.5 fold increase in total DNMT activity at day 8 compared with cells grown in complete medium and this difference was highly significant ($P=0.001$). Folate depletion alone did not influence total DNMT activity (**Figure 42**).

4.4.5 Folate and methionine repletion (only C4-II cells)

4.4.5.1 Effect on cell growth

After growth of cells in folate and methionine-deplete medium for 8 days, cells were grown in complete medium for a further 4 days. On day 12 cell number was still significantly greater in control cells than cells grown initially in either deficient media ($P<0.02$), and there were more cells for the folate-replete treatment than for the folate and methionine-replete treatment ($P=0.022$) (**Figure 43**). Cells transferred from a folate and methionine-deplete medium to a complete medium at day 8 showed a significant increase in cell number by day 12 ($P<0.001$). The growth rate of folate depleted cells after repletion also increased significantly between day 8 and 12 ($P<0.001$).

4.4.5.2 Effect on DNMT gene expression

In this depletion/repletion experiment, combined depletion of folate and methionine led to a significant loss of expression of DNMT1, 3a and 3b, which was recovered following transfer of depleted cells to a complete medium for 4 days (**Figure 44**).

Folate and methionine-depletion led to a downregulation in expression of DNMT1, such that by day 8 DNMT1 expression was lower in depleted cells than controls ($P=0.045$) (**figure 44A**). Following transfer to complete medium, there was an increase in expression of DNMT1 from day 8 to day 12 ($P<0.05$) and there was no longer any significant difference in DNMT1 expression between treatments.

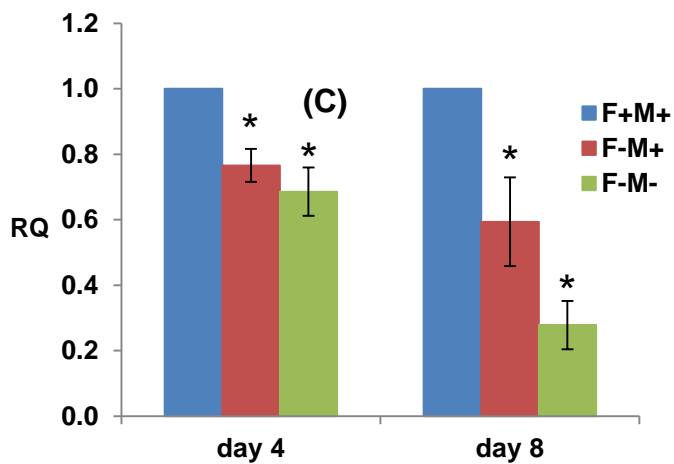
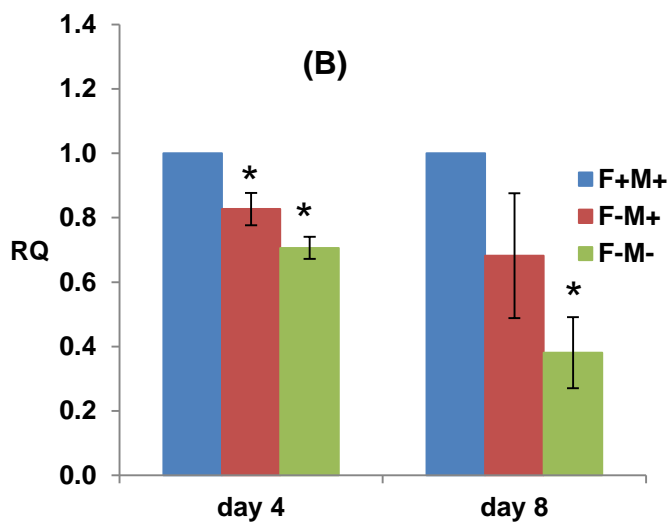
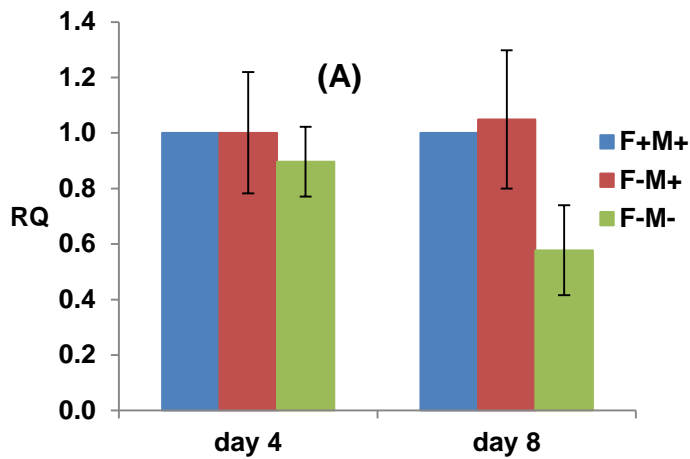


Figure 41: DNMT expression of C4-II cells grown in folat depleted medium, folate and methionine-depleted medium and complete medium

DNMT1, 3a, and 3b expression (A-C) respectively.

Each value shows the mean of four-independent experiments and error bars show SEM.

* Significantly different from control, $P < 0.05$ (one-way ANOVA, post hoc test)

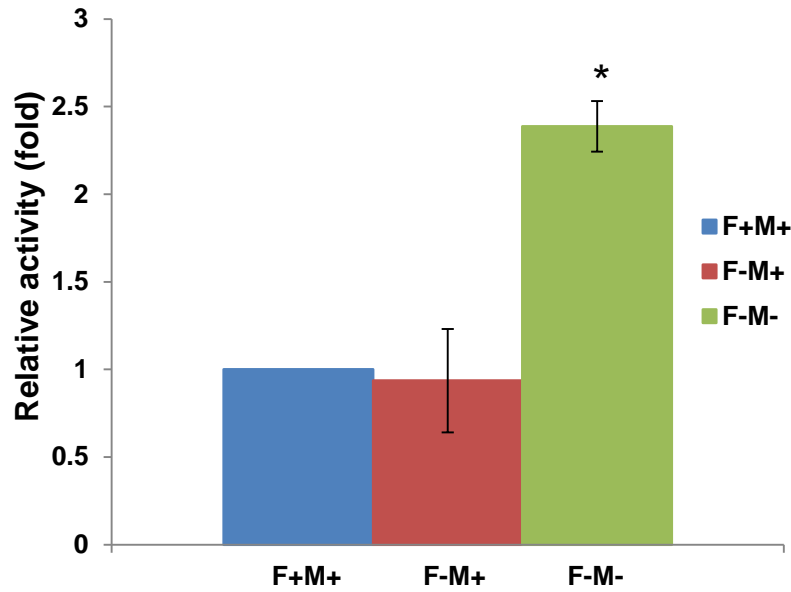


Figure 42: Total DNMT activity of methyl-donor depleted cells in comparison with control

Each value shows mean of four-independent experiments and error bars show SEM.
 * Significantly different from control and F-M+, $P < 0.05$ (one-way ANOVA, post hoc test)

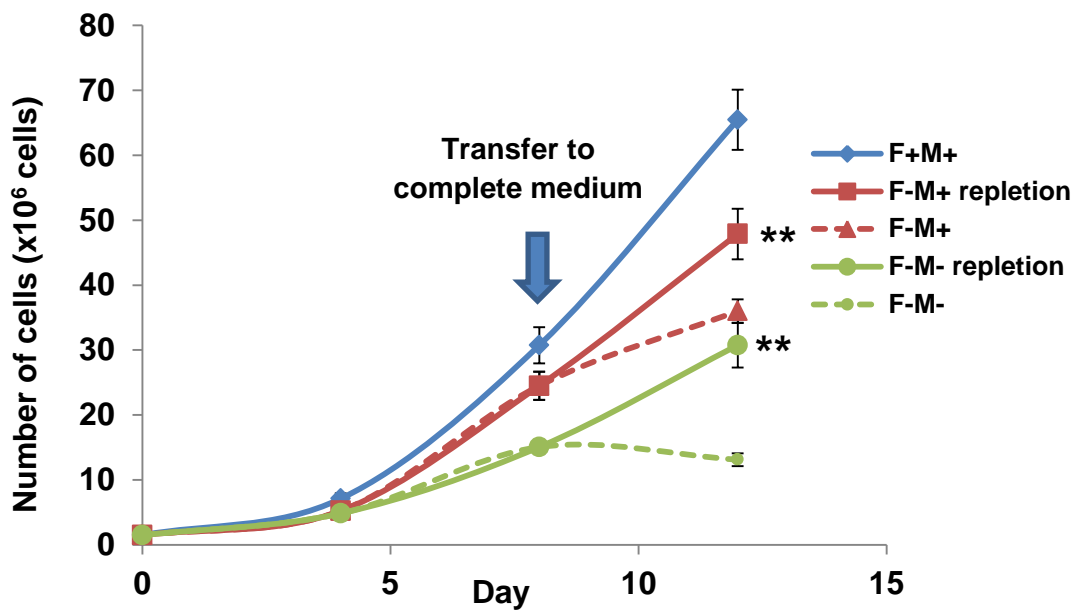


Figure 43: Growth of cells depleted of methyl donors for 8 days and then grown in complete medium for a further 4 days

The dotted lines refer to the growth rate of the 12-day depletion model and the solid lines refer to the growth rate of the repletion model.

Each value shows mean of five -independent experiments and error bars show SEM.
 ** Significantly different from value after 8 days of depletion, $P < 0.05$ (one-way ANOVA, post hoc test)

There was a significant fall in DNMT3a gene expression from days 4 to 8 in folate and methionine-depleted cells ($P=0.002$) such that after 8 days of depletion DNMT3a expression was significantly lower in folate deplete ($P=0.016$) and folate and methionine depleted cells ($P<0.001$) than in the control cells. It was also lower in folate and methionine-depleted cells than in folate deplete cells ($P = 0.014$) (**figure 44B**). Repletion led to a significant increase in DNMT3a gene expression ($P<0.001$) so that by day 12 there was no significant difference in DNMT3a expression between treatments.

DNMT3b expression behaved in a similar fashion. DNMT3b expression fell in response to 8 days of growth in folate and methionine depleted medium ($P=0.008$); following 4 days of repletion DNMT3b gene expression increased ($P=0.038$) (**figure 44C**). After 8 days of depletion, expression of DNMT3b was lower in folate and methionine depleted cells than control cells and cells depleted of folate alone ($P<0.01$). This difference was reversed by 4 days of repletion.

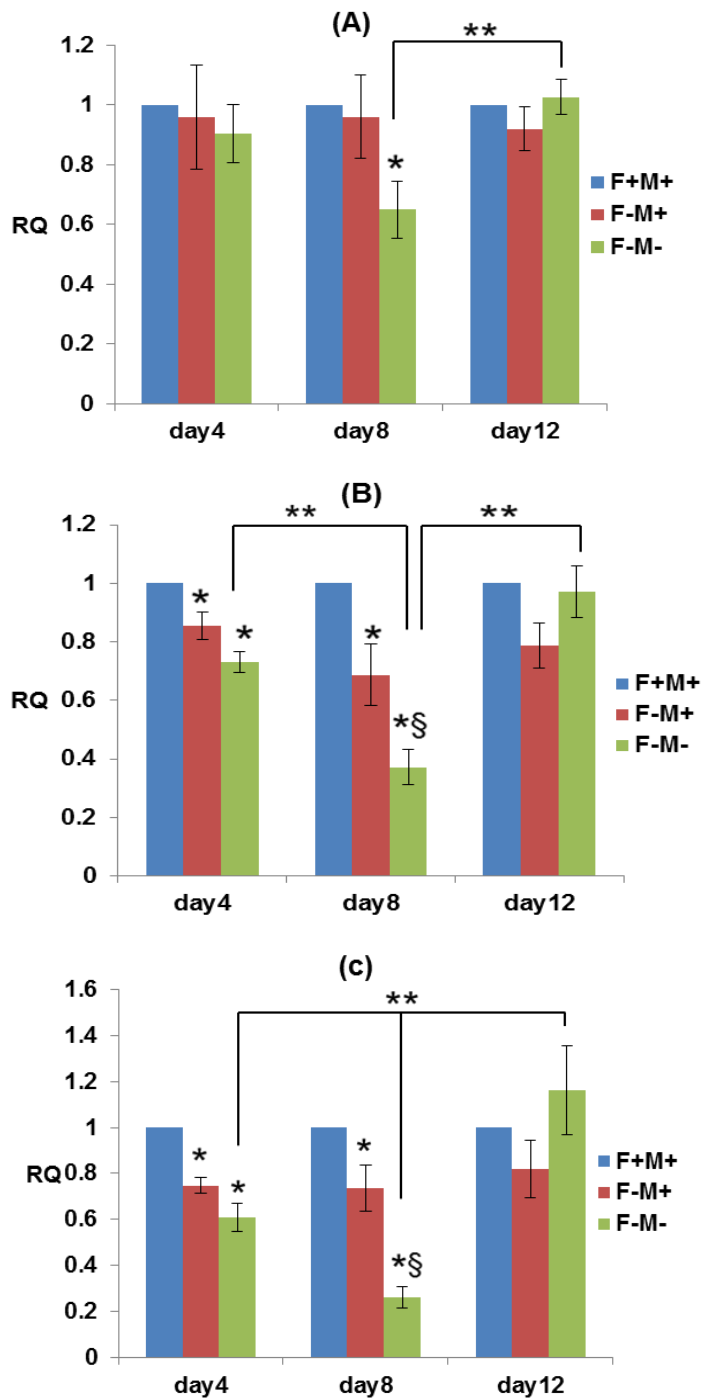


Figure 44: Effects of methyl donor depletion on DNMTs expression in C4-II cells

Cells were grown in folate or folate and methionine-depleted medium for 8 days, after which they were transferred to complete medium and grown for a further 4 days. (A) DNMT1 (B) DNMT3a (C) DNMT3b

Each value shows mean of five to seven-independent experiments and error bars show SEM.

*Significantly different from control, $P < 0.05$ (one-way ANOVA, post hoc test)

§ Significantly different from F-M+, $P < 0.05$ (one-way ANOVA, post hoc test)

** Significantly different by time, $P < 0.05$ (one-way ANOVA, post hoc test)

4.5 Discussion

4.5.1 Effect of methyl donor depletion on global DNA methylation

4.5.1.1 DNA methyl acceptor assay

In our study, this particular method for determining DNA methylation showed poor precision, despite intensive efforts to improve reproducibility. The coefficient of variation of this method was quite high (11.62%). Dahl & Guldborg (2003) suggested in their review paper that this may be partly due to instability of SAM and SssI methyltransferase. They also mentioned that although the DNA methyl acceptor assay appears to be relatively straightforward, others have reported many technical problems.

The [³H]-SAM donor assay for global DNA methylation did not reveal any effects of folate and methionine depletion, in either C4-II or SiHa cells, although with increased number of cell passages there was an increase in DNA hypomethylation. Whilst there are no explicit reports of an increase in hypomethylation of cells during successive passages there are reports describing a correlation between ageing and increasing hypomethylation, such as in reports of Catania *et al.* (Catania & Fairweather, 1991) and Kim *et al.* (Kim *et al.*, 2009). They concluded that 5-methylcytosine loss occurred during cell culture and appeared to be related to cell division. The rate of 5-methylcytosine loss was related to *in vitro* lifespan.

4.5.1.2 Immunocytochemistry for the detection of 5-methylcytosine

Piyathilake *et al.* (2000) used an immunohistochemistry method for the detection of 5-methylcytosine in squamous cell lung cancer specimens, in order to investigate the level of global DNA methylation (Piyathilake *et al.*, 2000). We examined the potential of this method for the quantification of 5-methylcytosine in C4-II cells. However, because of the high density of cells it was very difficult to reliably assess and score the intensity of staining after several days of culture. This problem was compounded by the appearance of multilayers after longer periods of growth in complete medium. The binding of primary antibody appeared problematic too, leading to probable false negative results. Therefore, it was concluded that determination of global DNA methylation using this method was not appropriate for C4-II cells.

4.5.1.3 Flow cytometric analysis of 5-methylcytosine

Although flow cytometry has been widely used in methylation studies of cells in culture we are not aware of its application to studies of effects of folate depletion in cell

culture. Flow cytometry was performed in order to detect 5-methylcytosine at a cellular level because it had been difficult to quantify the degree of staining in our immunocytochemistry owing to factors such as hyperconfluence over many days of cell growth, as well as operator subjectivity (Habib *et al.*, 1999; McManus *et al.*, 2006).

A protocol for the flow cytometric determination of 5-methylcytosine in cultured cells was developed and optimised. Using the optimised method it was possible to demonstrate an effect of methyl donor depletion on global DNA methylation in C4-II cells in culture. Staining for flow cytometry was also carried out on SiHa cells for three experiments. However, no difference was seen in the mean fluorescence intensities between the different growth conditions. One possible explanation for this is that the DNA methylation process in these cells may be preserved to some extent at the expense of other methyl acceptors.

The flow cytometric analysis of C4-II cells and SiHa cells was suggestive of two sub-populations of cells, for some conditions at certain time-points. It is not immediately apparent why this should be the case. However, differences in cell size, shape and internal complexity such as stage of life-cycle, might influence the results of flow cytometry (Shapiro, 2003). Since flow cytometry detects light scattering and fluorescence properties in order to sort cells and discriminate cell groups. The split peaks in some of the plots, which suggest sub-populations of cells, might reflect differences between cells in stages of the cell cycle and in cell size. Different stages of the cell cycle stage are associated with a distinct DNA content (Darzynkiewicz *et al.*, 2010) and differences between cells might lead to a non-homogeneity of 5-methylcytosine detection. Moreover, any hyperconfluency of C4-II cells at the later time point might have resulted in apoptosis or in limited access of the 5-aza-deoxycytidine to some cells; either possibility could have contributed to sub-populations of fluorescing cells. It is not possible to re-analysis the data because the original file has been removed from the database of our facility.

Results from other studies, using various methods, have been inconsistent and there are various reasons why this might be so, including differential responses of different cell lines to methyl donor depletion. The study by Stempak *et al.* (2005) suggested that effects might be cell-specific. Using the SAM donor assay they showed a lower global DNA methylation in folate-deficient untransformed cells (NIH/3T3 and CHO-K1), but not in folate-deficient transformed cells (HTC116 and Caco-2). Folate depletion in normal human colonic epithelial cell lines, HCEC, NCM356 and NCM460 using LC-MS (high-performance liquid chromatography/ electrospray ionization mass spectrometry), did not influence global DNA methylation (Crott *et al.*, 2008). A study of moderately folate-depleted rats showed no significant change in DNA methylation of liver or colonic mucosa, using the SAM donor

assay (Kim *et al.*, 1995). Moreover, using liquid chromatography-mass spectrometry, feeding a folate-deficient diet to mice for 8 months found only a 9% fall in global DNA methylation in splenocytes, a decrease of 4% in small intestinal epithelial cells and a 7.2% reduction in colon epithelial cells, only the latter reaching statistical significance ($P < 0.05$) (Heinz *et al.*, 2009).

Other studies, in various systems and using various methods, have reported effects of folate depletion on global DNA methylation. For example, folate depletion of immortalized colonic epithelial cells resulted in an increase in global DNA hypomethylation (Duthie *et al.*, 2000a). There have been few studies in humans, but Rampersaud *et al.* (2000) reported a fall in global DNA methylation in leukocytes in response to a moderate folate-depletion (118 μg folate/day) of elderly women (age 60-85) for 7 weeks, which was not reversed over a 7 week repletion period (200 or 415 μg folate/day).

S-adenosylmethionine is the methyl donor for very many methylation reactions, possibly more than 50, and DNA is only one substrate for methylation. Other substrates for methylation include guanidinoacetate (forming creatine), and phosphatidylethanolamine (forming phosphatidylcholine). To maintain other methylation activities, the DNA methylation profile may be preserved to some extent at the expense of other methyl acceptors. The effect of one-carbon depletion may be evident in changes in other methylated substrates before effects on DNA methylation are noted (Brosnan *et al.*, 2004). Furthermore, others have shown interactions between the activities of dietary methyl donors (Niculescu & Zeisel 2002); notably, choline may mitigate effects of folate depletion (Craciunescu *et al.*, 2010). Their study was conducted to investigate the effect of folate-deficiency (FD) and folate-deficiency with choline-supplementation (FDCS) on the neurogenesis and apoptosis of regions of fetal mouse brain. While folate deficiency led to a reduction in the mitosis rate and an increase in apoptosis of neural progenitor cells in different regions of the brain, choline supplementation mitigated some of these effects.

Serum choline concentration depends on the intake of choline in the diet and fluctuates during meals (Bligh, 1952; Zeisel, 1981). While the normal human plasma choline concentration is about 10 μM (Savendahl *et al.*, 1997), the choline concentration in the medium used to grow the C4-II cells is about 1.8mM (0.454g/L of choline bitartrate), compared with a choline concentration of 0.2-0.3 μM (0.003-0.004 g/L of choline chloride) in RPMI-1640 and DMEM media, which are commonly used to culture cells *in vitro*. As the medium used to grow the C4-II cells was particularly rich in choline, this may have compensated for the depletion of folate and methionine and maintained methionine synthesis and therefore SAM synthesis, through the betaine pathway.

The accumulation of homocysteine produced in our folate and methionine-depleted system may be another influence on DNA methylation. Jiang *et al.* (2007) investigated the effect of induced hyperhomocysteinemia in rats fed various concentrations of methionine. They demonstrated that a high plasma homocysteine concentration was associated with an increase in genome hypomethylation of B1 repetitive element (B1 is SINE: Short Interspersed Element in mouse which shares 70-80% sequence homology of *Alu* in human). However, there is no certainty that the effects were due to elevated homocysteine or decreased methionine. They also suggested that the different concentrations of homocysteine impacted on methyl metabolism (Jiang *et al.*, 2007a). It is known that SAH is a DNA methyltransferase inhibitor, the reversible reaction from accumulated homocysteine to SAH could increase the inhibition of DNA methyltransferase and thereby influence DNA methylation (James *et al.*, 2002).

Effects of methyl-donor depletion on global DNA methylation seem very dependent on the model system, the protocol for depletion, and the method of analysis.

4.5.2 Effect on DNMTs expression

To determine whether effects of methyl donor depletion on global DNA hypomethylation in C4-II cells could be explained by altered expression of DNMTs, mRNA was determined for DNMT1, 3a and 3b. A combined methionine and folate depletion resulted in a progressive reduction in the mean expression of all DNMTs with time, and this was especially so for DNMT3b. Folate depletion alone had less marked effects than the double-depletion, but did lead to a loss of DNMT3a and 3b expression. DNMT1 expression was more resistant to effects of methyl donor depletion than DNMT 3a and 3b, but did also show a reduced expression in response to a combined depletion of folate and methionine. Repletion of cells with folate or folate and methionine reversed effects on growth and DNMT expression.

Others have studied effects of methyl donor depletion on the expression of DNMTs but the direction of any effects observed are not consistent between studies, or between DNMTs. Hayashi *et al* (2007) observed a down regulation of DNMT3a and 3b in folate-depleted human colon adenocarcinoma cells but DNMT1 was upregulated in this system. They did not propose a mechanism for the effect. Stempak *et al* (2005) reported a decrease in DNMT1 and DNMT3a protein expression in folate-depleted untransformed NIH/3T3 mouse fibroblast cells, which was reported global DNA hypomethylation, but also in human HCT116 and Caco-2 colon cancer cells in which they did not observe DNA hypomethylation. Moreover, a rat model of multi methyl-donor deficiency (methionine, folate, and choline) showed an increase in the protein and mRNA of DNMT1 and DNMT3a in liver, but no

change in DNMT3b expression (Ghoshal *et al.*, 2006). Importantly, in our studies the additional depletion of methionine generated more pronounced effects than folate depletion alone, and the effects were reversible. This suggests a mechanism that is not specific to either folate or methionine but is rather underpinned by methyl group deficiency.

Several factors are thought to influence the expression of DNMTs, such as the expression level of microRNAs (miRNAs) and non-coding RNAs (ncRNAs), and chromatin conformation. The effect of methyl-donor deficiency on DNMTs expression might be explained in the context of a change in chromatin structure. A change in methyl-donor status may lead to aberrant DNA methylation and subsequent histone acetylation, leading to a reduced accessibility of transcription factors to the binding site of chromatin (Jones *et al.*, 1998; James *et al.*, 2003; Pogribny *et al.*, 2007; Delage & Dashwood, 2008). Kovacheva *et al.* (2007) were able to show that DNMT1 expression was influenced by methylation; specifically, hypomethylation at a key regulatory CpG within the DNMT1 locus led to upregulation of this gene. In contrast, in our study of C4-II cells, we did not observe the upregulation of DNMTs, even though global DNA hypomethylation was observed. The explanation in this case may be that the gene-specific hypomethylation did not function directly at DNMTs themselves. In contrast, the expression of other regulators, such as repressor proteins, involved in DNMTs transcription may be up-regulated by gene-specific hypomethylation mediated by methyl-donor depletion, resulting in the decrease in DNMTs expression.

The functional significance to cancer progression of altered expression of DNMTs in response to methyl donor depletion is unclear. DNMTs have been found to be overexpressed in some human cancers (De Marzo *et al.*, 1999; Mizuno *et al.*, 2001; Etoh *et al.*, 2004; Su *et al.*, 2013). On the other hand, Choi *et al.* demonstrated a loss of cytoplasmic expression of DNMT3a in hepatic carcinogenesis and suggested that dysregulation of DNMT3a expression might be involved in cancer progression (Choi *et al.*, 2003). There is also limited evidence that silencing of DNMT1 may be associated with demethylation and reactivation of some tumour suppressor genes, in various cancer cell lines, although effects were not wholly consistent (Zhang *et al.*, 2011). Two potentially important studies suggest an inverse relationship between DNMT3a and 3b expression and carcinogenesis; Hlady conducted a study in which he inactivated DNMT3b in a mouse model of lymphomagenesis and observed an accelerated lymphomagenesis. He showed a gradual demethylation of a tumour modifier gene MENT (methylated in normal thymocytes) and overexpressed in the DNMT3b knockout model. MENT expression was up-regulated over 60% of human lymphomas. His findings suggested that DNMT3b has a role in maintaining tumour modifier gene methylation in cancer and he proposed DNMT3b as a tumour suppressor (Hlady *et al.*,

2012) . Similarly, Gao showed that deletion of DNMT3a in a mouse model of lung cancer led to an enhanced tumour progression associated with increased expression of genes important to the cancer phenotype (Gao *et al.*, 2011). He proposed DNMT3a as a tumour-suppressor-like gene. Taken together these findings suggest that a down regulation of DNMT3a and 3b in response to methyl donor depletion may have cancer- promoting effects.

Time constraints meant that we were unable to progress these observations to a validation of DNMTs gene expression by investigating the protein expression. Preliminary studies showed non-specific bands, which precluded an accurate interpretation. Further investigation of a more suitable primary antibody could have been conducted to improve the quality of the result, but this was not possible within our time-frame.

4.5.3 Effect of methyl donor repletion on cell growth and DNMT expression

The diminished growth rate of both folate depleted cells and the folate and methionine depleted cells was corrected after 4 days repletion.

The effect of folate and methionine depletion on DNMT1 expression was equivocal, as our depletion/repletion experiment did suggest a down-regulation following folate and methionine depletion, and reversibility of this effect, but the effect seen in the earlier depletion experiment did not reach statistical significance. This may simply be a reflection of the greater number of independent experiments conducted for the depletion/repletion study. A repletion of methyl donor status from a combined-depletion state led to a significant recovery in the expression of all DNMTs. The effect of folate repletion alone was to improve expression of all DNMTs but to a more modest extent. Our result confirmed that DNA methyltransferase gene expression can be altered by the methyl donor depletion and reversed after repletion.

Relatively few studies have reported effects of methyl donor repletion. Wasson *et al.* conducted an experiment in human colonic adenocarcinoma cell lines (SW620). They grew the cells in folate depleted medium for 7 days and then transferred to a complete medium (3 μ mol/L folic acid) for further 7 days and found that folate deprivation led to DNA hypomethylation, and that this was reversed on folate repletion (Wasson *et al.*, 2006). Williams & Jacobson (2010) observed the growth rate of immortalized human epidermal keratinocytes (HaCaT cells) after 10-day folate depletion and then 10-day repletion and found that cell proliferation, which was decreased by depletion, was recovered after repletion. They reported an increase in the S- and G2-phase cells, during depletion and a reverse this trend on repletion (Williams & Jacobson, 2010). Results of the two studies are likely compatible to our results in which the growth rate and DNMTs expression were

resumed after repletion. Folate and methionine repletion initiated cell cycle and cell proliferation again by restoring DNA synthesis. The methyl cycle was also normalized resulting in the recovery of DNA methylation level and a rescue of gene expression of all relevant genes in DNMTs transcription.

Our results demonstrated that DNA methyltransferase gene expression can be reduced by methyl donor depletion and reversed by repletion, which may have implications for the effects of dietary restriction and supplementation on DNMT expression *in vivo*.

4.5.4 Effect on DNMT activity

Using a method for the measurement of total DNMT activity, rather than the activity of individual DNMTs, combined folate and methionine depletion led to an apparent increase in activity. This seemed counter-intuitive given the loss of expression of DNMT1, 3a and 3b by the same depletion regimen. Furthermore, it was surprising that there was no intermediate effect of folate depletion alone, which we had seen for all other outcomes. Unfortunately, we cannot differentiate between the individual DNMTs because of the limitations of the activity assay and therefore we do not know whether any particular DNMT is driving this apparent effect. The DNMT activity assay kit used in our research is an ELISA-based protocol in which the methylated DNA products can be detected with a 5-methylcytosine antibody. A discussion of the limitations of the kit used to measure total DNMT activity is warranted here. The percentage of coefficient of variation (%CV) of this protocol was very high (>20%). From 4-independent experiments, there was one experiment in which folate-depleted cells gave a 1.8 fold higher activity than complete cells while the other three experiments resulted in a modest lowering of activity. In addition, the activity detected was different from lot to lot of the kit. The actual activity value could not be obtained, even for the positive control enzyme provided from the manufacturer. The sensitivity of the assay is also a potential limitation because this kit requires a high protein concentration of nuclear extract in a tiny microlitre volume. Moreover, the protein concentration of the nuclear extract did not relate directly to the amount of DNMT, rather to the total protein concentration of the extract. There was also uncertainty about those factors which influenced enzyme stability, which depended on pH, temperature, amount of substrates and cofactors. Therefore, the interpretation of total DNMT activity should be considered cautiously. The lack of effect of folate depletion alone was in accordance with findings of Uthus *et al* (2006) in their study of 70-day folate deficiency in rats; using the SAM donor based assay, they found no change in total DNMT activity in the liver or colon of the rats (Uthus *et al.*, 2006).

Total DNMT activity was also studied in folate-deficient cells using the SAM-donor assay based protocol. They found a lower total DNMT activity in folate-deficient non-transformed cells HIH/3T3 but not in CHO-K1 cells. They also reported a lower DNMT activity in folate-deficient Caco-2, but not in HCT116 colon cancer cells (Stempak *et al.*, 2005), indicating a cell-specificity. According to the DNA methylation and DNMTs results of Stempak *et al.*, folate depletion has more influence on non-transformed cells than transformed cells. The depleted non-transformed NIH/3T3 cells have an increased DNA hypomethylation, despite increased DNMTs activity and DNMT1 and DNMT3a protein. Jiang *et al.* (2007) found an increased activity of DNMT3a and DNMT3b in vascular smooth muscle cells exposed to high homocysteine concentrations, which is usually interpreted as reflecting disturbance to the methylation cycle and is associated with folate deprivation as in our study (Jiang *et al.*, 2007b). However, they also found an increase in S-adenosylhomocysteine, which is understood to inhibit DNMT activity (Saavedra *et al.*, 2009) and therefore their results are difficult to interpret.

Most cancer cells have a genome-wide hypomethylation and Belinsky *et al.* (1996) suggested that an increase in total DNMT activity is a sign of neoplastic development and carcinogenesis (Belinsky *et al.*, 1996). Jiang *et al.* (2007) suggested that an increase in DNMT activity could be seen as a compensatory mechanism in order to maintain a DNA methylation profile (Jiang *et al.*, 2007a).

The anti-correlation between DNMTs expression and activity in the methyl donor depletion was unexpected. The underlying mechanism of this mismatch may be explained in the context of post-translational modification. For DNMT1, there are some documented examples of post-translational modifications which influence its stability/activity. For example, Goyal *et al.* removed the phosphorylated serine 515 from DNMT1 and found a severe loss of DNMT1 activity (Goyal *et al.*, 2007). Estève *et al.* showed that lysine methylation of DNMT1 mediated by SET7 (histone methyltransferase) influenced proteasome-mediated degradation of DNMT1 (Estève *et al.*, 2009). In the DNMT3 family, a study of sumoylation of DNMT3a at the N-terminal regulatory region, showed a disruption of interaction with HDAC interaction, leading to impaired stability and activity of DNMT3a (Ling *et al.*, 2004).

The existence of DNMT isoforms, especially splice variants of DNMT3b, could also explain the mismatch between expression and activity of DNMTs. Depending on the specific splice variant, there may be different effects on the function of a particular DNMT (Choi *et al.*, 2011). There are more than 30 isoforms of DNMT3b and several of them are inactive because the catalytic C-terminal domain is missing. Moreover, there is evidence that inactive

isoforms of DNMT3b could influence overall activity and lead to a difference in DNA methylation patterns. Godon *et al.* proposed that DNMT3b3 isoform binds to the regulatory site of DNMT3a and modestly increases DNMT3a activity. In contrast, DNMT3b4 isoform inhibits the DNMT3 family enzyme activity by competitive binding to DNA substrate (Gordon *et al.*, 2013).

4.6 Summary

Our results show for the first time that a combined folate and methionine deficiency in a cervical cancer cell line induces global DNA hypomethylation and this may be caused by the observed down regulation of the *de novo* DNA methyltransferases. There was a concordance between DNMT expression and global DNA methylation, but a lack of concordance between DNMT expression and activity. Loss of DNMT expression has been associated with enhanced cancer progression in some studies, which suggests that methyl donor depletion in people with an existing cancer might have adverse effects. However, there is also evidence that down-regulation of DNMT expression may lead to a re-activation of tumour suppressor genes which would have a beneficial effect. It is therefore difficult to be certain of the overall effect on cancer progression of a down-regulation of DNMTs.

Chapter 5 Gene expression

5.1 Introduction

Diets supplemented with methyl donors have been reported to influence gene expression, via the alteration of DNA methylation. Our research has demonstrated that methyl donor depletion can result in modest DNA hypomethylation which is linked to the down-regulation of *de novo* DNA methyltransferases. Changes in the gene expression profile of cancer cells are likely to lead to changes in cell behaviour; some changes may be relevant to cancer progression. Therefore, it was considered that an investigation of the role of methyl donors in determining the gene expression profile of cervical cancer cells may bring some benefits to understanding cancer prognosis.

Other studies have reported gene expression in cervical cancer. In the review of Dueñas-González *et al.* (Dueñas-González *et al.*, 2005), several genes were proposed as being causally linked with cervical carcinogenesis, through epigenetic mechanisms. Those altered genes involved several which are known to be involved in many important processes such as apoptosis, the cell cycle, Wnt signalling pathway, and DNA repair. In their study of cervical cancer progression, Hagemann *et al.* (2007) compared the molecular profile of lymph node micrometastases with primary tumours using Taqman Low-Density Arrays. They reported that *AKT*, *BCL2*, *CSFR1*, *EGFR1*, *FGF1*, *MMP3*, *MMP9* and *TGF- β* were upregulated by more than 2-fold (Hagemann *et al.*, 2007). Recently Rajkumar *et al.* (2011) carried out an oligo-microarray study in samples from various stages of cervical cancer. They identified seven genes which they proposed were involved in tumourigenesis, which were *UBE2C*, *CCNB1*, *CCNB2*, *PLOD2*, *NUP210*, *MELK*, and *CDC20*. In addition they demonstrated an upregulation of *IL8*, *INDO*, *ISG15*, *ISG20*, *AGRN*, *DTXL*, *MMP1*, *MMP3*, *CCL18*, *TOP2A*, and *STAT1* in cancers compared to normal, CIN1/2 or CIN3/CIS stages of cell abnormality (Rajkumar *et al.*, 2011). Those genes are likely to be important in cervical cancer progression.

In terms of methyl-donor depletion, some studies, in various cell types, have investigated the effects of folate depletion on gene expression. For example, Jhaveri *et al.* (2001) conducted a gene microarray of folate-depleted human nasopharyngeal epidermoid carcinoma KB. Surprisingly, they found only three genes showing up-regulation (Brain-expressed HHCPA78 homolog, Calmegin, and Insulin-induced protein 1) and five genes showing down-regulation (Keratin type 1 cytoskeleton 14, Cyclin D3, H-cadherin, Gravin, and Interferon-inducible protein 1-8U) (Jhaveri *et al.*, 2001). This result pointed that there seemed to be cell communication leading to cell proliferation and transformation genes affected by folate deficiency. In the study conducted by Katula *et al.* (Katula *et al.*, 2007) to

investigate global gene expression in folate-deficient normal human fibroblast cells (GM03349), effects were observed in the Wnt pathway, cell signalling, and the cytoskeleton and extracellular matrix. In the above depletion studies, the proteomic and pathway analysis was also investigated in folate-deficient NCM460 human colon epithelial cells by Duthie *et al.* (2008). They reported a significantly altered protein expression in proteins important to cell proliferation, DNA repair, apoptosis, cytoskeleton organization, and malignant transformation. They also suggested that folate status most associated with the regulation of actin cytoskeleton, which significantly affects cell motility and locomotion (Duthie *et al.*, 2008). All of the above studies showed that no matter what cell types are, folate deficiency seems to affect signalling pathways and cytoskeleton organization.

The gene expression in methyl-donor depleted cervical cancer cells has not been investigated so far. In order to determine the effects of folate and methionine depletion on global gene expression of cervical cancer cells, a gene microarray analysis was conducted.

5.2 Aims

To investigate the effects of methyl-donor depletion of C4-II cervical cancer cells on gene expression profile by gene microarray, in order to gain insight into possible implications for cancer progression.

5.3 Methods

5.3.1 Microarray

A genome-wide microarray analysis was processed by Dr Paul R Heath, Department of Neuroscience, SiTRans, University of Sheffield. Briefly, the C4-II RNA of F+M+ and F-M- cells was extracted as described (see section 2.2.8). The purity and integrity of C4-II RNA was determined by Agilent 2100 bioanalyzer and Agilent RNA 6000 Nano Kit before further processing (see section 2.2.11.1). The RNA was used for the microarray target preparation (see section 2.2.11.2) and hybridisation (see section 2.2.11.3).

5.3.2 Data analysis

The F+M+ and F-M- samples probe array images were merged for probe intensities and normalised by GeneChip® Command Console® Software (Affymetrix, UK). The data from each sample were analysed and compared by using GeneSpring Software version 11 (Agilent Technologies, Germany). The probe signals were filtered based on fold change and statistical significance (t-test). Genes were selected if there was a statistically significant difference ($P < 0.05$) in gene expression between F+M+ and F-M-. DAVID (The Database for

Annotation, Visualization and Integrated Discovery) Bioinformatics Resource 6.7 software was used to identify effects on specific gene clusters, according to biological function, as described by Huang *et al.* (Huang *et al.*, 2009) .

5.4 Results and discussion

From more than 54,000 probes detected in the microarray, there were about 10,000 probes which appeared to show a significant difference ($P < 0.05$, t-test) in gene expression between methyl-donor depleted cells and complete cells. The analysis did not take account of multiple testing because the use of the Bonferroni method to make such a correction led to an almost complete loss of differentiating genes. Therefore, results will be discussed primarily on the analysis of uncorrected data. However, some attempt has been made to use the Benjamini-Hochberg's method for correction of multiple testing, and results have been included as a brief summary at the end of this chapter.

Those 10,000 probes IDs were further clustered according to biological function. The expressed transcripts were clustered using the DAVID software (David Bioinformatics Resource 6.7). In order to maximize the possible benefit from the microarray, three thousand probe IDs, which was the maximum size of data for analysis with DAVID, were uploaded to DAVID software. The first 3000 probe IDs from up- and down-regulation in methyl donor depleted cells were analysed. All of the significant probes gave the difference in gene expression more than 1.5-fold change. Functional annotation clustering according to biological function revealed 464 clusters of up-regulated genes and 476 clusters of down-regulated genes (**figure 45-46**).

Each cluster was given an enrichment score which indicated the functional importance of the gene group. The clusters which have an enrichment score of more than 1.3 (Huang *et al.*, 2009), were considered further. There were 64 clusters of up-regulated genes and 51 clusters of down-regulated genes, for which the enrichment score was more than 1.3. Of these clusters seven were selected on the basis of a high enrichment score and the biological grouping. These are presented in **table 6**

Functional Annotation Clustering

[Help and Manual](#)

Current Gene List: F-M- vs F+M+ up-reg first 3000 IDs

Current Background: Homo sapiens

2175 DAVID IDs

Options Classification Stringency Medium

Rerun using options

Create Sublist

464 Cluster(s)

[Download File](#)

Annotation Cluster	Enrichment Score			Count	P_Value	Benjamini
Annotation Cluster 1 Enrichment Score: 15.49						
<input type="checkbox"/> GOTERM_CC_FAT	membrane-enclosed lumen	RT		309	5.0E-19	2.9E-16
<input type="checkbox"/> GOTERM_CC_FAT	nuclear lumen	RT		256	6.8E-19	2.0E-16
<input type="checkbox"/> GOTERM_CC_FAT	organelle lumen	RT		300	8.4E-18	1.7E-15
<input type="checkbox"/> GOTERM_CC_FAT	intracellular organelle lumen	RT		294	1.4E-17	2.1E-15
<input type="checkbox"/> GOTERM_CC_FAT	nucleolus	RT		145	2.7E-16	2.6E-14
<input type="checkbox"/> GOTERM_CC_FAT	nucleoplasm	RT		142	1.1E-7	9.5E-6
Annotation Cluster 2 Enrichment Score: 8.12						
<input type="checkbox"/> GOTERM_CC_FAT	nucleolus	RT		145	2.7E-16	2.6E-14
<input type="checkbox"/> GOTERM_CC_FAT	intracellular non-membrane-bounded organelle	RT		356	4.3E-9	4.2E-7
<input type="checkbox"/> GOTERM_CC_FAT	non-membrane-bounded organelle	RT		356	4.3E-9	4.2E-7
<input type="checkbox"/> GOTERM_CC_FAT	cytoskeleton	RT		142	6.5E-1	9.8E-1
Annotation Cluster 3 Enrichment Score: 7.13						
<input type="checkbox"/> GOTERM_BP_FAT	death	RT		134	9.1E-9	3.6E-5
<input type="checkbox"/> GOTERM_BP_FAT	cell death	RT		133	1.1E-8	2.1E-5
<input type="checkbox"/> GOTERM_BP_FAT	programmed cell death	RT		115	4.7E-8	4.6E-5
<input type="checkbox"/> GOTERM_BP_FAT	apoptosis	RT		113	7.3E-8	4.1E-5
<input type="checkbox"/> SP_PIR_KEYWORDS	Apoptosis	RT		71	6.9E-6	2.6E-4
Annotation Cluster 4 Enrichment Score: 5.79						

Figure 45: Example of functional annotation clustering using DAVID Bioinformatics. This screen shot shows a few clusters from the up-regulated gene list

Functional Annotation Clustering

[Help and Manual](#)

Current Gene List: F-M- vs F+M+ down-reg first 3000 IDs

Current Background: Homo sapiens

2203 DAVID IDs

Options Classification Stringency Medium ▾

Rerun using options

Create Sublist

476 Cluster(s)

[Download File](#)

Annotation Cluster 1		Enrichment Score: 23.85			Count	P_Value	Benjamini
<input type="checkbox"/>	GOTERM_BP_FAT	cell cycle phase	RT		129	1.3E-31	4.7E-28
<input type="checkbox"/>	GOTERM_BP_FAT	cell cycle	RT		189	1.6E-30	2.9E-27
<input type="checkbox"/>	SP_PIR_KEYWORDS	cell cycle	RT		132	8.5E-28	2.8E-25
<input type="checkbox"/>	GOTERM_BP_FAT	M phase	RT		106	2.5E-27	3.0E-24
<input type="checkbox"/>	GOTERM_BP_FAT	cell cycle process	RT		146	2.9E-26	2.6E-23
<input type="checkbox"/>	GOTERM_BP_FAT	mitotic cell cycle	RT		109	1.6E-24	1.2E-21
<input type="checkbox"/>	GOTERM_BP_FAT	M phase of mitotic cell cycle	RT		79	3.1E-23	1.9E-20
<input type="checkbox"/>	GOTERM_BP_FAT	organelle fission	RT		80	3.2E-23	1.7E-20
<input type="checkbox"/>	GOTERM_BP_FAT	nuclear division	RT		78	4.1E-23	1.9E-20
<input type="checkbox"/>	GOTERM_BP_FAT	mitosis	RT		78	4.1E-23	1.9E-20
<input type="checkbox"/>	GOTERM_BP_FAT	cell division	RT		88	2.8E-20	1.1E-17
<input type="checkbox"/>	SP_PIR_KEYWORDS	cell division	RT		81	2.6E-19	5.9E-17
<input type="checkbox"/>	SP_PIR_KEYWORDS	mitosis	RT		65	3.2E-19	5.3E-17
Annotation Cluster 2		Enrichment Score: 11.1			Count	P_Value	Benjamini
<input type="checkbox"/>	GOTERM_CC_FAT	condensed chromosome	RT		48	4.0E-15	1.2E-12
<input type="checkbox"/>	GOTERM_CC_FAT	chromosome, centromeric region	RT		45	9.1E-14	1.4E-11
<input type="checkbox"/>	GOTERM_CC_FAT	chromosome	RT		103	1.1E-13	1.4E-11
<input type="checkbox"/>	GOTERM_CC_FAT	chromosomal part	RT		91	1.6E-13	1.6E-11

Figure 46: Example of functional annotation clustering using DAVID Bioinformatics. This screen shot shows a few clusters from the down-regulated gene list

Table 6: Summary of selected gene clusters from both up- and down-regulated genes of methyl-donor depleted cells

Up-regulation	Enrichment score	Down-regulation	Enrichment score
Cell death	7.13	Cell cycle	23.85
Cell motion	4.05	Condensed chromosome	11.1
Protein kinase cascade	3.21	Cytoskeleton organization	9.6
Signal transduction	3.21	DNA metabolic process	5.43
Cell communication	3.21	Transferase	3.77
Blood vessel development	3.21	Lipid biosynthesis process	2.6
Focal adhesion	2.16	Chromosome organization	1.8

From the results of the DAVID resource, the gene list of each cluster could be examined. An example of a gene list from DAVID analysis is presented in **figure 47 and 48**. Gene lists were examined and a small number of genes on the basis of either having a high fold change for that cluster or appearing in more than one cluster were identified and considered more closely. **Table 7 and 8** show such genes and the fold change and direction of change, for the methyl donor depleted cells relative to the controls. In the arm of up-regulation, interesting genes were selected from each cluster and are considered further here. Transforming growth factor beta 2 (TGFB2), which is a secreted cytokine protein, was upregulated 3.76 fold in folate and methionine depleted cells compared with complete cells and this plays an important role in 6 of the 7 clusters considered in our study. TGFB2 functions as a signal to regulate the expression of the extracellular matrix and is linked to several biological processes important to cancer cell activity such as cell adhesion, migration, differentiation, and proliferation. Thrombospondin1 (THBS1) appeared in 4 of the 7 selected clusters. THBS1 expression of folate and methionine depleted cells was 2.2 fold greater than complete cells. This gene encodes the adhesive glycoprotein which is involved in the interaction between cells and cell-matrix. The key roles of THBS1 are in cell migration

and angiogenesis, both of which are important to cancer progression. Another gene which was regulated in folate and methionine depleted cells was transglutaminase 2 (TGM2). Its expression was 29 fold higher than in the complete cells and this gene was involved in 4 of the 7 selected clusters. TGM2 is the gene for a calcium-dependent enzyme which catalyses the transamidation of protein leading to altered protein conformation conferring resistance to proteolytic degradation. TGM2 function can be linked to various cell processes such as extracellular matrix stabilization, cell adhesion, wound healing, cell signalling, and cell motility (Griffin *et al.*, 2002). Tumour protein p63 (TP63) works as a transcription factor and in this way regulates several cell processes such as cell proliferation, cell adhesion, and apoptosis. TP63 expression was 14.18 fold higher in folate and methionine depleted cells compared with complete cells and appeared in 3 of the 7 clusters shown here.

According to the arm of down-regulation, interesting genes were selected from each cluster and some are described here. Breast cancer 1, early onset (BRCA1) which appeared in 5 of the 7 clusters, was down-regulated in folate and methionine depleted cells by 1.74 fold compared to complete cells. BRCA1 is known as a tumour suppressor gene. Aurora kinase B (AURKB) which is the gene for an enzyme involved in cell cycle check point, was down-regulated 3.36 fold and appeared in 3 of the 7 clusters. E1A binding protein p300 (EP300) was down-regulated 3.59 fold and appeared in 3 of the 7 clusters. This gene works as a histone acetyltransferase and is involved in chromosome remodelling. The last example is DNMT3b which we have already shown to be down regulated in folate and methionine depleted cells compared with complete cells, as described in chapter 4. From the microarray result, we also found a down regulation of this gene, the expression of which was 3.03 fold lower in the methyl donor depleted cells, and appeared in 2 of the 7 clusters.

Regarding cancer cell characteristics, Hanahan and Weinberg (2000) proposed six major characteristics of cancer cells which distinguish cancer cells from normal cells. Firstly, cancer cells have their own growth signals. The cells achieve an active proliferative state without relying on stimulatory signals. Secondly, cancer cells are insensitive to antigrowth signals. Thirdly, cancer cells are resistant toward apoptosis. Fourthly, cancer cells have a infinite replicative potential. Fifthly, to maintain their viability, cancer cells require angiogenesis. And finally, cancer cells can move and travel to their surrounding tissue, resulting in tissue invasion and metastasis (Hanahan & Weinberg, 2000). Moreover, in 2011, Hanahan and Weinberg (2011) suggested two more hallmarks of cancer cell potential which are (1) reprogramming of energy metabolism, and (2) evading immune destruction. In addition, they proposed four main intracellular signalling networks which support cancer cell activity. These are motility circuits, proliferation circuits, viability circuits, and cytoskeleton and differentiation circuits. To understand cervical cancer behaviour in methyl-donor depletion,

we need to look closely at all of those circuits. Unfortunately, within the time constraints of this study it was not possible for us to carry out such an exhaustive analysis.

As far as we know, there has been no other study conducted to examine the effects of folate and methionine deficiency on gene expression profile in cervical cancer cells. However, there have been studies focussing on aspects of gene expression profiles of cervical cancer cells and on methyl donor-depleted cells of various types. Perez-Plasencia *et al.* (2007) conducted a study to investigate the alteration of metabolic pathways in invasive squamous cervical cancer stage IIB of human biopsies harbouring HPV16 compared to normal cervical tissues. They demonstrated an upregulation of the Wnt signalling pathway, calcium signalling pathway, and MAPK signalling pathway in invasive cervical cancer and a down regulation of focal adhesion and TGF- β signalling pathways (Perez-Plasencia *et al.*, 2007). In addition, Liu *et al.* (2007) showed that a combined folate and multiple B vitamin (B2, B6, and B12) depletion in a mouse model led to an alteration of Wnt pathway metabolites in mouse colon cells (Liu *et al.*, 2007).

The alteration of Wnt signalling pathway is the most frequently cited in cancer development (Giles *et al.*, 2003) and the altered expression of genes involved in this pathway have been reported in cervical cancer (Dueñas-González *et al.*, 2005). For example, Chen *et al.* (2003) investigated methylation level at the promoter of E-cadherin gene in 5 cervical cancer cell lines and 20 cervical cancer samples. They found that all five cell lines and 8/20 of cervical cancer samples have hypermethylation. Protein expression of E-cadherin was absent in 3/5 of cell lines and 6/8 of cervical cancer sample. They also reported an increase of DNMT1 expression. However, E-cadherin expression was recovered when DNMT1 was interrupted. This cervical cancer study suggested a positive relation between promoter DNA methylation level and DNMT1 expression (Chen *et al.*, 2003). Another study, conducted by Cheung *et al.* (2004), was focused on PTEN (phosphatase and tensin homolog). They determined methylation level at promoter of PTEN in 10 samples of high-grade cervical intraepithelial neoplasia (CIN-H) and in 62 squamous cell carcinoma (SCC) tissues. Hypermethylation was found in 40% of CIN-H and 58% of SCC (Cheung *et al.*, 2004). Taken together, these findings encouraged us to focus primarily on the effects of methyl-donor depletion on the Wnt signalling pathway.

The Wnt signalling pathway involves the control of several cell functions. **Figure 49** shows the Wnt signalling pathway from KEGG (Kyoto Encyclopedia of Genes and Genomes) database. There are three major pathways activated downstream from the Wnt reaction.

- (1) The canonical pathways which is β -catenin dependent. This pathway affects gene transcription. Some important genes in this pathway are *Wnt*, *Frizzled*, *Dvl*, *GSK-3 β* , *APC*, and *β -catenin*.
- (2) The planar cell polarity pathway, which is important in cell polarization and plays a key role during neural tube closure. Some important genes in this pathway are *Wnt11*, *Frizzled*, *Dvl*, *RhoA*, *ROCK*, and genes in focal adhesion
- (3) The Wnt/ Ca^{2+} pathway (non-canonical pathway) which mediates cell adhesion and cell motility. Some important genes in this pathway are *Wnt5*, *Frizzled*, *PLC*, and *CaMKII*.

Within the whole picture of the Wnt signalling pathway there are several other pathways which work harmoniously to regulate cell behaviour. In order to select a part of the Wnt signalling pathway for further consideration, we found that several genes were significantly up-regulated in the cluster of cell motion, cell communication, and focal adhesion, which may be particularly related the planar cell polarity pathway and the Wnt/ Ca^{2+} pathway. Those two arms of the Wnt signalling pathway may direct us to understand the effect of methyl-donor depletion on cervical cancer motility. Therefore, the focal adhesion pathway is considered more closely.

Focal adhesion is the process whereby the integrins and glycoprotein receptors on the cell membrane interact with the extracellular matrix (e.g. collagen, laminin, and fibronectin) (Abercrombie *et al.*, 1971; Burridge *et al.*, 1988). Once focal adhesion has occurred, the consequent signals are transmitted to several parts of the cells. Two major participants are (1) the connection of membrane receptors and bundles of actin filaments, and (2) signalling molecules such as protein kinase and phosphatase which can transmit signals through several substrates and adaptor proteins (Petit & Thiery, 2000). The downstream signals can lead to cytoskeleton rearrangements which are involved in an alteration of cell shape and cell motility, and in changes in gene expression which lead to an alteration of cell proliferation and cell survival (Lo, 2006).

Table 7: Example of genes which were up-regulated in methyl-donor depleted cells and their relevance to biological function
Gene lists were chosen on the basis of either having a high fold change for that cluster or appearing in more than one cluster

Gene name	Fold change	Cluster						
		Cell death	Cell motion	Protein kinase cascade	Signal transduction	Cell communication	Blood vessel development	Focal adhesion
SMAD family member3 (SMAD3)	3.63	√	√					
adenomatous polyposis coli (APC)	1.68	√	√	√	√			
cyclin-dependent kinase inhibitor 1A (p21, Cip1, CDKN1A)	2.39	√			√			
insulin-like growth factor binding protein3 (IGFBP-3)	3.56	√	√					
transforming growth factor beta2 (TGFB2)	3.76	√	√	√	√	√	√	
transglutaminase2 (TGM2, protein-glutamine-gamma-glutamyl transferase)	29	√		√		√	√	
caspase1	3.03	√		√	√	√		
son of sevenless homolog1 (SOS1)	1.57	√			√			
tumor necrosis factor member2 (TNF2)	3.82	√		√				
tumor protein p63 (TP63)	14.18	√			√	√		
adrenergic, beta2 receptor (ADRB2)	3.06	√		√	√	√		

Table 7: Example of genes which were up-regulated in methyl-donor depleted cells and their relevance to biological function (continued).

Gene lists were chosen on the basis of either having a high fold change for that cluster or appearing in more than one cluster

Gene name	Fold change	Cluster						
		Cell death	Cell motion	Protein kinase cascade	Signal transduction	Cell communication	Blood vessel development	Focal adhesion
tensin 4 (TNS4)	2.14	√						√
nexilin (F actin binding protein) (NEXN)	2.65		√					
endothelin1 (ET-1)	4		√	√			√	
fibroblast growth factor 2 basic (FGF2)	2.16		√				√	
histone deacetylase 9 (HDAC9)	2.03		√					
interleukin 6 (IL-6)	2.06		√	√	√	√		
thrombospondin1 (THBS1)	2.22		√		√	√	√	
vascular endothelial growth factor C (VEGF-C)	1.74		√				√	
integrin alpha2 (ITGA2)	1.69		√			√		√
apolipoprotein L3 (APOL3)	2.3			√	√	√		
leptin receptor (LEPR)	2.29			√	√	√		

Table 7: Example of genes which were up-regulated in methyl-donor depleted cells and their relevance to biological function (continued)

Gene lists were chosen on the basis of either having a high fold change for that cluster or appearing in more than one cluster

Gene name	Fold change	Cluster						
		Cell death	Cell motion	Protein kinase cascade	Signal transduction	Cell communication	Blood vessel development	Focal adhesion
TNF receptor associate factor6 (TRAF6)	2.32			√	√	√		
protein phosphatase1A (PPM1A)	1.76			√	√			
epiregulin (EREG)	2.67				√	√	√	
cyclin-dependent kinase inhibitor 2B (CDKN2B, p15, inhibits CDK4)	3.37				√	√		
collagen, type I, alpha 1 (COL1A1)	2.4						√	
Rho GTPase activating protein 24 (ARHGAP24)	2.22						√	√
cadherin 1, type 1, E-cadherin (epithelial) (CDH1)	1.62							√

Table 8: Example of genes which were down-regulated in methyl-donor depleted cells and their relevance to biological function

Gene lists were chosen on the basis of either having a high fold change for that cluster or appearing in more than one cluster

Gene name	Fold change	Cluster						
		Cell cycle	Condensed chromosome	Cytoskeleton organization	DNA metabolic process	Transferase	Lipid biosynthesis process	Chromosome organization
H2A histone family, member X (H2AFX)	2.38	√			√			√
Cullin 4A (CUL4A)	1.79	√			√			
E1A binding protein p300 (EP300)	3.59	√				√		√
anillin, actin binding protein (ANLN)	2.44	√		√				
aurora kinase B (AURKB)	3.36	√	√			√		
cyclin-dependent kinase 2 (CDK2)	1.78	√			√	√		
aurora kinase A (AURKA)	2.56	√		√				
breast cancer 1, early onset (BRCA1)	1.74	√	√	√	√		√	
retinoblastoma 1 (RB1)	2.13	√						√
ErbB2 interacting protein (ERBB2IP)	1.75	√		√				

Table 8: Example of genes which were down-regulated in methyl-donor depleted cells and their relevance to biological function (continued).

Gene lists were chosen on the basis of either having a high fold change for that cluster or appearing in more than one cluster

Gene name	Fold change	Cluster						
		Cell cycle	Condensed chromosome	Cytoskeleton organization	DNA metabolic process	Transferase	Lipid biosynthesis process	Chromosome organization
epidermal growth factor receptor (EGFR)	2.23	√				√		
calcium/calmodulin-dependent protein kinase II gamma (CAMK2G)	2.16	√				√		
Holliday junction recognition protein (HJURP)	2.81	√	√					√
tubulin, beta (TUBB)	3.6	√		√				
stathmin 1 (STMN1)	3.25	√		√				
ras homolog gene family, member U (RHOU)	4.86	√		√				
O-6-methylguanine-DNA methyltransferase (MGMT)	5.32				√	√		
DNA (cytosine-5-)-methyltransferase 3 beta (DNMT3B)	3.02					√		√
NIMA (never in mitosis gene a)-related kinase 2 (NEK2)	2.41		√	√				√

Gene Report

[Help and Manual](#)

Current Gene List: F-M- vs F+M+ up-reg first 3000 IDs

Current Background: Homo sapiens

2175 DAVID IDs

134 record(s)

 [Download File](#)

AFFYMETRIX_3PRIME_IVT_ID	GENE NAME	Related Genes	Species
224788_at	ADP-ribosylation factor 6	RG	Homo sapiens
202511_s_at, 202512_s_at, 210639_s_at	ATG5 autophagy related 5 homolog (S. cerevisiae)	RG	Homo sapiens
205263_at	B-cell CLL/lymphoma 10; hypothetical LOC646626	RG	Homo sapiens
211692_s_at	BCL2 binding component 3	RG	Homo sapiens
230427_s_at, 202985_s_at, 202984_s_at	BCL2-associated athanogene 5	RG	Homo sapiens
206665_s_at, 212312_at	BCL2-like 1	RG	Homo sapiens
204493_at	BH3 interacting domain death agonist	RG	Homo sapiens
210563_x_at	CASP8 and FADD-like apoptosis regulator	RG	Homo sapiens
201743_at	CD14 molecule	RG	Homo sapiens
202221_s_at, 213579_s_at	E1A binding protein p300	RG	Homo sapiens
219002_at	FAST kinase domains 1	RG	Homo sapiens
219016_at	FAST kinase domains 5	RG	Homo sapiens
225262_at, 228188_at	FOS-like antigen 2	RG	Homo sapiens
216252_x_at, 215719_x_at, 204780_s_at	Fas (TNF receptor superfamily, member 6)	RG	Homo sapiens
210002_at	GATA binding protein 6	RG	Homo sapiens
205842_s_at	Janus kinase 2	RG	Homo sapiens
239944_at	NLR family, apoptosis inhibitory protein	RG	Homo sapiens
201844_s_at, 201845_s_at, 201846_s_at	RING1 and YY1 binding protein	RG	Homo sapiens
217828_at	SAFB-like, transcription modulator	RG	Homo sapiens
209090_s_at, 210101_x_at	SH3-domain GRB2-like endophilin B1	RG	Homo sapiens
205398_s_at, 205397_x_at	SMAD family member 3	RG	Homo sapiens
230459_s_at	Src homology 2 domain containing adaptor protein B	RG	Homo sapiens
221571_at, 208315_x_at	TNF receptor-associated factor 3	RG	Homo sapiens
235688_s_at, 242473_at, 202871_at	TNF receptor-associated factor 4	RG	Homo sapiens
227264_at	TNF receptor-associated factor 6	RG	Homo sapiens
215411_s_at	TRAF3 interacting protein 2	RG	Homo sapiens
204507_s_at	WD repeat domain 92	RG	Homo sapiens
206536_s_at, 206537_at	X-linked inhibitor of apoptosis	RG	Homo sapiens
228617_at, 206133_at	XIAP associated factor 1	RG	Homo sapiens
202541_at	aminoacyl tRNA synthetase complex-interacting multifunctional protein 1	RG	Homo sapiens
232184_at	amyotrophic lateral sclerosis 2 (juvenile)	RG	Homo sapiens

Figure 47: Example of genes from the cell death cluster which were up-regulated in methyl-donor depleted cells

Gene Report

[Help and Manual](#)

Current Gene List: F-M- vs F+M+ down-reg first 3000 IDs

Current Background: Homo sapiens

2203 DAVID IDs

189 record(s)

 [Download File](#)

AFFYMETRIX_3PRIME_IVT_ID	GENE NAME	Related Genes	Species
202641_at	ADP-ribosylation factor-like 3	RG	Homo sapiens
205345_at	BRCA1 associated RING domain 1	RG	Homo sapiens
205733_at	Bloom syndrome, RecQ helicase-like	RG	Homo sapiens
204170_s_at	CDC28 protein kinase regulatory subunit 2	RG	Homo sapiens
204126_s_at	CDC45 cell division cycle 45-like (S. cerevisiae)	RG	Homo sapiens
226569_s_at	CTF18, chromosome transmission fidelity factor 18 homolog (S. cerevisiae)	RG	Homo sapiens
238757_at	DBF4 homolog B (S. cerevisiae)	RG	Homo sapiens
219512_at	DSN1, MIND kinetochore complex component, homolog (S. cerevisiae)	RG	Homo sapiens
1562921_at	E1A binding protein p300	RG	Homo sapiens
2028_s_at, 204947_at	E2F transcription factor 1	RG	Homo sapiens
228361_at	E2F transcription factor 2	RG	Homo sapiens
228033_at	E2F transcription factor 7	RG	Homo sapiens
219990_at	E2F transcription factor 8	RG	Homo sapiens
219785_s_at, 219784_at	F-box protein 31	RG	Homo sapiens
218875_s_at	F-box protein 5	RG	Homo sapiens
203806_s_at, 236976_at, 203805_s_at	Fanconi anemia, complementation group A	RG	Homo sapiens
223545_at, 242560_at	Fanconi anemia, complementation group D2	RG	Homo sapiens
213008_at, 213007_at	Fanconi anemia, complementation group I	RG	Homo sapiens
215942_s_at, 211040_x_at, 204318_s_at, 204317_at	G-2 and S-phase expressed 1	RG	Homo sapiens
240452_at, 225276_at	G1 to S phase transition 1	RG	Homo sapiens
205436_s_at	H2A histone family, member X	RG	Homo sapiens
218383_at	HAUS auqmin-like complex, subunit 4	RG	Homo sapiens
213054_at, 213053_at, 36888_at	HAUS auqmin-like complex, subunit 5	RG	Homo sapiens
226308_at	HAUS auqmin-like complex, subunit 8	RG	Homo sapiens
218726_at	Holliday junction recognition protein	RG	Homo sapiens
228762_at	LFNG O-fucosylpeptide 3-beta-N-acetylglucosaminyltransferase	RG	Homo sapiens
206205_at, 215731_s_at, 221965_at, 1558369_at	M-phase phosphoprotein 9	RG	Homo sapiens
233921_s_at, 204857_at	MAD1 mitotic arrest deficient-like 1 (yeast)	RG	Homo sapiens
203362_s_at	MAD2 mitotic arrest deficient-like 1 (yeast)	RG	Homo sapiens
204162_at	NDC80 homolog, kinetochore complex component (S. cerevisiae)	RG	Homo sapiens
219542_at	NIMA (never in mitosis gene a)- related kinase 11	RG	Homo sapiens
1564093_at	NIMA (never in mitosis gene a)-related kinase 1	RG	Homo sapiens

Figure 48: Example of genes from the cell cycle cluster which were down-regulated in methyl-donor depleted cells

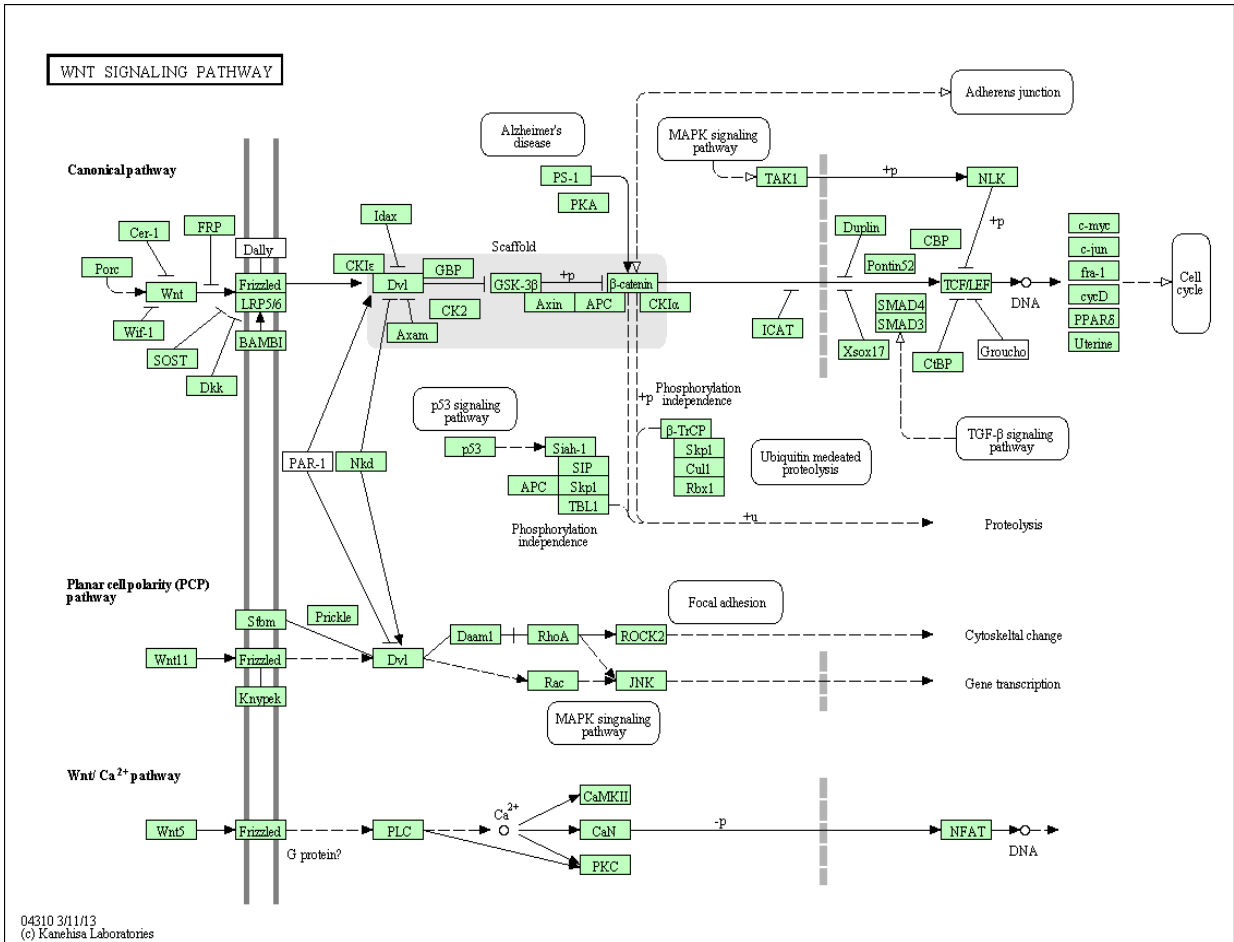


Figure 49: The Wnt signalling pathway from KEGG database

Wnt signalling pathway can be divided into 3 paths; (1) the canonical pathway which affects the stabilization of β -catenin in order to activate Wnt regulated gene through its interaction with TCF (2) the planar cell polarity pathway which leads to remodelling of cytoskeleton, cell adhesion and cell motility (3) the Wnt/ Ca^{2+} pathway which leads to an increase in free calcium to activate kinase and phosphatase

The KEGG database was interrogated, in order to identify genes involved in focal adhesion (**figure 50**). Among more than 200 genes involved in the focal adhesion pathway, we found 29 genes were up-regulated and 26 genes were down-regulated in our methyl-donor depleted cells (**table 9 and 10**). In addition to the genes shown in the KEGG focal adhesion pathway, there numerous genes identified from other sources, which are not shown in the KEGG figure. Some of those genes are also included in the table.

Our analysis and data interrogation show that folate and methionine depletion of C4-II cells leads to both an up- and down-regulation of genes in the integrin family. Some studies have suggested that the alteration of integrin expression or its activation results in more dense focal adhesion (Keely *et al.*, 1995; Palecek *et al.*, 1997). The cell region exhibiting stronger adhesion might restrict the protrusion of the membrane and lead to a decrease in cell migration. We also found an increase in the expression of RAC1 (1.98 fold, $P < 0.05$), slightly increased RhoA (1.15 fold, $P < 0.01$), and slightly decreased CDC42 (1.17 fold, $P < 0.01$) in our depletion model. RhoA, RAC1, and CDC42 are a gene group belonging to the Rho family of GTPases which functions as a transducer to convey the extracellular signal into cells. These genes contribute to cell motility by stimulating the re-organization of the actin cytoskeleton. RAC1 and CDC42 serve to stimulate cell protrusion while RhoA serves as a focal adhesion stimulator (Nobes & Hall, 1995). Even though up-regulation of RhoA and down-regulation of CDC42 may lead to a decrease in cell migration, RAC1 was up-regulated and would lead to increased cell motility. It should be noted that the fold change of RhoA and CDC42 were not high and may not be sufficient to influence cell migration compared with replete cells. In contrast, the upregulation of RAC1 was somewhat greater and may have the dominant effect.

To be more certain of the likely functional effects of methyl donor depletion on gene expression, on cell migration in particular, results from this microarray study need to be validated by other methods such as qRT-PCR and western blot.

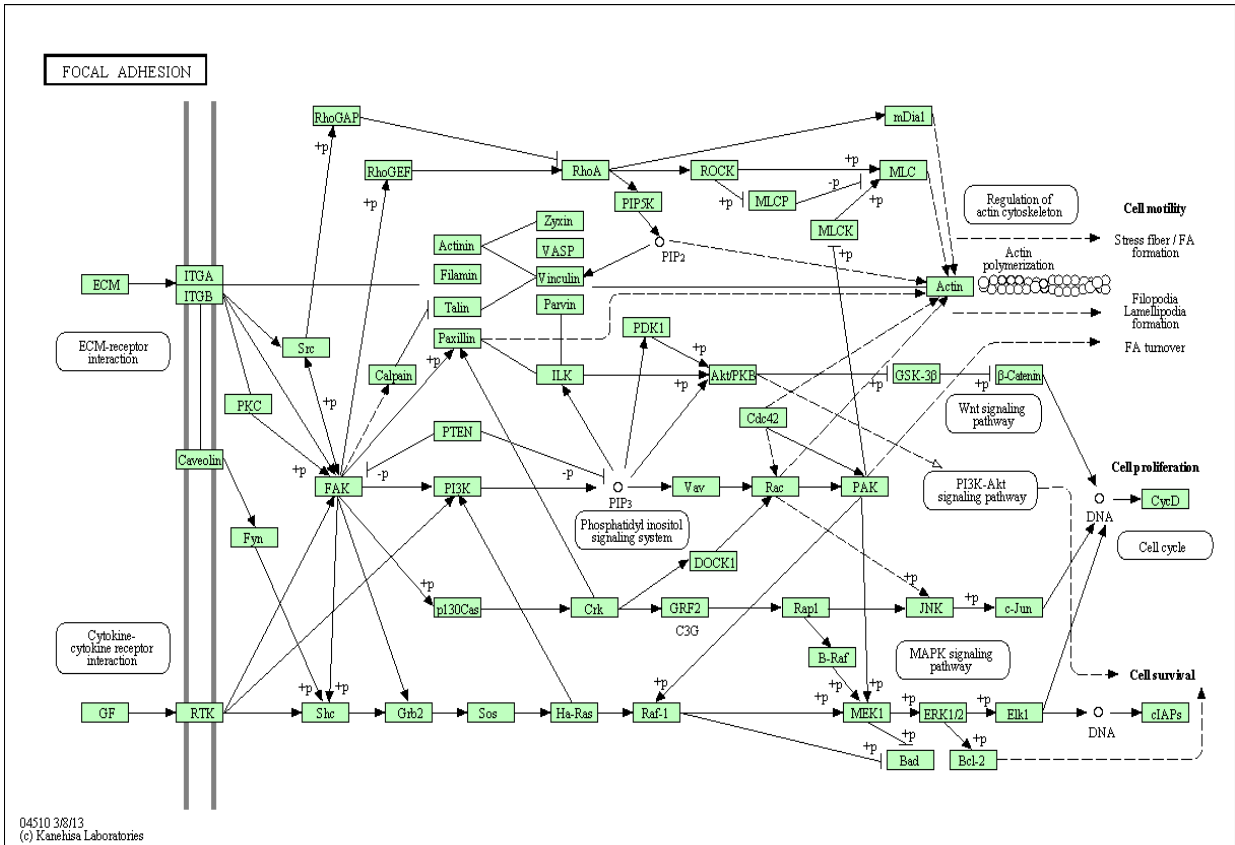


Figure 50: The focal adhesion pathway from KEGG database

Focal adhesion is the contact point in which ECM-integrin receptor and growth factor-receptor interaction take place. Downstream targets include actin skeleton and signalling molecule such as kinase and phosphatase which control cell motility, cell proliferation, and cell survival.

Table 9: The list of up-regulated genes of focal adhesion pathway in F-M- cells compared with in F+M+ cells

Gene name	Fold change
Up-regulation	
Integrin, alpha 2 (ITGA2)	1.7
Rho GTPase activating protein 5 (RhoGAP5)	2.28
Rho GTPase activating protein 24(RhoGAP24)	2.22
Rho GTPase activating protein 26(RhoGAP26)	2.29
Src homolog 2 domain containing transforming protein (SHC1)	1.65
Filamin B, beta (FLNB)	1.51
Calpain 2(CAPN2)	1.65
Phosphoinositide-3-kinase, regulatory subunit 1 alpha (PIK3R1)	1.7
Son of sevenless homolog 1 (SOS1)	1.57
v-crk sarcoma virus CT10 oncogene homolog (avain) (CRK)	1.76
vav 1 guanine nucleotide exchange factor (VAV1)	1.94
Ras-related C3 botulinum toxin substrate 1 (RAC1)	1.98
Dedicator of cytokinesis 1 (DOCK1)	2.13
Additional genes not appearing in the KEGG figure	
v-erb-b2 erythroblastic leukemia viral (ERBB2)	1.53
Baculoviral IAP repeat containing 3 (BIRC3)	4.73
Laminin, beta 3 (LAMB3)	5.03
Thrombospondin 1 (THBS1)	2.2
Tenascin R (TNR)	2.6
Vascular endothelial growth factor C (VEGFC)	1.75
Breast cancer anti-estrogen resistance 1 (BCAR1)	1.79
Insulin-like growth factor 1 receptor (IGF1R)	1.58

Table 10: *The list of down-regulated genes of focal adhesion pathway in F-M- cells compared with in F+M+ cells*

Gene name	Fold change
Down-regulation	
Integrin, beta 4 (ITGB4)	2.37
Integrin, beta 6 (ITGB6)	1.92
Integrin, beta 8 (ITGB8)	1.51
FYN oncogene (FYN)	1.83
Guanine nucleotide exchange factors for Rho/Rac/Cdc42-like GTPase (RhoGEF)	4.5
Actinin, alpha 2 (ACTN2)	13.57
Talin 1(TLN1)	1.55
Calpain 3(CAPN3)	1.74
Calpain 6(CAPN6)	1.52
Calpain 8(CAPN8)	2.61
Phosphatase and tensin homolog (PTEN)	1.92
Phosphoinositol-4,5-bisphosphate -3-kinase, catalytic subunit delta (PIK3CD)	2.36
Parvin, beta (PARVB)	1.98
Integrin-linked kinase (ILK)	1.53
Myosin light chain kinase (MLCK)	2.35
Ras-related C3 botulinum toxin substrate 3 (RAC3)	2.2
p21 protein (Cdc42/Rac) –activated kinase 4 (PAK4)	1.68
Additional genes not appearing in the KEGG figure	
Collagen, type I, alpha 1 (COL1A1)	3.54
Collagen, type IV, alpha 2 (COL4A2)	3.51
Collagen, type IV, alpha 3 (COL4A3)	2.22
Collagen, type V, alpha 1 (COL5A1)	2.52
Fibronectin 1(FN1)	1.62
Myosin light chain kinase (MYLK)	2.35
Thrombospondin 3 (THBS3)	3.98

Addendum:

The gene microarray data were re-analysed using Benjamini Hochberg's method to correct for multiple testing. The number of genes for which a significant effect on expression was observed, following methyl donor depletion reduced to about 4,700 probe genes ($P < 0.05$, t-test). The number of probe genes for which the differences according to treatment were more than a 1.5-fold change was about 3,900, of which 2,193 were down-regulated and 1,749 up-regulated. The identities of those 3,900 probes were further clustered according to biological function using the DAVID software (David Bioinformatics Resource 6.7) again. Functional annotation clustering according to biological function revealed 348 clusters of up-regulated genes and 374 clusters of down-regulated genes (**figure 51-52**).

There were 48 clusters of up-regulated genes and 47 clusters of down-regulated genes, for which the enrichment score was more than 1.3. Of these clusters seven were selected on the basis of a high enrichment score and the biological grouping. These are presented in **table 11**.

Table 11: Summary of selected gene clusters from both up- and down-regulated genes of methyl-donor depleted cells (re-analysis with multiple corrections)

Up-regulation	Enrichment score	Down-regulation	Enrichment score
Cell death	5.73	Cell cycle	18.4
Defense response	3.92	Condensed chromosome	12.75
Chromosome organisation	3.06	Cytoskeleton organization	5.97
Proteolysis	2.96	DNA metabolic process	5.24
Epithelial cell differentiation	2.89	Lipid biosynthesis process	2.92
Focal adhesion	2.76	Transferase	1.92
DNA damage response, signal transduction	2.17	Chromosome organization	1.8

Functional Annotation Clustering

[Help and Manual](#)

Current Gene List: F-M- vs F+M+ up-reg more than 1.5 FC with Benjamini
Current Background: Homo sapiens
1368 DAVID IDs

Options **Classification Stringency** Medium

348 Cluster(s)

[Download File](#)

Annotation Cluster 1		Enrichment Score: 6.41			Count	P_Value	Benjamini
<input type="checkbox"/>	GOTERM_CC_FAT	nuclear lumen	RT		150	1.8E-8	8.7E-6
<input type="checkbox"/>	GOTERM_CC_FAT	membrane-enclosed lumen	RT		181	3.3E-8	7.9E-6
<input type="checkbox"/>	GOTERM_CC_FAT	nucleolus	RT		85	5.5E-8	8.9E-6
<input type="checkbox"/>	GOTERM_CC_FAT	intracellular organelle lumen	RT		172	1.6E-7	1.9E-5
<input type="checkbox"/>	GOTERM_CC_FAT	organelle lumen	RT		174	2.7E-7	2.6E-5
<input type="checkbox"/>	GOTERM_CC_FAT	nucleoplasm	RT		81	2.4E-3	7.6E-2
Annotation Cluster 2		Enrichment Score: 5.73			Count	P_Value	Benjamini
<input type="checkbox"/>	GOTERM_BP_FAT	cell death	RT		90	4.1E-7	1.3E-3
<input type="checkbox"/>	GOTERM_BP_FAT	death	RT		90	5.5E-7	8.9E-4
<input type="checkbox"/>	GOTERM_BP_FAT	programmed cell death	RT		77	2.5E-6	1.6E-3
<input type="checkbox"/>	GOTERM_BP_FAT	apoptosis	RT		76	2.7E-6	1.5E-3
<input type="checkbox"/>	SP_PIR_KEYWORDS	Apoptosis	RT		50	1.5E-5	6.9E-4
Annotation Cluster 3		Enrichment Score: 3.92			Count	P_Value	Benjamini
<input type="checkbox"/>	GOTERM_BP_FAT	defense response	RT		72	6.5E-5	2.6E-2
<input type="checkbox"/>	GOTERM_BP_FAT	response to wounding	RT		64	7.2E-5	2.3E-2
<input type="checkbox"/>	GOTERM_BP_FAT	inflammatory response	RT		42	3.9E-4	5.5E-2
Annotation Cluster 4		Enrichment Score: 3.87			Count	P_Value	Benjamini
<input type="checkbox"/>	GOTERM_CC_FAT	nucleolus	RT		85	5.5E-8	8.9E-6
<input type="checkbox"/>	GOTERM_CC_FAT	intracellular non-membrane-bounded organelle	RT		217	1.0E-4	5.6E-3
<input type="checkbox"/>	GOTERM_CC_FAT	non-membrane-bounded organelle	RT		217	1.0E-4	5.6E-3
<input type="checkbox"/>	GOTERM_CC_FAT	cytoskeleton	RT		92	5.5E-1	9.6E-1
Annotation Cluster 5		Enrichment Score: 3.06			Count	P_Value	Benjamini
<input type="checkbox"/>	GOTERM_CC_FAT	nucleosome	RT		18	4.5E-7	3.7E-5
<input type="checkbox"/>	INTERPRO	Histone core	RT		15	1.6E-6	2.6E-3
<input type="checkbox"/>	SP_PIR_KEYWORDS	ubl conjugation	RT		72	2.1E-6	1.9E-4
<input type="checkbox"/>	SP_PIR_KEYWORDS	nucleosome core	RT		15	2.5E-6	1.9E-4
<input type="checkbox"/>	GOTERM_CC_FAT	protein-DNA complex	RT		20	2.7E-6	1.9E-4
<input type="checkbox"/>	INTERPRO	Histone-fold	RT		15	1.7E-5	1.4E-2
<input type="checkbox"/>	GOTERM_BP_FAT	nucleosome organization	RT		20	3.3E-5	1.5E-2
<input type="checkbox"/>	GOTERM_BP_FAT	protein-DNA complex assembly	RT		19	8.3E-5	2.2E-2
<input type="checkbox"/>	GOTERM_BP_FAT	nucleosome assembly	RT		18	9.6E-5	2.4E-2
<input type="checkbox"/>	GOTERM_BP_FAT	chromatin assembly	RT		18	1.5E-4	2.9E-2
<input type="checkbox"/>	PIR_SUPERFAMILY	PIRSF002048:histone H2A	RT		7	2.7E-4	1.3E-1
<input type="checkbox"/>	PIR_SUPERFAMILY	PIRSF002050:histone H2B	RT		7	2.7E-4	1.3E-1
<input type="checkbox"/>	SP_PIR_KEYWORDS	isopeptide bond	RT		40	3.1E-4	8.5E-3
<input type="checkbox"/>	SP_PIR_KEYWORDS	chromosomal protein	RT		23	3.5E-4	9.2E-3
<input type="checkbox"/>	KEGG_PATHWAY	Systemic lupus erythematosus	RT		19	3.6E-4	5.7E-2
<input type="checkbox"/>	GOTERM_BP_FAT	chromatin assembly or disassembly	RT		21	8.3E-4	7.4E-2
<input type="checkbox"/>	INTERPRO	Histone H2B	RT		7	1.1E-3	3.6E-1
<input type="checkbox"/>	UP_SEQ_FEATURE	cross-link:Glycyl lysine isopeptide (Lys-Gly) (interchain with G-Cter in ubiquitin)	RT		27	1.2E-3	4.4E-1
<input type="checkbox"/>	INTERPRO	Histone H2A	RT		7	1.6E-3	3.0E-1
<input type="checkbox"/>	GOTERM_CC_FAT	chromatin	RT		26	1.7E-3	5.6E-2
<input type="checkbox"/>	SMART	H2B	RT		7	2.0E-3	4.5E-1
<input type="checkbox"/>	SMART	H2A	RT		7	2.7E-3	3.4E-1
<input type="checkbox"/>	GOTERM_BP_FAT	chromatin organization	RT		43	4.0E-3	1.8E-1
<input type="checkbox"/>	GOTERM_BP_FAT	DNA packaging	RT		18	4.7E-3	1.9E-1
<input type="checkbox"/>	GOTERM_BP_FAT	chromosome organization	RT		51	7.8E-3	2.5E-1

Figure 51: Example of functional annotation clustering using DAVID Bioinformatics. This screen shot shows some clusters from the up-regulated gene list (re-analysis)

Functional Annotation Clustering

[Help and Manual](#)

Current Gene List: F-M- vs F+M+ down-reg more than 1.5 FC with Benjamini
Current Background: Homo sapiens
1710 DAVID IDs

Options Classification Stringency Medium

374 Cluster(s)

[Download File](#)

Annotation Cluster	Enrichment Score	Count	P_Value	Benjamini
Annotation Cluster 1 Enrichment Score: 18.4				
<input type="checkbox"/> GOTERM_BP_FAT	M phase	88	7.9E-24	2.5E-20
<input type="checkbox"/> GOTERM_BP_FAT	cell cycle phase	100	2.1E-23	3.4E-20
<input type="checkbox"/> GOTERM_BP_FAT	cell cycle	140	9.4E-20	9.9E-17
<input type="checkbox"/> GOTERM_BP_FAT	M phase of mitotic cell cycle	65	1.0E-19	8.3E-17
<input type="checkbox"/> SP_PIR_KEYWORDS	cell cycle	100	1.3E-19	8.3E-17
<input type="checkbox"/> GOTERM_BP_FAT	nuclear division	64	1.8E-19	1.1E-16
<input type="checkbox"/> GOTERM_BP_FAT	mitosis	64	1.8E-19	1.1E-16
<input type="checkbox"/> GOTERM_BP_FAT	organelle fission	64	1.6E-18	8.7E-16
<input type="checkbox"/> GOTERM_BP_FAT	cell cycle process	110	5.0E-18	2.2E-15
<input type="checkbox"/> GOTERM_BP_FAT	mitotic cell cycle	84	5.8E-18	2.3E-15
<input type="checkbox"/> SP_PIR_KEYWORDS	mitosis	54	9.1E-17	2.3E-14
<input type="checkbox"/> SP_PIR_KEYWORDS	cell division	66	3.6E-16	5.1E-14
<input type="checkbox"/> GOTERM_BP_FAT	cell division	70	5.2E-16	2.0E-13
Annotation Cluster 2 Enrichment Score: 12.75				
<input type="checkbox"/> GOTERM_CC_FAT	condensed chromosome	44	8.7E-16	4.9E-13
<input type="checkbox"/> GOTERM_CC_FAT	chromosome, centromeric region	43	1.1E-15	3.1E-13
<input type="checkbox"/> GOTERM_CC_FAT	chromosome	92	6.7E-15	1.2E-12
<input type="checkbox"/> GOTERM_CC_FAT	chromosomal part	82	7.5E-15	1.0E-12
<input type="checkbox"/> SP_PIR_KEYWORDS	kinetochore	27	7.8E-13	9.6E-11
<input type="checkbox"/> GOTERM_CC_FAT	condensed chromosome, centromeric region	27	5.8E-12	5.4E-10
<input type="checkbox"/> GOTERM_CC_FAT	kinetochore	28	5.6E-11	3.8E-9
<input type="checkbox"/> GOTERM_CC_FAT	condensed chromosome kinetochore	24	8.3E-11	5.1E-9
Annotation Cluster 3 Enrichment Score: 6.76				
<input type="checkbox"/> GOTERM_CC_FAT	microtubule cytoskeleton	97	2.9E-12	3.2E-10
<input type="checkbox"/> GOTERM_BP_FAT	microtubule-based process	52	1.2E-9	2.9E-7
<input type="checkbox"/> GOTERM_CC_FAT	microtubule	51	1.4E-7	7.2E-6
<input type="checkbox"/> SP_PIR_KEYWORDS	microtubule	43	7.0E-7	3.3E-5
<input type="checkbox"/> GOTERM_CC_FAT	cytoskeletal part	119	1.1E-5	3.6E-4
<input type="checkbox"/> GOTERM_MF_FAT	microtubule motor activity	19	3.5E-5	3.7E-3
<input type="checkbox"/> GOTERM_BP_FAT	microtubule-based movement	24	3.6E-5	3.8E-3
Annotation Cluster 4 Enrichment Score: 6.34				
<input type="checkbox"/> GOTERM_CC_FAT	microtubule cytoskeleton	97	2.9E-12	3.2E-10
<input type="checkbox"/> GOTERM_CC_FAT	intracellular non-membrane-bounded organelle	296	5.1E-9	2.8E-7
<input type="checkbox"/> GOTERM_CC_FAT	non-membrane-bounded organelle	296	5.1E-9	2.8E-7
<input type="checkbox"/> GOTERM_CC_FAT	microtubule organizing center	45	3.1E-6	1.1E-4
<input type="checkbox"/> GOTERM_CC_FAT	cytoskeletal part	119	1.1E-5	3.6E-4
<input type="checkbox"/> SP_PIR_KEYWORDS	cytoskeleton	83	2.4E-5	6.6E-4
<input type="checkbox"/> GOTERM_CC_FAT	centrosome	38	5.8E-5	1.5E-3
<input type="checkbox"/> GOTERM_CC_FAT	cytoskeleton	151	5.7E-4	1.2E-2
Annotation Cluster 5 Enrichment Score: 5.97				
<input type="checkbox"/> GOTERM_BP_FAT	microtubule-based process	52	1.2E-9	2.9E-7
<input type="checkbox"/> GOTERM_BP_FAT	microtubule cytoskeleton organization	32	7.6E-7	1.1E-4
<input type="checkbox"/> GOTERM_BP_FAT	cytoskeleton organization	55	1.4E-3	8.1E-2
Annotation Cluster 6 Enrichment Score: 5.24				
<input type="checkbox"/> GOTERM_BP_FAT	DNA metabolic process	80	1.4E-8	2.9E-6
<input type="checkbox"/> GOTERM_BP_FAT	response to DNA damage stimulus	61	2.8E-7	5.1E-5
<input type="checkbox"/> GOTERM_BP_FAT	cellular response to stress	80	1.6E-6	2.1E-4

Figure 52: Example of functional annotation clustering using DAVID Bioinformatics. This screen shot shows some clusters from the down-regulated gene list (re-analysis)

The result taking account of multiple corrections in re-analysis gave a similar outcome to the previous analysis, especially for those gene clusters which were down regulated. A few differences in up-regulated gene clusters were observed compared with the previous analysis, but the general effect profile was very similar. Moreover, in the new analysis gene clusters for epithelial cell differentiation, focal adhesion, blood vessel development and regulation of cell migration appeared again in those 48 clusters for which the enrichment score was more than 1.3, as was found in the uncorrected data analysis.

Interestingly, the gene cluster for chromosome organisation appeared to be both up- and down-regulated. This suggests chromatin remodelling may be central to effects of methyl donor depletion on gene expression, leading to phenotypic changes relevant to cancer progression.

5.5 Summary

Folate and methionine depletion led to an up-regulation of several genes involved in cell death, chromosome organisation, and cell signalling, but a down-regulation of genes important for the cell cycle, condensed chromosome, and cytoskeleton organization. The results from gene clustering directed us to an interest in signalling pathways leading to cell motility, which were the Wnt signalling pathway and focal adhesion. The focal adhesion pathway itself also has various signalling complexes. A single specific signal has to work in concert with others in order to drive specific cell behaviour and our results have identified a focus for further research of the effects of methyl donor depletion on cancer cell behaviour. It will be important to validate of the genes of interest to clearly indicate the mechanisms driving the specific behaviour of folate and methionine-depleted cancer cells.

Chapter 6 Cell Migration

6.1 Introduction

Cell migration and invasion are hallmarks of cancer progression (Hanahan & Weinberg, 2011). Cell migration is also a feature of non-pathological states and homeostasis, skin renewal, and wound healing (Webb *et al.*, 2005)

In our study methyl-donor depletion of cervical cancer cells gave rise to an altered expression of many genes in the 'cell motion' cluster, as defined by DAVID software (see chapter 5). Other studies have also indicated a possible link between methyl donor status and the expression of several genes involved in cell migration and invasion. Novakovic *et al.* (2006) reported that folate deficiency in human colon adenocarcinoma cell lines (HCT116) induced the up-regulation of integrin beta 1 and integrin alpha 6, but a down-regulation of vascular endothelial growth factor (VEGF). VEGF is known to be important in angiogenesis by primarily stimulating cell proliferation and cell migration. It is expressed and secreted from several tumours during their expansion. Crott *et al.* (2004) also found a decrease in the expression of VEGF in the colonic mucosa of rats fed a folate-deficient diet. This group also reported an elevation of E-cadherin (cell adhesion protein) and SMAD-4 (a protein which conveys the TGF- β signal from cell surface to nucleus) (Crott *et al.*, 2004). In normal human colon cells, NCM356, both these proteins are involved in cell migration, cell invasion, and cell adhesion (Crott *et al.*, 2008). In addition, the gene expression profile of lymph node micrometastases of invasive cervical cancer cells confirmed the up-regulation of fibroblast growth factor and transforming growth factor compared to the primary tumour (Hagemann *et al.*, 2007). Although limited, these gene expression studies suggest that cell migration and/or invasion might be influenced by methyl donor depletion.

There is a modest literature describing migration or invasion studies in cells deprived of one or more methyl donors. In their study of folate-deficient hepatocellular carcinoma cells (SK-Hep-1), WenChun & Huang (2009) demonstrated an approximate 25% inhibition of migration which was reversed when the cells were supplied by 100 μ M folate, when the migration rate increased 1.21-fold (WenChun & Huang, 2009). Cell migration rate was also investigated in a methionine-deficient model of gastric tumor cells. Graziosi *et al.* suggested that a decrease of migration was modulated by a methionine-deficient diet (Graziosi *et al.*, 2013). To my knowledge there have been no studies of cell migration in response to a combined folate and methionine-depletion.

Migration studies have been carried out in several cervical cancer cell lines. For example, SiHa cells were used to investigate effects on the migration rate of silencing MTA1 (metastasis-associated gene 1), using a wound-healing assay (Rao *et al.*, 2011). After

disruption of the gene expression of MTA1, cell adhesion, cell migration and cell invasion were decreased. The expression of E-cadherin and p53 were up-regulated by MTA1 silencing indicating a role for these genes in SiHa cell motility. Sun *et al* (2011) used the cervical cancer cells, CaSki, in order to investigate the effect of overexpressed autophagy-related gene *Beclin1* on cell migration. Using the trans-well migration assay they found that VEGF and MMP9 (matrix metalloproteinase-9) expression were down-regulated and that this was associated with inhibition of metastasis. This demonstrates the importance of angiogenesis and extracellular matrix degradation to cell migration (Sun *et al.*, 2011). Su *et al.* (2013) carried out a study in cervical cells to determine the consequence of knock down of DNMT3b in cell migration of HeLa3rd and CaSki by using an Oris Cell Migration Assay (Su *et al.*, 2013). They demonstrated that disrupted DNMT3b led to a re-expression of PTPRR (protein tyrosine phosphatase receptor type R), which was followed by the inhibition of downstream signalling of cell migration. This can be related to our research in which DNMT3b was down-regulated in methyl donor depletion. Therefore, the migration rate of methyl-donor deficient cervical cells in our model may be altered. However, no study has been conducted in C4-II cervical cancer cells.

Several different methods have been used to estimate cell migration rate. The basic method is a wound healing assay or a scratch assay. This method can be easily set up in cell culture ware and therefore, the first choice for our study was the scratch assay.

6.2 Aims

To determine whether methyl donor depletion influences cell migration, estimated using the scratch assay.

6.3 Methods

6.3.1 Cell culture

After culturing cells in complete and folate and methionine-depleted media for 8 days in T75 flasks, C4-II cells were transferred for growth in 96-well plates. Cells were plated at various seeding densities ranging from 10,000-500,000 cells/cm² in order to set up the mitomycin C optimisation assay and the scratch assay. We needed 50-70% confluence by 24 hours for the mitomycin C optimisation and 100% confluence by 24 hours for the scratch assay. In the first place, three-independent experiments were carried out and confluence observed to determine the appropriate seeding density. The suitable seeding density for mitomycin C optimisation was 50,000 cells/cm² (~50,000cells/well) and for the scratch assay was 100,000 cells/cm² (~100,000 cells/well). The experiment was set up using

100µl culture medium/well for at least 6 replicates for each sample (at least 6 wells). The culture period was up to 72 hours after setting up the plate for mitomycin C optimisation. The culture period for the scratch assay was 48-72 hours after confluence.

6.3.2 Mitomycin C optimisation

To determine cell migration, in order to avoid confounding from cell proliferation, the cells must be treated with mitomycin C (MMC), which is used to stop DNA synthesis. However, mitomycin C is very toxic against cell viability, and therefore an optimum concentration must be identified to ensure that cells can survive throughout the assay period. The mitomycin C optimisation method was used as described (see section 2.2.15.2). Cell proliferation was determined by using the method described (see section 2.2.15.1) at 24, 48, and 72 hours. The absorbance at 490nm was measured and set the A_{490} of control as 100% cell proliferation. Cell proliferation was determined for mitomycin-treated and untreated cells following growth in complete or methyl-donor deplete media. **Figure 53** shows the flow chart of mitomycin C optimisation protocol.

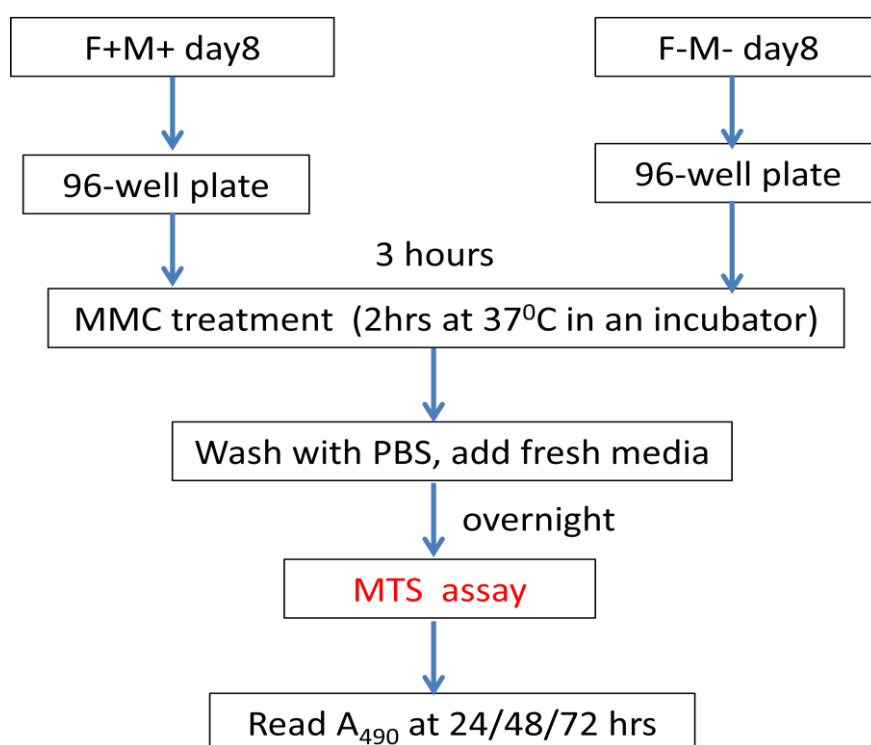


Figure 53: *The flow chart of mitomycin C optimisation protocol*

6.3.3 Scratch assay

The protocol for the scratch assay was followed as described (see section 2.2.15.3). Each scratch was visualised under a 4x objective microscope at 0, 24, and 48-hour time points. The migration rate was determined by measuring the width of a scratch for 20 areas of each scratch by using ImageJ tool and at least 6 technical replicates were determined for each sample. The experiment was conducted for at least three-independent cell culture batches. The migration rate was calculated as a mean percentage of gap closure of treated cells compared with the mean gap width of control (non-mitomycin C-treated F+M+ cells) at 0 hour. **Figure 54** shows the flow chart of scratch assay protocol.

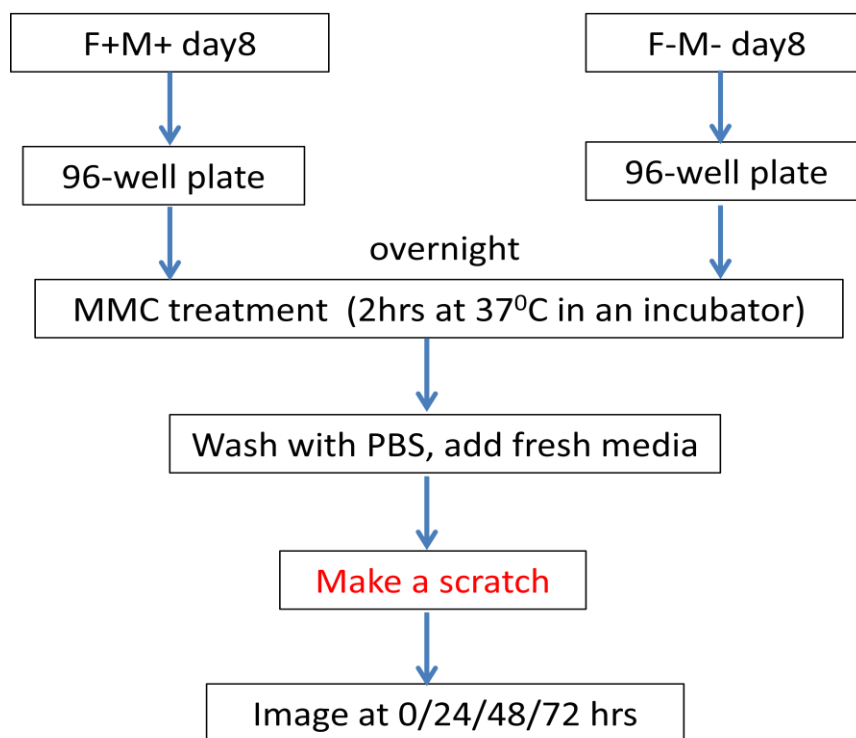


Figure 54: *The flow chart of the scratch assay protocol*

6.4 Results

6.4.1 Mitomycin C optimisation

Since we are not aware of any publication describing migration of C4-II cervical cancer cells, the optimal range of mitomycin C concentration had to be determined in the first instance. A broad range of concentrations (0-20 $\mu\text{g/ml}$) was set up as a single experiment to estimate the optimum concentration of mitomycin C and cell proliferation was measured after 24 and 48 hours.

Figure 55 shows the cell proliferation at 48 hours for cells grown in various concentrations of mitomycin C for cells grown in both complete medium, and folate and methionine-depleted medium. Results suggested that a concentration of mitomycin C greater than 1 $\mu\text{g/ml}$ was toxic to C4-II cells grown in complete medium, therefore, the optimum concentration range was thought likely to be 0-1 $\mu\text{g/ml}$. Cells depleted of folate and methionine showed evidence of toxic effects at only 0.5 $\mu\text{g/ml}$ of mitomycin C, therefore, the optimum concentration range of mitomycin C for these cells was thought to be 0-0.5 $\mu\text{g/ml}$. Mitomycin C concentrations of 0, 0.1, 0.3, 0.5, 0.7, and 1.0 $\mu\text{g/ml}$ were used for cells grown in complete medium. For cells depleted of folate and methionine mitomycin C was used at concentrations of 0, 0.1, 0.2, 0.3, 0.4, and 0.5 $\mu\text{g/ml}$.

From 3 independent experiments, cells treated with 0.1, 0.3, and 0.5 $\mu\text{g/ml}$ of mitomycin C continued to proliferate over 72 hours of culture. However, cells grown in complete medium appeared to stop proliferation after 48 hours (this was evident at 72 hours too) when treated with 0.7 or 1.0 $\mu\text{g/ml}$ (**figure 56**). Therefore, a mitomycin C concentration of 0.7 $\mu\text{g/ml}$ was chosen for the scratch assay experiment. In contrast, cells grown in methyl-donor depleted medium and exposed to 0.5 $\mu\text{g/ml}$ of mitomycin C continued to proliferate until 48 hours. Because of uncertainty remaining about the optimum concentration to prevent proliferation, 3 further replicate experiments were carried out at mitomycin C concentration of 0.7, 1.0, and 2.0 $\mu\text{g/ml}$ for methyl-donor depleted cells.

After 24 hours, the results showed that no matter which concentration of mitomycin C was used proliferation fell by about 20% (**figure 57**). The cells grown in methyl-donor deplete medium appeared to stop proliferating after 48 hours (this was evident at 72 hours too) when treated with 0.7 or 1.0 $\mu\text{g/ml}$. At the concentration of 2.0 $\mu\text{g/ml}$, cells also appeared to stop proliferating after 48 hours, but started to show signs of cell death before 72 hours. Thus, we decided to use 0.7 $\mu\text{g/ml}$, the same concentration used in cells grown in complete medium.

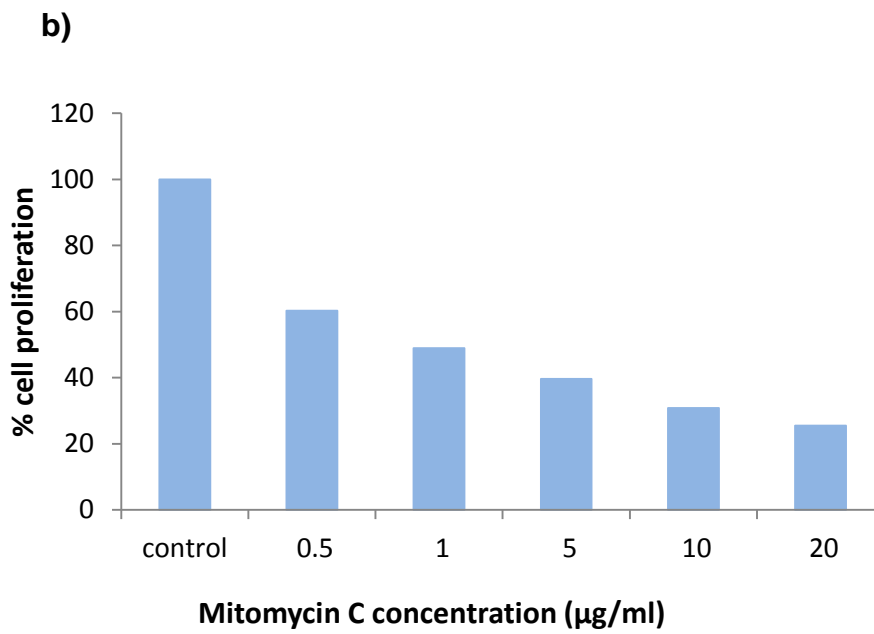
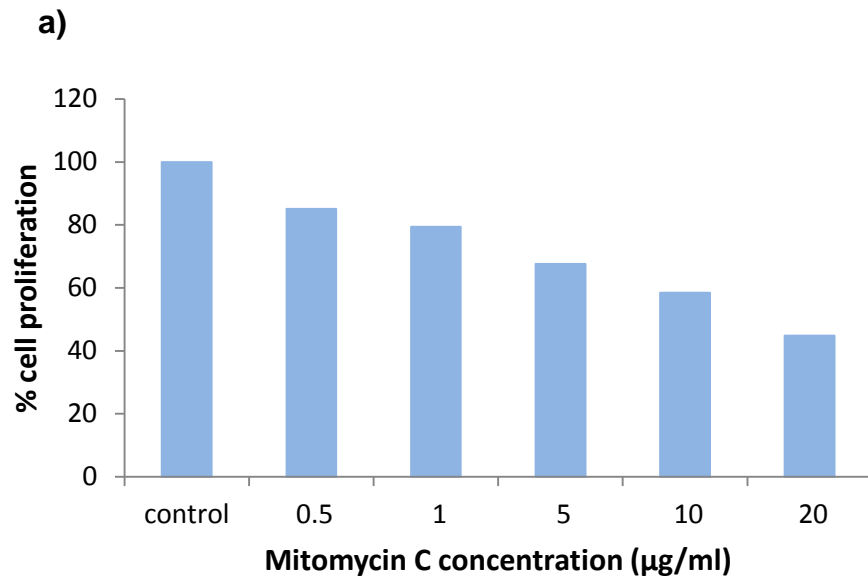
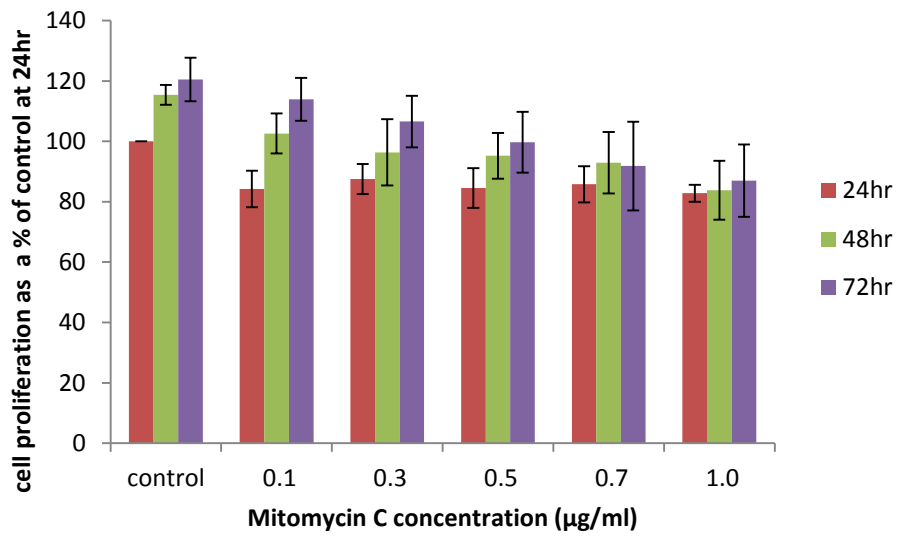


Figure 55: *The effect of mitomycin C on cell proliferation*
Cells grown in a) methyl-donor replete and b) methyl-donor depleted medium.

a)



b)

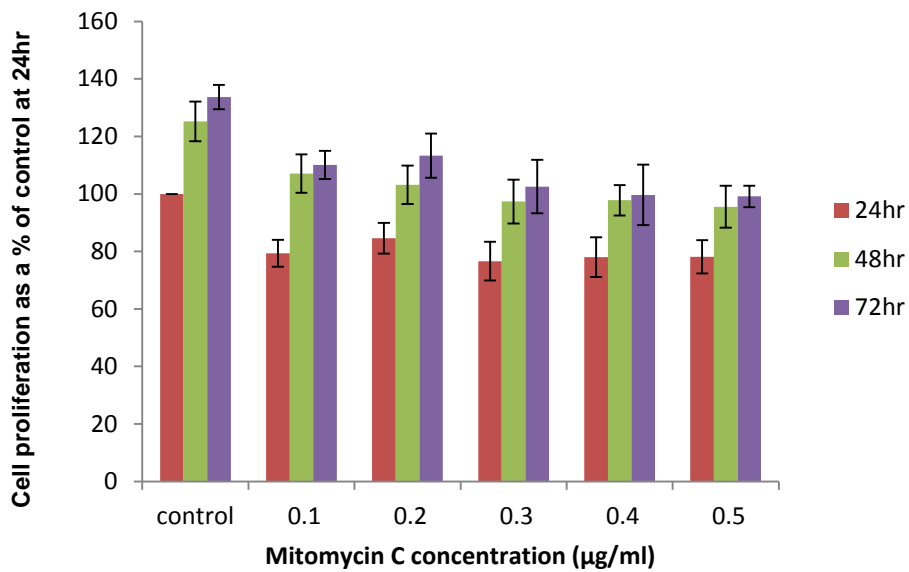


Figure 56: Mitomycin C optimisation considering the effect on cell proliferation

a) methyl-donor replete and b) methyl-donor depleted cells over 72 hours

Each value shows mean of four-independent experiments and error bars show SEM.

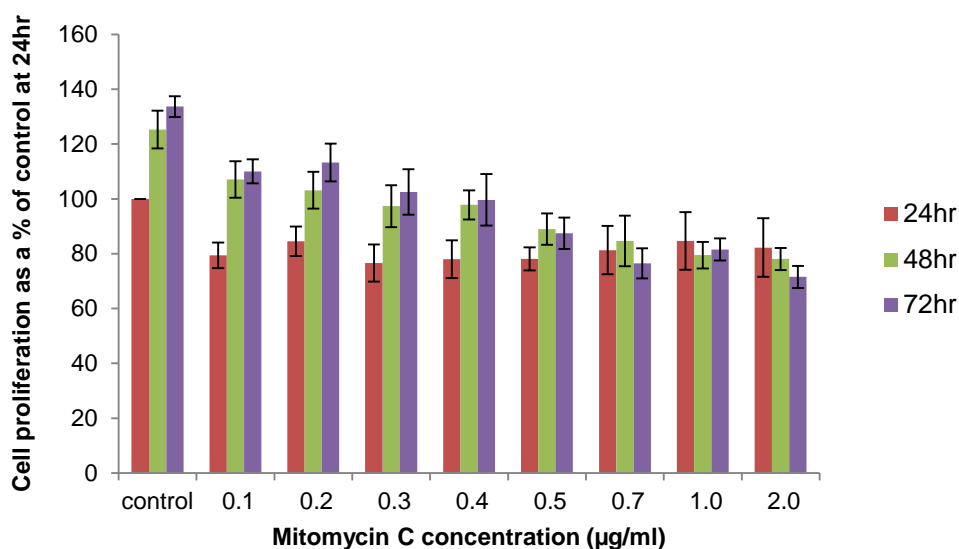


Figure 57: The effect of mitomycin C on F-M- cell proliferation (repeat)

The repeat experiment with increase mitomycin C concentration shows the effect of treatment on folate and methionine-depleted cells at the concentration of 0.7, 1.0, and 2.0 µg/ml

Each value shows mean of three-independent experiments and error bars show SEM.

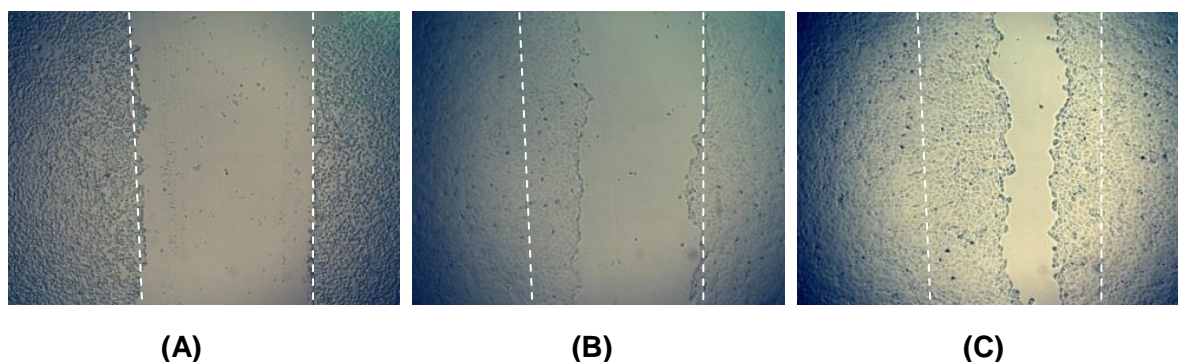


Figure 58: Scratch wound model

The pictures show C4-II cells that have been (A) freshly wounded (B) 24 hours after wounding, and (C) 48 hours after wounding at which time point cells can be clearly seen to have migrated to fill the wound. Dotted lines indicate the edge of the wound at 0-hour time point. The migration rate is evaluated at 24- and 48-hour time points by determining the reduction of mean gap width.

6.4.2 Scratch assay

As the scratches were made with a p200 pipette tip, the gap between cells was wide enough to investigate gap closure by cell migration over 48-72 hours. **Figure 58** illustrates that cell movement was sufficient to close the gap before 72 hours, and so an image at the 72-hour time point was not taken. From the gap width at 0, 24, and 48-hour time point, the gap closure was determined as a percentage of the gap width at 0 hours. One-way ANOVA with time as factor showed a significant increase in % gap closure with time under all conditions ($P < 0.003$) as expected. One-way ANOVA and post hoc analysis with treatment as factor showed no significant effect of methyl donor depletion at either the 24-hour or 48-hour time points (**figure 59**). The methyl donor depleted cells showed no significant difference in cell migration rate in comparison with complete cells, also the migration rate of the mitomycin C-treated F-M- cells and the mitomycin C-treated F+M+ cells were not different.

Regarding the migration rate, the mitomycin C optimisation was carried out at 50-70% cell confluence but the scratch assay was carried out at 100% cell confluence. So, we were curious to know whether cell proliferation had contributed to gap closure. A further experiment was carried out to examine mitomycin C efficiency but this time using cells at 100% cell confluence.

Cell proliferation was examined over 72 hours for cells grown in complete or methyl donor-deplete medium and exposed to mitomycin C or not. Cell proliferation rate seemed unaffected by methyl donor depletion or mitomycin C exposure (**figure 60**). Cells grown to 100% confluence showed no further proliferation. Therefore, we were absolutely sure that the cell movement to fill the gap resulted only from cell migration. Furthermore, time-lapse microscopy was carried out to investigate cell movement in real time and also confirmed these findings.

Time-lapse microscopy was set up with 5x objective bright phase microscopy. The cell images were captured every 20 minutes for 48 hours (**figure 61**). This experiment was set up for the observation of cell movement and cell morphology in real time in order to confirm that cell migration was occurring. From the observation, the cell movement was caused by only cell migration, not cell proliferation, since no cell division was detected. The **figure 61** shows the images from time-lapse microscopy for cells grown under methyl donor-replete and methyl donor deplete medium, in the presence or absence of mitomycin C. No difference in cell migration rate could be detected between these treatments.

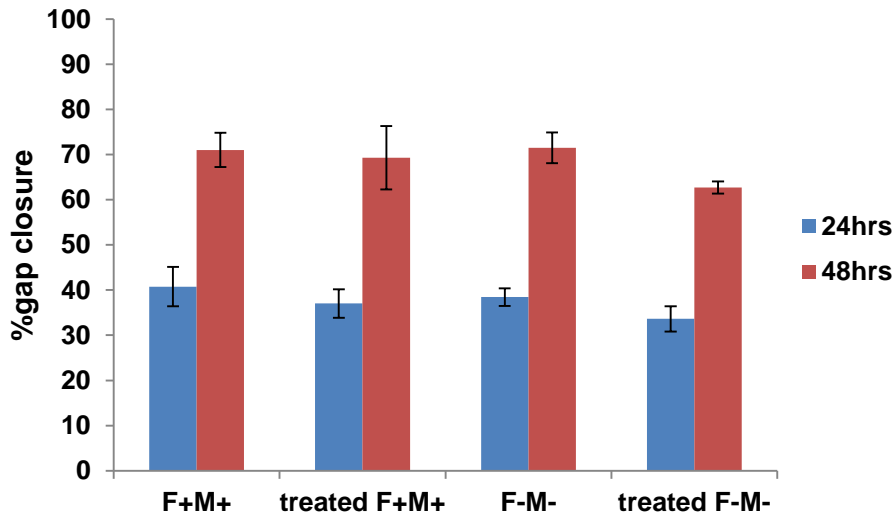


Figure 59: The percentage of gap closure of the C4-II cells grown under four different conditions

F+M+, mitomycin C-treated F+M+, F-M-, and mitomycin C-treated F-M-.

Each value shows mean of five-independent experiments and error bars show SEM.

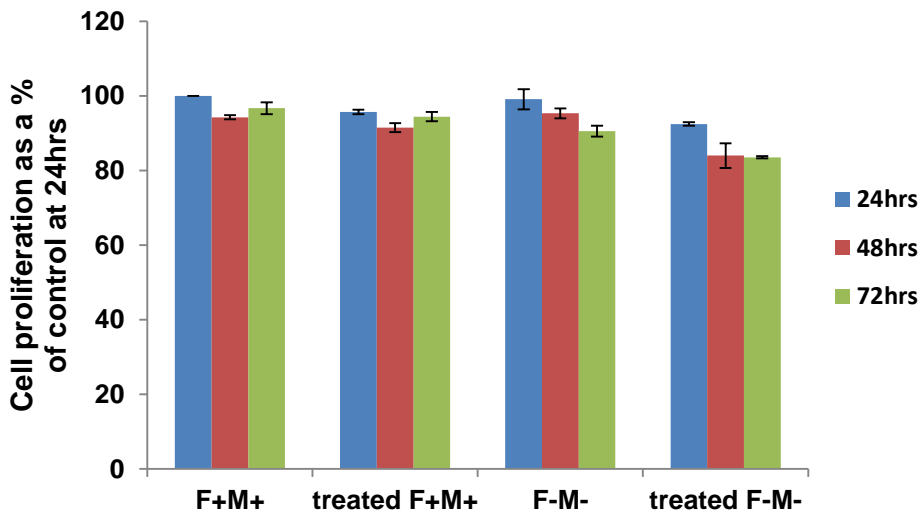


Figure 60: The effect of mitomycin C treatment on cell proliferation

Measurements were made at 100% confluence of both methyl-donor replete and methyl-donor depleted cells.

Each value shows mean of three-independent experiments and error bars show SEM.

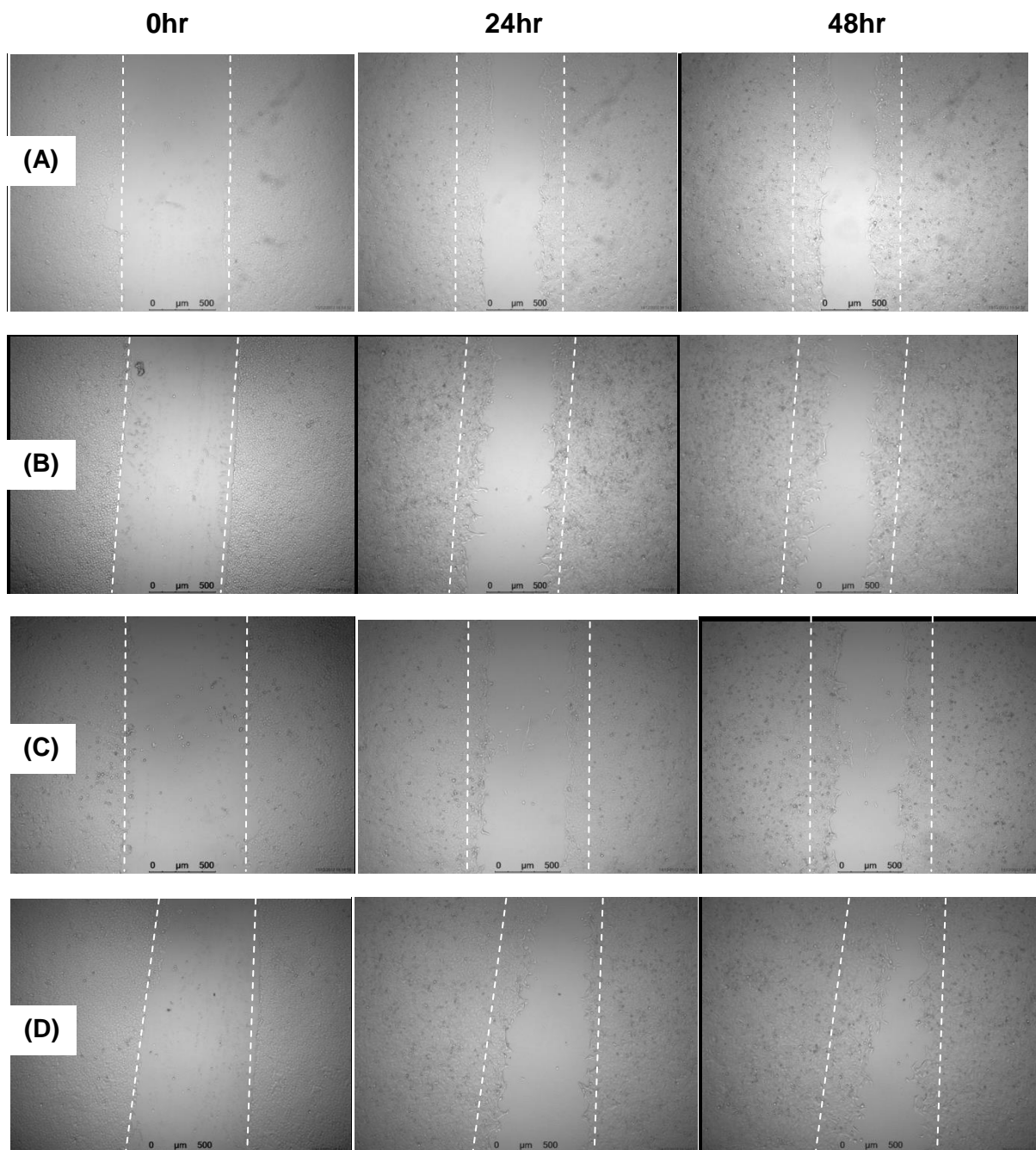


Figure 61: *Scratch wound model from time-lapse microscopy*

The pictures show the frame sequence recorded for C4-II cell migration at 0-, 24-, and 48-hr time points (left to right of each row) for (A) F+M+ cells (B) mitomycin C-treated F+M+ cells (C) F-M- cells, and (D) mitomycin C-treated F-M- cells. Dotted lines indicate the edge of the wound at 0-hour time point.

6.5 Discussion

In order to investigate a functional outcome from alterations in the expression of genes involved in cell motion, which we found in the gene microarray study, the scratch assay was carried out. The objective was to compare migration rates between methyl donor replete and folate and methionine-deplete cells.

The scratch assay is a two-dimensional (2D) investigation of cell migration. This assay determines the directed movement of the cell on a planar surface (in this case a plastic culture plate) without the barrier of fibre network in 3D migration. The whole protocol was modified from the wound-healing assay protocol of Rodriguez *et al* (Rodriguez *et al.*, 2004) and of Dr Carolyn Staton, Department of Oncology, University of Sheffield (personal contact). Since, to our knowledge, this is the first time cell migration has been investigated in C4-II cells, the appropriate seeding density for the assay had to be determined at the outset. The confluency of the cells is important for mitomycin C optimisation because, at hypoconfluency, the usage of mitomycin C becomes limiting at a lower concentration and at higher confluency mitomycin C efficiency falls. Furthermore, the scratch assay needs to be conducted at 100% confluency to avoid cell movement into the unoccupied space between cells rather than filling the gap made from a scratch.

Cell proliferation can confound results of the migration assay. Some protocols solve this problem by culturing the cells in serum-free medium to arrest or slow proliferation, but treatment with an anti-proliferation drug can also be used. Mitomycin C is an antineoplastic antibiotic used to stop DNA synthesis in cells by nucleotide alkylation; treated cells will not be able to proliferate and may die. An appropriate concentration needs to be selected so as to prevent cell proliferation but not cause cell death. The mitomycin C optimisation was set up for a broad range of concentrations in the first instance, and a more appropriate narrower range for the final experiment. The MTS assay used for the determination of cell proliferation in this study is widely accepted. MTS is a tetrazolium compound [3-(4,5-dimethylthiazol-2-yl)-5-(3-carboxymethoxyphenyl)-2-(4-sulfophenyl)-2H-tetrazolium] in a solution with an electron coupling reagent-phenazine ethosulfate. This assay is used to determine the number of living cells in culture by measuring the quantity of formazan product using absorbance at 490nm, which results from cell bio-reduction by NADPH or NADH (Berridge & Tan, 1993). The MTS assay is an improved version of the MTT assay.

From a single observation, we have seen that, to maintain healthy cells the mitomycin C concentration should not exceed 1.0 µg/ml for F+M+ and not exceed 0.5µg/ml for F-M-. However, after setting up the mitomycin C optimisation experiment 0.5 µg/ml seemed too low to stop cell proliferation and therefore, a concentration of 0.7 µg/ml of mitomycin C concentration was chosen for the scratch assay, for both F+M+ and F-M- cells.

Further experiments using cells at 100% confluence also confirmed the absence of cell proliferation and therefore it was concluded that gap closure would be due solely to cell migration.

We did not observe any effect of methyl donor status on migration rate. Since the protocol resulted in a large variance around a mean for gap closure, regardless of the treatment results should be interpreted cautiously. The scratch assay has many advantages as reviewed in Hulkower & Herber (2011) such as (1) the assay can be performed using any normal laboratory materials, (2) cell movement is in a defined direction which is easy to track, (3) the assay can be modified to investigate the cell migration on different extracellular matrices (ECMs), and (4) the cell movement and morphology can be observed under the microscope at any time point together with the capability of image capturing all through the assay period (Vogt, 2010).

However, the scratch assay also has some disadvantages. The size and shape of the assay scratches are difficult to reproduce perfectly from well to well, even in the same assay plate. In addition, it is not easy to reproduce equivalent characteristics of cells at the edge of the wound because monolayer cell confluence is difficult to standardise (Staton *et al.*, 2009), and the area of the wound may be imprecise. This means that cell damage occurs unequally between scratches, resulting in imprecision in the damage to the underlying ECM (Kam *et al.*, 2008; Staton *et al.*, 2009; Hulkower & Herber, 2011). **Figure 58** shows that the cells on the left-hand side move faster than cells on the other side. This suggested that even in the same well, the cell characteristics around the wound would be different.

Although we were not able to demonstrate an effect of methyl donor depletion on migration of cervical cancer cells others have investigated the role of DNA methylation in cervical cell metastasis. Su *et al.* (2013) found that DNMT3b was overexpressed in the highly invasive HeLa3rd and Caski cervical cancer cell lines. They knocked down DNMT3b and found that this led to a disruption of cell migration in both cell lines (Su *et al.*, 2013). It is important to note that they used the Oris cell migration assay rather than the scratch assay, and this is considered to have better reproducibility. They suggested that down-regulation of DNMT3b resulted in the demethylation of PTPRR (protein tyrosine phosphatase receptor type R) promoter and led to its re-expression. The PTPRR inhibited the MAPK (mitogen-activated protein kinase) signalling and EMT (epithelial-mesenchymal transition), thus disrupting cell migration. A study in DNMT3b-depleted prostate-derived PC3 cells also demonstrated a reduction in cell migration, this time using scratch assay (Yaqinuddin *et al.*, 2008).

Although we were able to demonstrate a down-regulation of DNMT3b in methyl-donor depleted C4-II cells this was not associated with altered cell migration characteristics, as determined using the scratch assay.

Effects of methyl donor depletion on cell migration may be cell-specific. The migration of human umbilical venous endothelial cells (HUVEC) was inhibited by treatment with a high concentration of folic acid (10 μ M) (Hou *et al.*, 2013). On the other hand, folate-depleted epithelial colon carcinoma cells (HCT116) showed enhanced cell migration (Wang *et al.*, 2012). These two studies suggest that high folate concentration decreases cell migration and that migration rate increases in response to folate depletion. Methionine deprivation in vascular smooth muscle cells was shown to increase cell migration, both *in vitro* and *in vivo* (Luo *et al.*, 2012). In contrast to vascular smooth muscle cells, Graziosi *et al.* (2013) found that methionine-depleted gastric cancer cells showed a decrease in cell migration, both *in vitro* and *in vivo* (Graziosi *et al.*, 2013).

It is not surprising that there is some inconsistency in the cell migration literature, given the complexity of the process being observed. Cell migration requires the concerted action of many molecules important to cell communication and cell adhesion and matrix degradation (Friedl & Wolf, 2003). The migration mechanism has been described in detail by Lauffenburger & Horwitz (1996). They proposed that the mechanism is initiated by cell polarization and a modification of the cell shape induced by protein interaction and signalling. Briefly, actin polymerization leads to a change in cell shape into a cylindrical finger-like shape (pseudopod). This change in cell shape pushes the cell membrane outwards, increasing contact with the adjacent ECM (extracellular matrix), and eliciting adhesion molecules and integrins. This stage of migration recruits various signalling pathways, both inside and outside the cell. Proteolysis is induced to degrade the ECM components, actin filaments bind to active myosin and form actomyosin contraction and the trailing edge of the cell detaches and allows the cell to move (Lauffenburger & Horwitz, 1996; Friedl & Wolf, 2003). The integrin-ligand interactions, integrin-ligand binding affinities, integrin levels, and ligand levels are all important for the migration speed (Palecek *et al.*, 1997).

Clearly, cell migration in our depletion model needs to be conducted using other methods. We propose that in further studies in this area we would adopt a method which gave a precise scratch or wound. For example, an electrical fence (Applied Biophysics) or a silicon stopper (Platypus Technologies Inc.) may be used, to create a standardised cell exclusion zone. This approach not only gives a similar size and shape of wound, but also avoids cell damage from the mechanical scraping.

6.6 Summary

There was no significant effect of methyl donor depletion on cell migration, using the scratch assay. However, it proved difficult to avoid a large deviation around the mean for each treatment and it is proposed that further work be carried out using alternative methods.

Chapter 7 Discussion and Conclusion

7.1 Conclusion

It was hypothesized that methyl-donor deficiency influenced the characteristics of the cervical cancer cell lines, C4-II, and SiHa cells. The research to investigate this hypothesis can be considered in four parts: development and validation of methyl donor depleted cervical cancer cell lines; investigation of the effects of methyl-donor status on global DNA methylation, DNMT expression and activity; global gene expression; and determination of altered phenotype in terms of cell migration.

The C4-II and SiHa cell models of methyl donor depletion were characterised by:

1. A fall in intracellular folate and methionine (measured in C4-II cells only).
2. Growth retardation in response to folate depletion alone and folate and methionine depletion. This occurred earlier in the depletion of C4-II cells than SiHa cells.
3. An increase in the accumulation of homocysteine in the extracellular medium, in response to folate depletion alone or folate and methionine depletion.
4. Global DNA hypomethylation in C4-II cells in response to depletion of folate and methionine.
5. A decrease in mRNA for DNMT3a and 3b in response to folate depletion and folate and methionine depletion in C4-II cells. This effect was reversed following repletion with folate and methionine. Effects on DNMT1 are equivocal but folate and methionine depletion led to a similar fall in DNMT1 mRNA but this effect was not consistent.
6. Total DNMT activity was increased in response to folate and methionine depletion in C4-II cells, but uncertainties about the quality of the assay temper the interpretation of these findings.
7. A high number of changes in gene expression occurred in response to folate and methionine depletion in C4-II cells. This included an upregulation of genes important for cell death, cell motion, protein kinase cascade, signal transduction, cell communication, blood vessel development, and focal adhesion. Genes were down regulated in clusters important for regulation of the cell cycle, condensed chromosome, cytoskeleton organization, DNA metabolic process, lipid biosynthesis, and chromosome organization.
8. Folate and methionine depletion of C4-II cells did not show an effect on cell migration this may be due to limitations of the method used.

7.2 Discussion

Methyl donor depleted model of cervical cancer cells

Two cell lines were selected to develop a methyl donor depletion model. Although C4-II is reported to be the most similar to cervical cancer biopsies, in terms of gene expression, the C4-II cervical cancer cell line has rarely been used in research. A lot of effort and time were spent to cope with the unique characteristics of C4-II cells in order to develop the model, and for this reason alone the research described here makes a unique contribution to our understanding of cervical cancer. Both C4-II cells and SiHa cells grew more slowly as a result of methyl donor depletion, is compatible with the role of folates in DNA synthesis and cell proliferation (Jackson *et al.*, 1997), albeit at odds with the high proliferative state of cancer cells. The accumulation of homocysteine in the extracellular medium is a reflection of disturbance to the methyl cycle and validation of the functional effects of methyl donor depletion (Svardal *et al.*, 1986; Nakano *et al.*, 2005), in both cell lines. This meant that further investigations were truly in cells in which methyl donor deficiency was shown to have a metabolic impact. Importantly, although the intracellular concentration of folate was markedly reduced in response to growth in a folate-deplete medium, the concentration of folate in the medium was quite comparable to that in the plasma of a moderately deficient person (Ruston *et al.*, 2004), and therefore the model is considered to be of moderate deficiency and not severe deficiency.

Effects of methyl donor depletion on global DNA methylation

Three approaches were used to determine global DNA methylation. In our experience only the flow cytometry approach generated results which were reproducible. Inconsistencies in the findings of other groups interested in effects of folate or other methyl donor depletion on global methylation may be partly due to effects of the different methods used (Dahl & Guldborg, 2003). Using the flow cytometry method folate depletion alone led to a modest effect on global DNA methylation, on the other hand, folate and methionine depletion led to a significant lowering of global DNA methylation level in C4-II cells, but not SiHa cells. Results suggest that only folate deficiency alone might not be sufficient to affect global DNA methylation (Liu *et al.*, 2010), particularly when the methyl donor choline was available in a high concentration, which we found, retrospectively, to be the case in our studies. Nonetheless, the modest, but not significant, global DNA hypomethylation did not mean that there was no alteration of DNA methylation level in specific genes (Cridler *et al.*, 2012).

Regarding epigenetic effects, histone methylation is another process known to be important for the control of gene expression (Fuks, 2005; Cedar & Bergman, 2009). Even

though we have not investigated the effect of methyl donor deficiency on histone methylation, we cannot exclude the possibility of an alteration of histone methylation status. It has been reported that dietary methyl donor may influence histone methylation status. For example, a study in rats found that choline supplementation during embryogenesis E11-E17 (embryo age day 11-17) led to an increase in global DNA methylation, DNMT1 gene expression, and mRNA and protein expression of histone methyltransferase (Davison *et al.*, 2009). Moreover, a study in cervical specimens from the pre- and post-fortification period of folic acid in USA reported a higher level of Lys-9 histone methylation in high grade cervical lesions than low-grade, and, that high-grade stage cervical lesions have a higher level of Lys-9 histone methylation in the post-fortification than in the pre-fortification period. This suggested that histone methylation effect may be adversely affected by folic acid fortification (Piyathilake *et al.*, 2009).

Effect on DNA methyltransferase gene expression

In order to investigate the DNA methylation machinery, DNA methyltransferase expression and activity were determined by qRT-PCR and ELISA-based enzyme activity assay, respectively. Although this result was not validated, more than 4-independent experiments were conducted and the result were very consistent. Furthermore, the findings were compatible with microarray data. Folate and methionine depletion affected *de novo* DNA methyltransferases (DNMT3a and 3b) expression more than the maintenance DNA methyltransferase (DNMT1). The decrease in gene expression of DNMTs may be causally associated with the decrease in DNA methylation level observed in this study. However, the higher activity of total DNMTs is not in concordance with the lower gene expression. This may be the consequence of post-translational modification to compensate for the lower mRNA expression (Jiang *et al.*, 2007a), or may be explained by altered gene expression of other components involved in DNMTs function (Robertson, 2001). Finally, the method used to measure total DNMT activity has important limitations which may have influenced the findings.

The effects of changes in DNMT expression and/or activity on cancer progression are not understood. Cheray *et al.* (2013), in a mouse glioma model by generating global DNA hypomethylation phenotype, suggested that inhibition of DNMT1 by 5-aza-2-deoxycytidine enhanced tumourigenesis (Cheray *et al.*, 2013). Similarly, Gao *et al.* who studied the effect of DNMT3a on lung tumourigenesis in a mouse model, and Hlady *et al.* who studied the effect of DNMT3b on lymphomagenesis, both suggested that loss of the DNMT3 family promotes cancer progression (Gao *et al.*, 2011; Hlady *et al.*, 2012). On the other hand, some studies have suggested that the loss of DNMTs inhibited cancer

progression. In their study of cervical cancer cell lines, Zhang *et al.* proposed that silencing of DNMT1 could reduce carcinogenesis/cancer progression by re-activation of tumour suppressor genes (Zhang *et al.*, 2011).

Even though animal studies may be more relevant to human carcinogenesis than *in vitro* studies, it is difficult to draw an informed conclusion about the effect of DNMTs expression on cancer progression, and more research in this field is warranted.

Effect on gene expression profile

Gene expression profiling was investigated using microarray analysis of folate and methionine deficient cervical cancer cells compared to replete cells, in order to gain some understanding of how phenotype might change in response to methyl donor depletion. Our investigation showed a significant alteration of expression in more than 10,000 probe genes. For example, the up-regulation of genes involved in cell death and the down-regulation of genes involved in the regulation of the cell cycle, which totally supports the observed growth retardation in depleted cells. The up-regulation of genes involved in cell communication, particularly in the Wnt signalling pathway and focal adhesion, was associated with a plausible change in genes involved in the actin cytoskeleton affecting cell motility, and a change in expression of signalling genes affecting cell proliferation and cell survival. This further supports the observed low proliferation rate in methyl donor depleted cells. Besides the important gene clusters mentioned above, there were several altered genes which play a role in cancer pathways, such as an up-regulation of *Myc*, *p15*, *Bcl2*, and *SMAD3*, and a down-regulation of *E2Fs* and *JUN*. These genes should be investigated further to understand overall cancer behaviour in a methyl donor-depleted system.

Effects on cell migration

Since the gene microarray results showed an up-regulation of genes involved in cell motion, cell migration rate was investigated in folate and methionine depleted cells in comparison to control cells. Several protocols have been used in the investigation of cell migration, but in the first instance, we set up the scratch assay. Although many groups use the scratch assay it became clear that this assay has important limitations. For example, the assay needs a very precise scratch, which is difficult to reproduce. The poor reproducibility cast doubt on the value of the results. It is difficult to be confident about the null findings of an effect of methyl donor depletion on cell migration and this is an area that should be investigated further.

Effect of methyl donor depletion on cancer progression

Folate/methyl donor status is altered by lifestyle factors including dietary/supplement intake, medication, and genetic variants in individual one-carbon metabolism enzymes (Thuesen *et al.*, 2010). The major methyl donors available from food are methionine (~10mmol of methyl group/day), 5-methylTHF (~5-10mmol of methyl group/day), and choline (~30mmol of methyl group/day) (Niculescu & Zeisel, 2002). In terms of dietary intake the prevalence of isolated deficiencies of methionine or choline is quite rare (Rogers, 1995). However, perturbing the metabolism of one methyl donor can affect another, therefore, indirect deficiency of methionine and choline may occur.

Regarding the effect of folate/methyl donor status on cancer, it has been stated that folate plays a role as a double edged sword (Kim, 2006; Lucock & Yates, 2009). In normal cells, folate deficiency leads to DNA instability and aberrant DNA methylation which is key to carcinogenesis. However, once the cancer is developed or in the pre-cancerous stage, folate plays a role in an adverse way by promoting cancer cell proliferation. Although our results suggest that folate depletion or combined folate and methionine depletion may have benefits for the cancer patient by inhibiting cancer cell proliferation, the effect on cancer progression is still unclear. As methyl donor depletion led to an up-regulation of genes related to cell communication, cell motion, and blood vessel development in our combined folate and methionine-depleted model, cancer cells may become more aggressive under methyl donor deficiency. This suggests that although the cervical cancer cells we studied showed a decreased proliferation rate in response to folate and methionine-depletion, this might not stop cell differentiation or metastasis.

Limitations

Most of the limitations of the studies are a result of time and cost constraints.

1. The effect of folate depletion alone could not be investigated in all experiments such as in the gene microarray experiment because of cost limitations. This meant that it was not possible to differentiate the effects of folate deficiency alone from the combined depletion.

2. DNMTs gene expression using qRT-PCR was not evaluated. In order to understand DNA methylation machinery, it will be necessary to validate the mRNA result. The correlation between transcriptional level (mRNA) and translational level (protein) are not always straight forward (Guo *et al.*, 2008). Therefore, it is important that protein expression is measured using Western blotting.

3. The method used to determine total DNMTs activity is not considered robust, and an

alternative method should be sought. The activity of individual DNMTs should be measured.

4. Since microarray measures a large number of gene expressions, a false positive or negative is unavoidable. The gene expression profile from microarray result should be validated using RT PCR or any other method in order to confirm whether the microarray method worked perfectly.

Future work

In order to build on the findings of the results described here the following studies are proposed.

1. DNMTs gene expression using qRT-PCR should be evaluated by western blot to determine protein expression.

2. The regulation mechanism of DNMTs should be investigated. For example, the expression of activator or repressor of DNMTs may be useful.

3. Candidate genes could be chosen from the findings of the microarray study to further validate effects on gene expression. qRT-PCR would be used, or another method such as in situ hybridization.

4. Specific methylation of target genes should be examined in order to determine whether alteration of gene expression resulted from aberrant DNA methylation.

5. Effects on gene expression should be interrogated in more depth. For example, pathway analysis should be considered in more depth and a proteomic study might be considered.

6. Cell behaviour in the methyl donor depleted model should be examined again including the determination of cell migration rate using a more satisfactory protocol. Other functional effects in addition to cell migration should also be investigated.

7. The intracellular choline concentration should be examined since choline is another methyl donor and the interaction between folate, methionine, and choline deficiency should be determined.

8. Besides the effect of methyl donor on DNA methylation, histone methylation may be another response which would also contribute to changes in gene expression. Therefore, determination of histone methylation may be conducted to provide some information about the effect of methyl donor on gene expression.

REFERENCES

- Abercrombie M (1979) Contact inhibition and malignancy. *Nature* **281**, 259-262.
- Abercrombie M, Heaysman JEM & Pegrum SM (1971) The locomotion of fibroblasts in culture: IV. Electron microscopy of the leading lamella. *Experimental Cell Research* **67**, 359-367.
- Ahluwalia A, Yan P, Hurteau JA, Bigsby RM, Jung SH, Huang THM & Nephew KP (2001) DNA Methylation and Ovarian Cancer: I. Analysis of CpG Island Hypermethylation in Human Ovarian Cancer Using Differential Methylation Hybridization. *Gynecologic Oncology* **82**, 261-268.
- Alberg AJ, Selhub J, Shah KV, Viscidi RP, Comstock GW & Helzlsouer KJ (2000) The risk of cervical cancer in relation to serum concentrations of folate, vitamin B12, and homocysteine. *Cancer Epidemiol Biomarkers Prev* **9**, 761-764.
- Ames BN (2001) DNA damage from micronutrient deficiencies is likely to be a major cause of cancer. *Mutation research* **475**, 7-20.
- Antequera F & Bird A (1993) Number of CpG islands and genes in human and mouse. *Proceedings of the National Academy of Sciences* **90**, 11995-11999.
- Antony A, Tang YS, Khan RA, Biju MP, Xiao X, Li QJ, Sun XL, Jayaram HN & Stabler SP (2004) Translational upregulation of folate receptors is mediated by homocysteine via RNA-heterogeneous nuclear ribonucleoprotein E1 interactions. *J Clin Invest* **113**, 285-301.
- Antony AC (1996) Folate Receptors. *Annual Review of Nutrition* **16**, 501-521.
- Appleby P, Beral V, Berrington de Gonzalez A, Colin D, Franceschi S, Goodhill A, Green J, Peto J, Plummer M & Sweetland S (2007) Cervical cancer and hormonal contraceptives: collaborative reanalysis of individual data for 16,573 women with cervical cancer and 35,509 women without cervical cancer from 24 epidemiological studies. *Lancet* **370**, 1609-1621.
- Appleby P, Beral V, Berrington de Gonzalez A, Colin D, Franceschi S, Goodill A, Green J, Peto J, Plummer M & Sweetland S (2006) Carcinoma of the cervix and tobacco smoking: collaborative reanalysis of individual data on 13,541 women with carcinoma of the cervix and 23,017 women without carcinoma of the cervix from 23 epidemiological studies. *Int J Cancer* **118**, 1481-1495.
- Apte R, Dotan S, Elkabets M, White M, Reich E, Carmi Y, Song X, Dvozkin T, Krelin Y & Voronov E (2006) The involvement of IL-1 in tumorigenesis, tumor invasiveness, metastasis and tumor-host interactions. *Cancer and Metastasis Reviews* **25**, 387-408.
- Auersperg N, Kruk PA, Maclaren IA, Watt FM & Myrdal SE (1989) Heterogeneous Expression of Keratin, Involucrin, and Extracellular-Matrix among Subpopulations of a Poorly Differentiated Human Cervical-Carcinoma - Possible Relationships to Patterns of Invasion. *Cancer Research* **49**, 3007-3014.
- Baeriswyl V & Christofori G (2009) The angiogenic switch in carcinogenesis. *Semin Cancer Biol.* **Oct;19(5)**, 329-337.
- Balada E, Ordi-Ros J, Serrano-Acedo S, Martinez-Lostao L, Rosa-Leyva M & Vilardell-Tarrés M (2008) Transcript levels of DNA methyltransferases DNMT1, DNMT3A and DNMT3B in CD4+ T cells from patients with systemic lupus erythematosus. *Immunology* **124**, 339-347.
- Balaghi M & Wagner C (1993) DNA Methylation in Folate-Deficiency - Use of Cpg Methylase. *Biochemical and Biophysical Research Communications* **193**, 1184-1190.
- Beaulieu N, Morin S, Chute IC, Robert M-F, Nguyen H & MacLeod AR (2002) An Essential Role for DNA Methyltransferase DNMT3B in Cancer Cell Survival. *Journal of Biological Chemistry* **277**, 28176-28181.

- Belinsky SA, Nikula KJ, Baylin SB & Issa JP (1996) Increased cytosine DNA-methyltransferase activity is target-cell-specific and an early event in lung cancer. *Proceedings of the National Academy of Sciences* **93**, 4045-4050.
- Berridge MV & Tan AS (1993) Characterization of the cellular reduction of 3-(4,5-dimethylthiazol-2-yl)-2,5-diphenyltetrazolium bromide (MTT): subcellular localization, substrate dependence, and involvement of mitochondrial electron transport in MTT reduction. *Archives of Biochemistry and Biophysics* **303**, 474-482.
- Berx G & van Roy F (2009) Involvement of Members of the Cadherin Superfamily in Cancer. *Cold Spring Harbor Perspectives in Biology* **1**.
- Bhowmick NA, Neilson EG & Moses HL (2004) Stromal fibroblasts in cancer initiation and progression. *Nature* **432**, 332-337.
- Biniszkiewicz D, Gribnau J, Ramsahoye B, Gaudet Fo, Eggan K, Humpherys D, Mastrangelo M-A, Jun Z, Walter Jr & Jaenisch R (2002) Dnmt1 Overexpression Causes Genomic Hypermethylation, Loss of Imprinting, and Embryonic Lethality. *Molecular and Cellular Biology* **22**, 2124-2135.
- Bistulfi G, VanDette E, Matsui S-I & Smiraglia D (2010) Mild folate deficiency induces genetic and epigenetic instability and phenotype changes in prostate cancer cells. *BMC Biology* **8**, 6.
- Blasco MA (2005) Telomeres and human disease: ageing, cancer and beyond. *Nat Rev Genet* **6**, 611-622.
- Bligh J (1952) The level of free choline in plasma. *J Physiol.* **June 27; 117(2)**, 234-240.
- Boulet GI, Horvath C, Broeck DV, Sahebali S & Bogers J (2007) Human papillomavirus: E6 and E7 oncogenes. *The International Journal of Biochemistry & Cell Biology* **39**, 2006-2011.
- Brinton LA, Reeves WC, Brenes MM, Herrero R, de Britton RC, Gaitan E, Tenorio F, Garcia M & Rawls WE (1989) Parity as a risk factor for cervical cancer. *Am J Epidemiol* **130**, 486-496.
- Brinton LA, Reeves WC, Brenes MM, Herrero R, de Britton RC, Gaitan E, Tenorio F, Garcia M & Rawls WE (1990) Oral contraceptive use and risk of invasive cervical cancer. *Int J Epidemiol* **19**, 4-11.
- Brock KE, Berry G, Mock PA, MacLennan R, Truswell AS & Brinton LA (1988) Nutrients in diet and plasma and risk of in situ cervical cancer. *J Natl Cancer Inst* **80**, 580-585.
- Brosnan JT, Jacobs RL, Stead LM & Brosnan ME (2004) Methylation demand: a key determinant of homocysteine metabolism. *Acta Biochim Pol* **51**, 405-413.
- Brown K, Huang Y, Lu Z-Y, Jian W, Blair I & Whitehead A (2006) Mild folate deficiency induces a proatherosclerotic phenotype in endothelial cells. *Atherosclerosis* **189**, 133-141.
- Buemi M, Marino D, Di Pasquale G, Floccari F, Ruello A, Aloisi C, Corica F, Senatore M, Romeo A & Frisina N (2001) Effects of homocysteine on proliferation, necrosis, and apoptosis of vascular smooth muscle cells in culture and influence of folic acid. *Thromb Res* **104**, 207-213.
- Burridge K, Fath K, Kelly T, Nuckolls G & Turner C (1988) Focal Adhesions: Transmembrane Junctions Between the Extracellular Matrix and the Cytoskeleton. *Annual Review of Cell Biology* **4**, 487-525.
- Butterworth CE, Jr., Hatch KD, Gore H, Mueller H & Krumdieck CL (1982) Improvement in cervical dysplasia associated with folic acid therapy in users of oral contraceptives. *Am J Clin Nutr* **35**, 73-82.
- Campbell PM & Szyf M (2003) Human DNA methyltransferase gene DNMT1 is regulated by the APC pathway. *Carcinogenesis* **24**, 17-24.
- CancerresearchUK (2009) Cervical cancer - UK incidence statistics (<http://info.cancerresearchuk.org/cancerstats/types/cervix/incidence/uk-cervical-cancer-incidence-statistics>)

- Carlson MW, Iyer VR & Marcotte EM (2007) Quantitative gene expression assessment identifies appropriate cell line models for individual cervical cancer pathways. *Bmc Genomics* **8**, -.
- Carmeliet P (2005) VEGF as a Key Mediator of Angiogenesis in Cancer. *Oncology* **69(suppl 3)**, 4-10.
- Castellano E & Downward J (2011) RAS Interaction with PI3K: More Than Just Another Effector Pathway. *Genes & Cancer* **2**, 261-274.
- Catania J & Fairweather DS (1991) DNA methylation and cellular ageing. *Mutat Res* **256**, 283-293.
- Cavallaro U & Christofori G (2004) Cell adhesion and signalling by cadherins and Ig-CAMs in cancer. *Nat Rev Cancer* **4**, 118-132.
- Cedar H & Bergman Y (2009) Linking DNA methylation and histone modification: patterns and paradigms. *Nat Rev Genet* **10**, 295-304.
- Chen CL, Liu SS, Ip SM, Wong LC, Ngan HYS & Ng TY (2003) E-cadherin expression is silenced by DNA methylation in cervical cancer cell lines and tumours. *European journal of cancer (Oxford, England : 1990)* **39**, 517-523.
- Chen T, Hevi S, Gay F, Tsujimoto N, He T, Zhang B, Ueda Y & Li E (2007) Complete inactivation of DNMT1 leads to mitotic catastrophe in human cancer cells. *Nat Genet* **39**, 391-396.
- Cheng N, Chytil A, Shyr Y, Joly A & Moses HL (2008) Transforming Growth Factor- β Signaling-Deficient Fibroblasts Enhance Hepatocyte Growth Factor Signaling in Mammary Carcinoma Cells to Promote Scattering and Invasion. *Molecular Cancer Research* **6**, 1521-1533.
- Cheray M, Pacaud R, Nadaradjane A, Vallette F & Cartron P-F (2013) Specific inhibition of one DNMT1-including complex influences tumor initiation and progression. *Clinical Epigenetics* **5**, 9.
- Chern CL, Huang RFS, Chen YH, Cheng JT & Liu TZ (2001) Folate deficiency-induced oxidative stress and apoptosis are mediated via homocysteine-dependent overproduction of hydrogen peroxide and enhanced activation of NF- κ B in human Hep G2 cells. *Biomedicine & Pharmacotherapy* **55**, 434-442.
- Cheung T-H, Lo KW-K, Yim S-F, Chan LK-Y, Heung M-S, Chan C-S, Cheung AY-K, Chung TK-H & Wong Y-F (2004) Epigenetic and genetic alternation of PTEN in cervical neoplasm. *Gynecologic Oncology* **93**, 621-627.
- Choi MS, Shim Y-H, Hwa JY, Lee SK, Ro JY, Kim J-S & Yu E (2003) Expression of DNA methyltransferases in multistep hepatocarcinogenesis. *Human pathology* **34**, 11-17.
- Choi SH, Heo K, Byun H-M, An W, Lu W & Yang AS (2011) Identification of preferential target sites for human DNA methyltransferases. *Nucleic Acids Research* **39**, 104-118.
- Chung-Tsen H & Dolnick BJ (1993) Altered folate-binding protein mRNA stability in KB cells grown in folate-deficient medium. *Biochemical Pharmacology* **45**, 2537-2545.
- Clements EG, Mohammad HP, Leadem BR, Easwaran H, Cai Y, Van Neste L & Baylin SB (2012) DNMT1 modulates gene expression without its catalytic activity partially through its interactions with histone-modifying enzymes. *Nucleic Acids Research*, 1-13.
- Collado M & Serrano M (2010) Senescence in tumours: evidence from mice and humans. *Nat Rev Cancer* **10**, 51-57.
- Collins K, Jacks T & Pavletich NP (1997) The cell cycle and cancer. *Proceedings of the National Academy of Sciences* **94**, 2776-2778.
- Craciunescu CN, Johnson AR & Zeisel SH (2010) Dietary Choline Reverses Some, but Not All, Effects of Folate Deficiency on Neurogenesis and Apoptosis in Fetal Mouse Brain. *The Journal of Nutrition* **140**, 1162-1166.
- Cravo ML, Pinto AG, Chaves P, Cruz JA, Lage P, Nobre Leitao C & Costa Mira F (1998) Effect of folate supplementation on DNA methylation of rectal mucosa in patients with colonic adenomas: correlation with nutrient intake. *Clin Nutr* **17**, 45-49.

- Crider KS, Yang TP, Berry RJ & Bailey LB (2012) Folate and DNA Methylation: A Review of Molecular Mechanisms and the Evidence for Folate's Role. *Advances in Nutrition: An International Review Journal* **3**, 21-38.
- Crott JW, Choi S-W, Ordovas JM, Ditelberg JS & Mason JB (2004) Effects of dietary folate and aging on gene expression in the colonic mucosa of rats: implications for carcinogenesis. *Carcinogenesis* **25**, 69-76.
- Crott JW, Liu Z, Keyes MK, Choi SW, Jang H, Moyer MP & Mason JB (2008) Moderate folate depletion modulates the expression of selected genes involved in cell cycle, intracellular signaling and folate uptake in human colonic epithelial cell lines. *J Nutr Biochem* **19**, 328-335.
- Czeizel AE & Dudas I (1992) Prevention of the first occurrence of neural-tube defects by periconceptional vitamin supplementation. *New England Journal of Medicine* **327**, 1832-1835.
- Dahl C & Guldborg P (2003) DNA methylation analysis techniques. *Biogerontology* **4**, 233-250.
- Darzynkiewicz Z, Halicka HD & Zhao H (2010) Analysis of Cellular DNA Content by Flow and Laser Scanning Cytometry. In *Polyploidization and Cancer*, pp. 137-147 [RC Poon, editor]: Springer New York.
- Davison JM, Mellott TJ, Kovacheva VP & Blusztajn JK (2009) Gestational choline supply regulates methylation of histone H3, expression of histone methyltransferases G9a (Kmt1c) and Suv39h1 (Kmt1a), and DNA methylation of their genes in rat fetal liver and brain. *Journal of Biological Chemistry* **284**, 1982-1989.
- De Marzo AM, Marchi VL, Yang ES, Veeraswamy R, Lin X & Nelson WG (1999) Abnormal Regulation of DNA Methyltransferase Expression during Colorectal Carcinogenesis. *Cancer Research* **59**, 3855-3860.
- DeBerardinis RJ, Lum JJ, Hatzivassiliou G & Thompson CB (2008) The Biology of Cancer: Metabolic Reprogramming Fuels Cell Growth and Proliferation. *Cell metabolism* **7**, 11-20.
- Delage B & Dashwood RH (2008) Dietary manipulation of histone structure and function. *Annual Review of Nutrition* **28**, 347-MC344.
- Denis H, Ndlovu MN & Fuks F (2011) Regulation of mammalian DNA methyltransferases: a route to new mechanisms. *Embo Reports* **12**, 647-656.
- Derynck R, Akhurst RJ & Balmain A (2001) TGF- β signaling in tumor suppression and cancer progression. *Nature genetics* **29**, 117-129.
- Ding Y, He J, Liu X, Chen X, Long C & Wang Y (2012) Expression of DNA methyltransferases in the mouse uterus during early pregnancy and susceptibility to dietary folate deficiency. *Reproduction*.
- Dueñas-González A, Lizano M, Candelaria M, Cetina L, Arce C & Cervera E (2005) Epigenetics of cervical cancer. An overview and therapeutic perspectives. *Molecular Cancer* **4**, 38.
- Dunn GP, Bruce AT, Ikeda H, Old LJ & Schreiber RD (2002) Cancer immunoediting: from immunosurveillance to tumor escape. *Nature immunology* **3**, 991-998.
- Duthie SJ & Hawdon A (1998) DNA instability (strand breakage, uracil misincorporation, and defective repair) is increased by folic acid depletion in human lymphocytes in vitro. *The FASEB Journal* **12**, 1491-1497.
- Duthie SJ, Mavrommatis Y, Rucklidge G, Reid M, Duncan G, Moyer MP, Pirie LP & Bestwick CS (2008) The Response of Human Colonocytes to Folate Deficiency in Vitro: Functional and Proteomic Analyses. *Journal of Proteome Research* **7**, 3254-3266.
- Duthie SJ, Narayanan S, Blum S, Pirie L & Brand GM (2000a) Folate deficiency in vitro induces uracil misincorporation and DNA hypomethylation and inhibits DNA excision repair in immortalized normal human colon epithelial cells. *Nutrition and Cancer-an International Journal* **37**, 245-251.
- Duthie SJ, Narayanan S, Brand GM & Grant G (2000b) DNA stability and genomic methylation status in colonocytes isolated from methyl-donor-deficient rats. *Eur J Nutr* **39**, 106-111.

- Duthie SJ, Narayanan S, Brand GM, Pirie L & Grant G (2002) Impact of folate deficiency on DNA stability. *J Nutr* **132**, 2444S-2449S.
- Duthie SJ, Narayanan S, Sharp L, Little J, Basten G & Powers H (2004) Folate, DNA stability and colo-rectal neoplasia. *Proc Nutr Soc* **63**, 571-578.
- Duursma AM, Kedde M, Schrier M, le Sage C & Agami R (2008) miR-148 targets human DNMT3b protein coding region. *RNA* **14**, 872-877.
- Eads CA, Danenberg KD, Kawakami K, Saltz LB, Danenberg PV & Laird PW (1999) CpG Island Hypermethylation in Human Colorectal Tumors Is Not Associated with DNA Methyltransferase Overexpression. *Cancer Research* **59**, 2302-2306.
- Ehrlich M (2009) DNA hypomethylation in cancer cells. *Epigenomics* **1**, 239-259.
- Ehrlich M, Gama-Sosa MA, Huang L-H, Midgett RM, Kuo KC, McCune RA & Gehrke C (1982) Amount and distribution of 5-methylcytosine in human DNA from different types of tissues or cells. *Nucleic Acids Research* **10**, 2709-2721.
- Eichholzer M, Luthy J, Moser U & Fowler B (2001) Folate and the risk of colorectal, breast and cervix cancer: the epidemiological evidence. *Swiss Medical Weekly* **131**, 539-549.
- Estécio MR, Gharibyan V, Shen L, Ibrahim AE, Doshi K, He R, Jelinek J, Yang AS, Yan PS & Huang TH (2007) LINE-1 hypomethylation in cancer is highly variable and inversely correlated with microsatellite instability. *PLoS ONE* **2**, e399.
- Esteller M, Hamilton SR, Burger PC, Baylin SB & Herman JG (1999) Inactivation of the DNA Repair Gene O6-Methylguanine-DNA Methyltransferase by Promoter Hypermethylation is a Common Event in Primary Human Neoplasia. *Cancer Research* **59**, 793-797.
- Estève P-O, Chin HG, Benner J, Feehery GR, Samaranyake M, Horwitz GA, Jacobsen SE & Pradhan S (2009) Regulation of DNMT1 stability through SET7-mediated lysine methylation in mammalian cells. *Proceedings of the National Academy of Sciences* **106**, 5076-5081.
- Etoh T, Kanai Y, Ushijima S, Nakagawa T, Nakanishi Y, Sasako M, Kitano S & Hirohashi S (2004) Increased DNA Methyltransferase 1 (DNMT1) Protein Expression Correlates Significantly with Poorer Tumor Differentiation and Frequent DNA Hypermethylation of Multiple CpG Islands in Gastric Cancers. *The American Journal of Pathology* **164**, 689-699.
- Evan GI & d'Adda di Fagagna F (2009) Cellular senescence: hot or what? *Current Opinion in Genetics & Development* **19**, 25-31.
- Fabbri M, Garzon R, Cimmino A, Liu Z, Zanesi N, Callegari E, Liu S, Alder H, Costinean S, Fernandez-Cymering C, Volinia S, Guler G, Morrison CD, Chan KK, Marcucci G, Calin GA, Huebner K & Croce CM (2007) MicroRNA-29 family reverts aberrant methylation in lung cancer by targeting DNA methyltransferases 3A and 3B. *Proceedings of the National Academy of Sciences of the United States of America* **104**, 15805-15810.
- Fang J-Y, Xiao S-D, Zhu S-S, Yuan J-M, Qiu D-K & Jiang S-J (1997) Relationship of plasma folic acid and status of DNA methylation in human gastric cancer. *Journal of Gastroenterology* **32**, 171-175.
- Fatemi M, Hermann A, Gowher H & Jeltsch A (2002) Dnmt3a and Dnmt1 functionally cooperate during de novo methylation of DNA. *European Journal of Biochemistry* **269**, 4981-4984.
- Ferrara N (2009) Vascular Endothelial Growth Factor. *Arteriosclerosis, Thrombosis, and Vascular Biology* **29**, 789-791.
- Fiala ES, Staretz ME, Pandya GA, El-Bayoumy K & Hamilton SR (1998) Inhibition of DNA cytosine methyltransferase by chemopreventive selenium compounds, determined by an improved assay for DNA cytosine methyltransferase and DNA cytosine methylation. *Carcinogenesis* **19**, 597-604.
- Finkelstein JD, Martin JJ, Harris BJ & Kyle WE (1982) Regulation of the betaine content of rat liver. *Archives of Biochemistry and Biophysics* **218**, 169-173.

- Flatley JE, McNeir K, Balasubramani L, Tidy J, Stuart EL, Young TA & Powers HJ (2009) Folate status and aberrant DNA methylation are associated with HPV infection and cervical pathogenesis. *Cancer Epidemiol Biomarkers Prev* **18**, 2782-2789.
- Fowler BM, Giuliano AR, Piyathilake C, Nour M & Hatch K (1998) Hypomethylation in cervical tissue: is there a correlation with folate status? *Cancer Epidemiol Biomarkers Prev* **7**, 901-906.
- Fridman JS & Lowe SW (2003) Control of apoptosis by p53. *Oncogene* **22**, 9030-9040.
- Friedl P & Wolf K (2003) Tumour-cell invasion and migration: diversity and escape mechanisms. *Nat Rev Cancer* **3**, 362-374.
- Fuks Fo (2005) DNA methylation and histone modifications: teaming up to silence genes. *Current Opinion in Genetics & Development* **15**, 490-495.
- Gabhann FM & Popel AS (2008) Systems Biology of Vascular Endothelial Growth Factors. *Microcirculation* **15**, 715-738.
- Gao Q, Steine EJ, Barrasa MI, Hockemeyer D, Pawlak M, Fu D, Reddy S, Bell GW & Jaenisch R (2011) Deletion of the de novo DNA methyltransferase Dnmt3a promotes lung tumor progression. *Proceedings of the National Academy of Sciences* **108**, 18061-18066.
- García-Closas R, Castellsagué X, Bosch X & González CA (2005) The role of diet and nutrition in cervical carcinogenesis: A review of recent evidence. *International Journal of Cancer* **117**, 629-637.
- Garlick PJ (2006) Toxicity of Methionine in Humans. *The Journal of Nutrition* **136**, 1722S-1725S.
- Garner EIO (2003) Cervical Cancer: Disparities in Screening, Treatment, and Survival. *Cancer Epidemiology Biomarkers & Prevention* **12**, 242s-247s.
- Geissler C & Powers H (2011) *Human Nutrition*, 12 ed: CHURCHILL LIVINGSTONE ELSEVIER.
- Gerhard DS, Nguyen LT, Zhang ZY, Borecki IB, Coleman BI & Rader JS (2003) A relationship between methylenetetrahydrofolate reductase variants and the development of invasive cervical cancer. *Gynecologic Oncology* **90**, 560-565.
- Ghoshal K, Li X, Datta J, Bai S, Pogribny I, Pogribny M, Huang Y, Young D & Jacob ST (2006) A Folate- and Methyl-Deficient Diet Alters the Expression of DNA Methyltransferases and Methyl CpG Binding Proteins Involved in Epigenetic Gene Silencing in Livers of F344 Rats. *The Journal of Nutrition* **136**, 1522-1527.
- Giles RH, van Es JH & Clevers H (2003) Caught up in a Wnt storm: Wnt signaling in cancer. *Biochimica et Biophysica Acta (BBA) - Reviews on Cancer* **1653**, 1-24.
- Goodman GE, Thornquist MD, Balmes J, Cullen MR, Meyskens FL, Omenn GS, Valanis B & Williams JH (2004) The Beta-Carotene and Retinol Efficacy Trial: Incidence of Lung Cancer and Cardiovascular Disease Mortality During 6-Year Follow-up After Stopping beta-Carotene and Retinol Supplements. *Journal of the National Cancer Institute* **96**, 1743-1750.
- Goodman MT, McDuffie K, Hernandez B, Wilkens LR, Bertram CC, Killeen J, Le Marchand L, Selhub J, Murphy S & Donlon TA (2001) Association of methylenetetrahydrofolate reductase polymorphism C677T and dietary folate with the risk of cervical dysplasia. *Cancer Epidemiol Biomarkers Prev* **10**, 1275-1280.
- Gordon CA, Hartono SR & Chédin F (2013) Inactive DNMT3B Splice Variants Modulate De Novo DNA Methylation. *PLoS ONE* **8**, e69486.
- Goyal R, Rathert P, Laser H, Gowher H & Jeltsch A (2007) Phosphorylation of Serine-515 Activates the Mammalian Maintenance Methyltransferase Dnmt1. *Epigenetics* **2**, 155-160.
- Graziosi L, Mencarelli A, Renga B, D'Amore C, Bruno A, Santorelli C, Cavazzoni E, Cantarella F, Rosati E, Donini A & Fiorucci S (2013) Epigenetic Modulation by Methionine Deficiency Attenuates the Potential for Gastric Cancer Cell Dissemination. *Journal of Gastrointestinal Surgery* **17**, 39-49.

- Greger V, Passarge E, Höpping W, Messmer E & Horsthemke B (1989) Epigenetic changes may contribute to the formation and spontaneous regression of retinoblastoma. *Human Genetics* **83**, 155-158.
- Griffin M, Casadio R & Bergamini CM (2002) Transglutaminases: nature's biological glues. *Biochem. J.* **368**, 377-396.
- Guenin S, Mouallif M, Deplus R, Lampe X, Krusy N, Calonne E, Delbecque K, Kridelka F, Fuks Fo, Ennaji MM & Delvenne P (2012) Aberrant Promoter Methylation and Expression of UTF1 during Cervical Carcinogenesis. *PLoS ONE* **7**, e42704.
- Guo Y, Xiao P, Lei S, Deng F, Xiao GG, Liu Y, Chen X, Li L, Wu S, Chen Y, Jiang H, Tan L, Xie J, Zhu X, Liang S & Deng H (2008) How is mRNA expression predictive for protein expression? A correlation study on human circulating monocytes. *Acta Biochimica et Biophysica Sinica* **40**, 426-436.
- Habib M, Fares F, Bourgeois CA, Bella C, Bernardino J, Hernandez-Blazquez F, de Capoa A & Niveleau A (1999) DNA global hypomethylation in EBV-transformed interphase nuclei. *Exp Cell Res* **249**, 46-53.
- Hagemann T, Bozanovic T, Hooper S, Ljubic A, Slettenaar VIF, Wilson JL, Singh N, Gayther SA, Shepherd JH & Van Trappen POA (2007) Molecular profiling of cervical cancer progression. *British Journal of Cancer* **96**, 321-328.
- Hanahan D & Weinberg RA (2000) The Hallmarks of Cancer. *Cell* **100**, 57-70.
- Hanahan D & Weinberg Robert A (2011) Hallmarks of Cancer: The Next Generation. *Cell* **144**, 646-674.
- Hansen RS, Wijmenga C, Luo P, Stanek AM, Canfield TK, Weemaes CMR & Gartler SM (1999) The DNMT3B DNA methyltransferase gene is mutated in the ICF immunodeficiency syndrome. *Proceedings of the National Academy of Sciences* **96**, 14412-14417.
- Hayashi I, Sohn K-J, Stempak JM, Croxford R & Kim Y-I (2007) Folate Deficiency Induces Cell-Specific Changes in the Steady-State Transcript Levels of Genes Involved in Folate Metabolism and 1-Carbon Transfer Reactions in Human Colonic Epithelial Cells. *The Journal of Nutrition* **137**, 607-613.
- Hazan RB, Phillips GR, Qiao RF, Norton L & Aaronson SA (2000) Exogenous Expression of N-Cadherin in Breast Cancer Cells Induces Cell Migration, Invasion, and Metastasis. *The Journal of Cell Biology* **148**, 779-790.
- He C & Klionsky DJ (2009) Regulation Mechanisms and Signaling Pathways of Autophagy. *Annual Review of Genetics* **43**, 67-93.
- Heinz GL, Aron T, George WB, Erika C, Wei Hsun C, Eva M, Eveline S, Timothy H & Rudolf J (2009) Folate Deficiency Induces Genomic Uracil Misincorporation and Hypomethylation But Does Not Increase DNA Point Mutations. *Gastroenterology* **136**, 227-235.e223.
- Herman JG, Umar A, Polyak K, Graff JR, Ahuja N, Issa J-PJ, Markowitz S, Willson JK, Hamilton SR & Kinzler KW (1998) Incidence and functional consequences of hMLH1 promoter hypermethylation in colorectal carcinoma. *Proceedings of the National Academy of Sciences* **95**, 6870-6875.
- Herrero R, Potischman N, Brinton LA, Reeves WC, Brenes MM, Tenorio F, de Britton RC & Gaitan E (1991) A case-control study of nutrient status and invasive cervical cancer. I. Dietary indicators. *Am J Epidemiol* **134**, 1335-1346.
- Hlady RA, Novakova S, Opavska J, Klinkebiel D, Peters SL, Bies J, Hannah J, Iqbal J, Anderson KM, Siebler HM, Smith LM, Greiner TC, Bastola D, Joshi S, Lockridge O, Simpson MA, Felsher DW, Wagner K-U, Chan WC, Christman JK & Opavsky R (2012) Loss of Dnmt3b function upregulates the tumor modifier Mnt and accelerates mouse lymphomagenesis. *The Journal of Clinical Investigation* **122**, 163-177.
- Hoffmann MJ & Schulz WA (2005) Causes and consequences of DNA hypomethylation in human cancer. *Biochemistry and Cell Biology* **83**, 296-321.
- Horne DW, Cook RJ & Wagner C (1989) Effect of Dietary Methyl Group Deficiency on Folate Metabolism in Rats. *The Journal of Nutrition* **119**, 618-621.

- Hou T-C, Lin J-J, Wen H-C, Chen L-C, Hsu S-P & Lee W-S (2013) Folic acid inhibits endothelial cell migration through inhibiting the RhoA activity mediated by activating the folic acid receptor/cSrc/p190RhoGAP-signaling pathway. *Biochemical Pharmacology* **85**, 376-384.
- Howley PM (1991) Role of the human papillomaviruses in human cancer. *Cancer Res* **51**, 5019s-5022s.
- Hsu PP & Sabatini DM (2008) Cancer Cell Metabolism: Warburg and Beyond. *Cell* **134**, 703-707.
- Hu J & Cheung N-KV (2009) Methionine depletion with recombinant methioninase: In vitro and in vivo efficacy against neuroblastoma and its synergism with chemotherapeutic drugs. *International Journal of Cancer* **124**, 1700-1706.
- Huang DW, Sherman BT & Lempicki RA (2009) Systematic and integrative analysis of large gene lists using DAVID bioinformatics resources. *Nature Protocols* **4**, 44-57.
- Hulkower KI & Herber RL (2011) Cell Migration and Invasion Assays as Tools for Drug Discovery. *Pharmaceutics* **3**, 107-124.
- Ifergan I, Jansen G & Assaraf YG (2005) Cytoplasmic Confinement of Breast Cancer Resistance Protein (BCRP/ABCG2) as a Novel Mechanism of Adaptation to Short-Term Folate Deprivation. *Molecular Pharmacology* **67**, 1349-1359.
- Ifergan I, Shafran A, Jansen G, Hooijberg JH, Scheffer GL & Assaraf YG (2004) Folate Deprivation Results in the Loss of Breast Cancer Resistance Protein (BCRP/ABCG2) Expression: A ROLE FOR BCRP IN CELLULAR FOLATE HOMEOSTASIS. *Journal of Biological Chemistry* **279**, 25527-25534.
- Irizarry RA, Ladd-Acosta C, Wen B, Wu Z, Montano C, Onyango P, Cui H, Gabo K, Rongione M, Webster M, Ji H, Potash JB, Sabunciyani S & Feinberg AP (2009) The human colon cancer methylome shows similar hypo- and hypermethylation at conserved tissue-specific CpG island shores. *Nat Genet* **41**, 178-186.
- Jackson CD, Weis C, Miller BJ & James SJ (1997) Dietary Nucleotides: Effects on Cell Proliferation Following Partial Hepatectomy in Rats Fed NIH-31, AIN-76A, or Folate/Methyl-Deficient Diets. *The Journal of Nutrition* **127**, 834S-837S.
- Jacob RA, Gretz DM, Taylor PC, James SJ, Pogribny IP, Miller BJ, Henning SM & Swendseid ME (1998) Moderate folate depletion increases plasma homocysteine and decreases lymphocyte DNA methylation in postmenopausal women. *Journal of Nutrition* **128**, 1204-1212.
- Jacobs EJ, Connell CJ, Chao A, McCullough ML, Rodriguez C, Thun MJ & Calle EE (2003) Multivitamin Use and Colorectal Cancer Incidence in a US Cohort: Does Timing Matter? *American Journal of Epidemiology* **158**, 621-628.
- James SJ, Melnyk S, Pogribna M, Pogribny IP & Caudill MA (2002) Elevation in S-Adenosylhomocysteine and DNA Hypomethylation: Potential Epigenetic Mechanism for Homocysteine-Related Pathology. *The Journal of Nutrition* **132**, 2361S-2366S.
- James SJ, Pogribna M, Pogribny IP, Melnyk S, Hine RJ, Gibson JB, Yi P, Tafoya DL, Swenson DH, Wilson VL & Gaylor DW (1999) Abnormal folate metabolism and mutation in the methylenetetrahydrofolate reductase gene may be maternal risk factors for Down syndrome. *The American Journal of Clinical Nutrition* **70**, 495-501.
- James SJ, Pogribny IP, Pogribna M, Miller BJ, Jernigan S & Melnyk S (2003) Mechanisms of DNA damage, DNA hypomethylation, and tumor progression in the folate/methyl-deficient rat model of hepatocarcinogenesis. *Journal of Nutrition* **133**, 3740s-3747s.
- Jemal A, Bray F, Center MM, Ferlay J, Ward E & Forman D (2011) Global cancer statistics. *CA: A Cancer Journal for Clinicians* **61**, 69-90.
- Jeong S, Liang G, Sharma S, Lin JC, Choi SH, Han H, Yoo CB, Egger G, Yang AS & Jones PA (2009) Selective Anchoring of DNA Methyltransferases 3A and 3B to Nucleosomes Containing Methylated DNA. *Molecular and Cellular Biology* **29**, 5366-5376.
- Jhaveri MS, Wagner C & Trepel JB (2001) Impact of Extracellular Folate Levels on Global Gene Expression. *Molecular Pharmacology* **60**, 1288-1295.

- Jiang Y, Sun T, Xiong J, Cao J, Li G & Wang S (2007a) Hyperhomocysteinemia-mediated DNA Hypomethylation and its Potential Epigenetic Role in Rats. *Acta Biochimica et Biophysica Sinica* **39**, 657-667.
- Jiang Y, Zhang J, Huang Y, Su J, Zhang J, Wang S, Han X & Wang S (2007b) Homocysteine-mediated expression of SAHH, DNMTs, MBD2, and DNA hypomethylation potential pathogenic mechanism in VSMCs. *DNA and Cell Biology*. **August 26(8)**, 603-611.
- Jones PA & Baylin SB (2007) The Epigenomics of Cancer. *Cell* **128**, 683-692.
- Jones PL, Jan Veenstra GC, Wade PA, Vermaak D, Kass SU, Landsberger N, Strouboulis J & Wolffe AP (1998) Methylated DNA and MeCP2 recruit histone deacetylase to repress transcription. *Nat Genet* **19**, 187-191.
- Jones RG & Thompson CB (2009) Tumor suppressors and cell metabolism: a recipe for cancer growth. *Genes & Development* **23**, 537-548.
- Kam Y, Guess C, Estrada L, Weidow B & Quaranta V (2008) A novel circular invasion assay mimics in vivo invasive behavior of cancer cell lines and distinguishes single-cell motility in vitro. *BMC Cancer* **8**, 198.
- Kanai Y, Ushijima S, Kondo Y, Nakanishi Y & Hirohashi S (2001) DNA methyltransferase expression and DNA methylation of CPG islands and peri-centromeric satellite regions in human colorectal and stomach cancers. *International Journal of Cancer* **91**, 205-212.
- Kane MA, Elwood PC, Portillo RM, Antony AC, Najfeld V, Finley A, Waxman S & Kolhouse JF (1988) Influence on immunoreactive folate-binding proteins of extracellular folate concentration in cultured human cells. *The Journal of Clinical Investigation* **81**, 1398-1406.
- Kang S, Kim JW, Kang GH, Park NH, Song YS, Kang SB & Lee HP (2005) Polymorphism in folate- and methionine-metabolizing enzyme and aberrant CpG island hypermethylation in uterine cervical cancer. *Gynecol Oncol* **96**, 173-180.
- Kastan MB & Bartek J (2004) Cell-cycle checkpoints and cancer. *Nature* **432**, 316-323.
- Katula KS, Heinloth AN & Paules RS (2007) Folate deficiency in normal human fibroblasts leads to altered expression of genes primarily linked to cell signaling, the cytoskeleton and extracellular matrix. *The Journal of Nutritional Biochemistry* **18**, 541-552.
- Kazerounian S, Yee KO & Lawler J (2008) Thrombospondins: from structure to therapeutics. *Cellular and Molecular Life Sciences* **65**, 700-712.
- Keely PJ, Fong AM, Zutter MM & Santoro SA (1995) Alteration of collagen-dependent adhesion, motility, and morphogenesis by the expression of antisense alpha 2 integrin mRNA in mammary cells. *Journal of Cell Science* **108**, 595-607.
- Kelemen LE (2006) The role of folate receptor alpha in cancer development, progression and treatment: cause, consequence or innocent bystander? *Int J Cancer* **119**, 243-250.
- Kessenbrock K, Plaks V & Werb Z (2010) Matrix Metalloproteinases: Regulators of the Tumor Microenvironment. *Cell* **141**, 52-67.
- Kim KC, Friso S & Choi SW (2009) DNA methylation, an epigenetic mechanism connecting folate to healthy embryonic development and aging. *Journal of Nutritional Biochemistry* **20**, 917-926.
- Kim Y-I (2004) Folate, colorectal carcinogenesis, and DNA methylation: Lessons from animal studies. *Environmental and Molecular Mutagenesis* **44**, 10-25.
- Kim Y-I (2005) Nutritional Epigenetics: Impact of Folate Deficiency on DNA Methylation and Colon Cancer Susceptibility. *The Journal of Nutrition* **135**, 2703-2709.
- Kim Y-I (2006) Folate: a magic bullet or a double edged sword for colorectal cancer prevention? *Gut* **55**, 1387-1389.
- Kim Y-I (2007) Folate and colorectal cancer: An evidence-based critical review. *Molecular Nutrition & Food Research* **51**, 267-292.

- Kim Y-I, Miller JW, da Costa K-A, Nadeau M, Smith D, Selhub J, Zeisel SH & Mason JB (1994a) Severe Folate Deficiency Causes Secondary Depletion of Choline and Phosphocholine in Rat Liver. *The Journal of Nutrition* **124**, 2197-2203.
- Kim Y, Christman J, Fleet J, Cravo M, Salomon R, Smith D, Ordovas J, Selhub J & Mason J (1995) Moderate folate deficiency does not cause global hypomethylation of hepatic and colonic DNA or c-myc-specific hypomethylation of colonic DNA in rats. *Am J Clin Nutr* **61**, 1083-1090.
- Kim YI, Giuliano A, Hatch KD, Schneider A, Nour MA, Dallal GE, Selhub J & Mason JB (1994b) Global DNA hypomethylation increases progressively in cervical dysplasia and carcinoma. *Cancer* **74**, 893-899.
- Kiviat NB & Koutsky LA (1993) Specific human papillomavirus types as the causal agents of most cervical intraepithelial neoplasia: implications for current views and treatment. *Journal of the National Cancer Institute* **85**, 934-935.
- Kobayashi Y, Absher DM, Gulzar ZG, Young SR, McKenney JK, Peehl DM, Brooks JD, Myers RM & Sherlock G (2011) DNA methylation profiling reveals novel biomarkers and important roles for DNA methyltransferases in prostate cancer. *Genome Research* **21**, 1017-1027.
- Kokkinakis DM, Liu X, Chada S, Ahmed MM, Shareef MM, Singha UK, Yang S & Luo J (2004) Modulation of Gene Expression in Human Central Nervous System Tumors under Methionine Deprivation-induced Stress. *Cancer Research* **64**, 7513-7525.
- Kokkinakis DM, Liu X & Neuner RD (2005) Modulation of cell cycle and gene expression in pancreatic tumor cell lines by methionine deprivation (methionine stress): implications to the therapy of pancreatic adenocarcinoma. *Molecular Cancer Therapeutics* **4**, 1338-1348.
- Kotsopoulos J, Sohn K-J & Kim Y-I (2008) Postweaning Dietary Folate Deficiency Provided through Childhood to Puberty Permanently Increases Genomic DNA Methylation in Adult Rat Liver. *The Journal of Nutrition* **138**, 703-709.
- Kroemer G & Pouyssegur J (2008) Tumor Cell Metabolism: Cancer's Achilles' Heel. *Cancer cell* **13**, 472-482.
- Lande-Diner L, Zhang J, Ben-Porath I, Amariglio N, Keshet I, Hecht M, Azuara V, Fisher AG, Rechavi G & Cedar H (2007) Role of DNA Methylation in Stable Gene Repression. *Journal of Biological Chemistry* **282**, 12194-12200.
- Lauffenburger D & Horwitz A (1996) Cell Migration: A Physically Integrated Molecular Process. *Cell* **84**, 359-369.
- Lee B & Muller MT (2009) SUMOylation enhances DNA methyltransferase 1 activity. *Biochemical Journal* **421**, 449-461.
- Lee PJ, Washer LL, Law DJ, Boland CR, Horon IL & Feinberg AP (1996) Limited up-regulation of DNA methyltransferase in human colon cancer reflecting increased cell proliferation. *Proceedings of the National Academy of Sciences* **93**, 10366-10370.
- Li E, Beard C & Jaenisch R (1993) Role for DNA methylation in genomic imprinting. *Nature* **366**, 362-365.
- Li E, Bestor TH & Jaenisch R (1992) Targeted mutation of the DNA methyltransferase gene results in embryonic lethality. *Cell* **69**, 915-926.
- Libbus BL, Borman LS, Ventrone CH & Branda RF (1990) Nutritional folate-deficiency in Chinese hamster ovary cells: Chromosomal abnormalities associated with perturbations in nucleic acid precursors. *Cancer Genetics and Cytogenetics* **46**, 231-242.
- Ling Y, Sankpal UT, Robertson AK, McNally JG, Karpova T & Robertson KD (2004) Modification of de novo DNA methyltransferase 3a (Dnmt3a) by SUMO-1 modulates its interaction with histone deacetylases (HDACs) and its capacity to repress transcription. *Nucleic Acids Research* **32**, 598-610.
- Lipkin G & Knecht ME (1974) A Diffusible Factor Restoring Contact Inhibition of Growth to Malignant Melanocytes. *Proceedings of the National Academy of Sciences* **71**, 849-853.

- Liu D, Zhou P, Zhang L, Wu G, Zheng Y & He F (2011) Differential expression of Oct4 in HPV-positive and HPV-negative cervical cancer cells is not regulated by DNA methyltransferase 3A. *Tumor Biology* **32**, 941-950.
- Liu J, Ward RL, Zdenko H & Toshikazu U (2010) Folate and One-Carbon Metabolism and Its Impact on Aberrant DNA Methylation in Cancer. In *Advances in Genetics*, pp. 79-121: Academic Press.
- Liu Z, Choi S-W, Crott JW, Keyes MK, Jang H, Smith DE, Kim M, Laird PW, Bronson R & Mason JB (2007) Mild Depletion of Dietary Folate Combined with Other B Vitamins Alters Multiple Components of the Wnt Pathway in Mouse Colon. *The Journal of Nutrition* **137**, 2701-2708.
- Livak KJ & Schmittgen TD (2001) Analysis of relative gene expression data using real-time quantitative PCR and the 2(-Delta Delta C(T)) Method. *Methods* **25**, 402-408.
- Lo SH (2006) Focal adhesions: what's new inside. *Developmental biology* **294**, 280-291.
- López de Silanes I, Gorospe M, Taniguchi H, Abdelmohsen K, Srikantan S, Alaminos M, Berdasco M, Urduñigo R, Fraga MF, Jacinto FV & Esteller M (2009) The RNA-binding protein HuR regulates DNA methylation through stabilization of DNMT3b mRNA. *Nucleic Acids Research* **37**, 2658-2671.
- Lowe SW, Cepero E & Evan G (2004) Intrinsic tumour suppression. *Nature* **432**, 307-315.
- Lowy DR, Kirnbauer R & Schiller JT (1994) Genital human papillomavirus infection. *Proceedings of the National Academy of Sciences* **91**, 2436-2440.
- Lowy DR & Schiller JT (2006) Prophylactic human papillomavirus vaccines. *The Journal of Clinical Investigation* **116**, 1167-1173.
- Lucock M & Yates Z (2009) Folic acid fortification: a double-edged sword. *Current Opinion in Clinical Nutrition & Metabolic Care* **12**, 555-564
510.1097/MCO.1090b1013e32833192bc.
- Luo X, Xiao Y, Song F, Yang Y, Xia M & Ling W (2012) Increased plasma S-adenosyl-homocysteine levels induce the proliferation and migration of VSMCs through an oxidative stress-ERK1/2 pathway in apoE^{-/-} mice. *Cardiovascular Research* **95**, 241-250.
- McManus KJ, Biron VL, Heit R, Underhill DA & Hendzel MJ (2006) Dynamic changes in histone H3 lysine 9 methylations: identification of a mitosis-specific function for dynamic methylation in chromosome congression and segregation. *J Biol Chem* **281**, 8888-8897.
- Miranda TB & Jones PA (2007) DNA methylation: The nuts and bolts of repression. *Journal of Cellular Physiology* **213**, 384-390.
- Mizuno S-i, Chijiwa T, Okamura T, Akashi K, Fukumaki Y, Niho Y & Sasaki H (2001) Expression of DNA methyltransferases DNMT1, 3A, and 3B in normal hematopoiesis and in acute and chronic myelogenous leukemia. *Blood* **97**, 1172-1179.
- Morey Kinney SR, Smiraglia DJ, James SR, Moser MT, Foster BA & Karpf AR (2008) Stage-Specific Alterations of DNA Methyltransferase Expression, DNA Hypermethylation, and DNA Hypomethylation during Prostate Cancer Progression in the Transgenic Adenocarcinoma of Mouse Prostate Model. *Molecular Cancer Research* **6**, 1365-1374.
- Muir CS, Waterhouse J, Mack T, Powell J & Whelan SL (1987) *Cancer incidence in five continents. Volume V, 1987/01/01* ed: IARC Scientific Publications No. 88, Lyon, IARC.
- Muñoz N, Bosch FX, de Sanjosé S, Herrero R, Castellsagué X, Shah KV, Snijders PJF & Meijer CJLM (2003) Epidemiologic Classification of Human Papillomavirus Types Associated with Cervical Cancer. *New England Journal of Medicine* **348**, 518-527.
- Muñoz N, Franceschi S, Bosetti C, Moreno V, Herrero R, Smith JS, Shah KV, Meijer CJ & Bosch FX (2002) Role of parity and human papillomavirus in cervical cancer: the IARC multicentric case-control study. *Lancet* **359**, 1093-1101.
- Najim N, Podmore ID, McGown A & Estlin EJ (2009) Biochemical Changes and Cytotoxicity Associated with Methionine Depletion in Paediatric Central Nervous System Tumour Cell Lines. *Anticancer Research* **29**, 2971-2976.

- Nakano E, Taiwo FA, Nugent D, Griffiths HR, Aldred S, Paisi M, Kwok M, Bhatt P, Hill MHE, Moat S & Powers HJ (2005) Downstream effects on human low density lipoprotein of homocysteine exported from endothelial cells in an in vitro system. *Journal of Lipid Research* **46**, 484-493.
- Narayan A, Ji W, Zhang XY, Marrogi A, Graff JR, Baylin SB & Ehrlich M (1998) Hypomethylation of pericentromeric DNA in breast adenocarcinomas. *International Journal of Cancer* **77**, 833-838.
- Narayan G, Arias-Pulido H, Koul S, Vargas H, Zhang FF, Vilella J, Schneider A, Terry MB, Mansukhani M & Murty VV (2003) Frequent promoter methylation of CDH1, DAPK, RARB, and HIC1 genes in carcinoma of cervix uteri: its relationship to clinical outcome. *Mol Cancer* **2**, 24.
- Niculescu MD & Zeisel SH (2002) Diet, methyl donors and DNA methylation: Interactions between dietary folate, methionine and choline. *Journal of Nutrition* **132**, 2333s-2335s.
- Nobes CD & Hall A (1995) Rho, Rac, and Cdc42 GTPases regulate the assembly of multimolecular focal complexes associated with actin stress fibers, lamellipodia, and filopodia. *Cell* **81**, 53-62.
- Novakovic P, Stempak JM, Sohn KJ & Kim YI (2006) Effects of folate deficiency on gene expression in the apoptosis and cancer pathways in colon cancer cells. *Carcinogenesis* **27**, 916-924.
- Oh BK, Kim H, Park HJ, Shim YH, Choi J, Park C & Park YN (2007) DNA methyltransferase expression and DNA methylation in human hepatocellular carcinoma and their clinicopathological correlation. *International journal of molecular medicine* **20**, 65-73.
- Ostor AG (1993) Natural history of cervical intraepithelial neoplasia: a critical review. *Int J Gynecol Pathol* **12**, 186-192.
- Oue N, Kuraoka K, Kuniyasu H, Yokozaki H, Wakikawa A, Matsusaki K & Yasui W (2001) DNA methylation status of hMLH1, p16 (INK4a), and CDH1 is not associated with mRNA expression levels of DNA methyltransferase and DNA demethylase in gastric carcinomas. *Oncology Reports* **8**, 1085.
- Pakneshan P, Têtu B & Rabbani SA (2004) Demethylation of Urokinase Promoter as a Prognostic Marker in Patients with Breast Carcinoma. *Clinical Cancer Research* **10**, 3035-3041.
- Palecek SP, Loftus JC, Ginsberg MH, Lauffenburger DA & Horwitz AF (1997) Integrin-ligand binding properties govern cell migration speed through cell-substratum adhesiveness. *Nature* **385**, 537-540.
- Panning B & Jaenisch R (1998) RNA and the Epigenetic Regulation of X Chromosome Inactivation. *Cell* **93**, 305-308.
- Park S-Y, Murphy SP, Wilkens LR, Nomura AMY, Henderson BE & Kolonel LN (2007) Calcium and Vitamin D Intake and Risk of Colorectal Cancer: The Multiethnic Cohort Study. *American Journal of Epidemiology* **165**, 784-793.
- Pathak S, Bhatla N & Singh N (2012) Cervical cancer pathogenesis is associated with one-carbon metabolism. *Molecular and Cellular Biochemistry* **369**, 1-7.
- Patterson D (2008) Folate metabolism and the risk of Down syndrome. *Down Syndrome Research and Practice* **12**, 93-97.
- Perez-Plasencia C, Vazquez-Ortiz G, Lopez-Romero R, Pina-Sanchez P, Moreno J & Salcedo M (2007) Genome wide expression analysis in HPV16 Cervical Cancer: identification of altered metabolic pathways. *Infectious Agents and Cancer* **2**, 16.
- Petit Vr & Thiery J-P (2000) Focal adhesions: structure and dynamics. *Biology of the Cell* **92**, 477-494.
- Phelan MC (1998) Basic Techniques for Mammalian Cell Tissue Culture. In *Current Protocols in Cell Biology*, pp. 1.1.1-1.1.10: John Wiley & Sons, Inc.
- Pitkin RM (2007) Folate and neural tube defects. *The American Journal of Clinical Nutrition* **85**, 285S-288S.
- Piyathilake CJ (2007) Update on micronutrients and cervical dysplasia. *Ethnicity & Disease* **17**, S14-S17.

- Piyathilake CJ, Celedonio JE, Macaluso M, Bell WC, Azrad M & Grizzle WE (2008) Mandatory fortification with folic acid in the United States is associated with increased expression of DNA methyltransferase-1 in the cervix. *Nutrition (Burbank, Los Angeles County, Calif.)* **24**, 94-99.
- Piyathilake CJ, Henao OL, Macaluso M, Cornwell PE, Meleth S, Heimbürger DC & Partridge EE (2004) Folate Is Associated with the Natural History of High-Risk Human Papillomaviruses. *Cancer Res* **64**, 8788-8793.
- Piyathilake CJ, Johanning GL, Frost AR, Whiteside MA, Manne U, Grizzle WE, Heimbürger DC & Niveleau A (2000) Immunohistochemical evaluation of global DNA methylation: Comparison with in vitro radiolabeled methyl incorporation assay. *Biotechnic & Histochemistry* **75**, 251-258.
- Piyathilake CJ, Macaluso M, Brill I, Heimbürger DC & Partridge EE (2007) Lower red blood cell folate enhances the HPV-16-associated risk of cervical intraepithelial neoplasia. *Nutrition* **23**, 203-210.
- Piyathilake CJ, Macaluso M, Celedonio JE, Badiga S, Bell WC & Grizzle WE (2009) Mandatory fortification with folic acid in the United States appears to have adverse effects on histone methylation in women with pre-cancer but not in women free of pre-cancer. *International journal of women's health* **1**, 131.
- Pogribny IP, James SJ, Jernigan S & Pogribna M (2004) Genomic hypomethylation is specific for preneoplastic liver in folate/methyl deficient rats and does not occur in non-target tissues. *Mutation Research/Fundamental and Molecular Mechanisms of Mutagenesis* **548**, 53-59.
- Pogribny IP, Karpf AR, James SR, Melnyk S, Han T & Tryndyak VP (2008) Epigenetic alterations in the brains of Fisher 344 rats induced by long-term administration of folate/methyl-deficient diet. *Brain Research* **1237**, 25-34.
- Pogribny IP, Tryndyak VP, Muskhelishvili L, Rusyn I & Ross SA (2007) Methyl Deficiency, Alterations in Global Histone Modifications, and Carcinogenesis. *The Journal of Nutrition* **137**, 216S-222S.
- Pomfret EA, daCosta KA & Zeisel SH (1990) Effects of choline deficiency and methotrexate treatment upon rat liver. *The Journal of Nutritional Biochemistry* **1**, 533-541.
- Potischman N (1993) Nutritional epidemiology of cervical neoplasia. *J Nutr* **123**, 424-429.
- Potischman N & Brinton LA (1996) Nutrition and cervical neoplasia. *Cancer Causes Control* **7**, 113-126.
- Potischman N, Brinton LA, Laiming VA, Reeves WC, Brenes MM, Herrero R, Tenorio F, de Britton RC & Gaitan E (1991) A case-control study of serum folate levels and invasive cervical cancer. *Cancer Res* **51**, 4785-4789.
- Powers HJ (2005) Interaction among folate, riboflavin, genotype, and cancer, with reference to colorectal and cervical cancer. *J Nutr* **135**, 2960S-2966S.
- Rajkumar T, Sabitha K, Vijayalakshmi N, Shirley S, Bose M, Gopal G & Selvaluxmy G (2011) Identification and validation of genes involved in cervical tumorigenesis. *BMC Cancer* **11**, 80.
- Rampersaud GC, Bailey LB & Kauwell GP (2002) Relationship of folate to colorectal and cervical cancer: review and recommendations for practitioners. *J Am Diet Assoc* **102**, 1273-1282.
- Rampersaud GC, Kauwell GP, Hutson AD, Cerda JJ & Bailey LB (2000) Genomic DNA methylation decreases in response to moderate folate depletion in elderly women. *Am J Clin Nutr* **72**, 998-1003.
- Rao Y, Wang H, Fan L & Chen G (2011) Silencing MTA1 by RNAi reverses adhesion, migration and invasiveness of cervical cancer cells (SiHa) via altered expression of p53, and E-cadherin/β²-catenin complex. *Journal of Huazhong University of Science and Technology [Medical Sciences]* **31**, 1-9.
- Reddel RR (2000) The role of senescence and immortalization in carcinogenesis. *Carcinogenesis* **21**, 477-484.
- Robertson KD (2001) DNA methylation, methyltransferases, and cancer. *Oncogene* **20** 3139-3155

- Robertson KD, Uzvolgyi E, Liang G, Talmadge C, Sumegi J, Gonzales FA & Jones PA (1999) The human DNA methyltransferases (DNMTs) 1, 3a and 3b: coordinate mRNA expression in normal tissues and overexpression in tumors. *Nucleic Acids Research* **27**, 2291-2298.
- Rodriguez LG, Wu X & Guan J-L (2004) Wound-Healing Assay, pp. 23-29.
- Rogers AE (1995) Methyl donors in the diet and responses to chemical carcinogens. *The American Journal of Clinical Nutrition* **61**, 659S-665S.
- Roll JD, Rivenbark A, Jones W & Coleman W (2008) DNMT3b overexpression contributes to a hypermethylator phenotype in human breast cancer cell lines. *Molecular Cancer* **7**, 15.
- Romestaing C, Piquet M-A, Letexier D, Rey B, Mourier A, Servais Sp, Belouze M, Rouleau V, Dautresme M, Ollivier I, Favier R, Rigoulet M, Duchamp C & Sibille B (2008) Mitochondrial adaptations to steatohepatitis induced by a methionine- and choline-deficient diet. *American Journal of Physiology - Endocrinology And Metabolism* **294**, E110-E119.
- Ross SA & Davis CD (2006) Differential effects of dietary selenium (Se) and folate on methyl metabolism in liver and colon of rats. *Biological Trace Element Research* **109**, 201-214.
- Ruston D, Hoare J, Handerson L & Gregory J (2004) The National Diet and Nutritional Survey : adult age 19 to 64 years. Volumn 4. London:TSO.
- Saavedra OM, Isakovic L, Llewellyn DB, Zhan L, Bernstein N, Claridge S, Raepfel F, Vaisburg A, Elowe N, Petschner AJ, Rahil J, Beaulieu N, MacLeod AR, Delorme D, Besterman JM & Wahhab A (2009) SAR around (l)-S-adenosyl-l-homocysteine, an inhibitor of human DNA methyltransferase (DNMT) enzymes. *Bioorganic & Medicinal Chemistry Letters* **19**, 2747-2751.
- Saito Y, Kanai Y, Sakamoto M, Saito H, Ishii H & Hirohashi S (2001) Expression of mRNA for DNA methyltransferases and methyl-CpG-binding proteins and DNA methylation status on CpG islands and pericentromeric satellite regions during human hepatocarcinogenesis. *Hepatology* **33**, 561-568.
- Saito Y, Kanai Y, Sakamoto M, Saito H, Ishii H & Hirohashi S (2002) Overexpression of a splice variant of DNA methyltransferase 3b, DNMT3b4, associated with DNA hypomethylation on pericentromeric satellite regions during human hepatocarcinogenesis. *Proceedings of the National Academy of Sciences* **99**, 10060-10065.
- Savendahl L, Mar MH, Underwood LE & Zeisel SH (1997) Prolonged fasting in humans results in diminished plasma choline concentrations but does not cause liver dysfunction. *The American Journal of Clinical Nutrition* **66**, 622-625.
- Sawada M, Kanai Y, Arai E, Ushijima S, Ojima H & Hirohashi S (2007) Increased expression of DNA methyltransferase 1 (DNMT1) protein in uterine cervix squamous cell carcinoma and its precursor lesion. *Cancer Letters* **251**, 211-219.
- Schoell WM, Janicek MF & Mirhashemi R (1999) Epidemiology and biology of cervical cancer. *Semin Surg Oncol* **16**, 203-211.
- Schreiber RD, Old LJ & Smyth MJ (2011) Cancer Immunoediting: Integrating Immunity's Roles in Cancer Suppression and Promotion. *Science* **331**, 1565-1570.
- Schroeder A, Mueller O, Stocker S, Salowsky R, Leiber M, Gassmann M, Lightfoot S, Menzel W, Granzow M & Ragg T (2006) The RIN: an RNA integrity number for assigning integrity values to RNA measurements. *BMC Molecular Biology* **7**, 3.
- Sedjo RL, Inserra P, Abrahamsen M, Harris RB, Roe DJ, Baldwin S & Giuliano AR (2002) Human Papillomavirus Persistence and Nutrients Involved in the Methylation Pathway among a Cohort of Young Women. *Cancer Epidemiology Biomarkers & Prevention* **11**, 353-359.
- Selhub J, Seyoum E, Pomfret EA & Zeisel SH (1991) Effects of Choline Deficiency and Methotrexate Treatment upon Liver Folate Content and Distribution. *Cancer Research* **51**, 16-21.

- Semenza GL (2010a) Defining the role of hypoxia-inducible factor 1 in cancer biology and therapeutics. *Oncogene* **29**, 625-634.
- Semenza GL (2010b) HIF-1: upstream and downstream of cancer metabolism. *Current Opinion in Genetics & Development* **20**, 51-56.
- Shane B (2010) Folate Chemistry and Metabolism. In *Folate in health and disease*, pp. 1-24 [LB Bailay, editor]. New York: CRC Press, Taylor & Francis Group.
- Shapiro HM (2003) *Practical flow cytometry*, 4th ed. New Jersey, USA: John Wiley & Sons, Inc.
- Shay JW & Wright WE (2000) Hayflick, his limit, and cellular ageing. *Nat Rev Mol Cell Biol* **1**, 72-76.
- Shortt J & Johnstone RW (2012) Oncogenes in Cell Survival and Cell Death. *Cold Spring Harbor Perspectives in Biology* **4**.
- Shuangshoti S, Hourpai N, Pumsuk U & Mutirangura A (2007) Line-1 hypomethylation in multistage carcinogenesis of the uterine cervix. *Asian Pacific Journal of Cancer Prevention* **8**, 307.
- Sikalidis AK & Stipanuk MH (2010) Growing Rats Respond to a Sulfur Amino Acid-Deficient Diet by Phosphorylation of the β Subunit of Eukaryotic Initiation Factor 2 Heterotrimeric Complex and Induction of Adaptive Components of the Integrated Stress Response. *The Journal of Nutrition* **140**, 1080-1085.
- Sohn K-J, Stempak JM, Reid S, Shirwadkar S, Mason JB & Kim Y-I (2003) The effect of dietary folate on genomic and p53-specific DNA methylation in rat colon. *Carcinogenesis* **24**, 81-90.
- Stanley M (2006) HPV and pathogenesis of cervical cancer. *European Journal of Obstetrics & Gynecology and Reproductive Biology*, (doi;10.1016/j.ejogrb.2006.06.022).
- Staton CA, Reed MWR & Brown NJ (2009) A critical analysis of current in vitro and in vivo angiogenesis assays. *International Journal of Experimental Pathology* **90**, 195-221.
- Stempak JM, Sohn KJ, Chiang EP, Shane B & Kim YI (2005) Cell and stage of transformation-specific effects of folate deficiency on methionine cycle intermediates and DNA methylation in an in vitro model. *Carcinogenesis* **26**, 981-990.
- Stokstad EL & Koch J (1967) Folic acid metabolism. *Physiol Rev* **47**, 83-116.
- Su PH, Lin YW, Huang RL, Liao YP, Lee HY, Wang HC, Chao TK, Chen CK, Chan MWY, Chu TY, Yu MH & Lai HC (2013) Epigenetic silencing of PTPRR activates MAPK signaling, promotes metastasis and serves as a biomarker of invasive cervical cancer. *Oncogene* **32**, 15-26.
- Sun Y, Liu J, Sui Y, Jin L, Yang Y, Lin S & Shi H (2011) Beclin1 overexpression inhibits proliferation, invasion and migration of CaSki cervical cancer cells. *Asian Pac J Cancer Prev.* **12(5)**, 1269-1273.
- Svardal ArM, Djurhuus R, Refsum H & Ueland PM (1986) Disposition of Homocysteine in Rat Hepatocytes and in Nontransformed and Malignant Mouse Embryo Fibroblasts following Exposure to Inhibitors of S-Adenosylhomocysteine Catabolism. *Cancer Research* **46**, 5095-5100.
- The American Cancer Society Advisory Committee on Diet N & Cancer P (1996) Guidelines on diet, nutrition, and cancer prevention: Reducing the risk of cancer with healthy food choices and physical activity. *CA: A Cancer Journal for Clinicians* **46**, 325-341.
- Thorstensen L, Lind GE, Lågvidt T, Diep CB, Meling GI, Rognum TO & Lothe RA (2005) Genetic and epigenetic changes of components affecting the WNT pathway in colorectal carcinomas stratified by microsatellite instability. *Neoplasia (New York, NY)* **7**, 99.
- Thuesen BH, Husemoen LLN, Ovesen L, Jørgensen T, Fenger M & Linneberg A (2010) Lifestyle and genetic determinants of folate and vitamin B12 levels in a general adult population. *British Journal of Nutrition* **103**, 1195.
- Trasler J, Deng L, Melnyk S, Pogribny I, Hiou-Tim F, Sibani S, Oakes C, Li E, James SJ & Rozen R (2003) Impact of Dnmt1 deficiency, with and without low folate diets, on tumor numbers and DNA methylation in Min mice. *Carcinogenesis* **24**, 39-45.

- Ueland PM, Refsum H, Stabler SP, Malinow MR, Andersson A & Allen RH (1993) Total homocysteine in plasma or serum: methods and clinical applications. *Clinical Chemistry* **39**, 1764-1779.
- Uthus E, Ross S & Davis C (2006) Differential effects of dietary selenium (Se) and folate on methyl metabolism in liver and colon of rats. *Biological Trace Element Research* **109**, 201-214.
- VanEenwyk J, Davis FG & Colman N (1992) Folate, vitamin C, and cervical intraepithelial neoplasia. *Cancer Epidemiol Biomarkers Prev* **1**, 119-124.
- Virmani AK, Muller C, Rathi A, Zochbauer-Mueller S, Mathis M & Gazdar AF (2001) Aberrant methylation during cervical carcinogenesis. *Clin Cancer Res* **7**, 584-589.
- Vogt A (2010) Advances in two-dimensional cell migration assay technologies. *European Pharmaceutical Review* **Issue 5**, 26-29.
- Walsh CP, Chaillet JR & Bestor TH (1998) Transcription of IAP endogenous retroviruses is constrained by cytosine methylation. *Nat Genet* **20**, 116-117.
- Wang T-P, Hsu S-H, Feng H-C & Huang R-FS (2012) Folate deprivation enhances invasiveness of human colon cancer cells mediated by activation of sonic hedgehog signaling through promoter hypomethylation and cross action with transcription nuclear factor-kappa B pathway. *Carcinogenesis* **33**, 1158-1168.
- Wasson GR, McGlynn AP, McNulty H, O'Reilly SL, McKelvey-Martin VJ, McKerr G, Strain JJ, Scott J & Downes CS (2006) Global DNA and p53 region-specific hypomethylation in human colonic cells is induced by folate depletion and reversed by folate supplementation. *Journal of Nutrition* **136**, 2748-2753.
- Webb DJ, Zhang H & Horwitz AF (2005) Cell migration. In *Cell Migration*, pp. 3-11: Springer.
- Weinstein SJ, Ziegler RG, Frongillo EA, Jr., Colman N, Sauberlich HE, Brinton LA, Hamman RF, Levine RS, Mallin K, Stolley PD & Bisogni CA (2001) Low serum and red blood cell folate are moderately, but nonsignificantly associated with increased risk of invasive cervical cancer in U.S. women. *J Nutr* **131**, 2040-2048.
- Weisenberger DJ, Campan M, Long TI, Kim M, Woods C, Fiala E, Ehrlich M & Laird PW (2005) Analysis of repetitive element DNA methylation by MethyLight. *Nucleic Acids Research* **33**, 6823-6836.
- WenChun C & Huang RFS (2009) Effects of folate and macrophages activation on migration of human hepatocellular carcinoma cell lines. *Nutritional Sciences Journal* **Vol. 34 No. 2**, 68-75.
- Whidden P (1994) Cigarette smoking and cervical cancer. *Int J Epidemiol* **23**, 1099-1100.
- Whitehead N, Reyner F & Lindenbaum J (1973) Megaloblastic changes in the cervical epithelium. Association with oral contraceptive therapy and reversal with folic acid. *JAMA* **226**, 1421-1424.
- Wild L & Flanagan JM (2010) Genome-wide hypomethylation in cancer may be a passive consequence of transformation. *Biochimica Et Biophysica Acta-Reviews on Cancer* **1806**, 50-57.
- Wilke CM, Hall BK, Hoge A, Paradee W, Smith DI & Glover TW (1996) FRA3B Extends Over a Broad Region and Contains a Spontaneous HPV16 Integration Site: Direct Evidence for the Coincidence of Viral Integration Sites and Fragile Sites. *Human Molecular Genetics* **5**, 187-195.
- Williams JD & Jacobson MK (2010) Photobiological implications of folate depletion and repletion in cultured human keratinocytes. *Journal of photochemistry and photobiology. B, Biology* **99**, 49-61.
- Yanagisawa Y, Ito E, Yuasa Y & Maruyama K (2002) The human DNA methyltransferases DNMT3A and DNMT3B have two types of promoters with different CpG contents. *Biochimica et Biophysica Acta (BBA) - Gene Structure and Expression* **1577**, 457-465.
- Yaqinuddin A, Qureshi S, Qazi R & Abbas F (2008) Down-regulation of DNMT3b in PC3 cells effects locus-specific DNA methylation, and represses cellular growth and migration. *Cancer Cell International* **8**, 13.

- Yin L-J, Zhang Y, Lv P-P, He W-H, Wu Y-T, Liu A-X, Ding G-L, Dong M-Y, Qu F, Xu C-M, Zhu X-M & Huang H-F (2012) Insufficient maintenance DNA methylation is associated with abnormal embryonic development. *BMC Medicine* **10**, 26.
- Zeisel SH (1981) Dietary choline: biochemistry, physiology, and pharmacology. *Annu Rev Nutr* **1**, 95-121.
- Zeisel SH, Zola T, daCosta KA & Pomfret EA (1989) Effect of choline deficiency on S-adenosylmethionine and methionine concentrations in rat liver. *The Biochemical journal* **259**, 725-729.
- Zhang Y, Chen F-q, Sun Y-h, Zhou S-y, Li T-y & Chen R (2011) Effects of DNMT1 silencing on malignant phenotype and methylated gene expression in cervical cancer cells. *Journal of Experimental & Clinical Cancer Research* **30**, 98.
- Zittoun J & Zittoun R (1999) Modern clinical testing strategies in cobalamin and folate deficiency. *Seminars in hematology* **36**, 35-46.
- Zondervan KT, Carpenter LM, Painter R & Vessey MP (1996) Oral contraceptives and cervical cancer--further findings from the Oxford Family Planning Association contraceptive study. *Br J Cancer* **73**, 1291-1297.